

FINAL REPORT

CONSTRUCTION LOADS AND VIBRATIONS

Project IA-H1, 1994

Report No. ITRC FR 94-3

Prepared by

Mohsen A. Issa
Department of Civil and Materials Engineering
University of Illinois at Chicago
Chicago, Illinois

March 1998

Front cover

Illinois Transportation Research Center
Illinois Department of Transportation

ILLINOIS TRANSPORTATION RESEARCH CENTER

This research project was sponsored by the State of Illinois, acting by and through its Department of Transportation, according to the terms of the Memorandum of Understanding established with the Illinois Transportation Research Center. The Illinois Transportation Research Center is a joint Public-Private-University cooperative transportation research unit underwritten by the Illinois Department of Transportation. The purpose of the Center is the conduct of research in all modes of transportation to provide the knowledge and technology base to improve the capacity to meet the present and future mobility needs of individuals, industry and commerce of the State of Illinois.

Research reports are published throughout the year as research projects are completed. The contents of these reports reflect the views of the authors who are responsible for the facts and the accuracy of the data presented herein. The contents do not necessarily reflect the official views or policies of the Illinois Transportation Research Center or the Illinois Department of Transportation. This report does not constitute a standard, specification, or regulation.

Neither the United States Government nor the State of Illinois endorses products or manufacturers. Trade or manufacturers' names appear in the reports solely because they are considered essential to the object of the reports.

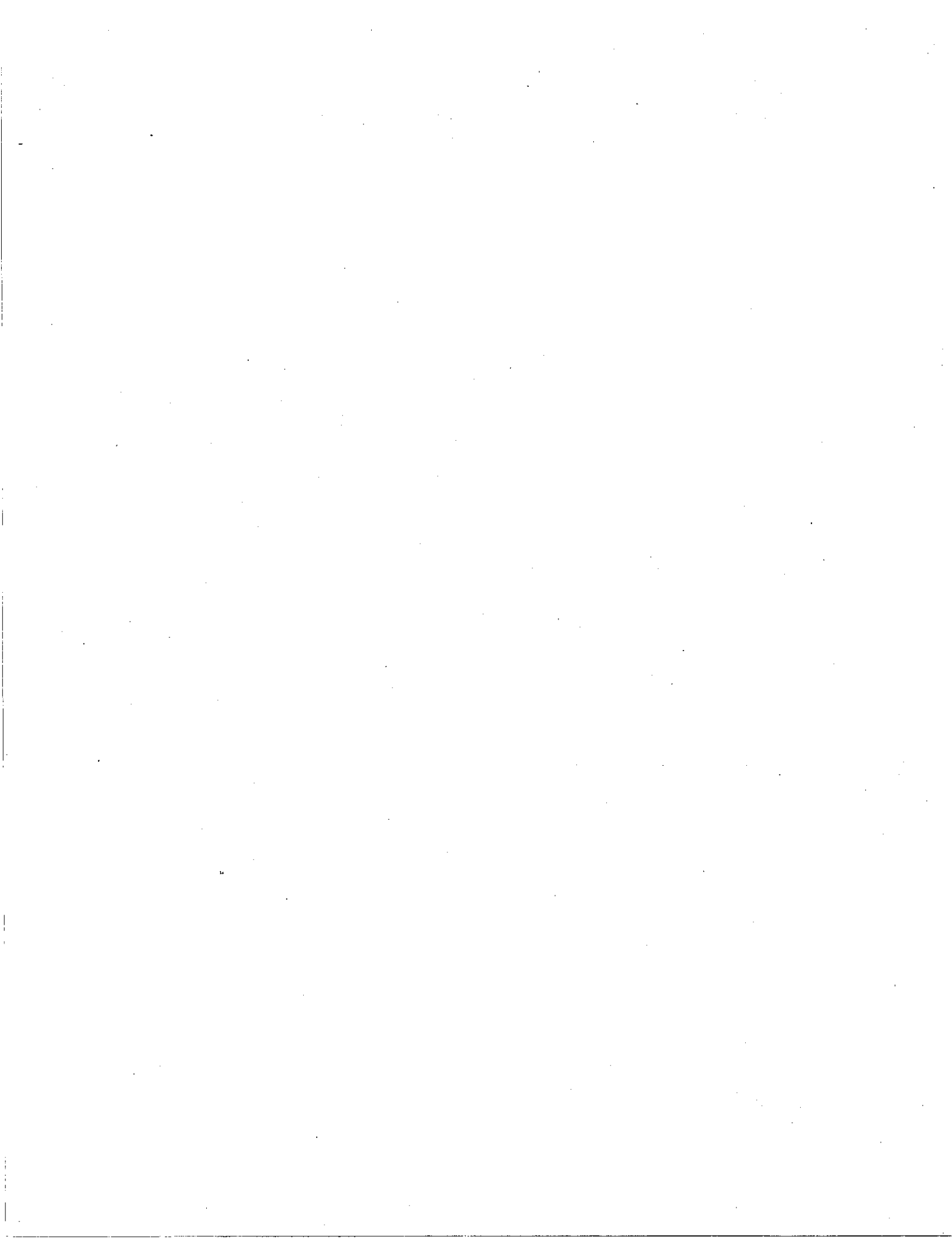
Illinois Transportation Research Center

Bradley University
DePaul University
Eastern Illinois University
Illinois Department of Transportation
Illinois Institute of Technology
Lewis University
Northern Illinois University
Northwestern University
Southern Illinois University - Carbondale
Southern Illinois University at Edwardsville
University of Illinois at Chicago
University of Illinois at Urbana-Champaign
Western Illinois University

Back side of Front cover

Reports may be obtained by writing to the administrative offices of the Illinois Transportation Research Center at 200 University Park, Edwardsville, IL 62026-1806 [telephone (618) 692-2972], or you may contact the Engineer of Physical Research, Illinois Department of Transportation, at (217) 782-6732.

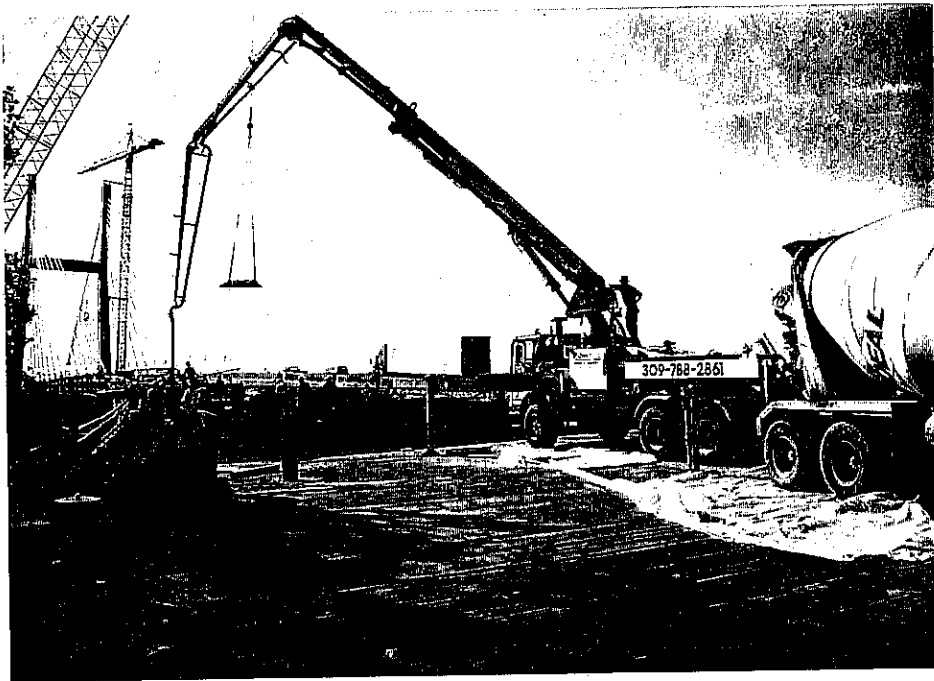
1. Report No. ITRC FR 94-3		2. Government Accession No.		3. Recipient's Catalog No.	
4. Title and Subtitle Construction Loads and Vibrations				5. Report Date March 1998	
				6. Performing Organization Code	
				8. Performing Organization Report No.	
7. Author(s) Mohsen A. Issa				10. Work Unit No. (TRAIS)	
9. Performing Organization Name and Address University of Illinois at Chicago Department of Civil and Materials Engineering 2095 ERF, M/C 246 842 W. Taylor St., Chicago, IL 60607				11. Contract or Grant No. IA-H1, 1994	
				13. Type of Report and Period Covered Final Report June 1995 to March 1997	
12. Sponsoring Agency Name and Address Illinois Transportation Research Center 200 University Park, Room 2210 Edwardsville, IL 62025				14. Sponsoring Agency Code	
15. Supplementary Notes					
16. Abstract <p>The objective and scope of this research was to investigate the effects of construction loads and vibrations on typical newly poured reinforced concrete bridge decks. A compendium was developed that takes into consideration all the factors influencing the effects of construction loads and vibrations on the performance of reinforced concrete bridge decks, in particular, the structural cracking of the concrete. The parameters considered for the evaluation stages were age of concrete, stage and sequence of pours, curing procedures, heat of hydration, strength gain, thermal changes, type of construction, adjacent traffic, adjacent pile driving, and construction equipment. The identification process consisted of a comprehensive literature review and questionnaire survey. Due to the complexity of the subject, limited and often conflicting information were identified. An experimental program was conducted to determine the modulus of elasticity of concrete as well as the maximum curvatures that fresh concrete can withstand. A computer program was developed to identify the best possible pouring sequence for continuous span bridges.</p> <p>Two bridges for which the plans and other relevant information were made available by the Illinois Department of Transportation (IDOT), were modeled for construction loads and vibrations. The time history and dynamic analysis indicated that the sequence of pour has a significant effect on the deformation of the concrete at early ages. The mode shapes obtained by the finite element analysis were used to optimize sensor locations for the dynamic field testing. Locations at the supports and along the two exterior girders of both bridges were selected for instrumentation based on the dynamic analysis results.</p>					
17. Key Words Bridge decks, construction loads, cracking curvature, instrumentation, mode shapes, pour sequence, reinforced concrete, time history, vibration.			18. Distribution Statement No Restrictions. This document is available to the public through the National Technical Information Service (NTIS), Springfield, Virginia 22161		
19. Security Classif. (of this report) Unclassified		20. Security Classif. (of this page) Unclassified		21. No. of Pages 268	22. Price



FINAL REPORT

CONSTRUCTION LOADS AND VIBRATIONS

Project IA-H1, FY 1994



Prepared by

Mohsen A. Issa
Department of Civil and Materials Engineering
University of Illinois at Chicago
Chicago, Illinois

March 1998

Illinois Transportation Research Center
Illinois Department of Transportation

DISCLAIMER

This document is disseminated under the sponsorship of the Department of Transportation and Illinois Department of Transportation in the interest of information exchange. Neither the United States Government nor the State of Illinois assumes liability for its contents or use thereof. The contents of this report reflect the views of the authors who are responsible for the facts and the accuracy of the data presented herein. The contents do not necessarily reflect the policy of the Department of Transportation or the Illinois Department of Transportation. This report does not constitute a standard, specification, or regulation. Neither the United States Government nor the State of Illinois endorses products or manufacturers. Trade or manufacturers' names appear herein only because they are considered essential to the objective of this document.

CONVERSION FACTORS, US CUSTOMARY TO METRIC UNITS

Multiply	by	to obtain
in.	25.4	mm
ft	0.3048	m
in. ²	645	mm ²
yd ³	0.765	m ³
pound (lb)	4.448	newtons (N)
kip (1000 lb)	4.448	kilo newtons (kN)
kip/ft	14.59	kN/m
psi	0.0069	MPa
ksi	6.895	MPa
ft-kip	1.356	kN·m
in.-kip	0.113	kN·m

PREFACE

This study was funded by a contract awarded to the University of Illinois at Chicago (UIC) by the Illinois Transportation Research Center (ITRC) and the Illinois Department of Transportation (IDOT). Their financial support is gratefully acknowledged. Thanks are due to the members of the Technical Review Panel, Rao Ghanta, Iraj I. Kaspar, Christopher Hahin, Salah Y. Khayyat, Jeff South, and William Mann. The author acknowledges the continuous support of Eric Harm and Richard Smith of IDOT, and Dr. Steven Hanna of ITRC.

Thanks are due to the U.S. Departments of Transportation and the nine Illinois Districts of Transportation for responding to the questionnaire and for providing helpful technical information on bridges related to this study.

We are indebted to Dr. Chien H. Wu, Chairman of the Department of Civil and Materials Engineering at UIC for the critical financial support for the students working on the project. Thanks are due to the graduate students Alfred Yousif, Stanislav Dekic, Mahmoud Issa, and Ahmad Hammad for their valuable contributions.

EXECUTIVE SUMMARY

The objective and scope of this research was to investigate the effects of construction loads and vibrations on typical newly poured reinforced concrete bridge decks. A compendium was developed that takes into consideration all the factors influencing the effects of construction loads and vibrations on the performance of reinforced concrete bridge decks, in particular, the structural cracking of the concrete. The parameters considered for the evaluation stages were age of concrete, stage and sequence of pours, curing procedures, heat of hydration, strength gain, thermal changes, type of construction, adjacent traffic, adjacent pile driving, and construction equipment. A methodology was developed for characterizing the types of loads and vibrations having adverse effects on the concrete during construction. The identification process consisted of a comprehensive literature review and questionnaire survey. Due to the complexity of the subject, limited and often conflicting information were identified.

An experimental program was conducted to determine the modulus of elasticity of concrete as well as the maximum curvatures that fresh concrete can withstand. The determination of the modulus of elasticity at early ages was necessary in order to establish a criteria for predicting the modulus of elasticity to be used as the basis for the theoretical part of the study, i.e., for the sequence of pour program. As a result, a computer program was developed to identify the best possible pouring sequence for continuous span bridges. It was experimentally determined that curvature does not contribute towards the cracking of fresh concrete for certain sequences of pour.

Two bridges for which the plans and other relevant information were made available by the Illinois Department of Transportation (IDOT), were modeled for construction loads and vibrations

by effectively simulating the loads encountered during construction in addition to the moving loads in adjacent lanes. The time history and dynamic analysis indicated that the sequence of pour has a significant effect on the deformation of the concrete at early ages. The deflections in the case when negative moment regions (not normal practice), i.e., over the interior supports, were poured first were twice as great as those obtained if the positive moment regions were poured prior to the negative moment regions. The deflections and stresses observed in the fresh concrete due to the construction loads and equipment were also significant. However, the largest contribution was due to the dead weight of the superstructure. This was prominent due to the fact that the span lengths were significantly long, especially in the case of the steel girder bridge.

The mode shapes obtained by the finite element analysis were used to optimize sensor locations for the dynamic field testing. Locations at the supports and along the two exterior girders of both bridges were selected for instrumentation based on the dynamic analysis results. This instrumentation was necessary in order to measure the vertical and longitudinal movement of the bridge deck. Detailed description of instrumentation, data collection, and construction monitoring procedures were proposed for Phase II of the research incorporating field investigations on the two selected bridges. The collected data from the field investigation will mainly be used to verify the finite element models and allow refinement of the models as well as determine the dynamic effects experienced by the bridges during construction.

TABLE OF CONTENTS

PREFACE	3
EXECUTIVE SUMMARY	4
LIST OF FIGURES	8
LIST OF TABLES	13
1. INTRODUCTION	14
1.1 General	14
1.2 Objectives of Study	15
2. LITERATURE REVIEW	16
2.1 General	16
2.2 Background	16
3. SURVEY	46
3.1 Introduction	46
3.2 Survey Results	46
4. EXPERIMENTAL PROGRAM	54
4.1 Introduction	54
4.2 Specimen Geometry	54
4.3 Materials	55
4.4 Specimen Preparation	56
4.5 Experimental Test Setup	57
4.6 Testing Procedure	59
4.7 Results and Discussion	59
5. SEQUENCE OF POUR	64
5.1 Introduction	64
5.2 Program Overview	64
5.3 Results of Program Executions	70
5.4 Description of Two Selected Bridges	76
5.5 Description of Sequences of Pour	76
5.6 Results of Program Execution	80
6. CATEGORIZATION OF VARIOUS TYPES OF LOADS AND VIBRATIONS	82
6.1 Introduction	82
6.2 Categorization	90
6.2.1 Heat of Hydration	93
6.2.2 Shrinkage	93
6.2.3 Temperature Effect	94
6.2.4 Wind	94

TABLE OF CONTENTS - Continued

6.2.5	Concrete Protection	95
6.2.6	Concrete Cover over Reinforcing Bar and Bar Size	95
6.2.7	Compaction of Concrete	95
6.2.8	Reinforcing Details	96
6.2.9	Self-Weight of the Slab	96
6.2.10	Joint Between Newly Poured and Old Concrete	97
6.2.11	Construction Procedures	97
6.2.12	Weight of Construction Machinery	97
6.2.13	Weight of Adjacent Traffic	98
6.2.14	Vibrations Due to Construction Machinery	98
6.2.15	Weight of Forms and Other External Dead Loads	99
6.2.16	Deflection of Formwork	99
6.2.17	Adjacent Traffic Vibrations	100
6.2.18	Other Factors	100
7.	BRIDGE VIBRATION ANALYSIS	103
7.1	Introduction	103
7.2	Finite Element Analysis	108
7.2.1	Illinois River Bridge Number 050-0219	108
7.2.2	Sangamon River Bridge Number 084-0206	109
7.2.3	Modeling of Illinois River Bridge	109
7.2.4	Modeling of Sangamon River Bridge	110
7.2.5	Loading	110
7.2.6	Results and Discussion	113
7.3	Effect of Damping	120
8.	DETAILED INSTRUMENTATION OF BRIDGES	175
9.	CONCLUSIONS	186
9.1	Literature Review and Survey	186
9.2	Dynamic and Vibration Analysis	189
9.3	Phase II of Study	189
10.	REFERENCES	192
	APPENDIX A	200
	APPENDIX B	209
	APPENDIX C	213
	APPENDIX D	261

LIST OF FIGURES

Figure:

4.1	Test setup scheme	57
4.2	Experimental test setup	58
4.3	Determination of curvature	60
5.1	Example of node numbering	65
5.2	Example of load position coordinates	66
5.3	System solving subroutine flowchart	68
7.1	Steel girder bridge	119
7.2	Prestressed concrete girder bridge	119
7.3	Detailed plan of steel bridge model	123
7.4	Detailed cross section of steel bridge model	124
7.5	Detailed framing plan of concrete bridge model	125
7.6	Detailed cross section of concrete bridge model	126
7.7	Prestressing details of concrete bridge girders	127
7.8	Close-up view of steel bridge model	128
7.9	Steel bridge model	128
7.10	Close-up view of concrete bridge model	129
7.11	Loading condition No. 1	130
7.12	Loading condition No. 6	130
7.13	Loading condition No. 10	131
7.14	Loading condition No. 19	131
7.15	Close-up view of HS-20 truck	132
7.16	Close-up view of construction loads	132
7.17	Loading patterns for HS20 truck loading and construction loads	133
7.18	Mode shape 1 for steel bridge	134
7.19	Mode shape 2 for steel bridge	134
7.20	Mode shape 3 for steel bridge	135
7.21	Mode shape 4 for steel bridge	135
7.22	Mode shape 5 for steel bridge	136
7.23	Mode shape 6 for steel bridge	136
7.24	Mode shape 7 for steel bridge	137
7.25	Mode shape 8 for steel bridge	137
7.26	Mode shape 9 for steel bridge	138
7.27	Mode shape 10 for steel bridge	138
7.28	Mode shape 1 for concrete bridge	139
7.29	Mode shape 2 for concrete bridge	139
7.30	Mode shape 3 for concrete bridge	140
7.31	Mode shape 4 for concrete bridge	140
7.32	Mode shape 5 for concrete bridge	141
7.33	Mode shape 6 for concrete bridge	141
7.34	Mode shape 7 for concrete bridge	142

LIST OF FIGURES - Continued

Figure:

7.35	Mode shape 8 for concrete bridge	142
7.36	Mode shape 9 for concrete bridge	143
7.37	Mode shape 10 for concrete bridge	143
7.38	Frequencies vs mode shape numbers for various bridges	144
7.39	Low frequency bridges for various mode shapes	145
7.40	Frequencies vs span length for simply supported bridges	146
7.41	Frequencies vs span length for continuous bridges	147
7.42	Maximum displacement in steel bridge due to moving vehicle	148
7.43	Maximum displacement in concrete bridge due to moving vehicle	148
7.44	Typical deflection mode in steel bridge	149
7.45	Displacement in steel bridge due to dead load	150
7.46	Displacement in concrete bridge due to dead load	150
7.47	Maximum top & bottom stresses in slab	151
7.48	Normal stresses in longitudinal direction at top surface of slab (load case 1)	152
7.49	Normal stresses in longitudinal direction at top surface of slab (load case 2)	152
7.50	Normal stresses in longitudinal direction at top surface of slab (load case 3)	153
7.51	Normal stresses in transverse direction at top surface of slab (load case 1)	153
7.52	Maximum stresses at top surface of slab (load case 1)	154
7.53	Minimum stresses at top surface of slab (load case 1)	154
7.54	Normal stresses in longitudinal direction at bottom surface of slab (load case 1) ..	155
7.55	Normal stresses in transverse direction at bottom surface of slab (load case 1) ..	155
7.56	Maximum stresses at bottom surface of slab (load case 1)	156
7.57	Von Mises stresses (load case 1)	156
7.58	Normal stresses in longitudinal direction at bottom surface of slab (load case 2) ..	157
7.59	Normal stresses in longitudinal direction at top surface of slab (load case 3)	157
7.60	Normal stresses in longitudinal direction at bottom surface of slab (load case 3) ..	158
7.61	Maximum stresses at top surface of slab (load case 2)	158
7.62	Mode shape 1 for steel bridge - stage construction	159
7.63	Mode shape 2 for steel bridge - stage construction	159
7.64	Mode shape 3 for steel bridge - stage construction	160
7.65	Mode shape 4 for steel bridge - stage construction	160
7.66	Mode shape 5 for steel bridge - stage construction	161
7.67	Mode shape 6 for steel bridge - stage construction	161
7.68	Mode shape 7 for steel bridge - stage construction	162
7.69	Mode shape 8 for steel bridge - stage construction	162
7.70	Mode shape 9 for steel bridge - stage construction	163
7.71	Mode shape 10 for steel bridge - stage construction	163
7.72	Maximum displacement in steel bridge due to moving vehicle - stage construction .	164
7.73	Displacement in steel bridge due to dead load - stage construction	164
7.74	Displacement in wet concrete region due to dead load - stage construction	165

LIST OF FIGURES - Continued

Figure:		
7.75	Displacement in wet concrete region due to live load - stage construction	165
7.76	Normal stresses in longitudinal direction in wet concrete due to dead load	166
7.77	Normal stresses in transverse direction in wet concrete due to dead load	166
7.78	Shearing stresses in wet concrete due to dead load	167
7.79	Maximum displacement in steel bridge due to two trucks	167
7.80	Normal stresses in longitudinal direction at top surface of slab (two trucks)	168
7.81	Normal stresses in longitudinal direction at top surface of slab (two trucks)	168
7.82	Normal stresses in longitudinal direction at bottom surface of slab (two trucks)	169
7.83	Normal stresses in longitudinal direction at bottom surface of slab (two trucks)	169
7.84	Normal stresses in longitudinal direction at top surface of slab (two trucks)	170
7.85	Time history function corresponding to vehicle location	171
7.86	Sinusoidal time history function corresponding to vehicle location	171
7.87	Time history, maximum displacement in z-direction as a function of time	172
7.88	Time history plot for typical shell element in respect to σ_{11}	172
7.89	Time history plot for typical shell element in respect to σ_{11} (Mode 1)	173
7.90	Time history plot for typical shell element in respect to σ_{11} (Mode 2)	173
7.91	Time history plot for typical shell element in respect to σ_{11} (Mode 3)	174
8.1	Instrumentation layout for dynamic test	180
8.2	Measurement locations	181
8.3	Plan view & instrumentation of steel girder bridge	182
8.4	Instrumentation for typical transverse section	183
8.5	Plan view & instrumentation of concrete girder bridge	184
8.6	Instrumentation for transverse section	185
B.1	Flexible mold	210
B.2	Load-displacement-curvature diagrams for specimens set 1, concrete without additives	211
B.3	Load-displacement-curvature diagrams for specimens set 1, concrete with plasticizer	212
C.1	Main menu screen	216
C.2	New input filename screen	216
C.3	File overwrite warning screen	217
C.4	Span data screen	217
C.5	Vertical supports screen	218
C.6	Rotational supports screen	218
C.7	Beam properties screen	219
C.8	Element properties data screen	219
C.9	Program trace screen	220
C.10	Choosing output file name for changed data	220
C.11	Change input data submenu	221
C.12	Change system of units screen	221

LIST OF FIGURES - Continued

Figure:

C.13	Sequence of pour for bridge AL-2 Case "a"	222
C.14	Sequence of pour for bridge OT-3 Case "c"	223
C.15	Bridge AL-2 deflections for sequence of pour Case "a"	224
C.16	Bridge AL-2 curvatures for sequence of pour Case "a"	225
C.17	Bridge AL-2 deflections for sequence of pour Case "aa"	226
C.18	Bridge AL-2 curvatures for sequence of pour Case "aa", first four sequences	227
C.19	Bridge AL-2 deflections for sequence of pour Case "aa", last two sequences	228
C.20	Bridge AL-2 curvatures for sequence of pour Case "b"	229
C.21	Bridge AL-2 curvatures for sequence of pour Case "c"	230
C.22	Bridge AL-2 curvatures for sequence of pour Case "cc"	231
C.23	Bridge AL-2 curvatures for sequence of pour Case "d"	232
C.24	Typical cross section	234
C.25	Cross section for bridge Al-2	235
C.26	Three span steel bridge - span sections cast prior to support sections	236
C.27	Three span steel bridge - span sections cast prior to support sections (continued) ..	237
C.28	Three span steel bridge - slab cast from the left end sections	238
C.29	Three span steel bridge - slab cast from the left end sections (continued)	239
C.30	Three span prestressed concrete bridge - span sections cast prior to support sections	240
C.31	Three span prestressed concrete bridge - span sections cast prior to supports (continued)	241
C.32	Three span prestressed concrete bridge - slab cast from the left end sections	242
C.33	Three span prestressed concrete bridge - slab cast from the left end sections (continued)	243
C.34	Curvatures for three span steel bridge - spans cast prior to supports	244
C.35	Curvatures for three span steel bridge - spans cast prior to supports (continued) ..	245
C.36	Curvatures for three span steel bridge - slab cast from the left end	246
C.37	Curvatures for three span steel bridge - slab cast from the left end (continued)	247
C.38	Curvatures for three span prestressed concrete bridge - spans cast prior to supports	248
C.39	Curvatures for 3-span prestressed concrete bridge - spans cast prior to supports (continued)	249
C.40	Curvatures for three span prestressed concrete bridge - slab cast from the left end ..	250
C.41	Curvatures for 3-span prestressed concrete bridge - slab cast from the left end (continued)	251
D.1	Time history plot for typical shell element in respect to σ_{11} (Mode 4)	262
D.2	Time history plot for typical shell element in respect to σ_{11} (Mode 5)	262
D.3	Time history plot for typical shell element in respect to σ_{11} (Mode 6)	263
D.4	Time history plot for typical shell element in respect to σ_{11} (Mode 7)	263
D.5	Time history plot for typical shell element in respect to σ_{11} (Mode 8)	264

LIST OF FIGURES - Continued

Figure:

D.6	Time history plot for typical shell element in respect to σ_{11} (Mode 9)	264
D.7	Time history plot for typical shell element in respect to σ_{11} (Mode 10)	265
D.8	Time history plot for typical joint in respect to displacement in z-axis (Mode 1) . . .	265
D.9	Time history plot for typical joint in respect to displacement in z-axis (Mode 2) . . .	266
D.10	Time history plot for typical joint in respect to displacement in z-axis (Mode 3) . . .	266
D.11	Time history plot for typical joint in respect to displacement in z-axis (Mode 4) . . .	267
D.12	Time history plot for typical joint in respect to displacement in z-axis (Mode 5) . . .	267
D.13	Time history plot for typical joint in respect to displacement in z-axis (Mode 6) . . .	268
D.14	Time history plot for typical joint in respect to displacement in z-axis (Mode 7) . . .	268

LIST OF TABLES

Table:

2.1	Development of Concrete Strength [10]	22
2.2	Coefficients for Finding Natural Bridge Frequency [19]	31
3.1	Departments of Transportation Response Summary	47
3.2	Departments of Transportation Question Response Summary	47
3.3	DOT Response Summary to Question 1	49
3.4	DOT Response Summary to Question 2	49
3.5	DOT Response Summary to Question 3	49
3.6	DOT Response Summary to Question 4	50
3.7	DOT Response Summary to Question 5 (Full Depth)	52
3.8	DOT Response Summary on Question 6	53
4.1	Concrete Mix Proportions Used to Make Specimens	56
4.2	Maximum Stresses at Cracking and Corresponding Curvatures	61
4.3	Concrete Compressive Strengths Modulus of Elasticity	63
5.1	Basic Properties of Examined Bridges	71
5.2	Sequences of Concrete Pour, SI Units	73
5.3	Sequences of Concrete Pour, in-lb Units	74
5.4	Maximum Curvature in Previously Poured Concrete	75
5.5	Steel Plate Girder Bridge Section Properties	78
5.6	Prestressed Concrete Girder Bridge Section Properties	79
5.7	Span Lengths	79
5.8	Sequence Positions and Time	79
5.9	Maximum Curvature in Previously Poured Concrete	80
7.1	Front Axle Truck Locations for Various Load Cases	112
7.2	First Ten Natural Frequencies and Mode Types	114
7.3	Mode Shape Frequencies	115
A.1	Summary of Answers by State	204
A.2	Summary of Answers by Illinois Districts	208

1. INTRODUCTION

1.1 General

Modern construction techniques enable reinforced concrete bridge decks to be constructed rapidly. However, it is vital to understand the type and magnitude of loads that are imposed on the structure during construction. The loads influence the performance of the bridge deck as well as its structural integrity. In addition, the construction procedures carried out at the specific job site are of critical importance since mistakes can cause detrimental effects on the concrete deck. Construction loads can be very large, especially considering the low early-age strength of concrete. Vibrations due to machinery and adjacent traffic during construction may adversely influence the concrete properties, and in turn cause cracking in the concrete deck. Inadequate concreting and concrete protection at early ages may also contribute to concrete cracking.

This research was conducted in order to identify the probable causes of cracking in reinforced concrete bridge decks, particularly at early ages. This task was accomplished through a literature review, and a comprehensive survey distributed to various departments of transportation as well as other federal and state agencies. This task has further revealed the current opinions and state of knowledge with respect to the effects of construction loads and vibrations on newly constructed concrete bridge decks. Efforts were made to categorize the causes of cracking in order of importance and to identify appropriate procedures that may control cracking.

1.2 Objectives of Study

The objectives of the study are to:

- Identify and evaluate current knowledge on the effect of construction loads and vibrations on cracking of reinforced concrete bridge decks.
- Determine the effects of the various loads and vibrations on cracking of reinforced concrete bridge decks.
- Arrange the types of loads and vibrations in their order of importance, influence, and magnitude, in order to determine their effects.
- Perform analyses with respect to construction loads and vibrations.
- Develop a detailed scheme for instrumentation, data collection and analysis, and construction monitoring procedures.
- Provide a recommendation plan for the reduction and control of cracks caused by loads and vibrations encountered during construction.

2. LITERATURE REVIEW

2.1 General

The literature review presented in this report was accomplished with respect to the current views and opinions concerning the effects of construction loads and vibrations, traffic induced vibrations, construction procedures, and environmental elements on the cracking of reinforced concrete decks at early ages, as well as on the bond to reinforcement and previously placed concrete. Efforts were made to include all aspects necessary to understand the above-mentioned phenomena. Limited and often conflicting information was identified with respect to the effect of construction loads and vibrations. This was determined to be the case due to the complexity of the subject.

2.2 Background

A statistical evaluation of different aspects that may influence deck cracking was conducted by Prenger for the Maryland DOT [1]. Thirty bridges, built between 1985 and 1989, which exhibited excessive cracking, were included in the study. The parameters considered were: type of bridge, location of cracks, span length, concrete compressive strength, rebar coating, type of cement, type and brand of admixtures, source of aggregates, water cement ratio, type of curing, location of reinforcing steel, presence of adjacent traffic, time of year and day, and air temperature. Unfortunately, no relationships were found between deck cracking and the addressed bridge parameters. Bridges with cracked and uncracked decks were identified in approximately the same amount in all bridge groups. The only relationship that seemed to exist was between the longitudinal and transverse cracks and the area of negative moment in continuous bridge decks. However, the study did not explain cracking that occurred in all other decks. It should be noted that due to the lack

of records, many areas that were suspected of contributing to bridge deck cracking could not be examined. Construction records on concrete placement sequences, time in which traffic was allowed on the bridge, staged construction, and air and concrete temperature differentials were not available.

Some researchers conducted studies on the materials aspect of the concrete. Fouad and Furr [2] studied the behavior of cement mortar under flexure. They tested a total of 32 specimens at ages between 3 and 11 hours. Since mortar was very fragile at the time of testing, the specimens were tested while inside the mold. Load was applied by moving the machine cross head at a rate of 1.25 mm/min (0.05 in./min). The primary concern of the study was the curvature that mortar could tolerate before cracking. The modulus of elasticity was computed as:

$$E = s \times \frac{L^3}{48I}$$

where:

L = span length of the tested beam

I = moment of inertia of the beam cross section

s = slope taken from load-deflection diagram as the secant between the maximum load and one-half of its value

Results showed that the curvature at first cracking decreased as time increased from 3 to 5 hours. For the same period of time, the modulus of elasticity increased more rapidly than the flexural strength. The average curvature at first cracking was found to be $596 \times 10^{-7} \text{ mm}^{-1}$ ($149 \times 10^{-5} \text{ in.}^{-1}$) at 3 hours. At 5 hours, which was approximately the time of setting, this value decreased to a minimum of $108 \times 10^{-7} \text{ mm}^{-1}$ ($27 \times 10^{-5} \text{ in.}^{-1}$). However, they noted that the age at which the deformation capacity reaches a minimum is dependent on the mix proportions and type of cement.

Dakhil et al. [3] studied the influence of cover, diameter of reinforcing bars, total slab depth, and slump on crack formation in plastic concrete. They reported that the tendency for crack occurrence seems to decrease with increasing cover, smaller bar sizes, and lower slumps. Experiments were performed on specimens with a single reinforcing bar with a cover of 19, 25, 38, and 50 mm ($\frac{3}{4}$, 1, $1\frac{1}{2}$, and 2 in.). The concrete slumps used were 50, 75, and 100 mm (2, 3, and 4 in.). Although the tendency toward cracking increased with decreasing cover, greater bar size, and higher slumps, it was concluded that the most critical variable affecting the cracking over the reinforcement was the depth of the cover. A 50 mm (2 in.) cover appeared to resist cracking due to subsidence, except in cases of larger bar sizes. Multiple regression analysis was used to determine a possible correlation between the probability of crack occurring and the concrete cover, size of the bar, and the concrete slump. An equation denoting the probability of crack occurrence was given as:

$$p = \frac{1.5 e^y - 0.5}{1 + e^y}$$

where

$$y = 1.37 - 0.58x_1 - 0.56x_2 + 0.27x_3$$

and

- p = probability of crack occurrence
- x_1 = concrete cover, in.
- x_2 = ratio of concrete cover and bar size
- x_3 = concrete slump, in.

They observed that the tensile stresses over the reinforcing bar increased from 2.1 to 8.3 kPa (0.3 to 1.2 psi) as the cover decreased from 50 to 19 mm (2 to $\frac{3}{4}$ in.).

Halvorsen [4] noted some of the common reasons for cracking and how to avoid cracks in concrete. The lowest possible concrete slump and a larger steel cover were recommended. Flexible forms, insufficient vibration, and premature removal of formwork were noted as possible causes of early age concrete cracking. Misplaced or poorly detailed reinforcement, especially at the corners, around openings, or at splice locations were also indicated as possible causes of cracking.

Hadje-Ghaffari et al. [5] studied the bond of epoxy coated reinforcement. Effects of cover, casting position, slump, and consolidation were considered. Specimens were made with bar sizes 16 mm (#5), 19 mm (#6), 25 mm (#8), and 35 mm (#11) and bond lengths of 89, 114, 203, and 229 mm (3.5, 4.5, 8, and 9 in.), respectively. The reinforcing steel was made of epoxy coated Grade 60 bars with different deformation patterns. Non-air entrained concrete had a compressive strength ranging between 34.5 and 41.4 MPa (5000 to 6000 psi). The researchers concluded that the casting position affects bond strength between reinforcement and concrete. A decrease in bond strength was observed with an increase in the amount of concrete settlement. This effect increased with the slump and the amount of concrete below the bar. Bars cast in high slump concrete exhibited reduced bond strength in the case of non-vibrated concrete. The epoxy coating also reduced the bond strength of the bars.

Hughes and Videla [6] studied early age bond strength in reinforced concrete. Their main objective was to provide a bond strength criteria between deformed bars and concrete in models to predict early age cracking. The major variables taken into account were bar diameter, concrete cover, age of concrete, transverse reinforcement, and anchorage length. Results showed that concrete age significantly influenced bond strength. The effect was more pronounced for the first three days and in specimens with smaller bar sizes. Compressive and splitting strengths increased less rapidly than

the bond strength at early ages. Comparison of data with the American Concrete Institute Building Code (ACI 318-83 Code) showed that it overestimates bond strength for early age concrete (1 to 7 days) and underestimates bond strength thereafter. However, the placement of deck reinforcement often varies widely, as an average deviation of ± 9.5 mm ($\frac{3}{8}$ in.) was reported. To maintain a projected minimum cover over the reinforcement, the study recommended that these tolerances be added to the thickness of the deck, resulting in a minimum slab thickness of about 200 mm (8 in.) [7]. There is no evidence that deterioration is more likely to occur in thinner decks. However, it was observed that once deterioration started, it was likely to progress more rapidly in thinner decks. A deviation of ± 12 mm ($\frac{1}{2}$ in.) should be expected during construction and might be considered normal, but engineers should anticipate and allow for conditions that may make accurate steel placement more difficult.

The primary goal of a survey that was accomplished by Ayoub et al. [8] was to collect data for live loads on new concrete slabs as well as to develop a probability live load model. They discussed loads on slabs that were supported by formwork and were one to several days old. Each surveyed slab was divided into six different grid sizes, from 0.093 m² (1 ft²) to 58 m² (625 ft²), and the load in each square was observed. They found high localized surface loads that may present problems. Given examples include: air compressors that can weigh up to about 13.34 kN (3000 lb) and be supported on just a few small wheels; bundles of reinforcement; and large storage boxes, sometimes supported on short pieces of lumber or legs.

Observations showed that one of the most important factors is the contractor's field personnel who control the lifting and placing of materials and equipment. The maximum observed load was

48.5 kN/m² (1012 psf) which is about 160 times higher than the average (mean) load found during the survey and calculated to be 304 N/m² (6.35 psf).

Gardner [9] investigated the effect of temperature in the early age properties of concrete. Six different concrete mixes were used: Type I, Type III, and Type I with fly ash, each at water/cement ratios of 0.55 and 0.35. Specimens were cured at temperatures between 0 and 30°C. The measured properties included compression and tensile strength. Results showed that the strength of Type III cement concretes was not influenced by the curing temperature after three days. Strength of Type I cement with a w/c of 0.35 was not affected by the curing temperature either. For concretes with fly ash, temperature proved to be critical. All specimens cured at temperatures of 0 or 10°C showed a decrease in compressive strength. New relationships for modulus of elasticity and tensile strength as functions of concrete compressive strength were given and compared with ACI-CSA, CEB-FIP and British Standards. The conclusion was that ACI formulas overestimate the early age modulus of elasticity and tensile strength. Gardner reported the modification factors for the development of concrete strength at various temperatures as shown in Table 2.1.

Pull-out tests were performed by Harsh and Darwin [10] on specimens that were vibrated by simulated traffic vibrations. Vibrations were selected to match those measured in the field and included simulated intermittent truck traffic. Test results were compared with the predicted values of bond strength obtained from the expression for development length, for bars 35 mm in diameter (#11) and smaller, according to American Association of State Highway Transportation Officials (AASHTO):

$$T = 1.25 \times 25 L \sqrt{f'_c}$$

and ACI specifications:

$$T = 1.25 \times 625 \pi L d_b$$

TABLE 2.1

DEVELOPMENT OF CONCRETE STRENGTH [9]

Age, Days	Type I cement			Type II cement		
	22.8°C 73°F	12.8°C 55°F	4.4°C 40°F	22.8°C 73°F	12.8°C 55°F	4.4°C 40°F
1	0.31	0.15	0.03	0.54	0.33	0.11
2	0.47	0.28	0.11	0.65	0.50	0.30
3	0.59	0.40	0.18	0.74	0.62	0.43
4	0.66	0.49	0.24	0.78	0.66	0.54
5	0.72	0.57	0.32	0.81	0.70	0.63
6	0.76	0.63	0.39	0.83	0.73	0.70
7	0.79	0.68	0.44	0.85	0.75	0.77
8	0.81	0.72	0.48	0.86	0.77	0.80
9	0.83	0.75	0.52	0.88	0.79	0.82
10	0.85	0.77	0.56	0.89	0.81	0.84
11	0.86	0.80	0.59	0.90	0.82	0.86
12	0.88	0.82	0.62	0.91	0.84	0.88
13	0.89	0.84	0.64	0.92	0.86	0.89
14	0.90	0.86	0.67	0.92	0.86	0.90
21	0.96	0.94	0.80	0.97	0.93	0.99
28	1.00	1.02	0.88	1.00	0.96	1.07

where:

f'_c = concrete compressive strength, psi

L = embedment length, in.

d_b = nominal bar diameter, in.

T = bond strength, lb

Results showed that the failure mode depended on cover thickness and bar size for the same concrete type. For the 16 mm (#5) bar with 38 mm (1.5 in.) cover and the 25 mm (#8) bar with

38 mm and 75 mm (1.5 and 3 in.) cover, failure was by longitudinal splitting. The 16 mm (#5) bar under 75 mm (3 in.) cover failed without surface cracking. For low slump concrete and cover thicknesses of 75 mm (3 in.), traffic induced vibrations increased the average bond strength up to 14.1 percent, with large scatter. Using a 75 mm (3 in.) cover for the 25 mm (#8) bars, the average bond strength increased for high slump concrete with 100 mm (4 in.) slump and decreased for 187 mm (7.5 in.) slump, but not significantly. However, for the 16 mm (#5) bars, some of the specimens had a very low bond strength of only 88 percent of the control group. In the case of the 38 mm (1.5 in.) cover, the average bond strength was as low as 63 percent for the 25 mm (#8) bars compared to the bars with 75 mm (3 in.) cover [10]. Usage of concrete with a slump of less than 100 mm (4 in.) did not have an adverse effect on the strength of concrete and bond strength. A concrete slump in the 100 to 125 mm (4 to 5 in.) range can be detrimental to the reinforcing steel bond to concrete, while slumps in the range of 175 to 200 mm (7 to 8 in.) have a measurable adverse effect when combined with traffic induced vibrations.

The influence of adjacent traffic on bridge deck repairs was considered by Manning [11, 12]. Research looked at influences on partial-depth repairs, bridge-deck overlays, as well as barrier walls, full-depth repairs, widenings, and deck replacement. Manning noted that closing traffic may be safe for the structure but it may also be expensive due to the need for temporary widening or detours. Most agencies prefer to maintain traffic on part of the bridge while the other part is under construction, however, the possibility of damage to fresh concrete is what makes the decision difficult. It is considered that concrete in widenings is vulnerable to longitudinal cracking across the joint between the old and new deck and loss of bond between the reinforcing steel and concrete. Differential consolidation of the concrete, lack of bond between the reinforcing steel and the concrete,

and bond failure between the new and old concrete have been considered results of vibration of the concrete, which is induced by the adjacent traffic [11].

Manning theorized that as a vehicle crosses, the existing bridge structure deflects but the widened portion, which is under construction, does not deflect as much as the existing structure. Reinforcing bars protruding from the existing deck into the newly poured concrete move according to the displacement and vibration of the existing structure, displacing the plastic concrete. While concrete is still in a plastic state it flows back, but as it stiffens it loses this ability. Segregation due to repeated displacement may occur which may lead to the formation of voids. In addition, as formwork deflects, concrete particles slide with respect to each other. When concrete stiffens, it is subjected to tensile stresses, which may cause early cracking. Furthermore, reinforcement of the new deck is welded or tied to dowels or reinforcement of the existing structure. It may induce reinforcement vibrations and displacements which, if different to that of concrete, may lead to the creation of voids and incipient fracture planes at the level of the steel. However, in the case of well proportioned and compacted fresh concrete, it was reported that traffic vibration does not cause segregation, slow setting of concrete, poor bond to existing structure, poor strength development of concrete, differential consolidation, or cracking.

In considering the behavior of bridge structures, researchers often perform impact studies to determine the distribution effects of the loads in terms of the supporting system. In related impact studies performed by Huang et al. [13], seven multi-girder bridges were tested. The bridges were modeled as grillage beam systems and loaded by a simulated MS18 (HS20-44) vehicle. Parameters taken into account were vehicle weight, number of loading lanes, transverse rigidities, effect of spacing, and bridge length. The researchers concluded that the number of lanes has little effect in

case of long span bridges compared to short span bridges where the impact factor increased with an increase in the number of loaded lanes. For short span bridges, an increase in transverse stiffness increased the impact factor in the interior beams and decreased it in the exterior beams. This had no influence on long span bridges. In the case of girder spacing, it drastically increased the impact factor of the center girders while the impact factor of the exterior girders changed only slightly. One of the conclusions was that the AASHTO impact formula underestimates the impact value for short span bridges and overestimates it in the case of bridges longer than 24.4 m (80 ft), assuming good road surface.

The factors influencing bridge deck slabs placed adjacent to moving loads were studied by Furr [14]. The study's topics included visual inspection of bridges, analysis of cores taken from bridge decks, laboratory beam tests, and a laboratory beam core study. All of the inspected bridges were widened after carrying normal traffic over a period of time. Inspection showed some bond problems between the steel and concrete, and that concrete from different bridges varied in color and density. Voids of air bubble size or larger pointed to the level of aggregate compaction, or lack thereof. As reported, visual inspection revealed few occasions of distress, and none that could definitely be attributed to the influence of traffic during construction. Except for a thin longitudinal crack along the construction joint, the crack patterns in the newer material were approximately the same as those in the older parts. During the study, ends of 109 cores from 9 bridges were sawed, polished, and examined under a magnifying glass and microscope. Some of the cores that were taken from the joint between the old and new concrete deck provided clear evidence of disturbance. The top surface cracked in the general direction of traffic and the concrete above the top layer of steel was badly damaged. The appearance of puddled plastic concrete was reported at the interface of steel and

concrete. It was believed that the intermittent deflections caused by traffic on the old deck caused the fresh concrete to puddle at the level of top steel. In some specimens, the relative movement of the dowel, which extended from the old slab to the fresh concrete, was evident. Dye tests showed that only a few feet from the joint between the old and new deck specimens, debonding problems were not apparent due to the vibration of steel. Measurements of transverse curvatures showed that a maximum curvature of $4.6 \times 10^{-7} \text{ mm}^{-1}$ ($1.17 \times 10^{-5} \text{ in.}^{-1}$) was about three times less than the experimentally established value of $14.4 \times 10^{-7} \text{ mm}^{-1}$ ($3.7 \times 10^{-5} \text{ in.}^{-1}$) needed to crack fresh concrete. Laboratory tests were performed on reinforced beams in order to establish the previously mentioned values of curvature at which fresh concrete cracks. All specimens were subjected to cyclic deflections and one of the beams had a superimposed vibration of 6 Hz and 0.5 mm (0.020 in.) amplitude.

A closure pour was used for some bridges to reduce the effect of deformation and shrinkage. The pours varied in width, but were usually in the neighborhood of 0.6 m (2 ft). Some of the specimens were reported to lack bond between the concrete and the reinforcing bars crossing from the old concrete into the new. It seemed that dowels bent 90° in the plane parallel to the surface of the deck were more vulnerable to debonding. Laboratory experiments showed that concrete under controlled conditions can be flexed from the time of casting until about the time of setting without flexural cracking.

Conclusions included the following: most of the wider cracks found in the cores taken from the bridge decks were perpendicular to the direction of traffic, as would be expected of shrinkage cracks; traffic caused no strength reduction because the measured strengths ranged from 19.3 to 48.3 MPa (2800 to 7000 psi); evidence of relative movement between the reinforcing steel and concrete was found in specimens from disturbed areas near the joint between the new and old

concrete; bent dowels should not be used instead of straight dowels; and the bridge carrying normal traffic load can be opened to traffic during placement and curing of concrete.

A study by Hearn and Ghia [15] examined the vibration response of highway bridges under normal traffic, particularly dynamic strains of the bridge member. Dynamic strains were measured for a group of twenty-nine highway bridges, including steel beam bridges, concrete I-beam bridges, multicell concrete bridges, and concrete spread box girders. The study included bridges with span lengths varying from 12 m to 45 m (39.4 to 148 ft). To estimate the modal parameters, a circle-fit technique was used.

Results showed as many as five peaks, while more peaks were observed for the steel than for the concrete bridges. For steel bridges, the minimum observed frequency for the first mode was 1.4 Hz and the maximum was 7.0 Hz. These values were 1.9 and 4.32 Hz, respectively, for concrete I-beam bridges.

The frequency and amplitude of the vibration are the result of the interaction between the vehicle suspension system and the surface roughness of the bridge deck, and it depends on the dynamic response of the bridge. When the natural frequencies of the vehicle and the bridge are the same, usually within the range of 2 to 5 Hz, the largest amplitudes of vibration may be expected. However, the peak particle velocity was found to be a more appropriate indicator of the risk of vibration damage than the amplitude or acceleration [12]. Various effects and aspects of the influence of vibration were established.

The dynamic response of a simply supported box girder bridge and stresses that are introduced to a bridge by the dead load of the vehicle and the vehicle pavement interactive force were studied by Inbanathan and Wieland [16]. They listed the following factors as the most probable

parameters influencing these forces: type of bridge; vehicle characteristics such as mass distribution, vehicle natural frequencies, and vehicle suspension; speed of vehicle; profile of approach roadway and bridge deck; traffic intensity; damping characteristics of bridge and vehicle; and driver behavior.

The force due to the pavement roughness was given as a function of the predominant excitation frequency f :

$$f = \frac{\bar{c}}{\lambda}$$

where:

\bar{c} = speed of the vehicle, km/hr

λ = predominant wave length of surface roughness

The bridge was modeled as a one-dimensional beam and the structure was assumed to behave as a linear-elastic body. The vehicle was modeled as a single point mass moving at a constant speed over the bridge. Results showed that the average impact factors for the absolute maximum peaks were considerably higher than the values prescribed by the AASHTO Code. The study confirmed that the effect of the vehicle mass on the bridge response is significant at high speeds and high ratios of vehicle mass to total bridge mass. They also concluded that the maximum response for the moment and deflection does not occur simultaneously, and that the influence of passenger cars may be neglected.

A similar study by Chang and Lee [17] confirmed these results. They suggested that an impact factor due to a running heavy vehicle should be represented in terms of surface roughness, and bridge and vehicle characteristics. In their study, the impact factor was almost constant with respect to span length, and it was higher for the moment than for deflection.

Some factors are associated with the road characteristics of the traffic adjacent to the freshly poured concrete sections on a bridge. One of the aspects studied by Gaunt et al. [18] was the influence of surface roughness on the roadway vertical acceleration. Simply supported, as well as two and three-span bridges were analyzed. The parameters that affected bridge accelerations were classified as bridge parameters, such as beam span and stiffness; vehicle parameters, such as velocity and transverse position of wheels; and construction parameters, such as roadway roughness. The most significant parameters were shown to be vehicle speed and weight, bridge span length and surface roughness. The influence of beam stiffness was insignificant compared to the above parameters.

Duseau and Dubaisi [19, 20] analyzed field vibration on fifty concrete bridges along interstate highways I-5 and I-405. The fundamental frequencies were found from amplitude versus frequency plots and used to derive empirical formulas that were used to estimate the fundamental vertical and lateral frequencies of other concrete bridges in the Pacific Northwest. A database for 1000 bridges containing design information was developed. The general empirical formulas used were:

$$f_v = \frac{K_v D^m}{L_s^n}$$

and

$$f_l = \frac{K_l W^{m'}}{L_b^{n'} H^p}$$

where:

- f_v = estimated fundamental vertical frequency, Hz
- L_s = span length, ft
- D_s = beam depth, box girder depth, or slab thickness, in.
- f_l = estimated fundamental lateral frequency, Hz
- L_b = span length, ft
- W = deck width, ft
- H = maximum support height, ft

The constants K_v , m , n , K_l , m' , n' , and p are given in Table 2.2 for different types of bridges.

TABLE 2.2**COEFFICIENTS FOR FINDING NATURAL BRIDGE FREQUENCY [19]**

Type of bridge	K_r	m	n	K_l	m'	n'	p
Pretensioned concrete	1230	0.5	1.7	836	0.5	1	1
RC box	1760	0.5	1.8	9.17	0.6	0.4	0.3
RC slab	615	0.4	1.5	17.4	0.4	0.5	0

Revibration of retarded concrete for continuous bridge decks was studied by Hilsdorf and Lott [21]. Since transverse cracks may be formed or initiated in fresh concrete, they considered revibration as a possible method for closing the cracks. They indicated that the formation of cracks while concrete is still in a fresh state seems to be of greater importance than cracking due to shrinkage of hardened concrete. The influencing factors found were early shrinkage of cement paste restrained by aggregate, reinforcement or other obstacles resulting in tensile stresses and cracking of concrete, and stresses in the fresh concrete due to deflection of formwork and/or supporting structure under weight of fresh concrete. The top fibers near the supports are the most sensitive regions where tensile stresses may develop, and the top reinforcement may present a problem in deeper slabs. Restraints presented by the reinforcement may form planes-of-weakness zones.

For the types of concrete used in their study, results showed significant cracking only when curvature of the surface exceeded $390 \times 10^{-7} \text{ mm}^{-1}$ (0.001 in.^{-1}). Exposure of the fresh concrete to high winds and high temperature resulted in shrinkage cracking and surface crusting. Surface revibration was found to be an effective way to repair the surface cracks and horizontal cracks at the

steel level. They also noted that the time at which form deflection may cause flexural cracking has not been significantly explored, and they suggested more testing.

Research by Karakouziam et al. [22] showed that crack creation is possible even when ACI recommendations are followed. Measured temperatures in the steel showed that time of crack forming coincides with peak temperatures in concrete. They suggested that in hot and dry climates, as in Nevada, solar energy may increase the reinforcement temperature above the concrete temperature, resulting in moisture loss around the bars. As a result, a weak plane is formed and cracks appear at the surface immediately above the reinforcing bars.

A study accomplished in Canada [23] addressed quality assurance in bridge construction, particularly bridge inspection. Recommendations for inspection procedures and some statistical data of interest were presented in this study. They showed that half of the bridge was represented with an adequate number of cylinders. However, there was a tendency to make more cylinders than necessary in case of concrete strengths of 34 MPa (5000 psi), and less than necessary in case of 28 MPa (4000 psi) concrete strength. Slump tests on 14 bridge decks revealed that in each case the mean value of slump was greater than the maximum specified slump of 6.4 cm (2.5 in.). A survey of concrete temperatures showed that some decks were constructed with concrete with a temperature higher than required. In other cases of cold weather concreting, concrete temperature coincided with the minimum specified value, or even lower. The study also showed that site drawings, particularly details of reinforcing bars, should be simpler.

In a study by Kostem [24], the dynamic response of beam-slab bridges was analyzed. Eighteen simple-span bridges of this type were used as test bridges. The bridge superstructure was considered as a combination of plate bending and beam elements. The first three natural periods of

vibration were found and no vehicle was assumed on the bridge. The calculated values were not in good agreement with those found using the equivalent beam approach:

$$T_i = \frac{2\pi}{A_i} \sqrt{\frac{ML^4}{EI}}$$

where:

M = beam mass per unit length

L = beam length

E = beam modulus of elasticity

I = beam moment of inertia

A_i = coefficient used to obtain different natural frequencies. For the first three natural periods A_i is equal to 9.87, 39.5, and 88.9, respectively.

However, when this formula was used with a corrected value for beam properties, assuming that the beams act as T-beams, the first natural period calculated according to the above formula was in very good agreement with the actual values. Nevertheless, higher orders of natural frequency were not close to the actual values. The first natural period was predominantly dependent on bridge length.

An investigation of bridge decks by Lane [25] revealed indications of severe longitudinal cracking of the concrete deck shortly after construction. The average crack width was 1.25 mm (0.05 in.), with a maximum observed width of 2 mm (0.08 in.). The contractor suggested that vibrations due to adjacent traffic may influence fresh concrete. Petrographic analysis was performed since core specimens had many large voids, and the percentage of air in large voids was 2.1 percent, indicating inadequate consolidation. The cracks had a dry powdery surface and bridging of the surface, which indicated that cracks formed while concrete was in a plastic state. Poor liquid

membrane coverage was also noticed, especially where most of the cracking occurred. It was concluded that the cracking occurred while the concrete was still in a plastic state and that the primary cause of the cracking was plastic shrinkage due to a rapid loss of moisture. The concrete was not adequately protected and was not properly compacted. Settlement of the poorly consolidated concrete may have adversely influenced plastic shrinkage, and traffic vibration may have contributed to the settlement.

Retempering of concrete was the subject of a study by Cheong and Lee [26]. Since concrete exhibits a decrease in strength after retempering, they proposed a relationship between water-cement ratio and concrete strength before and after retempering. They mentioned that although retempering is not recommended, there are occasions when some retempering of the concrete is needed, e.g., due to loss of workability after a long distance haul. The time rate of slump loss depended on the initial slump, low slump concrete loses slump much slower than the high slump concrete. It was stated that concrete that undergoes prolonged mixing exhibited an increase of strength up to 20 percent. However, when water was added to restore the slump, strength loss was observed. An exponential curve was found to fit the data in the form:

$$\frac{f'_c}{f_c} = 3.265 \times 0.321^{\frac{(w/c)'}{(w/c)}}$$

where:

- f_c = compressive strength before retempering
- f'_c = compressive strength after retempering
- w/c = water cement ratio before retempering
- w/c' = water cement ratio after retempering

The suggested formula was given only as a helpful guidance to site engineers, since in most occurrences, unauthorized retempering of concrete takes place.

A study undertaken to determine the influence of different parameters on shrinkage cracking [27] revealed that the number of cracks increased with length of the member. However, the final crack spacing was the same: the number of cracks increased with area of steel between 0.2 and 0.5 percent, with a corresponding decrease in crack spacing for a given length; the crack affected-zone increased with bar diameter; the member with larger bars experienced a larger reduction in stiffness; and the number of cracks is smaller and the crack widths are larger if larger bar sizes are used. However, it was concluded that the number of cracks is relatively insensitive to variations in reinforcement ratio and bar size.

Research by Ravina and Soroka [28] enlightened some aspects of the behavior of concrete made with water reducing retarders (WWR) and high-range water reducing admixtures (HRWR). They pointed out that use of WWR and HRWR unexpectedly increased the stiffening rate of fresh concrete. They noted that this effect may not be observed in all combinations of retarders, but must be considered as a possibility. A clear reason for this behavior was not given. However, some practical procedures were recommended. The use of the above-mentioned admixtures may be recommended if used to increase the slump of the concrete. If they are used to reduce the amount of mixing water, they are not recommended.

De Schutter and Taerwe [29] studied heat of hydration for portland cement and blast furnace slag cement, and its influence on massive concrete elements. First, tests performed on a cement paste with a water-cement ratio equal 0.5 at three different temperature levels, 5°C, 20°C and 35°C (41°F, 68°F and 95°F) showed that peak of heat production occurs in the first minutes after the addition of

water. Since this peak only amounts to a small percentage of the total heat and is never produced inside the concrete element, it is not considered in further analyses. Additional tests were performed on the concrete consisting of 300 kg/m³ of cement, 150 kg/m³ of water, 670 kg/m³ of sand and 1280 kg/m³ of coarse aggregate (18.7, 9.4, 41.8, and 79.9 lb/ft³, respectively), under adiabatic conditions. Three different cement types were used. The heat production rate, as a function of time, t , in hours, was established for the above mentioned concretes.

Branco et al. [30] studied the nonlinear temperature distribution in concrete structures caused by developing heat of hydration. As noted, high temperature gradients associated with the exothermic chemical reaction of cement hydration may occur between the interior and the surface of a structural element at early ages, or between parts of an element during sequential concreting phases. When these nonlinear temperature distributions lead to tensile stresses that exceed tensile strength in fresh concrete, cracks occur. Since methods to predict temperature distributions in massive structures had already been developed, Branco et al.'s study concentrated on predicting temperature for slender or less massive elements. In this case, influence of the environmental variables on the hydration temperature gradients had to be taken into account. The numerical technique to estimate concrete heat of hydration temperatures was presented.

A study of the influence of different additives on portland cement hydration heat was performed by Rojas et al. [31]. The additives included in the study were natural pozzolan, volcanic tuff, diatomaceous earth, opaline rock, fly ash, rice husk ash, and limestone filler. All additives, except fly ash and limestone, increased the heat of hydration for the first 5 hours. The conclusion was that the use of fly ash may be favorable with respect to the decrease of hydration heat, however, strengths of mixed concretes did not improve.

In research performed by Emborg and Bernander [32], thermal stresses due to heat of hydration were analyzed. The rheological model of thermal stress analysis at early ages was presented. It consisted of three elements in a series: (1) an element describing the fracture behavior at high tensile stresses; (2) a viscoelastic element for creep and shrinkage; and (3) an element representing the thermal displacement. Increments of the elastic and creep deformation, thermal movement, and fracturing behavior for each time step were considered in this model.

A parametric study was conducted by Mamdouh and Ghali [33] in order to determine the effects of continuity and eigen stresses in simple and continuous span bridges due to nonlinear temperature variation over the cross section. A finite element program was developed based on equations of heat flow and it was used to study the influence of different parameters on concrete box-girder, cellular slab, and solid slab bridges. The researchers concluded that the largest curvature may develop in the case of the following conditions: (1) in a summer when the solar energy received on the deck surface is at a maximum; (2) in case of a large daily range of ambient temperature; (3) when there is no wind, or wind speed is low; and (4) when the deck is covered with an asphalt wearing surface.

Also, they noted that bridges with the same depth and different cross sections had almost the same temperature distribution and curvatures. However, temperature distribution varied significantly in the case of bridges with different depths.

The factors influencing girder deflections were studied by Hilton [34]. This study included field measurements of girder deflections during construction and theoretical frame analysis of the girder deflections. The study was limited to a simple supported steel-plate girder and longitudinal screeding techniques. Since deflections of girders may be influenced by the interconnecting

diaphragms between the bridge girders, the effect of rigidity of diaphragm connections was investigated. Differential thermal conditions between the upper and lower flanges of the steel girders were included in the study. The measured air temperatures ranged from 18.9°C to 33.3°C (66°F to 92°F). Hilton reported the maximum temperatures in the upper flange due to solar radiation in the order of 49.9°C (120°F). However, he noted that the measured differential temperatures between the lower and upper flanges were in the order of 13.9°C (25°F), although extreme temperature differences may be much higher. Analysis of the theoretical versus actual deflection showed that frame analysis, including thermal effects, agrees favorably with the measured deflections. Similar analyses, excluding thermal effects, showed that girder deflections would be considerably greater, and that both field and frame analysis were markedly different from the conventionally calculated deflections.

A general observation was that the final screeding pass lag of 3 bays behind concrete placement would be ideal if conventionally calculated deflections are used to establish the elevations. However, only two, and sometimes only one bay lag, were noted over some areas. It was concluded that if concrete placement is closely followed by the screeding machine, dead-load deflection values should be reduced by about 25 percent.

The influence of wind flow to shrinkage of concrete was studied by Dutt et al. [35]. The recommended evaporation rates were examined and their validity was tested. Concrete cubes and slabs of different concrete grades were subjected to simulated wind speeds between 7.2 and 18 km/h (4.5 and 11.3 mph). The specimens were inspected for cracks after 72 hours. Air temperature was 35°C (95°F) and the concrete temperature was 50°C (122°F). One set of specimens was cast under direct exposure of sunlight and hot water, and subjected to a low wind speed of 4 km/h (2.5 mph).

Cracks were found on all the specimens in that set. Cracks were also found in most of the other specimens. Recommendations for concrete casting under hot weather were given as follows: subgrade and formwork should be dampened; aggregate should be dampened if it is dry or absorptive; windbreaks should be erected to reduce speed velocity over concrete surface; reflective sunshades should be provided to control concrete surface temperature; excessive temperature difference should be avoided between concrete, curing water and air; concrete temperature should be lowered in hot weather; surface of concrete should be reworked near the time of initial set of cement; and the time between placing of concrete and the start of curing should be reduced.

Effects of curing conditions on various concrete properties were studied by Alsayed [36]. This study was concerned with the effect of intermittent wet and dry curing methods in hot and dry climates on different concrete properties. The addressed properties were strength, porosity, absorptivity, and shrinkage. Four groups of specimens were cast and kept for 24 hours in steel molds covered with wet burlap. Then each group was subjected to different environmental conditions. The first group (A) was sprinkled with water twice a day; the second group (B) was covered with burlap and then sprinkled with water twice a day; the third group (C) was covered with an impervious polythene sheet; and the fourth group (D) was exposed to air without curing. Results of the tests showed that groups C and D had significantly lower compressive strengths. In the case of group C, a polythene sheet worked as an insulator and led to insufficient cement hydration. Results for groups A and B were almost the same, proving that a burlap cover did not improve concrete strength. This may be due to the fact that the burlap becomes dry and hot as soon as water evaporates from it, which occurs shortly after sprinkling stops. In fact, it was concluded that a burlap cover may increase

the concrete temperature and adversely influence the concrete properties. However, none of the mentioned curing methods reduced the rate of shrinkage at the early ages of curing.

A study by Ho et al. [37] confirmed the importance of early age curing conditions on the quality of concrete. Specimens prepared with Type I (normal) and Type II (low heat) portland cements and a fly ash were cured under different humidity levels and tested. It was shown that the effectiveness of curing drops rapidly as the relative humidity falls below 100%. The duration of curing, in the case of a 6% drop in relative humidity of 100%, should be extended to one year in order to achieve the quality of a concrete cured for 7 days at 100% relative humidity. The importance of saturating concrete for the first few days after casting was emphasized.

The Kansas DOT in cooperation with Kansas State University performed research on the cracking of concrete bridge decks [38]. Data for a total of 40 steel girder bridges were collected and variables that may influence bridge deck cracking were analyzed. They concluded that cracking increases with increasing concrete slump, water content, cement content, compressive strength, and water-cement ratio. However, cracking in monolithic bridge decks decreased with an increase in air content, particularly for concretes with an air content greater than 6.0 percent. A high level of cracking was noticed in the case of overlays placed with zero slump concrete. A significant increase of cracking in overlays was found when silica fume was used if precautions were not taken to prevent plastic shrinkage. Also, cracking increased with an increase in the top reinforcement size (diameter), placement length, and average daily temperature. According to previous indications, it was recommended that the volume of water and cement should not exceed 27.0 percent of the total volume of concrete. Secondly, the air content of concrete should be greater than 6.0 percent, and finally, concrete for bridge deck overlays should not have zero slump. The researchers recommended

limiting the size of the top transverse reinforcing bars to 13 or 16 mm (#4 and #5) spaced at less than 150 mm (6.0 in.) apart.

Durability of bridge decks was the subject of a study performed by Jackson for the Arkansas State Highway and Transportation Department [39]. This study was divided into three phases: a field survey, shrinkage tests and crack monitoring, and petrographic examination of cores. Preliminary results indicated that no particular area of the state had greater occurrence of bridge deck cracking. Though use of fly ash was not found to be a major contributing factor, adjustments to the current mixing procedures were suggested. Shrinkage graphs have shown that the majority of shrinkage does not always occur at the same time.

In a technical report for the Washington State Department of Transportation, performed by Babaei [40], concrete overlays were evaluated for bridge applications. Protection of reinforced bridge decks with respect to salt infiltration was the primary concern of the study. Surface wear and friction resistance, surface cracking, overlay bond, chloride permeability, corrosion-induced deterioration, protective system selection, and service life expectancy were evaluated. Although the findings indicated that many overlays were cracked, cracking of the latex modified concrete (LMC) overlays was less severe than the cracking in the low slump dense concrete (LSDC). Analysis of cracking patterns revealed that cracks appeared as a result of initial plastic shrinkage in the overlays. As a result of thermal cycling, wetting and drying, and structure flexing, these initial cracks later propagated. The overlay bond to underlying deck was generally stronger in the case of the LMC. To minimize overlay cracking, it was recommended that a maximum evaporation rate of $0.73 \text{ l/m}^2\text{h}$ (0.15 lb/ft^2 per hour) be permitted while placing overlays. Prolongation of a wet cure period to at least 48 hours for LMC was also suggested.

In a report for the Illinois Department of Transportation [41], petrographic examination of three concrete cores taken from two bridge decks was discussed. In order to identify the causes of the cracking and debonding of microsilica overlay, five concrete cores from several different locations on the bridge were examined. The overlay exhibited prominent vertical cracks extending from the top surface. In some cases, cracks were 48 mm (1.9 in.) deep, while in other cases, cracks extended all the way to the bottom of the overlay surface. The cracking style indicated that stresses due to shrinkage were primarily the cause of cracking. Fully carbonated top portions of the base concrete indicated mediocre concrete quality. Delamination was present in all specimens below the interface between the concrete overlay and concrete base. The presence of loose particles adhering to the concrete overlay, as well as irregular voids in the concrete grout layer, indicated that delamination was the result of poor surface preparation.

Bridge widening problems were studied in a report for the State of California Highway Transportation Agency [42]. The study revealed that widened structures are a proportionally greater source of bridge maintenance. Spalling of bituminous concrete over the longitudinal joint, high escarpments along the longitudinal joint, and spalling of patches that were placed over the cut off curb dowels were found. The report suggested that "smoother riding surface is obtained, bridge deck maintenance reduced, and deck aesthetics improved by attaching widened decks to the original through lapped deck reinforcing steel." A six week period of curing was also recommended before the closure pour was provided.

Pile driving can cause significant movements in nearby newly constructed structures due to the displacement of soil and due to the high pore pressures developed in clay subsoils. Driving piles into clay can cause structure movements for a distance approximately equal to the length of the piles

driven [43]. The hammer impulse travels down the pile, where the impulsive pile displacements produce both impulsive ground motions or vibrations as well as permanent pile displacement equal to the penetration per blow. Vibration is radiated outward cylindrically from the length of the pile as well as spherically from the pile tip. Within distances equal to pile penetration, vibration is dominated by compressive and shear body waves. Distinct impact hammer pulses decay to zero between hammer blows, which occur at a rate of tens of times a minute. The dominant frequency of the impact motions is dependent on driving conditions and pile and hammer properties, but will range between 10 and 50 Hz for typical hammers. Vibratory hammers produce ground motions at the hammer frequency, which typically operate between 900 and 1400 rpm or 15 to 20 Hz [44].

One of the concerns on any construction project is the strength of the cast-in-place concrete, and most engineers assume that its resistance to vibration is proportional to its strength, which is very small before it cures. Therefore, construction vibrations are usually greatly restricted near setting or curing concrete on the basis of this intuitive concept. On the other hand, experiments performed to investigate the validity of the assumption of vibratory sensitivity reveal curing concrete to be surprisingly robust [44]. Pile driving near curing concrete is erroneously prohibited on many sites due to fear of vibratory degradation. Many state highway departments have conducted field tests that confirm the vibratory robustness of cast-in-place concrete piles even when cast immediately adjacent to piling.

Pile drivers, forge hammers, and rail and highway traffic are frequent causes for disturbance. In objective terms, unless the observer is very close to the vibration source, the vibration magnitude at the point of observation is likely to be less than the generally accepted threshold particle velocity of 50 mm/sec [45].

At distances greater than 70 m, there is little difference in the magnitude of peak particle velocity produced by either a vibrator pile driver or diesel hammer. At lesser distances (23 m), there is a marked difference, as the diesel hammer produces a peak particle velocity of 2.5 mm/sec compared with 0.75 mm/sec by the vibrator pile driver. In objective terms, either value is much less than the suggested threshold of 50 mm/sec. However, subjectively, both machines are highly objectionable and cause much complaint, the diesel hammer producing impact and noise, and the vibrator producing resonance in neighboring buildings and other structures [45].

At an industrial site, the ground vibrations produced by the impact of forge hammers were compared with those produced by heavy highway traffic. The maximum particle velocities due to a forge hammer weighing 18 tons at distances of 15 to 21 m away measured 1.0 mm/sec on the radial and transverse modes, and 1.8 mm/sec on the vertical mode. The peak vibration from the forge hammer was almost instantaneous. The vibrations from highway traffic also peaked at 1 mm/sec on the shear mode, and the peaks on all three modes were sustained over periods of 0.25 seconds. Nevertheless, from a subjective viewpoint, the operation of the forge hammers was objectionable, while the highway traffic vibrations and noise were accepted without complaint [45].

Proper finishing is essential to reduce the risk or severity of transverse deck cracking. The concrete should be vibrated and struck with a mechanical screed. The concrete should then be smoothed using a float, if necessary. Final floating should be delayed until after the early bleeding to prevent crusting of the surface that traps bleed water and weakens the surface, making it susceptible to rapid scaling. The California Department of Transportation (Caltrans) [46] found that late finishing and hand finishing increased cracking. The New Mexico Department of Transportation

also reported that early finishing reduced cracking. Early finishing reduced the number and width of cracks, and double-floating decreased cracking even further [46,47].

There are many mechanical finishing machines, and their effects on early cracking vary. Finishing machines that can rapidly consolidate and finish the concrete with the minimum amount of manipulation are best suited for decks. To reduce surface drying before curing, the concrete deck surface should be misted using fog nozzles specifically designed for concrete placement or evaporation-reducing films should be applied. Fogging should commence immediately after strike off. Water should never be sprinkled directly onto the new concrete surface and worked into the surface. At least three vibrators are recommended for placement rates of 22 m³/hr (30 yd³/hr) or higher. Generally, vibrator frequency, size, and time of insertion can vary without affecting consolidation [48].

3. SURVEY

3.1 Introduction

In order to identify the effects of construction loads and vibrations as well as the form of deterioration in newly poured bridge decks, an integral survey was prepared and sent to 59 departments of transportation in the United States as well as all nine districts in the State of Illinois. The questionnaire was presented in the format as shown in Appendix A. A summary of responses for each agency is also given in Appendix A. The results reported herein are those corresponding to full depth construction. Although some aspects of the survey included partial deck construction, those results have been omitted.

3.2 Survey Results

Table 3.1 presents the total response from the departments of transportation, the number of departments reported using this concept, and the number of departments interested in the results of this survey. Since all the questions were not answered in each survey, Table 3.2 presents the total response for each question. Tables 3.3 and 3.4 present the number of affirmative or negative answers on questions 1 and 2. Table 3.5 presents the response on the third question, which asked for the rationale behind the policy of either permitting or prohibiting traffic in adjacent lanes. Answers for this question were divided into 8 groups, and categorized according to the following:

TABLE 3.1**DEPARTMENTS OF TRANSPORTATION RESPONSE SUMMARY**

Surveys mailed out	59	%
Responses received	54	91.5
Interested in results of this survey	52	96.3
Not interested in results of this survey	2	3.7

- **Economy and Inconvenience:** Many organizations base their policy of not closing a bridge to traffic on factors other than those concerned with the quality of the bridge deck. Some based their policy on economy (since it is too expensive to provide detours), some on inconvenience to the public, and others on lack of detour routes. In some cases, safety of workers as well as safety of the public was indicated. Since none of these policies are related to bridge performance and deck quality, they are listed separately.
- **Vibrations Do Not Present the Problem:** A number of respondents believe, based on reports and research, that vibrations due to adjacent traffic flow do not present problems to fresh concrete and consequently allow traffic on the bridge during construction of bridge decks.

TABLE 3.2**DEPARTMENTS OF TRANSPORTATION QUESTION RESPONSE SUMMARY**

Question Number	1	2	3	4	5	6	7
Responded to question	52	52	49	47	35	41	53
Percentage	96.3	96.3	90.7	87.0	64.8	75.9	98.2
Did not respond to question	2	2	5	7	19	13	1
Percentage	3.7	3.7	9.3	13.0	35.2	24.1	1.9

- **Experience:** A number of respondents do not close traffic on the bridge during rehabilitation based on previous experience. They either had no problems with bridge cracking or had it with bridges that were closed to traffic.
- **Vibrations Present the Problem:** Some of the respondents believe that vibrations present problems and generally do not allow traffic on the bridge during reconstruction. However, their policy is not backed with any substantial data.
- **Undertake Measures to Reduce Vibrations:** Some agencies permit traffic if certain measures to reduce vibrations are considered. In one case, a closure pour is used and traffic is allowed only if parts of the bridge under construction and traffic are not structurally connected.
- **Decisions on Individual Basis:** These agencies do not have firm policies but rather make the decisions individually. Their decisions are based on availability of routes, safety, convenience as well as concern with work quality.
- **Other:** In one state, full deck replacement is not used, so the policy cannot be included.
- **No opinion:** In a few cases, agencies expressed no opinions on question three.

Table 3.6 presents the number of agencies that conduct research on bridge deck cracking problems. In Table 3.7, the factors that are the cause for specific defects in the case of full depth concrete deck rehabilitation are shown. The number indicated presents the frequency of occurrence of a specific condition. Table 3.8 gives an overview of the answers to Question 6. Since only cement type and concrete strength were mentioned in most of the answers, only these two parameters are listed. Additional information on for instance, additives, fly ash, silica, etc., were not systematically mentioned in the answers, therefore, it was not feasible to present them in this table. Table 3.9 is a summary of the responses to Question 7.

TABLE 3.3**DOT RESPONSE SUMMARY TO QUESTION 1**

Does your agency permit regular vehicular traffic to continue using one or more lanes of a bridge when concrete is being placed on the same structure?	Full deck replacement		Partial deck overlay	
	Answered "YES"	48	92.3%	49
Answered "NO"	4	7.7%	3	5.8%
Answered the Question	52		52	

TABLE 3.4**DOT RESPONSE SUMMARY TO QUESTION 2**

Do you impose any restrictions on the traffic related to construction loads, e.g., limit on speed or truck weight, or the concreting operation, e.g., time of day?	Full deck replacement		Partial deck overlay	
	Answered YES	25	48.1%	25
Answered NO	27	51.9%	27	51.9%
Answered the Question	52		52	

TABLE 3.5**DOT RESPONSE SUMMARY TO QUESTION 3**

What is the rationale behind your agency's policy of either permitting or prohibiting traffic to continue in adjacent lanes?	Number of responses	Percentage
Economy and Inconvenience	25	48.1
Experience	4	7.7
Vibrations Do Not Present the Problem	14	26.9
Vibrations Present the Problem	2	3.8
Undertake Measures to Reduce Vibrations	4	7.7
Decision on Individual Basis	1	1.9
Other	1	1.9
Have No Opinion	1	1.9
Total	52*	

* 3 departments indicated 2 explanations each

TABLE 3.6

DOT RESPONSE SUMMARY TO QUESTION 4

Does your agency conduct research or field studies on the factors most likely to inflict any damage on newly poured concrete during construction, and if so, could you provide us with your own specifications for these construction techniques, or any published reports?		
Conducting research, etc.	11	23.4%
Not conducting research, etc.	36	76.6%
Responded to Question	47	

Most of the respondents, i.e., more than 95%, answered questions 1 thru 3. The majority of respondents confirmed permitting regular traffic on the bridge during reconstruction. In both bridge deck overlay and full deck replacement cases, more than 90 percent of the answers were affirmative. However, on the second question opinions are almost equally divided. Slightly more agencies impose restrictions than not (55 versus 45 percents in the case of full deck bridge replacement, and 56 versus 44 percent in the case of partial overlays). A small number of agencies prohibit heavy vehicle traffic, or they limit the weight of the vehicle as additional measures to the speed restriction.

The opinion that vibrations are not a problem was expressed by 27 percent of the respondents, who based their policy on research and reports. Approximately 7.3 percent based their opinion on previous experiences, since cracking had occurred in bridges regardless of whether they were closed or open to traffic. Approximately 9.8 percent of the respondents attempt to reduce vibrations on the bridge during construction by either closing the bridge during the pouring of concrete and some time after that, using closure pours, or allowing traffic only if the portion under construction is not structurally connected to the traffic lane(s). However, they did not have explanations for these requirements. Only 2.4 percent decide on an individual basis, while about 4.9 percent believe that

vibrations are harmful to newly constructed decks in the presence of traffic. Only a small number of agencies, 21.6 percent, conduct their own research in this field.

Table 3.7 presents the distribution of answers to Question 5 in the case of full deck replacements. It is clearly visible that the concentration of answers is in the case of transverse cracks, followed by random cracking, cracking over supports, and midspan cracking. A somewhat lower rating was given to longitudinal cracking. Other defects, such as diagonal cracking, were sometimes mentioned.

The opinions on causes of cracking are presented in Table 3.7. For the full depth concrete decks, the most significant reasons are thought to be time of year, thermal changes, and curing procedures, totaling 50 percent of all responses. They are combined since they are mutually dependent and may be categorized as concrete curing. Other reasons for cracking were mentioned in 13.9 percent of the answers. Sequence of pour was indicated in 9.8 percent, concrete age in 7.4 percent, deflections caused by moving equipment in 5.7 percent, and traffic induced vibrations in 4.9 percent. Concrete cover was mentioned only once, which represents 0.8 percent of all responses.

The cement type used varies from case to case. Predominantly Type I and Type II, have been used, 66.6 percent. However, type of cement was unknown in a relatively high number of cases (19.0 percent). Among concrete properties, compressive strength was mentioned in twenty responses. Most of the agencies reported strengths of more than 27.6 MPa (4000 psi). However, a high percentage of responses (33 percent), noted unknown concrete strength.

TABLE 3.7

DOT RESPONSE SUMMARY TO QUESTION 5 (FULL DEPTH)

Have you experienced a significant premature occurrence of any of the following defects in bridge deck concrete that had been *subjected to construction loads and vibrations* during construction, rehabilitation, widening, or overlaying of the deck?

Prevailing Condition	Defect								
	Longitudinal cracks	Transverse cracks	Random cracks	Cracking over supports	Cracking at midspan	Bond failure at overlay-deck	Delamination at rebar level	Inadequate concrete strength	Other
a - Traffic-induced vibrations during placement of concrete	1	7	1	1		1			2
b - Vibrations caused by construction equipment		1		1					
c - Adjacent pile driving									
d - Deflections caused by moving equipment	1	3	2		2	1			
e - Clean concrete cover						1			
f - Concrete age associated with pour stages		3	2	5	1				
g - Sequence of pours	1	4	1	6	2				
h - Curing procedures	4	7	6	1	2	1		1	
I - Thermal changes	3	9	4	4	2			1	
j - Heat of hydration		1	1					1	
k - Type of concrete	1	3	1	1	1				
l - Time of year and conditions prevalent at pour stages	2	8	3	4	4			2	
m - Type of paving and/or finishing equipment used									
n - Adjacent railroad traffic									
o - Shear connector design									
p - Other	4	8	2	4	3			1	

TABLE 3.8

DOT RESPONSE SUMMARY TO QUESTION 6

What type of concrete and cement type (if known) was used?							
Cement	Type I	13	36.1%	Concrete	< 24.1 MPa (3500 psi)	1	4.8%
	Type II	6	16.7%		24.1 MPa (3500 psi)	0	0.0%
	Type III	1	2.8%		27.6 MPa (4000 psi)	5	23.8%
	Type I or II	6	16.7%		31.0 MPa (4500 psi)	6	28.6%
	Type I or II or III	1	2.8%		24.1 to 31.0 MPa (3500 to 4500 psi)	1	4.8%
	Other	2	5.6%		20.7 to 27.6 MPa (3000 or 4000 psi)	1	4.8%
	Unknown	7	19.4%		Unknown	7	33.3%
Total	Cement	36		Total	Concrete	21	

Most of the DOTs (98.1 percent), indicated that bridge deck construction, rehabilitation, widening, or overlay projects were scheduled for the 1996 construction season (question 7).

The comprehensive survey suggested that cracking of full depth concrete bridge decks is not believed to be related to vibrations and loads imposed by adjacent traffic. However, experience with concrete bridge deck overlays indicates that the significance of these effects on this particular type of rehabilitation is more prominent. In addition, the conclusions from the survey are not substantial due to the lack of information in this field. Adjacent traffic as well as other factors that were addressed in the survey, such as construction loads and equipment (concrete mixer trucks and concrete pump trailer units), disturb the setting of concrete at early ages.

4. EXPERIMENTAL PROGRAM

4.1 Introduction

One of the factors considered to possibly affect cracking in fresh concrete is sequence of pour. Bridge deck construction is normally planned in accordance with the most effective sequence of pour. Distinct pour sequences can yield different curvatures in concrete. However, since fresh concrete has specific properties at early ages, an experimental program was necessary to determine the modulus of elasticity of concrete as well as the maximum curvatures that fresh concrete can withstand. The determination of the modulus of elasticity at early ages was necessary in order to establish a criteria for predicting the modulus of elasticity to be used as the basis for the theoretical part of the study, i.e., for the sequence of pour program.

Concrete Standard Specifications for Road and Bridge Construction by the Illinois Department of Transportation (IDOT), particularly the sections referring to bridge deck concrete, were used to design the concrete mixes. Three types of concrete mix designs were adopted: plain, with super-plasticizer, and with retarder. Nine specimens were cast for each of the three different concrete sets used. Each set included three specimens that were tested at 5 hours, three at 8 hours, and three at 12 hours. As a result, a total of 27 specimens were tested.

4.2 Specimen Geometry

Specimens consisted of concrete beams 75 mm wide and deep, and 500 mm long (3 x 3 x 20 in.). For the first two concrete mixes, specimens were cast in simple plywood board molds. A third series utilizing concrete with a retarder were cast in flexible plexiglass molds in which

they were later tested, as shown in Figure B.1. This was done since it was not possible to take the specimens out of the molds without incurring damage. Accompanying beam specimens, concrete cylinders 10 cm in diameter and 20 cm in length (4 and 8 in., respectively), were cast to determine the compressive strength of the specimens at the time of testing.

4.3 Materials

The concrete mix used corresponds to IDOT Standard Specifications for Road and Bridge Construction. Type I cement, locally available fine and coarse aggregate, and tap water were used. The amounts of additives used in the mix were according to manufacturer specifications. The maximum aggregate size was 9.5 mm ($\frac{3}{8}$ in.) and had a specific gravity of 2.83. The fine aggregate conformed to the specification for FA-2 aggregate and had a specific gravity of 2.71. The water/cement ratio used was between 0.42 to 0.44, depending on the admixtures used. Basically, the same mix proportions were used for the cement and the aggregate except additives (Table 4.1). However, different additives were added while the water content was adjusted correspondingly.

TABLE 4.1

CONCRETE MIX PROPORTIONS USED TO MAKE SPECIMENS

Concrete Series	Cement	Fine aggregate	Coarse aggregate	Water	Super-plasticizer	Retarder	Air-entrainment
	kg (lb)	kg (lb)	kg (lb)	l (gal)	ml (fl. oz.)	ml (fl. oz.)	ml (fl. oz.)
	per m ³ (per yd ³)						
I	376 (634)	771 (1299)	1155 (1946)	165 (33.3)			
II	376 (634)	793 (1336)	1155 (1946)	159 (32.1)	730 (19)		
III	376 (634)	793 (1336)	1155 (1946)	158 (31.9)		852 (22)	183 (4.7)

4.4 Specimen Preparation

The specimens were prepared in the laboratory using a 0.057 m³ (2 cubic ft) mixer. Dry materials were mixed for three minutes. The mixing process continued for another three minutes after the water was added. Concrete was placed in the molds in three layers, and each layer was compacted according to ASTM Standards. Furthermore, specimens were vibrated on the vibrating table for one minute. The top surface was then smoothed with a trowel, and allowed to cure for one hour. Simultaneously, the concrete cylinders were prepared. All specimens and cylinders were covered after one hour to minimize evaporation and possible shrinkage cracking.

4.5 Experimental Test Setup

The specimens prepared without a retarder were tested after being taken out of the molds. These specimens were positioned into a testing frame, as shown in Figures 4.1 and 4.2. The load was applied at the center of the span using a simple fixture connected to a 4.45 kN (1000 lb) load cell. As the cross-head of the Instron 8500 Series Testing Machine traveled upward, it applied an upward load onto the specimen.

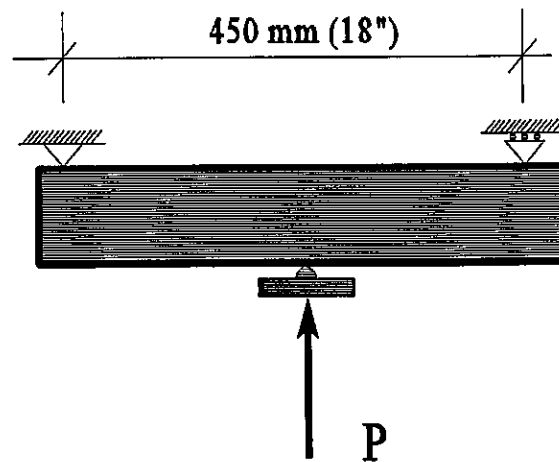
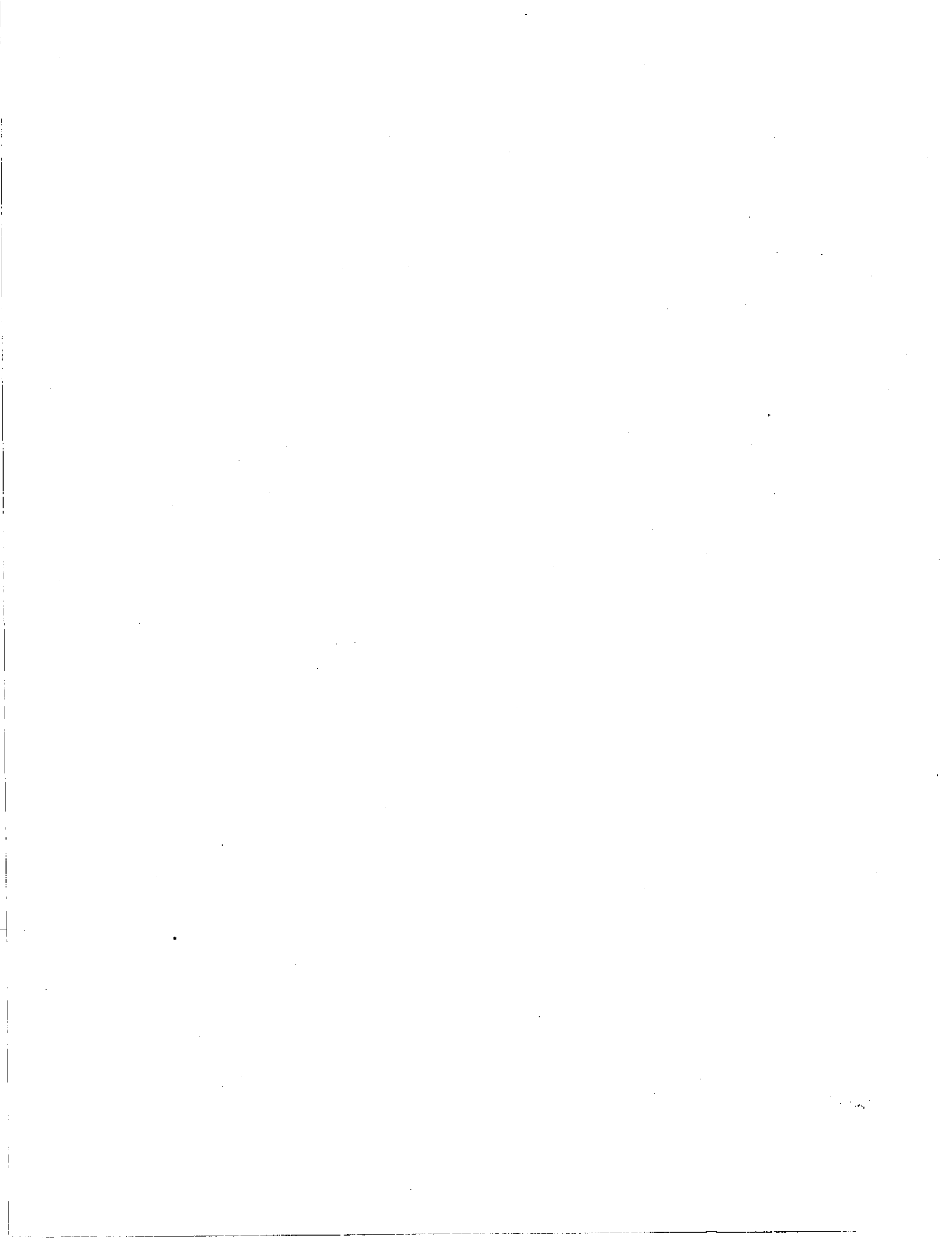


Figure 4.1 Test setup scheme



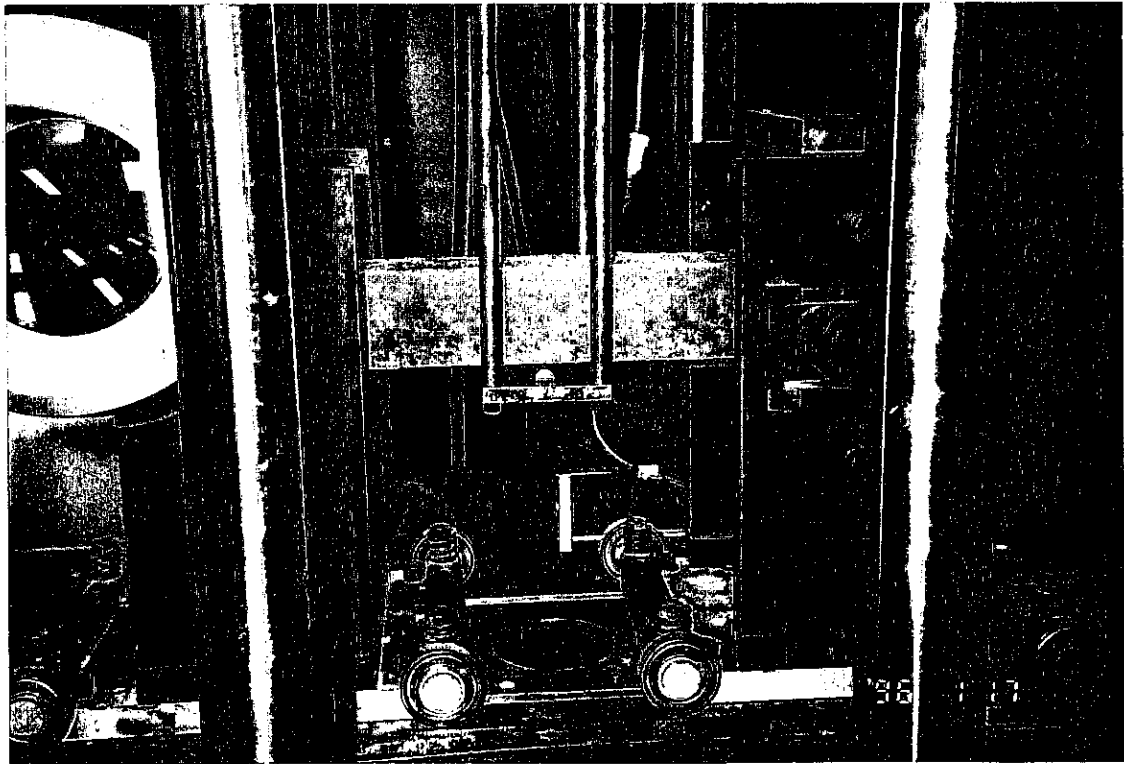
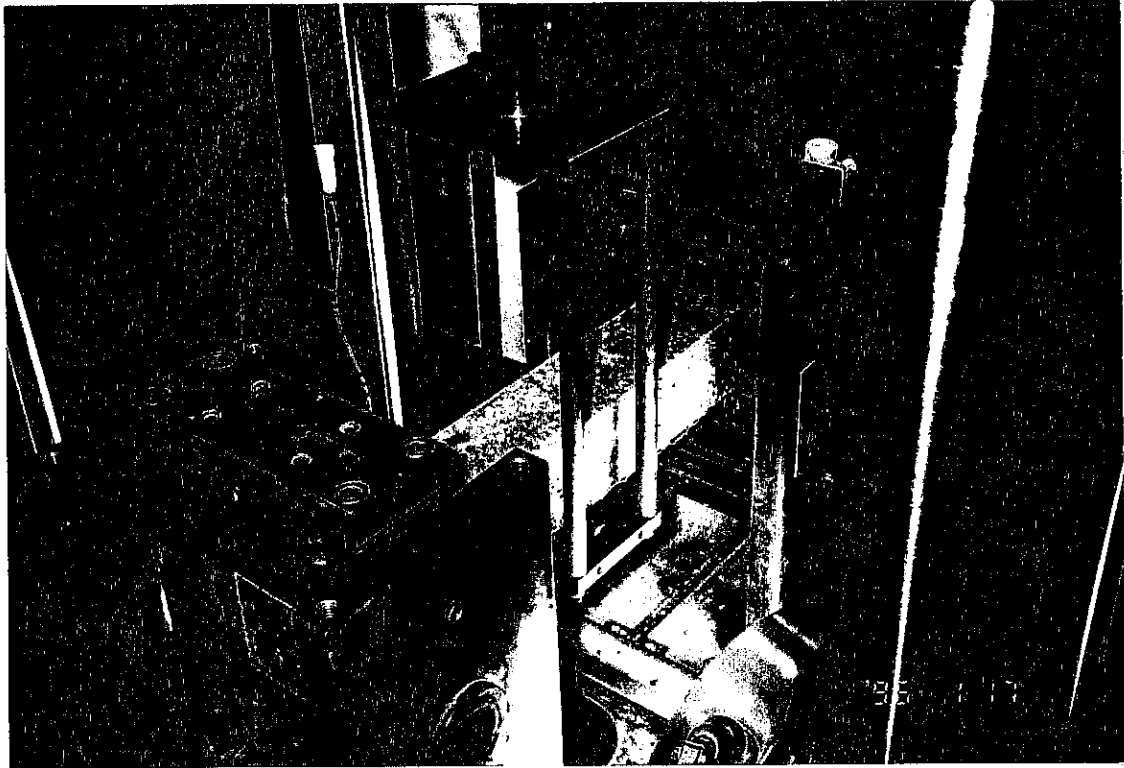


Figure 4.2 Experimental test setup

The specimens made of concrete with a retarder were tested while inside the flexible plexiglass molds since they were too fragile to be taken out at the specific time without damage. Otherwise, the test setup was as described earlier.

4.6 Testing Procedure

After the specimen was placed in the frame, the load was applied at the rate of 0.025 mm/min (0.01 in./min) under displacement control. Displacement and load values were recorded using a computer and Instron software. The test was continued after the point of concrete cracking until the load showed no significant changes. Load-deflection diagrams were then plotted taking into account the weight of the specimens, and in the case of the concrete with retarder, stiffness of the forms. The modulus of elasticity was then calculated from Eq. 4.1, where s is the slope of the load-deflection diagram, ℓ is the span length, b is the width of the specimen, and I is the moment of inertia of the cross section.

$$E = \frac{s \ell^3}{8 b I} \quad (4.1)$$

4.7 Results and Discussion

Typical load-deflection curves are shown in Figures B.2 and B.3, which depict the actual data recorded after the influence of the self-weight and stiffness of the mold were taken into account. The maximum flexural stresses and curvatures are presented in Table 4.2. The curvature for the experimental setup was calculated in accordance with the illustration shown in Figure 4.3, where the equation presented was used; Δ is the maximum deflection and ℓ is the span length.

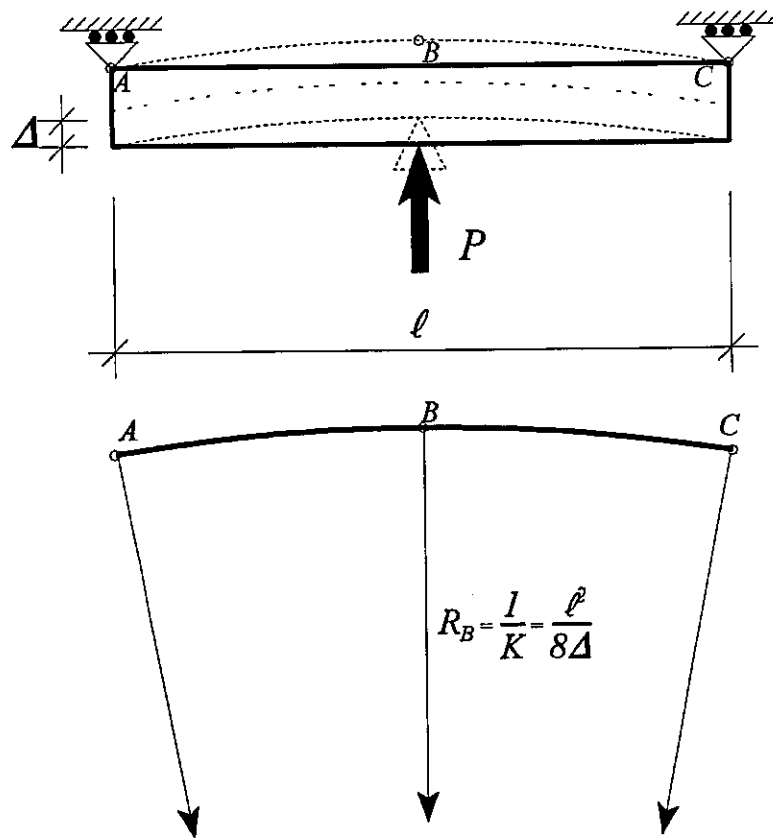


Figure 4.3 Determination of curvature

Comparison of data for the same type of concrete at the same age showed that cracking of the specimens occurs at approximately the same curvature and at the peak load. After the specimens cracked, a sudden drop of the load was recorded at approximately a quarter of the value in the case of specimens prepared with plain concrete and concrete with super-plasticizer. After the specimens cracked, the load decreased more slowly. In the case of the specimens at 5 hours, this drop was less pronounced and the slope of the curve decreased more slowly compared to the specimens at 8 and

12 hours. This was expected since first setting of concrete occurs between 3 and 5 hours. The only deviation was for the specimens made with the concrete with a retarder, which did not crack at the peak load, and cracked at much higher deflections. This was not unusual since the concrete behaved as concrete without retarder at ages less than 5 hours, i.e., it was still in a plastic state. Note that the load for these specimens was not given although it was measured.

TABLE 4.2

MAXIMUM STRESSES AT CRACKING AND CORRESPONDING CURVATURES

Concrete Series	Hours	Flexural stress					Curvature				
		Specimen Series			Average	Standard Deviation	Series			Average	Standard Deviation
		1	2	3			1	2	3		
		kPa (psi)					$\times 10^{-7} \text{ mm}^{-1} (\times 10^{-5} \text{ in}^{-1})$				
Plain concrete	5	846 (123)	672 (97.5)	427 (62.0)	649 (94.2)	148 (21.5)	84 (21)	76 (19)	84 (21)	81 (20.3)	4.0 (0.9)
	8	2555 (371)	2309 (335)	2073 (301)	2312 (336)	161 (23.4)	120 (30)	144 (36)	104 (26)	123 (30.7)	14.0 (3.6)
	12	3520 (511)	3307 (480)	2722 (395)	3183 (462)	308 (44.7)	164 (41)	208 (52)	160 (40)	177 (44.3)	20.0 (5.1)
Concrete with super-plasticizer	5	443 (64.3)	688 (99.9)	578 (83.9)	570 (82.7)	84.6 (12.3)	76 (19)	108 (27)	88 (22)	91 (22.7)	12.0 (2.9)
	8	1408 (204)	1892 (275)	1376 (200)	1559 (226)	222 (32.2)	140 (35)	140 (35)	112 (28)	131 (32.7)	12.0 (3.1)
	12	2855 (414)	3300 (479)	2967 (431)	3040 (441)	172 (25.0)	252 (63)	236 (59)	224 (56)	237 (59.3)	10.0 (2.4)

Due to the properties of the concrete with retarder at early ages, the load at cracking is very dependent on rate of loading. It is difficult to determine the load the specimens can withstand without

cracking. For both concrete without additives and concrete with super-plasticizer, the minimum curvature required to crack the specimens was reached at five hours and its value was in the vicinity of $80 \times 10^{-7} \text{ mm}^{-1}$ ($20 \times 10^{-5} \text{ in.}^{-1}$). This value increased to $120 \times 10^{-7} \text{ mm}^{-1}$ ($30 \times 10^{-5} \text{ in.}^{-1}$) at 8 hours and $170 \times 10^{-7} \text{ mm}^{-1}$ ($42.5 \times 10^{-5} \text{ in.}^{-1}$). Correspondingly, the minimum modulus of elasticity was reached at the age of 5 hours as shown in Table 4.3. The modulus of elasticity was calculated by taking the slope between the point of maximum load and zero load. Since the load-displacement curve was not linear at age 5 hours, the modulus of elasticity had to be a function of displacement. However, the range of values for the modulus of elasticity was not high for the given concrete at this age. This presents a better indication of the increase of stiffness over time. In the range between 5 and 8 hours, the modulus of elasticity increased more rapidly than that between 8 and 12 hours, which may be attributed to the slopes of the load-deflection diagrams at different ages. The modulus of elasticity for concrete with retarder was not calculated due to the extreme nonlinearity of the load-deflection curve and the plastic behavior of this concrete at early ages.

TABLE 4.3

CONCRETE COMPRESSIVE STRENGTHS AND MODULUS OF ELASTICITY

Concrete	Age of Specimen	Compression Strength Test Stress	Modulus of Elasticity	
			Average Value	Standard Deviation
	Hours	MPa (psi)	MPa (psi)	
Plain concrete	5	1.61 (233)	2499 (362700)	644 (93400)
	8	4.11 (596)	5651 (820200)	760 (110300)
	12	7.02 (1019)	5790 (840300)	711 (103200)
	5	1.38 (201)	2499 (362700)	644 (93400)
	8	4.24 (615)	5651 (820200)	760 (110300)
	12	6.95 (1009)	5790 (840300)	711 (103200)
Concrete with super- plasticizer	5	1.57 (228)	1971 (286000)	102 (14800)
	8	3.51 (510)	3573 (518600)	375 (54400)
	12	8.07 (1171)	4053 (588300)	351 (50900)
	5	1.54 (223)	1971 (286000)	102 (14800)
	8	4.01 (582)	3573 (518600)	375 (54400)
	12	7.85 (1140)	4053 (588300)	351 (50900)

Cracking of specimens of the same concrete type and age occurs at approximately the same curvature and at the peak load. After cracking occurred in the specimens, a sudden drop of the load was recorded at approximately a quarter of the value in the case of specimens prepared with plain concrete and concrete with super-plasticizer. For both concrete without additives and concrete with super-plasticizer, the minimum curvature required to crack the specimens was reached at five hours and its value was in the vicinity of $80 \times 10^{-7} \text{ mm}^{-1}$ ($20 \times 10^{-5} \text{ in.}^{-1}$). This value increased to $120 \times 10^{-7} \text{ mm}^{-1}$ ($30 \times 10^{-5} \text{ in.}^{-1}$) at 8 hours and $170 \times 10^{-7} \text{ mm}^{-1}$ ($42.5 \times 10^{-5} \text{ in.}^{-1}$) at 12 hours. The curvature obtained at 12 hours was smaller than that reported by Hilsdorf and Lott [21] ($390 \times 10^{-7} \text{ mm}^{-1}$).

5. SEQUENCE OF POUR

5.1 Introduction

To investigate the possibility of concrete deck cracking due to loads induced by the sequence of pour, a computer program was developed. This program was used to calculate, among other parameters, deflections and curvatures for different sequences of pour. The objective of this theoretical analysis was to identify the various parameters associated with the intensity of construction loads and vibrations that ultimately produce cracking in the concrete. As stated earlier, the program utilized the concrete modulus of elasticity at early ages determined in the experimental portion of the study.

5.2 Program Overview

The program was written in FORTRAN language (see listing in Appendix C) where the following input variables were considered:

- number of spans
- span length
- number of elements for each span
- supporting beam material properties for each span
- cross-section properties for each element of supporting beam
- additional external loads that effect only supporting beam
- concrete deck material properties for each sequence
- concrete deck section properties for each element

- starting time for each sequence
- additional external live loads acting at time of given sequence

The user can choose to work in International System (SI) or "inch-pound" units. The user has to choose the number of elements each span is divided into. Coordinates of the nodes, measured from the left end of the bridge, are then calculated by the program, Figure 5.1. Material and cross section properties for each element are used to calculate the self weight of the elements. This weight is applied as a uniform load on the element. If there are any additional external loads, they are taken into account and equivalent nodal forces are calculated. External loads may be point loads (concentrated loads) or uniform loads. Note that the position of the concentrated load is given from the left end of the bridge and *does not* have to correspond with the location of the node.

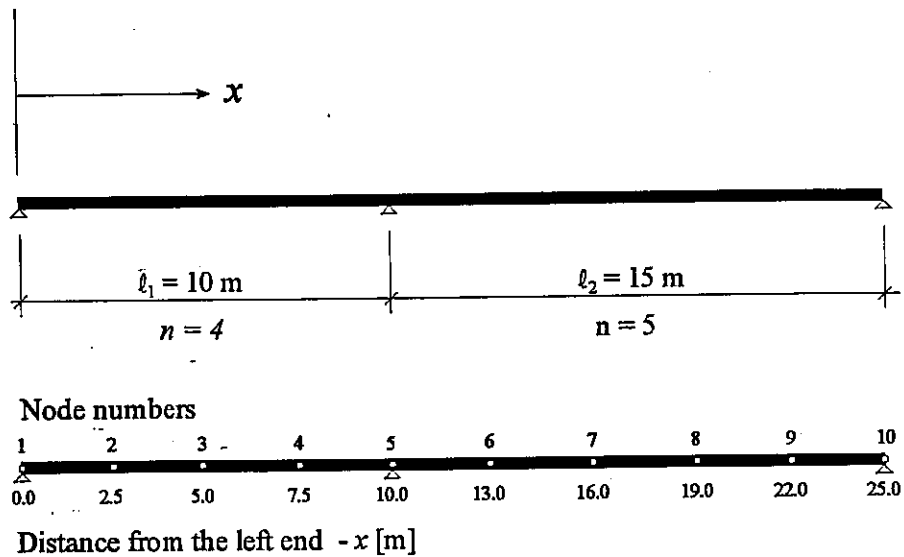


Figure 5.1 Example of node numbering

The program automatically calculates where the element force acts and gives the corresponding equivalent nodal forces for the element. Similarly, uniformly distributed loads may start and end anywhere on the bridge, Figure 5.2. Loaded elements are automatically found and equivalent nodal forces are calculated. However, the uniform load must spread on at least two consecutive elements.

The load due to the self-weight of concrete for the first sequence is then calculated according to the material and section properties for each element. Since concrete is still fresh, no changes in the element stiffness matrices are made. The calculations are similar to those related to the uniform load previously mentioned. If any external load is given, it is treated in the same manner as before. The only difference is that the external loads associated with self-weight of the beam are taken into

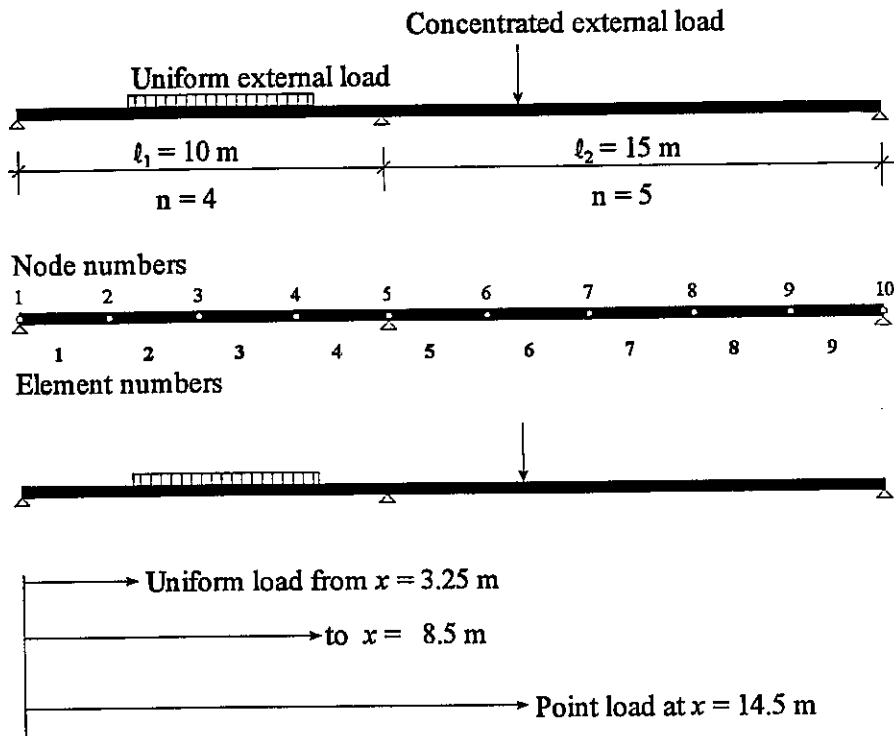


Figure 5.2 Example of load position coordinates

account as dead load acting at all times, while any external loads associated with a given sequence are taken into account only while calculating the given sequence.

Consecutive sequences may then be calculated. This process is similar to that of the first sequence except in one detail. For each sequence, stiffness of each element changes due to the hardening of the previously poured concrete. Since each sequence starts at a specific time, age of concrete for each of the previous sequences is calculated. According to the concrete age, change in element stiffness matrix for each *affected* element is calculated and the stiffness matrix for the system is adjusted. Note that in calculations of the n th sequence of pour, the properties for $n - 1$ previous sequences, each with different concrete age, have to be recalculated, Figure 5.3. The formulae for concrete stiffness as a function of time, for ages greater than 24 hours is taken as [49]:

$$f'_c(t) = f'_c \frac{t^{3/4}}{at^{3/4} + b} \quad (5.1)$$

$$E_c(t) = 4700 \sqrt{f'_c(t)} \quad \text{MPa} \quad (5.2)$$

$$E_c(t) = 57000 \sqrt{f'_c(t)} \quad \text{psi} \quad (5.3)$$

where:

f'_c = 28 day concrete compressive strength, in MPa or psi

t = time in days > 24 hours

$f'_c(t)$ = concrete strength at time t , in MPa or psi

a = 2.8, 3.4, and 1.0 for cement Type I, II, and III, respectively

b = 0.77, 0.72, and 0.92 for cement Type I, II, and III, respectively

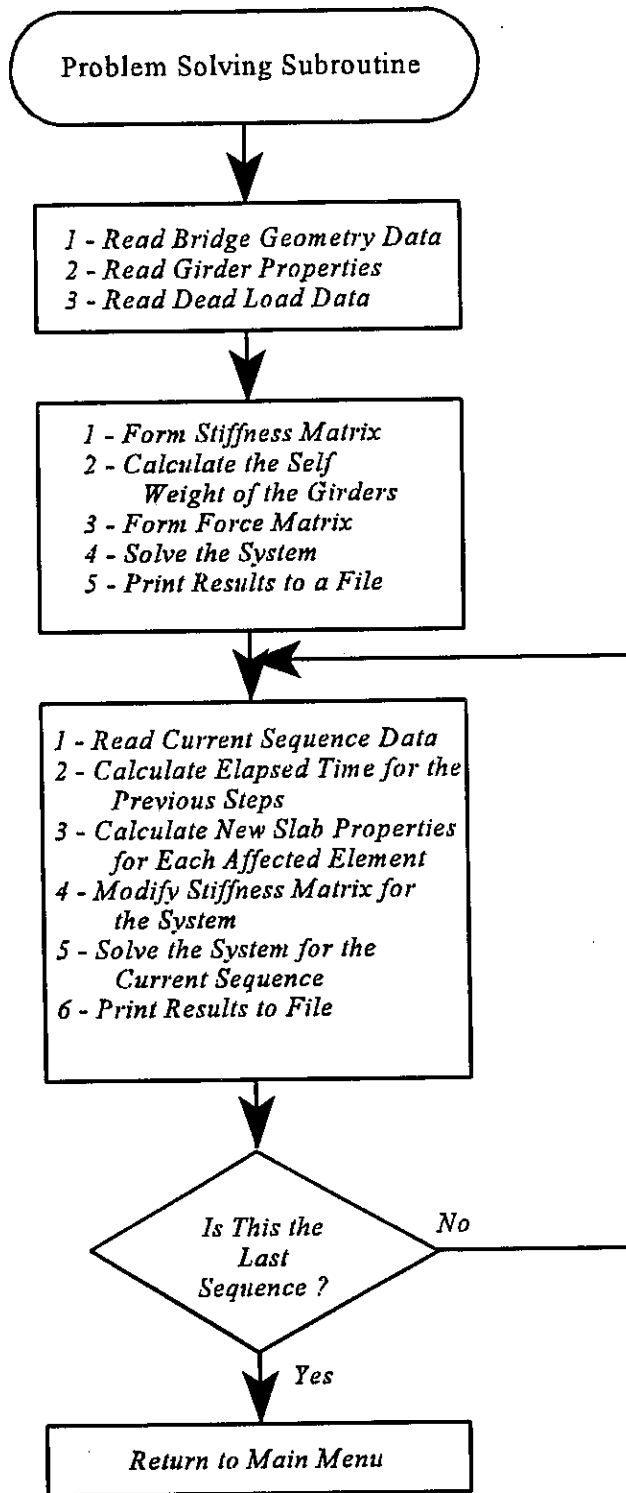


Figure 5.3 System Solving Subroutine Flowchart

Based on the experimental test results, the next procedure was used to calculate the modulus of elasticity for ages between 0 and 24 hours. For less than 4 hours, it had been assumed to be zero. Between 4 and 12 hours, the following equation is proposed for the modulus:

$$E_c(t) = \left(a - \frac{b}{t^2} \right) E_c \quad (5.4)$$

where:

- a = Dimensionless coefficient equal to 0.186
- b = Coefficient equal to 2.93 h²
- $E_c(t)$ = Modulus of elasticity of concrete, in MPa or psi
- t = Age in hours

Since the expression in brackets is dimensionless, units for the modulus of elasticity as a function of time are the same units used for the modulus of elasticity E_c in Eqs. 5.2 and 5.3. Equation 5.4 is preliminary and needs more testing for verification.

The system is solved for each sequence of pour and the results are printed into a file. Note that the program creates two temporary files, which are automatically deleted upon program completion. If the program was stopped during execution for any reason, these files would not be deleted. However, they will be deleted the first time the system is solved using *the same* file. Several steps are followed in solving the system of equations. The preprocessor prepares the system of equations to be solved and gives the formatted output from the input file as well as preprocessed data to the output file. In the second step, the system is solved for the current stage and prints the results to the same output file. It includes the results that correspond to the current load, as well as the

results for the combined total loads. This process is repeated as long as the last sequence is not completed.

5.3 Results of Program Executions

The program was run using data for existing structures. The goal was to examine the maximum curvatures and deflections on several bridges and compare them to the maximum values that fresh concrete may sustain before it cracks.

The bridge properties used are given in Table 5.1. Data for a total of five bridges and an average of three different sequences of pour are calculated for each bridge. Only two types of loads are considered on the structure; the self-weight of the supporting beam and the weight of the concrete. Sequence of pour was divided into sections between 4 and 24 hours. The order of sequence on a particular bridge is shown in Tables 5.2 and 5.3 and illustrated in typical figures, i.e., Figures C.13 and C.14. The influence of each sequence of pour on the *previously* poured partially hardened concrete was of primary interest, while curvatures that resulted in compression of concrete were not significant. Curvatures that result in tension of concrete were found as expected in the regions over the supports, except in a few cases where midspan had uplift. However, curvatures in those cases were negligible.

TABLE 5.1

BASIC PROPERTIES OF EXAMINED BRIDGES

Bridge designation	Span lengths			Beam Properties		Slab Properties		Beam to Slab Distance c-c
	1	2	3	Area	M. of Inertia	Area	M. of Inertia	
	m (ft)			10^{-4} m^2 (in. ²)	10^{-6} m^4 (in. ⁴)	10^{-4} m^2 (in. ²)	10^{-6} m^4 (in. ⁴)	m (in.)
AL-2	9 (30)	18 (60)		91.1 (14.7)	257 (659)	1380 (221)	519.5 (1330)	0.310 (12.38)
AL-3	9 (30)	9 (30)	9 (30)	91.1 (14.7)	257 (659)	1380 (221)	519.5 (1330)	0.310 (12.38)
OT-3	14.63 (48)	14.86 (48.75)	14.63 (48)	239 (37.0)	2621 (6297)	9330 (1446)	3474 (8346)	0.526 (20.71)
IN-3	21 (70)	21 (70)	18 (60)	276 (44.2)	3531 (9040)	3930 (630)	1570 (4020)	0.558 (22.30)
NW-3	9 (30)	18 (60)	9 (30)	125 (20)	578 (1480)	2680 (429)	590 (1510)	0.345 (13.81)

In the case of one bridge, designated AL2, each sequence of pour was modeled in two ways. First, each sequence was treated as one step (Figure C.13). Then, each sequence was represented by a higher number of smaller sequences, Table 5.3. For example, the time needed to cover the length of 9 m (30 ft) at time zero had been taken as 8 hours in the first case. In the second case, the same step was modeled as two separate steps. One step was assumed for the period of 4 hours, covering 4.5 m (15 ft), at time zero. The second step was assumed to cover the remaining 4.5 m (15 ft) for the period of 4 hours, immediately following the previous step. The aim was to determine if there was any change in the results. The results for both cases differed by less than two percent (Table 5.4, Figures C.16 and C.18). Since each sequence was taken for a maximum of eight hours, this was expected. Concrete was only four hours old if the sequence was divided into two equal parts. Presumably, concrete at such early ages could not change significantly the total stiffness of a bridge. However, combining sequences of more than 8 hours old may yield unreliable results due to

the fact that concrete stiffness increases much faster after the age of 5 hours. Comparison of the results for the same bridge and the same order of sequences, taking different construction times, revealed no significant difference. In the first case, the period between the beginning of each sequence was assumed to be 24 hours, and in the second it was 8 hours. Although, the plots showed a different bridge behavior, the maximum curvature over the support was practically the same (Table 5.4, Figures C.19 and C.20). The difference between this value and the previously calculated value was less than 0.1 percent. Changing the order of pour sequence, i.e., starting the pour from the right end instead of the left end, showed a drastic reduction of curvature. The maximum value for this case was about 3.7 times smaller than the highest calculated value for the bridge.

The highest curvature value was found to be in the vicinity of $16 \times 10^{-7} \text{ mm}^{-1}$ ($4 \times 10^{-5} \text{ in.}^{-1}$) in the case of the asymmetrical (9 + 18 m (30 + 60 ft)), bridge (Table 5.4 and Figure C.20). For the bridges with three equal spans, the highest calculated values were approximately $12 \times 10^{-7} \text{ mm}^{-1}$ ($3 \times 10^{-5} \text{ in.}^{-1}$) (Table 5.4). Comparing this value with a value required to crack the fresh concrete reported by Hilsdorf and Lott [21], which is one order of magnitude higher, we may conclude that there is no danger of concrete cracking. However, Hilsdorf and Lott's experiments were performed under static loading and that value may be considered too high for concrete under dynamic loading. A much lower value of $13.2 \times 10^{-7} \text{ mm}^{-1}$ ($3.3 \times 10^{-5} \text{ in.}^{-1}$) was reported in the case of the dynamically loaded specimens, which is close to the calculated values [14]. Also, the different sequences of pour on the same bridge gave significantly different curvature values (Table 5.4, Figures C.21 and C.22). Any additional load introduced on the structure during any sequence of pour may increase the calculated values, hence increasing the likelihood of crack formation.

TABLE 5.2

SEQUENCES OF CONCRETE POUR, SI UNITS

Bridge sequence		Sequence 1		Sequence 2		Sequence 3		Sequence 4		Sequence 5		Sequence 6	
		Position	t										
		(m)	(h)										
AL-2	a	0-9.1	0	9.1-18.3	24	18.3-27.4	48						
	aa	0-4.6	0	4.6-9.1	4	9.1-13.7	20	13.7-18.3	24	18.3-22.9	44	22.9-27.4	48
	b	0-9.1	0	9.1-18.3	4	18.3-27.4	8						
	c	0-13.7	0	13.7-27.4	24								
	cc	0-6.9	0	6.9-13.7	4	13.7-20.4	20	20.6-27.4	24				
	d	13.7-90	0	0-13.7	24								
AL-3	a	0-9.1	0	9.1-18.3	24	18.3-27.4	48						
	b	0-9.1	0	18.3-27.4	24	9.1-18.4	48						
	c	0-6.9	0	6.9-13.7	24								
OT-3	a	0-14.6	0	14.6-29.5	24	29.5-45.3	48						
	b	0-14.6	0	29.5-45.3	24	14.6-29.5	48						
	c	14.6-29.5	0	0-14.6	4	29.5-44.1	8						
IN-3	a	0-15.2	0	15.2-30.5	8	30.5-45.7	16	45.7-61.0	24				
NW-3	a	9.1-27.4	0	0-9.1	12	27.4-36.6	24						
	b	0-12.2	0	12.2-24.4	12	24.4-36.6	24						
	c	27.4-36.6	0	0-9.1	12	9.1-27.4	24						
	d	0-18.3	0	18.3-36.6	12								

TABLE 5.3

SEQUENCES OF CONCRETE POUR, IN-LB UNITS

Bridge sequence		Sequence 1		Sequence 2		Sequence 3		Sequence 4		Sequence 5		Sequence 6	
		Position	t	Position	t	Position	t	Position	t	Position	t	Position	t
		(ft)	(h)	(ft)	(h)	(ft)	(h)	(ft)	(h)	(ft)	(h)	(ft)	(h)
AL-2	a	0-30	0	30-60	24	60-90	48						
	aa	0-15	0	15-30	4	30-45	20	45-60	24	60-75	44	75-90	48
	b	0-30	0	30-60	4	60-90	8						
	c	0-45	0	45-90	24								
	cc	0-22.5	0	22.5-45	4	45-67.5	20	67.5-90	24				
	d	45-90	0	0-45	24								
AL-3	a	0-30	0	30-60	24	60-90	48						
	b	0-30	0	60-90	24	30-60	48						
	c	0-45	0	45-90	24								
OT-3	a	0-48	0	48-96.75	24	96.75-148.75	48						
	b	0-48	0	96.75-148.75	24	48-96.75	48						
	c	48-96.75	0	0-48	4	96.75-144.75	8						
IN-3	a	0-50	0	50-100	8	100-150	16	150-200	24				
NW-3	a	30-90	0	0-30	12	90-120	24						
	b	0-40	0	40-80	12	80-120	24						
	c	90-120	0	0-30	12	30-90	24						
	d	0-60	0	60-120	12								

TABLE 5.4

**MAXIMUM CURVATURE IN PREVIOUSLY POURED CONCRETE
IMPOSED BY CURRENT SEQUENCE OF POUR**

Bridge		Units	Sequence				
			2	3	4	5	6
AL-2	a	$\times 10^{-7} \text{ mm}^{-1}$ ($\times 10^{-5} \text{ in.}^{-1}$)	3.5 (0.89)	11 (2.8)			
	aa	$\times 10^{-7} \text{ mm}^{-1}$ ($\times 10^{-5} \text{ in.}^{-1}$)	5.0 (1.3)	3.5 (0.89)	5.0 (1.3)	10 (2.5)	16 (4.1)
	b	$\times 10^{-7} \text{ mm}^{-1}$ ($\times 10^{-5} \text{ in.}^{-1}$)	2.0 (0.51)	16 (4.1)			
	c	$\times 10^{-7} \text{ mm}^{-1}$ ($\times 10^{-5} \text{ in.}^{-1}$)	4.0 (1.0)				
	cc	$\times 10^{-7} \text{ mm}^{-1}$ ($\times 10^{-5} \text{ in.}^{-1}$)	4.0 (1.0)	4.0 (1.0)	16 (4.1)		
	d	$\times 10^{-7} \text{ mm}^{-1}$ ($\times 10^{-5} \text{ in.}^{-1}$)	4.0 (1.0)				
AL-3	a	$\times 10^{-7} \text{ mm}^{-1}$ ($\times 10^{-5} \text{ in.}^{-1}$)	7.5 (1.9)	3.0 (0.76)			
	b	$\times 10^{-7} \text{ mm}^{-1}$ ($\times 10^{-5} \text{ in.}^{-1}$)	6.0 (1.5)	4.0 (1.0)			
	c	$\times 10^{-7} \text{ mm}^{-1}$ ($\times 10^{-5} \text{ in.}^{-1}$)	4.5 (1.1)				
OT-3	a	$\times 10^{-7} \text{ mm}^{-1}$ ($\times 10^{-5} \text{ in.}^{-1}$)	9.0 (2.3)	7.5 (1.9)			
	b	$\times 10^{-7} \text{ mm}^{-1}$ ($\times 10^{-5} \text{ in.}^{-1}$)	3.0 (0.76)	7.0 (1.8)			
	c	$\times 10^{-7} \text{ mm}^{-1}$ ($\times 10^{-5} \text{ in.}^{-1}$)	9.0 (2.3)	9.5 (2.4)			
IN-3	a	$\times 10^{-7} \text{ mm}^{-1}$ ($\times 10^{-5} \text{ in.}^{-1}$)	0.40 (0.10)	0.40 (0.10)	0.40 (0.10)		
NW-3	a	$\times 10^{-7} \text{ mm}^{-1}$ ($\times 10^{-5} \text{ in.}^{-1}$)	10 (2.5)	5.0 (1.3)			
	b	$\times 10^{-7} \text{ mm}^{-1}$ ($\times 10^{-5} \text{ in.}^{-1}$)	2.0 (0.51)	6.5 (1.7)			
	c	$\times 10^{-7} \text{ mm}^{-1}$ ($\times 10^{-5} \text{ in.}^{-1}$)	4.5 (1.1)	1.5 (0.38)			
	d	$\times 10^{-7} \text{ mm}^{-1}$ ($\times 10^{-5} \text{ in.}^{-1}$)	3.0 (0.76)				

5.4 Description of Two Selected Bridges

Data for the two bridges furnished by the Illinois Department of Transportation (IDOT) were used to examine the influence of sequence of pour on the maximum curvature in the concrete. Both bridges were composite structures, one supported on steel plate girders, and the other supported by prestressed AASHTO beam girders.

The steel girder geometric section properties used in the calculations are given in Table 5.5, while the geometric section properties for the prestressed concrete girder are given in Table 5.6. The third column presents the distance from the center of gravity of the girder to the center of gravity of the slab. In both bridges, the modulus of elasticity E_c for the slab was based on an $f'_c = 24$ MPa. In the case of the prestressed concrete girder bridge, the modulus of elasticity E_c of the girder was based on $f'_c = 50$ MPa. Both bridges were modeled as three-span continuous bridges. The span lengths are given in Table 5.7.

5.5 Description of Sequences of Pour

Two distinct pouring sequences were examined for both bridges. It was first assumed that the positive moment regions of the concrete bridge deck were poured first, followed by pours on the regions of the deck over the supports. This case has been reported to occur on some occasions. The second sequence scheme assumed that the concrete deck was cast starting from the "left" side of the bridge and proceeded towards the "right" side of the bridge. The exact locations of each sequence of pour are given in Table 5.8 for both bridges. These locations are also presented in Figures C.26-C.29 for the steel girder bridge, and in Figures C.30-C.33 in the case of the prestressed concrete girder bridge. No other loads were considered on the bridge at this stage.

A sequence refers to the cumulative pours applied at a specified instance. For example, sequence two refers to the combined effect of pours one and two, etc. However, the order of pour is controlled by that respective sequence. A pour is related to an individual concrete pour at the specified time of application. Sequence number one is always associated with pour number one since at that instance only the initial concrete pour is applied. In some illustrations, various pours are added to show their cumulative effect on the deflection or curvature in previously poured concrete due to the the latest pour.

TABLE 5.5
STEEL PLATE GIRDER BRIDGE SECTION PROPERTIES

Element Number	Area	Moment of Inertia	Distance c-c	Element Number	Area	Moment of Inertia	Distance c-c
	m ²	m ⁴	m		m ²	m ⁴	m
1	0.064032	0.033292	0.111700	35	0.066440	0.065192	0.151100
2	0.064764	0.035268	0.114200	36	0.066440	0.065192	0.151100
3	0.065496	0.037311	0.116800	37	0.066440	0.065192	0.151100
4	0.066228	0.039421	0.119300	38	0.066440	0.065192	0.151100
5	0.066960	0.041601	0.121800	39	0.066440	0.065192	0.151100
6	0.067692	0.043850	0.124300	40	0.066440	0.065192	0.151100
7	0.068424	0.046169	0.126800	41	0.066440	0.065192	0.151100
8	0.069156	0.048559	0.129300	42	0.088620	0.098140	0.143200
9	0.069888	0.051021	0.131700	43	0.088620	0.098140	0.143200
10	0.070620	0.053556	0.134200	44	0.088620	0.098140	0.143200
11	0.071352	0.056164	0.136700	45	0.088620	0.098140	0.143200
12	0.063584	0.048827	0.139200	46	0.088620	0.098140	0.143200
13	0.064316	0.051170	0.137200	47	0.088620	0.098140	0.145300
14	0.065048	0.053579	0.139600	48	0.130620	0.173559	0.145300
15	0.065780	0.056057	0.142000	49	0.130620	0.173559	0.145300
16	0.092326	0.093974	0.144400	50	0.130620	0.173559	0.145300
17	0.093150	0.097956	0.133600	51	0.095620	0.110476	0.142700
18	0.093973	0.102028	0.138200	52	0.094936	0.106920	0.140900
19	0.094797	0.106203	0.140500	53	0.094252	0.103432	0.138900
20	0.095620	0.110476	0.142700	54	0.093568	0.100012	0.137100
21	0.103062	0.173559	0.145300	55	0.092884	0.096659	0.135100
22	0.103062	0.173559	0.145300	56	0.066400	0.058209	0.146500
23	0.103062	0.173559	0.145300	57	0.065792	0.056098	0.144500
24	0.088620	0.098140	0.142300	58	0.065184	0.054035	0.142500
25	0.088620	0.098140	0.142300	59	0.064576	0.052018	0.140500
26	0.088620	0.098140	0.142300	60	0.072468	0.060283	0.142900
27	0.088620	0.098140	0.142300	61	0.071860	0.058018	0.140900
28	0.088620	0.098140	0.142300	62	0.071252	0.055803	0.138800
29	0.066440	0.065192	0.151100	63	0.070644	0.053640	0.136800
30	0.066440	0.065192	0.151100	64	0.070036	0.051528	0.134700
31	0.066440	0.065192	0.151100	65	0.069428	0.049466	0.132700
32	0.066440	0.065192	0.151100	66	0.068820	0.047153	0.130600
33	0.066440	0.065192	0.151100	67	0.068212	0.045490	0.128500
34	0.066440	0.065192	0.151100	68	0.067604	0.043576	0.126500
35	0.066440	0.065192	0.151100	69	0.066996	0.041710	0.124400
36	0.066440	0.065192	0.151100	70	0.066338	0.039892	0.122300
Slab	0.502100	0.001591					

TABLE 5.6
PRESTRESSED CONCRETE GIRDER BRIDGE SECTION PROPERTIES

Element Number	Area	Moment of Inertia	Distance c-c
	m ²	m ⁴	m
All Elements	0.37760	0.08869	0.78400
Slab	0.39975	0.00127	

TABLE 5.7
SPAN LENGTHS

Bridge	Span 1	Span 2	Span 3
	m (ft)	m (ft)	m (ft)
Steel Girder	71.55 (234.74)	90.68 (297.51)	71.55 (234.74)
Prestressed Concrete	29.48 (96.72)	29.48 (96.72)	29.48 (96.72)

TABLE 5.8
SEQUENCE POSITIONS AND TIME

Bridge	Sequence									
	1		2		3		4		5	
	from - to m (ft)	t h	from - to m (ft)	t h	from - to m (ft)	t h	from - to m (ft)	t h	from - to m (ft)	t h
Steel Bridge positive moment first	86.55-147.23 (288.5-490.77)	0	0-50.0 (0-166.67)	6	183.78-233.78 (612.6-779.27)	72	147.23-183.78 (490.77-612.6)	76	50.0-86.55 (166.67-288.5)	80
Steel Bridge from the left end	0-50.0 (0-166.67)	0	50.0-86.55 (166.7-288.5)	6	86.55-147.23 (288.5-490.77)	72	147.23-183.78 (490.77-612.6)	76	183.78-233.78 (612.6-779.27)	80
Concrete Bridge positive moment first	33.98-54.42 (113.27-181.4)	0	0-22.0 (0-73.33)	6	66.4-88.4 (221.33-294.67)	72	54.42-66.4 (181.4-221.33)	76	22.00-33.98 (73.33-113.27)	80
Concrete Bridge from the left end	0-22.0 (0-73.33)	0	22.00-33.98 (73.3-113.27)	6	33.98-54.42 (113.27-181.4)	72	54.42-66.48 (181.4-221.33)	76	66.48-88.4 (221.33-294.67)	80

5.6 Results of Program Execution

The output from the program was used to plot graphs that present curvatures in the concrete due to the self-weight of concrete. Two plots are given for each bridge and each sequence of pour. The first plot presents the influence of concrete weight for each individual sequence, and the second presents the influence of the concrete weight combining all sequences. Figures C.34-C.37 correspond to the steel girder bridge, while Figures C.38-C.41 correspond to the prestressed concrete girder bridge.

Inspection of these plots revealed that the maximum curvatures in the previously poured concrete due to self-weight of the sequential pours are small when positive regions were cast prior to sections over support. The maximum values found were approximately 1.0 and $0.8 \times 10^{-7} \text{ mm}^{-1}$ (0.25 and $0.8 \times 10^{-5} \text{ in.}^{-1}$) for the steel and concrete girder bridges, respectively, as shown in Table 5.9. This is significantly less than the curvature needed to crack dynamically loaded concrete specimens.

TABLE 5.9
MAXIMUM CURVATURE IN PREVIOUSLY Poured CONCRETE
IMPOSED BY CURRENT SEQUENCE OF POUR

Bridge	Units	Sequence			
		2	3	4	5
Steel Bridge positive moment first	$\times 10^{-7} \text{ mm}^{-1}$ ($\times 10^{-5} \text{ in.}^{-1}$)	1.0 (0.25)	0.90 (0.22)	0.40 (0.10)	0.40 (0.10)
Steel Bridge from the left end	$\times 10^{-7} \text{ mm}^{-1}$ ($\times 10^{-5} \text{ in.}^{-1}$)	0.50 (0.12)	2.3 (0.56)	0.30 (0.06)	1.9 (.48)
Concrete Bridge positive moment first	$\times 10^{-7} \text{ mm}^{-1}$ ($\times 10^{-5} \text{ in.}^{-1}$)	0.80 (0.2)	0.80 (0.2)	0.20 (0.05)	0.20 (0.05)
Concrete Bridge from the left end	$\times 10^{-7} \text{ mm}^{-1}$ ($\times 10^{-5} \text{ in.}^{-1}$)	0.20 (0.05)	1.0 (0.24)	0.20 (.04)	1.2 (0.30)

However, curvature values in the concrete when the deck was cast from the "left" side of the bridge were significantly greater. The maximum calculated curvatures were 2.3 and $1.2 \times 10^{-7} \text{ mm}^{-1}$ (0.56 and $0.3 \times 10^{-5} \text{ in.}^{-1}$) for the steel and concrete girder bridges, respectively. The increase is particularly high for the steel girder bridge due to the fact that this bridge has unequal span lengths. The middle span is 27 percent longer than the exterior spans. High curvatures over the first interior support is the consequence of the concrete weight that is imposed on this span.

The calculated curvatures for these bridges are smaller than the curvatures needed to crack dynamically loaded fresh concrete in a laboratory environment. However, significant differences in curvatures for the different sequences of pour confirm the importance of initiating the sequence of pour in the positive moment regions prior to the negative moment regions. It was experimentally determined for concrete without additives and concrete with super-plasticizer, that the minimum curvature required to crack the specimens was reached at five hours and its value was $81 \times 10^{-7} \text{ mm}^{-1}$ ($20.3 \times 10^{-5} \text{ in.}^{-1}$). This value increased to $123 \times 10^{-7} \text{ mm}^{-1}$ ($30.7 \times 10^{-5} \text{ in.}^{-1}$) at 8 hours, and $177 \times 10^{-7} \text{ mm}^{-1}$ ($44.3 \times 10^{-5} \text{ in.}^{-1}$) at 12 hours. The curvature obtained at 12 hours was smaller than that reported by Hilsdorf and Lott [21] ($390 \times 10^{-7} \text{ mm}^{-1}$).

6. CATEGORIZATION OF VARIOUS TYPES OF LOADS AND VIBRATIONS

6.1 Introduction

One of the objectives of this study was to categorize the various loads and vibrations associated with concrete at early ages. As a result, the information obtained from previous chapters was summarized and grouped in accordance with the relevant aspects. However, prior to the categorization, a brief description of the effects of construction loads and vibrations are presented here.

Hydration of cement in concrete starts the moment water is added to the concrete mixture. About fifty percent of the cement hydrates in the first three days (Type I portland cement). Nevertheless, the process of hydration may continue for months, if not years. However, the most critical period is during early strength development. A specific amount of water is needed to completely hydrate the cement. Realistically, loss of water is expected, hence an increase in the water amount is needed due to:

- Evaporation of water — during mixing and transportation, as well as during construction.
- Porosity of aggregate — porous aggregate may soak up water from the mixture and decrease the amount of water left for hydration.
- Porosity of forms or existing structure — dry, porous forms may soak up water. It is less dangerous due to the limited exposed surface of forms compared to the total area of aggregates.
- Amount of fines in aggregate — if the amount of fines in the aggregate mixture is higher than prescribed, extra water is needed to provide enough water for hydration and to maintain workability.

However, it seems that the greatest amount of water is added to maintain the desired workability. This amount is not used for hydration purposes and usually bleeds to the surface, which causes settlement of the concrete. Extreme settlement may cause cracking of concrete. If the obstructions in the concrete, i.e., reinforcing steel, void forms, etc., are present it will not allow the concrete above it to subside. At these locations, settlement of concrete may introduce tensile stresses in the concrete above the obstruction. A typical example of this is the cracking over the top reinforcing bars, which is sometimes referred to as pattern cracking. This effect may be reduced by:

- Increasing the concrete cover, particularly over the top reinforcement. It appears that a minimum cover of 50 mm (2 in.) is needed to prevent cracking due to a subsidence.
- Decreasing bar sizes. Smaller bars at smaller distances are preferred over bigger bars at higher distances. A 50 mm (2 in.) cover over the top reinforcement is sufficient for the concrete to resist cracking for all but bigger size bars.
- Thorough vibration of concrete. Dangers of overvibrating the concrete are minuscule in comparison to undervibrating.
- Reducing the concrete slump.

Since it is unusual that the amount of water added to the concrete is insufficient, extra efforts should be made to keep the water content to a minimum. Adding water at the construction site should be prohibited. The reason for this is not only the detrimental effect of extra water in fresh concrete (sensitivity to vibrations, cracking due to increased subsidence, etc.), but also the fact that retempered concrete (concrete to which water is added some time after mixing) shows a significant decrease in strength. Use of high slump concrete must be avoided. In fact many codes discourage the use of concrete with a slump of more than 63 to 75 mm (2.5 to 3 in.). The recommended slump should be in the vicinity of 50 mm (2 in.). An increased slump may not only increase the probability

of pattern cracking, but may decrease bond strength between the concrete and the reinforcing bars. It should be mentioned that low slump concrete is less vulnerable to the effects of vibrations as well. The influence of concrete properties at the early ages, particularly concrete tensile strength, on its behavior are of great importance. Concrete passes through several stages before it reaches the necessary design strength and necessary levels in other properties. At first, concrete is in a plastic state and at that stage it is not particularly vulnerable to any external loads imposed upon it. As concrete starts to harden, its modulus of elasticity increases over time and it becomes sensitive to external, as well as internal, influences. Since stresses in concrete due to external loads are proportional to the concrete modulus of elasticity, they increase with an increase in the modulus of elasticity. However, at very early ages, approximately 3 to 5 hours after mixing, the modulus of elasticity increases more rapidly than the concrete strength. This is the period when the concrete may "attract" more stresses than it can tolerate. After approximately ten hours, this trend changes and strength increases more rapidly than the modulus of elasticity, making it less vulnerable to the external stresses. That is why any load that may be imposed on the structure in the hours immediately following a pour must be carefully examined.

Loads due to the weight of forms and similar dead loads are usually known with a relatively high degree of accuracy. Deflections due to these loads may be calculated and easily taken into account. Since these loads are imposed on the structure before concrete is poured, they do not introduce stresses in the concrete and, accordingly, they do not present any danger to the concrete. However, it seems that these deflections may be overestimated. Inaccurately estimated deflections may lead to insufficient deck thickness and insufficient steel cover, which may present danger not to the concrete as a material but to the integrity of the structure as a whole.

Loads due to fresh concrete weight are of special interest since they may be the greatest of all at the early stages of construction. In fact, stresses on a previously poured and partially hardened concrete introduced by new pours are important. Visits to a bridge under construction in Burlington, Iowa, revealed several factors that may be attributed to concrete cracking. Vibrations due to adjacent traffic and machinery were clearly observed at the construction site, which may have induced hairline cracks in the deck. Finishing was also a problem as a result of workmanship inconsistencies. Certain sections of the cast-in-place deck exhibited crack formation that were credited to sequence of concrete pouring.

In some instances, part of the finished deck is used as storage for the material to be used in the future or for the necessary construction machinery. This may present danger in several ways:

- The influence of weight of such equipment and material to a structure as a whole. Since concrete on some parts of the structure may still be very weak, as previously explained, deflections and stresses invoked by such loads present danger. The potentially vulnerable zones are above the supports of continuous span bridges due to the invoked tensile stresses. It appears that zones under compression stresses are not in danger compared to tension zones.
- The local influence of the weight of materials and equipment on the concrete deck. Some machines and materials may present small loads on the structure as a whole. However, due to the small dimensions of the supporting elements (wheels, wood blocks, etc.), these loads may introduce high localized surface stresses on the concrete. This may lead to a punching failure of the concrete. Even if the equipment is adequately supported by, for example, a larger block of wood, they may present danger for the concrete slab. In case that equipment

is located between the girders, or on the overhangs, it may introduce high forces to concrete which has not reached its design strength.

- Construction machinery may produce vibrations which could spread through the structure influencing fresh concrete. The influence of the vibration is, however, discussed later.

The temperature in the concrete is the result of a combination of separate phenomena, namely: heat of hydration, environmental temperature (air temperature), and solar radiation. None of these parameters may be treated separately. Higher heat of hydration or solar radiation may be desired during winter concreting, and may have disastrous consequences during the summer. The temperature affects a concrete deck in terms of the properties of fresh and hardened concrete, and the deformation of the structure.

Concrete placed on a hot supporting structure during a hot day may develop a high temperature that may lead to inadequate concrete properties due to incomplete hydration. Furthermore, in combination with direct sunlight, lack of protection, and inadequate curing causes cracking in the concrete. Cracking of the concrete due to high temperature differences between the inside and face of the concrete is generally not a problem since the concrete deck thickness is limited. Adequate curing and preparation is extremely important. To minimize the effects of warm weather on concreting, it is recommended that concreting be planned during the periods of decreased temperatures, as overnight or during morning. The following may be necessary for hot-weather concreting:

- Adding ice during mixing.
- Dampening the aggregate before use, especially if the aggregate is porous.
- Thorough dampening of forms and/or supporting structure, as well as reinforcing steel with water.

- Protecting concrete from direct sunlight.
- Limiting evaporation with covers or protective barriers.
- Regular dampening of concrete to keep it wet.
- Use of retarders.

It is not possible to separate each of these procedures since they are interconnected. However, lowering the concrete mix temperature prior to its use reduces its maximum temperature. Use of Type III concrete should be avoided since its heat of hydration is high. During hot days, temperature of the forms and reinforcing steel may be very high. Pouring of concrete directly over such warm elements will increase its temperature. Even if the influence is localized, such as in the case of a concrete surrounding warm reinforcing bars, it should not be neglected. Dry forms may soak water from the concrete, reducing the quantity left for proper cement hydration. Direct sunlight may raise the already high temperature in the concrete. Note that the high rate of evaporation may lead to severe cracking of concrete due to shrinkage. Concrete must be protected against it with a protective barrier, such as wet burlap, curing membrane, vinyl covers, or other measures. However, the burlap must be kept wet at all times. Failure to do so may in fact increase the temperature of the concrete since burlap acts as an insulation. Curing membranes are effective if applied according to the manufacturers directions, i.e., coverage must be sufficient and uniform. Effectiveness of polyethylene sheets is a subject of disagreement. Although it protects concrete from drying, it also increases its temperature. Regular dampening of concrete until it reaches the design strength is of vital interest. It not only helps concrete reach its desired strength, but it also reduces shrinkage cracking. Dampening should be started as soon as possible after setting. Retarders should be used whenever possible, since they slow down the process of hydration and the maximum concrete temperature is lowered. However, it was reported that prolonged mixing of retarded concrete may

in fact increase the rate of hydration, which is the opposite of what is needed. Since not all retarders have the same chemical composition, further studies are needed to confirm this effect.

In contrast to the procedures applied during hot weather, concreting procedures during cold weather should increase the temperature of the concrete. The use of cements with higher heat of hydration is recommended. Whenever it is possible, concrete should be placed in periods of sunny weather. Insulated concrete covers should be used to keep heat produced by hydration and to protect it from drying.

It should be noted that wind may greatly influence the temperature of the concrete, as well as the rate of evaporation. On windy days, temperature differences in the structure are lower than during calm days. However, it is more significant that wind drastically increases the rate of evaporation. At air temperatures over 35°C (95°F) and concrete temperatures over 50°C (122°F), even light wind may cause a high rate of evaporation. Higher winds may have this effect on the lower temperatures. During cold weather, wind may decrease the temperature of concrete, which may lead to inadequate concrete properties. In both cases, if wind combined with very high or very low temperatures is expected, wind barriers should be erected to protect the concrete. To minimize the effects of cold weather, concreting should be planned during the day. Windy days in both cases should be avoided if possible.

Temperature differential between the top and bottom of the beams may introduce stresses into a structure during construction, but these stresses usually are not of a great concern. However, deflections due to thermal changes are of great importance. Due to these deflections, screeding machines may not maintain proper deck thickness during construction. Deck thickness deficiency may be expected at midspan. Since the top reinforcement is held at proper locations from the forms, this yields insufficient cover thickness.

Vibration due to adjacent traffic may present a problem to fresh concrete. Under its influence, bond between concrete and reinforcing steel can be degraded. However, this is noticed in a narrow region close to the joint between the new and old deck only, particularly in case of the dowels protruding from the old to new concrete. Dowels with 90° hooks have the worst bond to concrete. Straight dowels and reinforcing bars protruding out from the old concrete are in better condition. However, a decrease in the concrete properties, such as strength, air content, etc., due to adjacent traffic vibrations is not noticed. In fact most of the laboratory studies showed an increase in the concrete strength due to prolonged vibration. Longitudinal cracks between the new and old deck exist in almost all widened or rehabilitated bridges where traffic is maintained during construction. These cracks are generally in good condition and did not present any problem to the structure. In some cases, settlement cracking of concrete due to adjacent traffic is reported. However, studies showed that it occurred when concrete had not been adequately compacted during construction. This is consistent with the studies showing that undervibrated concrete may be vulnerable to the cracking. This cracking is very often related to the location of reinforcement. Pattern cracks were found directly over the top reinforcement. This cracking may be affected by the location of the top reinforcement and the thickness of the concrete cover. The concrete above the reinforcing steel with a cover of less than 50 mm (2 in.) appears to be sensitive to settlement cracking. The probability of cracking increases with depth of the deck and size of the reinforcing bar, and with decreasing concrete cover. If the concrete is atop undervibrated concrete, settlement may be more pronounced with the presence of traffic vibration leading to cracking.

Displacements due to adjacent traffic have the greatest effect in the transverse direction, over the beam closest to the joint. Curvatures of the concrete are the greatest there, but no detrimental effects to the concrete were found. However, reinforcing steel may be displaced and have inadequate

cover. To eliminate this as well as reduce free vibration of the reinforcing bars, it is recommended to securely tie all reinforcement. Reinforcement that was left protruding out of the old concrete is preferred over dowels, and straight bars are preferred over bars with hooks.

Bridge vibrations due to adjacent traffic are influenced by several factors. The most critical are: bridge length, vehicle weight, vehicle suspension characteristics, surface roughness, and speed. Modes of vibration are determined primarily by the bridge length. However, amplitudes depend on the other four factors. Personal vehicles are too light to significantly influence bridge vibrations. This influence increases with the weight of the vehicle, its speed, and roughness of the driving surface. Heavy trucks seem to have a major influence on the amplitude of bridge vibration. Its effect is also influenced by the characteristics of the vehicle suspension, as well as suspension, tire, and deck interface. This leads to a recommendation to limit the speed of traffic over the bridge during widening. Influence of the deck roughness on bridge vibrations is determined not only by amplitude but also by period. If the period is close to that of the bridge, wheels push the bridge in the same direction in a repetitive pattern in accordance with the bridge natural frequency. This resonant effect may drastically increase the influence on the bridge.

6.2 Categorization

The most important factor of categorization is to determine which factors contribute the most to bridge deck cracking. The factors influencing the cracking of concrete bridge decks are (in descending order of importance):

1. High evaporation rate, hence high magnitude of shrinkage, as a result of inadequate concrete curing procedures during hot weather conditions, especially at very early concrete ages. This effect is attributed to:

- lack of concrete protection
 - inadequate uniform coverage with a curing compound
 - delay of concrete protection application
2. Use of high slump concrete.
 3. Excessive amount of water in the concrete as a result of:
 - inadequate mix proportions
 - retempering of concrete
 4. Insufficient top reinforcement cover due to:
 - inadequate reinforcing detail plans
 - improper placement of reinforcement
 - insufficient deck depth due to deflections during construction
 5. Insufficient vibration of the concrete.
 6. Inadequate reinforcing details of the joint between the new and old deck.
 7. Sequence of pour.
 8. Weight and vibration of machinery.
 9. Weight of the forms.
 10. Deflection of forms.

Note that although vibrations due to different sources are not directly included in the previous list, their influence is given through other categories such as slump and reinforcement cover.

The following sections present a more detailed description of the reasons for concrete bridge deck cracking. They may be divided into two basic groups. The first group consists of all types of loads applied on the concrete, and the second includes other factors that may contribute to cracking of concrete.

Loads:

- Weight of forms and other external dead loads
- Weight of construction machinery
- Self-weight of the slab
- Weight of adjacent traffic
- Adjacent traffic vibrations
- Vibrations due to construction machinery
- Deflection of formwork

Other factors:

- Heat of hydration
- Shrinkage
- Temperature at early ages
- Wind
- Concrete protection
- Concrete cover over reinforcing bar and bar thickness
- Reinforcing details
- Compaction of concrete
- Joint between newly poured and old concrete
- Construction procedures

6.2.1 Heat of Hydration

Concrete gains strength as it undergoes a complex chemical reaction. As a result of this chemical reaction, heat is developed internally. The effect of this temperature depends on other factors such as the influence of air temperature, sun radiation, and wind. In case of high temperatures, this may have an extremely detrimental effect in reducing the concrete strength and inducing cracking in the deck. These conditions may worsen in case of additional sun radiation, wind, and inadequate curing. Also, regions near the surface lose the heat more rapidly, which results in a nonlinear temperature distribution over the depth of the deck. Since most of the heat is developed at very early ages, i.e., when concrete strength, especially tensile strength, is very low, the probability of cracking in the concrete is very high. Since the influence of the heat of hydration is closely related to that of the temperature, both factors must be taken into account simultaneously.

6.2.2 Shrinkage

As concrete loses water due to evaporation and hydration, it shrinks. If water is not readily supplied in sufficient quantities during this process, stresses in the concrete may exceed the concrete tensile strength, resulting in cracking. Additional problems present many restraints that exist in the concrete deck. For example, reinforcing bars and void forms present obstacles to the free displacement of concrete as it shrinks or settles, which introduce tensile stresses in the concrete. As soon as these stresses reach the concrete tensile strength, cracking occurs. Shrinkage cracks usually appear randomly over the deck. Severity of this type of cracking is a function of rate of shrinkage, and is closely related to the quality of concrete protection, particularly at early ages.

6.2.3 Temperature Effect

It is difficult to distinguish the effects of temperature, especially at early ages, from the heat of hydration. A temperature increase in the concrete due to solar radiation or change in environmental temperature increases the rate of hydration producing even more heat. An increase in the ambient temperature influences temperature primarily on the exposed concrete, resulting in a nonlinear temperature distribution in the concrete deck. This phenomenon is similar to the previously explained effect in case of heat of hydration, although distribution over the deck thickness is different. In cold climates, heat induced by the sun and the heat of hydration may in fact help maintain a proper concrete temperature. Prior to deck casting, temperature changes affect the girders supporting the forms and deck. These variations of temperature may result in change of deflections during a day and may be significantly different from the design deflections. Depending on screeding techniques, this may result in insufficient deck thickness and concrete cover, particularly at midspan. Finally, during hot sunny weather, temperature of the forms and top flanges of supporting girders may become very high. Following the pouring of concrete, these additional elements warm up the concrete increasing the probability of cracking.

6.2.4 Wind

The importance of wind is not related to the possibility of creating pressure on the structure, but in increasing the rate of evaporation of water from the fresh concrete. The increased water evaporation may lead to a shortage of water in the concrete cement paste, hence not allowing proper hydration and leading to inadequate concrete properties such as concrete strength, resistance to abrasion, etc. It may also increase the shrinkage of concrete causing severe cracking. Wind speed and air temperature are the most important parameters that determine the magnitude of influence of

wind on concrete. During hot weather, even moderate wind speed may result in dangerous levels of drying shrinkage.

6.2.5 Concrete Protection

Concrete protection at early ages is essential for good quality concrete. Lack of maintenance at early ages cannot be compensated for with proper maintenance later on. Some common mistakes in concrete protection are the use of inadequate cover or improperly maintained cover, the use of burlap covers that are not wetted regularly, uneven coverage with curing compound, and late application. Any of these factors may lead to severe cracking. In the case of windy or sunny conditions, wind barriers and sun shades, respectively, should be used.

6.2.6 Concrete Cover over Reinforcing Bar and Bar Size

Thickness of concrete cover is vital to prevent cracking over the top reinforcement due to concrete settlement. It is not possible to separate this factor from the others. The thickness necessary to resist cracking is a function of concrete depth under the bar, bar diameter, and concrete properties, particularly slump. These are closely related to the other factors such as shrinkage, settlement of concrete, slump, vibrations due to adjacent traffic, etc. High slump concrete exhibiting high settlement combined with insufficient cover may lead to cracking over the top reinforcement. Vibrations may increase this effect leading to even more severe cracking.

6.2.7 Compaction of Concrete

Proper compaction of concrete by vibration is essential. For concrete bridge decks, this is even more significant. Insufficiently compacted concrete is highly susceptible to cracking due to the

influence of any additional vibration after the time of setting. Concrete under the influence of vibration due to traffic or construction machinery exhibits high settlement and shrinkage, which may lead to cracking of concrete. The possibility of voids in insufficiently compacted concrete is also increased and bond between the steel and concrete is jeopardized. Freeze-thaw resistance of such concrete may also be unsatisfactory. Otherwise, well compacted concrete is highly resistant to any form of vibrations due to its low amount of shrinkage or settlement, assuming proper care.

6.2.8 Reinforcing Details

One usually ignored factor is reinforcement detailing. Details that are hard to read are easily misinterpreted resulting in the improper placement of reinforcement. Congested reinforcement details also make the placement of steel and concrete difficult, increasing the probability of voids or insufficient compaction. Variations in rebar position in the field must be taken into account when detailing, especially in the case of complicated details. Minimum reinforcement cover in such cases may lead to insufficient cover, due to variations in the position of steel.

6.2.9 Self-Weight of the Slab

The most significant problem with the weight of a fresh concrete slab is its influence on previously poured concrete in the case of continuous bridges and the possibility of cracking of the fresh concrete deck over the piers. This is more pronounced if areas over piers are poured before midspan sections. In the case of bridges where span lengths differ considerably, concrete surface curvatures in the longitudinal direction may become considerably high if a longer span is poured first. This effect may be significant in bridges with composite cross sections, since at early ages the contribution of a concrete slab is very small and girders carry the majority of the load. This

emphasizes the importance of the sequence of pour of concrete for bridges with composite cross sections.

6.2.10 Joint Between Newly Poured and Old Concrete

Longitudinal cracks between new and old concrete appear in all cases of bridge widening or reconstruction where one side of the bridge deck was poured first. In cases of reinforcing details that include hooked reinforcing bars between the newly poured and old concrete, some unwarranted effects may appear. Voids around reinforcement may form, resulting in insufficient bond between concrete and steel and the cracking of concrete, particularly if vibrations are present. Some states practice the use of closure pour, one to two feet wide, between the new and old concrete. However, an insufficient amount of data does not allow the determination of these two methods with respect to cracking of concrete.

6.2.11 Construction Procedures

Although construction procedures seem to have a significant influence on the performance of the bridge decks, limited data in this field restrict drawing any conclusions concerning the influence of construction procedures on the cracking of concrete bridge decks. In the reviewed studies, most of the Departments of Transportation (DOTs) involved in surveys were unwilling to reveal data, or did not have any.

6.2.12 Weight of Construction Machinery

Trucks, cranes, screeding machines, and other equipment present more danger to fresh concrete decks than dead loads since their position is less predictable and since their presence is a

necessity during construction. The weight of these machines is also considerably high. The stresses induced by these machines may be significant especially since they are present while concrete is still very young. The stresses induced must be examined, particularly if they will introduce tensile stresses in either the longitudinal or transverse direction. Due to their small foot prints, these machines may introduce stresses that are localized over small areas.

6.2.13 Weight of Adjacent Traffic

In case of widening and new construction, where one side of the bridge is open to the traffic, the bridge deflects due to the weight of traffic adjacent to the section with newly poured concrete. Differential deflections between sections under traffic, with the old deck and section under construction, may lead to high transverse curvatures in concrete. Since curvature is usually highest in the region over the girder closest to the joint between the new and old deck, longitudinal cracks may occur in fresh concrete. Also, transverse reinforcement near the old concrete may be dislocated. A repetitive pattern of these deflections may lead to the creation of voids around reinforcing bars, which decrease slab performance.

6.2.14 Vibrations Due to Construction Machinery

These vibrations may have an effect similar to the vibrations due to adjacent traffic. However, due to smaller magnitude, compared to the vibrations due to adjacent traffic, they are much less likely to do any serious damage.

6.2.15 Weight of Forms and Other External Dead Loads

These loads usually do not present danger to fresh concrete in a bridge deck since they are easily estimated. Forms are placed prior to concrete placement and do not introduce any stresses in the concrete. However, the dead loads introduced to a structure other than the weight of forms may present a problem, particularly if they are added while concrete is still young. For example, concrete traffic dividers added on the bridge may induce stresses in the bridge deck. Bending stresses in concrete over the piers in the longitudinal direction due to these loads is not usually of concern. However, the concrete stresses in the transverse directions over the girder closest to the joint between the old and new deck may be of concern. However, since its weight is small compared to the other loads, these effects may be neglected. Significant stresses may be expected only in the case of storing materials such as reinforcing steel, concrete, etc.

6.2.16 Deflection of Formwork

Deflection of formwork usually occurs due to the weight of fresh concrete. Since concrete is at that time still in a plastic state, these deflections present no harm. As concrete stiffens, deflections of formwork due to other loads may present problems. However, since other loads applied to a bridge at that time induce stresses in the concrete with a magnitude greater than the loads due to deflection of formworks, its influence may be neglected, assuming the forms are properly constructed.

Other types of form deflections may be attributed to the influence of temperature on the deflection of the supporting structure, and to the deflection of forms. This may lead to adverse results while placing concrete and, consequently, lead to insufficient concrete deck thickness and reinforcement cover.

6.2.17 Adjacent Traffic Vibrations

When a vehicle passes over a bridge under construction, it introduces vibrational effects on the bridge. The magnitude of these vibrations is a function of vehicle weight, speed, suspension system, deck roughness, bridge length, and damping. However, these vibrations inflict damaging effects on *fresh* concrete depending on many parameters, and they may be negligible or critical.

Insufficiently compacted or high slump concretes are vulnerable to cracking due to the influence of vibrations. The addition of a small concrete cover and large size bars magnifies this problem. The bond between the rebars and concrete may also be destroyed, particularly in the regions of fresh concrete near a joint. However, dangers of cracking of concrete due to vibrations decrease as the slump and level of compaction of concrete decrease. Assuming proper compaction, the same is true when bar size decreases and cover increases.

6.2.18 Other Factors

As expected, the magnitude of the influence of the previously mentioned loads and factors on the cracking of concrete bridge decks is mutually dependent. The influence of one factor may be reduced or increased by an increase in another factor. This is also highly dependent on the following concrete components:

- Cement type and amount:

Cement, which is a vital component, has a great influence on the concrete properties. Finer ground cements and higher amounts in the mix result in an increase in strength, increase in heat of hydration, and they tend to reduce the amount of bleeding.

- **Aggregate: granular composition, mineral composition, shape, and porosity:**

Aggregate mineral composition may increase or decrease the final strength of concrete. Some aggregates have lower compressive or tensile strengths than others. Some aggregates are also more porous, which increases the amount of water needed for proper hydration. Shape of the aggregate influences the behavior of concrete at limit states. For example, concrete made of crushed stone usually has greater tensile strength than one made of river gravel.

- **Water and concrete slump:**

The amount of water used is directly related to the amount of cement. Good quality concretes for bridge decks have a water/cement ratio not greater than 0.44. Higher water/cement ratios increase bleeding and shrinkage, decreasing concrete quality and increasing the probability of cracking. Concretes with higher water/cement ratios and higher slumps are more sensitive to the influence of the other factors such as vibrations, drying, setting, etc.

- **Additives: retarders, super-plasticizers, and air-entrainment:**

Additives enable the production of higher quality concrete by:

- slowing down the hydration process, which decreases the heat of hydration and allows extra time for concrete placement (retarders).
- increasing the workability of concrete with a low water/cement ratio, or reducing the amount of water for the same workability (super-plasticizers).
- increasing air-entrained in the concrete, hence increasing its resistance to damage due to freeze and thaw.

Although it is difficult to distinguish one factor from the other, it seems that in most cases cracking of concrete may be attributed to the high evaporation rate, and by that high magnitude of shrinkage as a result of inadequate concrete curing procedures during hot weather conditions, especially at very early concrete ages. This effect is attributed to: lack of concrete protection, inadequate uniform coverage with a curing compound, and delay of concrete protection application. Other factors include use of high slump concrete, excessive water in the concrete, insufficient top reinforcement cover, insufficient vibration of the concrete, inadequate reinforcing details of the joint between the new and old deck, sequence of pour, weight and vibration of machinery, weight of the forms, and deflection of forms. The influence of vibrations due to different sources is depicted through slump and reinforcement cover.

7. BRIDGE VIBRATION ANALYSIS

7.1 Introduction

Vibration of a bridge structure under the passage of vehicles is an important consideration in the design of bridges. The interaction between the vehicle and the bridge makes the dynamic response analysis very complex [50]. In studying the vehicle-bridge system, a great number of parameters, such as stiffness, damping, and inertial properties of the vehicles and the bridge, velocity of the vehicle, and pavement roughness, may affect the dynamic response of the bridge. In studying the vehicle-bridge interactions, different frequencies should be considered. One is the driving frequency caused by the motion of the vehicle, as represented by $\pi v/L$, while the other is the fundamental frequency ω of vibration of the bridge [51].

A structure's dynamic behavior is defined by a discrete spectrum of an infinite number of natural frequencies and corresponding mode shapes, which are determined by geometry, distribution of mass, stiffness, and boundary conditions. Within these parameters, changes in stiffness are directly related to changes in the safety condition of the structure. Therefore, it is essential to identify the damage in the structure by comparing the measured natural frequencies and mode shapes. Numerous studies have indicated that an increase in damage corresponds with decreased natural frequencies of a structure [52].

The following are some of the important parameters in bridge vibration analysis [50]:

- Characteristics of the vehicle, which include the number of axles, axle spacing, axle loads, natural frequencies, and the damping provided by the shock absorbers and inter-leaf friction in the springs.

- Characteristics of the bridge structure, such as the bridge geometry, support conditions, and mass and stiffness distribution.
- Vehicle speed.
- Profile of the bridge deck, in particular pavement roughness and surface misalignments at the abutments and expansion joints.
- The number of vehicles and their travel paths.

A vehicle traveling over a highway containing surface irregularities experiences vertical and horizontal motions. Associated with the vertical motion are forces between the highway and the vehicle that are developed in addition to the dead load of the vehicle. These forces are frequently referred to as the dynamic reactions or the dynamic forces [17].

A bridge, like any other structure, has a number of natural frequencies and associated mode shapes. These modes could be bending, longitudinal, transverse, torsional or a combination thereof. The stiffness and mass distribution of the bridge will determine the shapes of the fundamental and other modes in a free vibration analysis. Due to the passage of vehicles, one or more of these modes could be excited. In a symmetric bridge subjected to a symmetric flow of traffic, the first flexural mode will generally be excited, whether or not it is the fundamental mode. However, this may not be the case in a bridge loaded by an asymmetric forcing function, due to a heavy vehicle traveling in an extreme lane of the bridge [53].

The effect of higher modes is included simply by considering more than one mode in the modal superposition analysis, or one can simply consider the effect of all modes by performing direct time history analysis rather than modal superposition [54].

For straight superstructures of equal span lengths, the fundamental frequency of the entire structure is equivalent to the fundamental frequency of one of the spans when simply supported. For straight, nonskewed bridges of approximately uniform mass and stiffness, a single beam idealization will usually underestimate the fundamental frequency observed in the field by approximately 5%. This is especially so when the higher modes are excited by vehicular traffic. The desired accuracy for design purposes is $\pm 10\%$, hence a single beam idealization is sufficiently accurate for bridges of this type [53].

For longitudinally asymmetric or skewed, continuous superstructures, a single beam idealization is not appropriate and should not be used. The only recommended calculation procedure is an eigenvalue analysis of a finite beam element grillage. For simply supported structures where the supports are fixed with respect to transverse rotation, the fundamental frequency significantly increases as the degree of skew is increased. Furthermore, it is suggested that precast deck unit superstructures inherently exhibit this support condition due to their method of construction. Therefore, a single beam idealization can be grossly inappropriate for calculating the fundamental frequency of a skewed deck unit structure. The skewing of simply supported structures when the supports are released with respect to transverse rotation, i.e., girder-slab construction, theoretically has no significant effect on the calculated fundamental frequency [53].

Since the dynamic response of structures is governed by system parameters such as stiffness, mass, and damping, changes in these parameters would lead to changes in the vibrational response as characterized by the modal parameters, natural frequencies, mode shapes, and modal damping values. Due to the fact that each vibration mode has a different energy distribution, any localized damage will affect each mode differently depending on the location and severity of the damage. Modal parameters are also sensitive to boundary conditions, i.e., physical constraints of the structure

[55]. The variation in the first natural frequency can be associated either to cracking in the beam or to a change in the deformation modulus of the whole beam or in bearing conditions. Therefore, the measurement of only one frequency is not enough for the damage identification technique [56].

Parameter studies show that the fundamental frequency of the structure is not sensitive to changes in boundary conditions, width of the structure, and local damage to the bridge deck [57]. The frequency range of interest for most highway bridges lies between 0 and 10 Hz. and occasionally goes up to 20 Hz. This range is usually wide enough to observe the first 10 vibration mode shapes [58]. Vehicle natural frequencies are also a design parameter. Ideally, vehicles would be designed so their natural frequencies do not coincide with natural bridge frequencies. However, in practice most heavy vehicles apply dynamic loads in the 1.5 to 4.5 Hz. frequency range [59]. Since vehicle frequencies occupy a relatively narrow frequency band, one possible design solution is to build bridges that avoid the 1 to 5 Hz. frequency range [60].

A study by Law et al. [61] of the field measurements of vibrational response of a full-scale bridge deck due to environmental excitation and traffic-generated excitation showed there was no significant change in the first modal frequency of the structure, provided the mass of the structure was more than ten times that of the vehicle [57]. The natural frequencies of a bridge do not change significantly as a result of structural repairs. The localized nature of the repairs was the reason for the modest changes. There was no definite trend in the changes in damping values due to the repairs [55].

It should be possible, at least in theory, to estimate the flexural stiffness and its longitudinal distribution in the main members of the bridge deck by developing the best match to the measured first modal frequency. The fundamental modal frequency is selected because the vibrational mode

shape will involve large amplitudes of vibration in most likely the cracked zone of the members, namely the midspan [57].

Results from dynamic analyses are used to select instrumentation locations on the bridge as well as to predict static displacements. They are then calibrated using the experimental frequencies and mode shapes, and they provide a basis for the study of the influence of certain elements such as barrier walls and sidewalks, cracking of deck slabs, effect of long-term concrete creep and shrinkage, etc. [58].

In performing vibration analysis, the fundamental modal frequency of the structure should be measured in free vibration. A finite element model (FEM) should be selected to best represent the bridge deck. The modal frequencies depend on vertical stiffness at the supports, the moduli of elasticity of the materials, and the moment of inertia of the beam. For normal types of rubber pads underneath bridge beams, the stiffness at the support was shown not to impose any significant effect on the modal frequencies, and therefore, a rigid support can be assumed in most cases [62-63]. The static modulus of elasticity of concrete can be used because the modal frequencies in civil engineering structures are usually low, well below 100 Hz. This means that the rate of loading in the vibration is too low to justify the use of a larger dynamic modulus of elasticity. The moment of inertia of beams in the FEM is adjusted to have the best match between the measured and analytical fundamental modal frequency in free vibration. Uniform distribution of the cracked moment of inertia is assumed over the length of the main beams. The value of inertia that gives the closest fit of the measured first modal frequency is the best estimate of the moment of inertia [57].

Variable dampers may be superior to existing dampers and damper stoppers. The damping coefficient is very large during small deck vibrations for preventing deck vibration due to braking

loads of vehicles and wind effects. The damper is movable in low-rate motions such as the elongation of a deck by temperature change [64].

7.2 Finite Element Analysis

In order to determine the dynamic behavior of composite bridges under truck loading, two bridge structures were examined using finite element analysis. Both bridges were continuous composite structures. The first bridge was a welded steel plate girder, three-span bridge with a composite concrete slab (see Figure 7.1). The second bridge was a three-span continuous bridge with precast prestressed concrete girders and a cast-in-place concrete slab (see Figure 7.2).

7.2.1 Illinois River Bridge Number 050-0219

This bridge was not symmetrical, although the two exterior spans were the same length due to different girder sectional properties in the two spans. The depth of the girder in the first span varied from 1.675 to 2.59 m. In the second span, the girder had a constant cross-section of 2.59 m, while the cross-section for the third span depth varied from 2.59 to 1.83 m. The flange width and thickness varied from 0.50 to 0.70 m and 20 to 60 mm, respectively, having the greatest area over the interior supports. The central span was 27 percent longer than the exterior spans (90.68 and 71.55 m, respectively), as shown in Figure. 7.1. Plan and cross section details of the bridge are presented in Figures 7.3-7.4. The total width of the bridge was 12 m, which allowed two traffic lanes, one in each direction.

7.2.2 Sangamon River Bridge Number 084-0206

This bridge consisted of three practically equal spans (29.48 m) as shown in Figure 7.2. Plan and cross section details of the bridge are presented Figures 7.5-7.6. Seven precast prestressed concrete bridge girders acted compositely with a 195 mm thick concrete slab that is 14.2 m wide. The precast concrete girders were 1.372 m deep, and spaced at 2.05 m center-to-center. Twenty-six strands were used to prestress the precast concrete girders (see Figure 7.7). These strands were straight at midspan, while six strands were draped at the ends.

7.2.3 Modeling of Illinois River Bridge

This bridge was modeled using shell and frame elements. Shell elements were used to model the concrete slab as well as the web of the steel plate girders. The top and bottom flanges of the steel plate girders were modeled using frame elements, where appropriate dimensions were given for each section along the span length. The web height was modeled with the exact lower flange position along the bridge axis as shown in Figures 7.8-7.9. The top and bottom flanges are not visible in the diagram due to the fact that frame elements are only shown as lines in the finite element analysis program used. The thickness was varied accordingly to the given bridge geometry, however, locations of the changes in thickness were approximated to the nearest node position. This process simplified generation of nodes and elements and is insignificant in terms of accuracy of the results. The restraints were modeled at real support positions allowing displacement in the bridge axis direction and rotation in the y direction (bridge having been modeled with slab in the x-y plane, x along the bridge centerline, direction of z perpendicular to the plane of the slab directed upward). The supports were restrained appropriately to simulate the pinned and roller conditions. The nodes in lower flange were also restrained against movement in the y direction.

7.2.4 Modeling of Sangamon River Bridge

This bridge was modeled using shell elements, except for the AASHTO girders, for which frame elements were used (Figure 7.10). The prestressed concrete girders were modeled using a modified I-section. The flanges were modeled as rectangular elements, hence eliminating the triangular portions of the beam. However, thickness of the elements was increased to maintain the same geometric properties as the original beam. The cross section was constant over the bridge length. The concrete slab was modeled with 195 mm thick shell elements. The modulus of elasticity for each concrete type was calculated according to the AASHTO formula:

$$E_c = 4700\sqrt{f'_c} \quad (MPa)$$

where the concrete compressive strength f'_c was given as 42 MPa for the beams and 24 MPa for the slab. The restraints were applied in a similar manner as that of the steel bridge.

The prestressing strands in the prestressed concrete girders were modeled as prestressing elements with the appropriate locations away from the neutral axis along the midspan and ends. A prestressing force of 2700 kN was calculated and used for each girder.

7.2.5 Loading

Excluding self weight of the bridge, the only loading applied to the bridge was truck loading and construction equipment. Typical HS-20 truck loading conditions are depicted in Figures 7.11 to 7.14, while Figures 7.15 and 7.16 present close-up views of the moving loads and construction loads, respectively. The wheel loads were distributed over adjacent nodes to avoid stress concentration under the applied load (see Figures 7.15-7.16). The length of the load arrow indicates the magnitude of the wheel loads. Two separate runs were performed to simulate one truck as well

as two side-by-side trucks. Separate runs were also performed to simulate the loads during construction and pouring sequence. The concrete mixer trucks were taken to be 276 kN, which included a full load of concrete (see Figure 7.17). The load imposed by the trailer unit carrying the pump was taken as approximately 94 kN. The modulus of elasticity was reduced to simulate fresh concrete, i.e., at 4 to 8 hours. It was applied to each of the bridges as outlined hereafter. The truck was assumed to travel on the bridge from the left side at a time, $t = 0$, and a speed of 90 km/h (55 mph). The total time needed to reach the other end of the bridge was calculated according to the length of the bridge and speed of the truck. The position of the truck was calculated every 0.2 and 0.5 seconds yielding 17 to 18 locations for the concrete and steel bridges, respectively.

Dynamic eigenvector time history analysis of the structures was performed. The damping values used for the different mode shapes (Ritz vectors) were specified. Two types of analyses were possible, transient and periodic. For periodic analysis, the period of the cyclic function was assumed to be the product of the number of steps and the time increment, Δt , i.e., the time span over which the time history analysis was carried out. Responses were calculated after every Δt seconds. The loading from each wheel was then transferred to the four adjacent joints. Table 7.1 presents the load cases used and the distances of the front axle with respect to the left end of the bridge.

TABLE 7.1**FRONT AXLE TRUCK LOCATIONS FOR VARIOUS LOAD CASES**

Load Case	Distance of front axle from end (m)
1	8.0
2	20.5
3	33.0
4	45.5
5	58.0
6	70.5
7	83.0
8	95.5
9	108.0
10	120.5
11	133.0
12	145.5
13	158.0
14	170.5
15	183.0
16	195.5
17	208.0
18	220.5

7.2.6 Results and Discussion

The results obtained consisted of vibration modes and frequencies for each structure in addition to top and bottom stresses in each principal direction. The first ten modes were observed. The resulting mode shapes are given in Figures 7.18 to 7.27 for the steel girder bridge and Figures 7.28 to 7.37 for the prestressed concrete girder bridge. The maximum deflections are associated with the various mode shapes. These deflections are observed at corresponding critical locations based on each mode shape. The maximum vertical deflections were traced along the length of the bridges collectively for all ten mode shapes. Figure 7.18 depicts the first mode shape (1st bending mode) for the steel bridge, where the maximum deflections are 40 and 29 mm for the middle span and end spans, respectively. Figure 7.19 presents the second mode shape (2nd bending mode), where the maximum upward and downward deflections are 40 and 41 mm in the end spans, respectively. The maximum vertical deflections for the remaining mode shapes, i.e., modes 3 through 10 (Figures 7.20-7.27), are 38, 105, 102, 95, 41, 94, 102, and 117 mm, respectively.

Figure 7.28 depicts the first mode shape (1st bending mode) for the prestressed concrete girder bridge, where the maximum deflection is 43 mm for the middle span and end spans. Figure 7.29 presents the second mode shape (1st torsional mode), where the maximum deflection is 71 mm. The maximum vertical deflections for the remaining mode shapes, i.e., modes 3 through 10 (Figures 7.30-7.37), are 53, 88, 82, 64, 105, 102, 122, and 85 mm, respectively. As a result, the corresponding locations for the LVDTs were proposed (Chapter 8). The corresponding locations along the steel bridge were obtained from the output file corresponding to the maximum vertical deflections already found. The same procedure was followed for Figures 7.28-7.37 for the concrete bridge.

The natural frequencies along with the mode shape types are also presented in Table 7.2. The natural frequencies for several bridges are also listed in Table 7.3. Figures 7.38-7.41 represent mode shape numbers versus frequency and mode shape numbers versus span length for both simply supported and continuous bridges. It is apparent that the natural frequencies of long span bridges are much less than those of short span bridges.

TABLE 7.2

FIRST TEN NATURAL FREQUENCIES AND MODE TYPES

Mode Shape Number	Steel Girder Bridge		Prestressed Concrete Bridge	
	Frequency (Hz)	Mode Type	Frequency (Hz)	Mode Type
1	1.21	1st bending	2.01	1st bending
2	1.41	2nd bending	2.24	1st torsional
3	1.86	3rd bending	2.56	2nd bending
4	2.22	1st torsional	2.76	2nd torsional
5	2.28	2nd torsional	3.69	1st bending/torsional
6	2.30	3rd torsional	3.71	3rd bending
7	3.49	4th bending	3.86	3rd torsional
8	4.36	4th torsional	4.05	2nd bending/torsional
9	4.36	5th torsional	4.90	3rd bending/torsional
10	4.38	6th torsional	7.51	4th bending/torsional

The first natural frequency for the steel girder bridge was 1.21 Hz. This low frequency was due to the long bridge spans, however, this result compares well with the results obtained for similar bridges.

TABLE 7.3

MODE SHAPE FREQUENCIES

Frequency (Hz.)	Illinois River ¹	Sangamo n ²	Englan d ³ [55]	Milnike k ⁴ [58]	Grand-Mere ⁵ [58]	Omerville e ⁶ [58]	Pirton Lane ⁷ [60]	Lower Early ⁸ [60]	Drift Road ⁹ [60]	Colquitz River ¹⁰ [65]
Mode 1	1.21	2.01	6.8	1.26	1.09	2.34	3.2	5.7	6.8	1.67
Mode 2	1.41	2.24	8.3	1.82		2.45	12.7	6.9	8.6	2.91
Mode 3	1.86	2.56	9.4	2.19	2.11		28.6		18.0	5.97
Mode 4	2.22	2.76	10.3	2.46		5.26		9.7		6.19
Mode 5	2.28	3.69	11.1	2.87		5.30		11.3		7.33
Mode 6	2.30	3.71	19.0		3.60					7.45
Mode 7	3.49	3.86	22.3		3.91			18.0		8.77
Mode 8	4.36	4.05			5.24			24.4		8.86
Mode 9	4.36	4.90			5.48					
Mode 10	4.38	7.51								

- 1 IDOT three-span steel girder bridge (71.90-71 m)
- 2 IDOT three-span prestressed concrete girder bridge (29.5-29.5-29.5 m)
- 3 Two-lane, six-span reinforced concrete, voided slab construction bridge (12.373-16.7-19.698-20.478-18.519-16.529 m)
- 4 Arch bridge (91 m), pillar reinforcement was added to limit torsional motion of deck
- 5 Segmentally constructed box-girder bridge (181 m), post-tensioned cables added to control creep and shrinkage induced midspan deflection
- 6 Skewed bridge (71 m), concrete slab supported by four steel girders
- 7 Simply-supported bridge (40 m)
- 8 Three-span, slab-on-girder, prestressed concrete bridge (22.2-22.4-22.2 m)
- 9 Four-span prestressed concrete, box-girder bridge (12.52-21.95-21.95-12.52 m)
- 10 Five-span steel girder bridge (14.07-18.08-18.33-18.08-14.12 m)

The displacements for each loading condition were then found, including the maximum deflection. The maximum displacement found due to live load for the steel girder bridge and prestressed concrete girder bridge were 20.6 and 17.1 mm, respectively (Figures 7.42-7.43). Figure 7.44 shows a close-up view of a typical deflection mode for the steel girder bridge, while Figures 7.45-7.46 show the deflection due to only the dead load for the steel and concrete bridges, respectively. The critical locations corresponding to these maximum displacements were also found in order to instrument the bridges accordingly. The maximum top and bottom tensile stresses in the slab were also found for each loading condition as shown in Figure 7.47. Note that the maximum stresses appear under the wheel loads and decrease sharply with the distance from the loading points. The load conditions correspond to the location of the HS20 truck as presented in Table 7.1.

The output obtained as a result of the finite element analysis is in metric units, hence, the stresses are in kPa, the displacements are in mm, and the forces are in kN. It seems that localized stresses under the point loads are of much greater importance with respect to bridge deck cracking than stresses away from these loads. A direct comparison of the calculated stresses with concrete strength was not possible due to the configuration of the slab model. Figures 7.48-7.57 present typical top and bottom stresses for a typical location on the bridge. These stresses correspond to one moving truck on the steel girder bridge. A maximum normal stress in the longitudinal direction of 1350 kN/m^2 is observed at joint number 2103 (Figure 7.48). As expected, this maximum stress is located under the wheel loads as shown in the figure. The critical stresses tend to follow the path of the truck as shown in Figures 7.49-7.50. The maximum stress is reduced as the truck reaches the interior support. Figures 7.58-7.61 present typical stresses for the prestressed concrete girder bridge. The slabs were treated as homogenous materials, hence neglecting the influence of steel and cracking. The maximum stress locations were determined due to the moving load and dead weight. The strains

that are associated with these stresses will be obtained by monitoring the corresponding critical locations with strain gages and vibrating wire strain gages.

A separate analysis was performed that took into account the sequence of pour. One half of the bridge was considered to have hardened concrete with moving loads simulated on it, while the other half of the bridge was under construction. Hardened concrete was placed over the positive moment region spanning the middle span, while fresh concrete was placed over the negative moment regions over the interior supports. The remaining portions of the end spans were modeled without concrete. This analysis was performed in order to determine the effect of moving loads as well as construction loads on the fresh concrete. As a result, that section was isolated in an effort to distinguish the amount of deflection due to all live load combinations and dead loads. The maximum deflection due to dead load was 60 mm, while the maximum upward and downward live load deflections were observed at 11.4 and 23.4 mm, respectively.

The corresponding first ten mode shapes are shown in Figures 7.62-7.71. Figure 7.62 depicts the first mode shape (1st bending mode) for the steel bridge under stage construction, where the maximum deflections are 44 and 32 mm for the middle span and end spans, respectively. Figure 7.63 presents the second mode shape (2nd bending mode), where the maximum upward and downward deflections are 60 and 55 mm in the end spans, respectively. The maximum vertical deflections for the remaining mode shapes, i.e., modes 3-10 (Figures 7.64-7.71), are 62, 93, 139, 141, 191, 187, 127, and 125 mm, respectively. The maximum deflection due to live loads as well as the deflection due to dead load are shown in Figures 7.72-7.73, respectively. Figures 7.74-7.75 show the deflection of the isolated wet concrete region due to dead and live loads (60 and 23 mm), respectively, while Figures 7.76-7.78 present the top stresses in that section of the slab. The locations depicting maximum displacements and stresses were determined in an effort to enhance the instrumentation

process. The maximum deflection as well as some typical stress diagrams for the case when two adjacent moving trucks were considered are presented in Figures 7.79-7.84.

Two different time history functions were used for the vibration analysis. One corresponding to the vehicle load cases (Figure 7.85), while the other implements a sinusoidal function to simulate the vibrational mode in addition to the mass of the trucks (Figure 7.86). Figure 7.87 presents the time history (displacement in the z direction as a function of time) for the node under maximum amplitudes. The maximum upward and downward displacements, corresponding to the vibrations imposed at node number 7017, are 22 and 23 mm, respectively. Comparison of the maximum displacement values from these graphs with the maximum deflection values for the same nodes indicates that the increase in the deflection due to vibrations is insignificant. The vibrations from the moving trucks, concrete mixer trucks, and concrete pumps were simulated as a sinusoidal curve function and implemented as force vibrations that are associated with the vehicle moving mass. These vibrations were also insignificant when compared to the moving vehicle effects. Figures 7.88-7.91 represent the time history plots for a typical element with respect to normal stresses for the combined case as well as first three modes, while Figures D.1-D.17 show typical time history plots for a typical element and a typical joint. These plots are associated with each of the first ten mode shapes of the bridge. If the mode shape selection in the program was chosen as zero, the maximum response due to all the mode shapes is shown.

The time history plots served as an indication for the maximum displacements and stresses due to vibrations. The critical locations associated with these displacements and stresses were also incorporated into the instrumentation process. The time history and dynamic analysis indicated that the sequence of pour has a significant effect on the deformation of the concrete at early ages. The deflections in the case when negative moment regions, i.e., over the interior supports, were poured

first were twice as great as those obtained if the positive moment regions were poured prior to the negative moment regions. The deflections and stresses observed in the fresh concrete due to the construction loads and equipment were somewhat significant. However, the largest contribution was observed to be as a result of the dead weight of the superstructure. This was prominent due to the fact that the span lengths were significantly long, especially in the case of the steel girder bridge.

Note however, that in this analysis, the influence of roughness of the surface could not be taken into account. Other researchers have indicated that the truck suspension natural frequency as well as roughness of the surface may greatly influence the bridge response to dynamic loads.

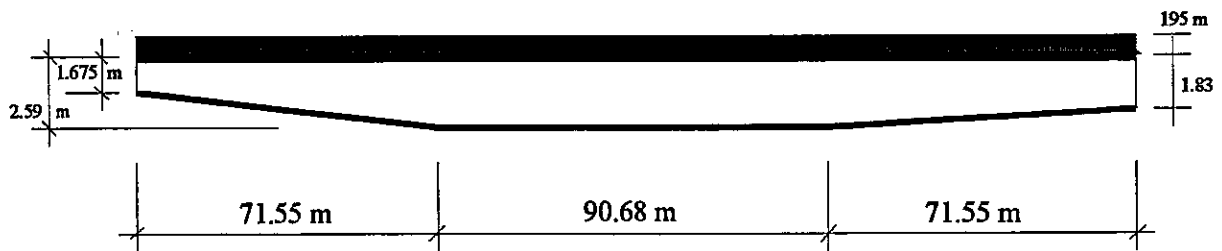


Figure 7.1 Steel girder bridge

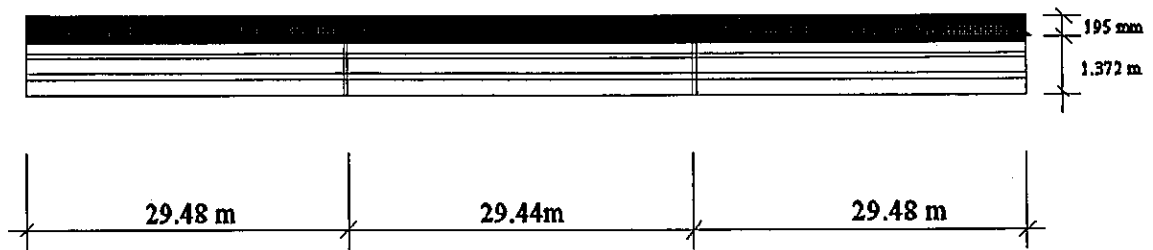


Figure 7.2 Prestressed concrete girder bridge

7.3 Effect of Damping

Damping of structures is normally associated with earthquake resistant techniques and the measures taken to attenuate the irregular behavior of the structures under seismic conditions. The effects of construction loads and vibrations were categorized to determine whether these loads are significant enough to require damping measures to be taken.

The dynamic and vibration analysis indicated that the simulated moving loads, construction loads, and vibrations do have an effect on the behavior of fresh concrete. Significant deflections were observed as a result of the finite element analysis for the portions considered to have wet concrete, i.e., concrete with a lower modulus of elasticity. These deflections would be detrimental to the concrete in that they can cause significant settlement, hence reducing the concrete cover for the main steel reinforcement. Furthermore, the mode shapes for the bridge under stage construction were more pronounced than those of the normal bridge structure.

Other factors that were not considered in the dynamic and vibration analysis include the fact that in stage construction, the steel reinforcement protruding from the finished deck into the portion of the deck under construction would cause significant cracking of the concrete at early ages due to the vibration from any dynamic load source.

With modern concrete structures and components becoming lighter and more flexible, vibration is often a problem. As a result, measurements can help in evaluating and solving vibration-related problems. If necessary, improvements to the two typical structures can be made taking into consideration the factors studied analytically as well as in the field. Action to reduce construction related vibrations can be introduced in the form of dampers or by imposing limitations on the speed of moving vehicles in adjacent lanes, especially heavy trucks.

Bridge behavior can be improved, i.e, improve serviceability to reduce cracking and excessive deflection throughout the structure due to vibration related problems, by stiffening the structure as follows:

- Modifying existing structural elements.
- Adding new elements.
- Localizing bracing and stiffening near the critical regions.
- Increasing stability of members and structures.
- Increasing strength for higher service loads.

Transverse stiffness of a bridge is an important factor that is considered in the study of static lateral load distribution. There is no doubt that it will affect the impact behavior of the bridge. Transverse stiffnesses of short span bridges distinctly affect the maximum impact factors. Increasing the lateral rigidities decreases the impact factors of exterior girders and increases those of interior girders. For long span bridges, a reasonable change of transverse stiffnesses gives little effect on the impact of each girder.

In general, very little difference is observed between the deflections obtained by assuming end fixity factors ranging from 0.10 to 1.0. An end fixity factor of 0.20, however, appears to match the actual deflection patterns the closest.

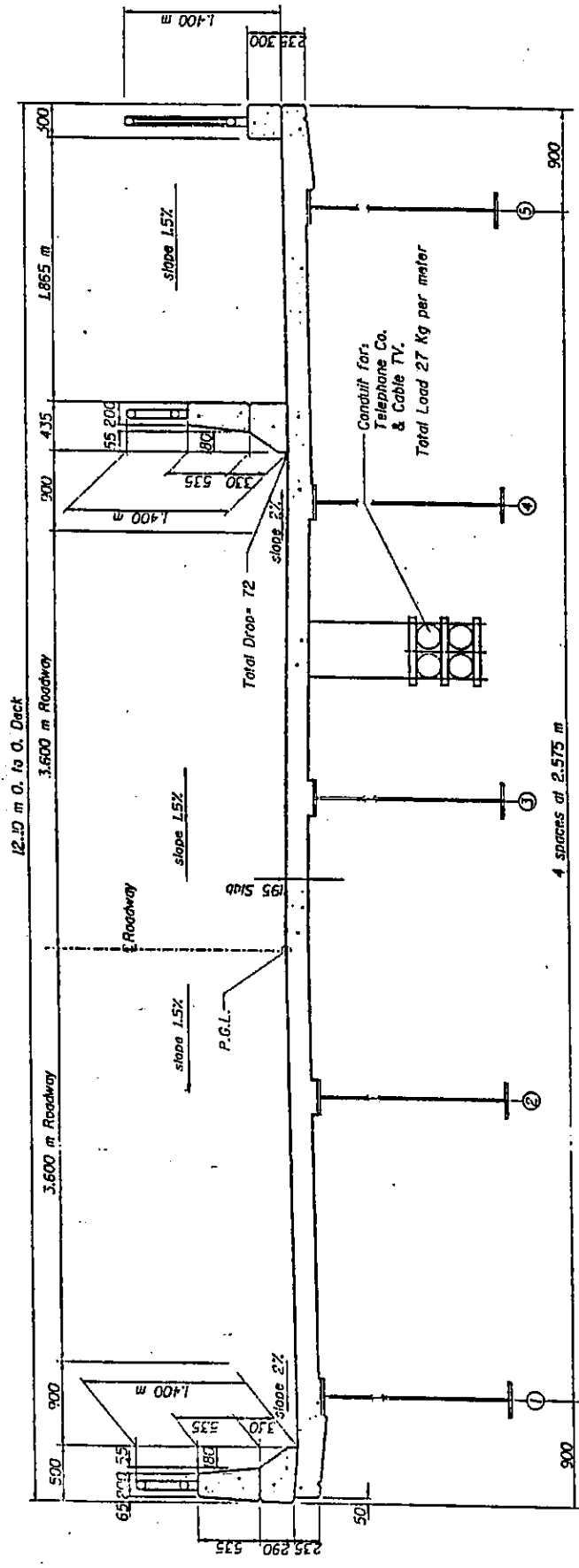
Differential deflections from live loading and plastic deformation produce numerous spalls on both the surface and soffit of decks under widening. Horizontal separation can be prevented more effectively through the more positive connection of exposing and lapping the original deck steel and/or diaphragms between the new and original girders.

The number of widenings designed with attached decks have been few and have usually been restricted to one girder widenings. Perhaps the reluctance to use this method more often has been

influenced by the theoretical overstress that results in the original exterior girder when analyzed by the usually accepted design criterion of placing all of the dead load that results from plastic deformation in the widening girders on the original exterior girder. This design approach is too conservative because in actuality, this dead load will be distributed to several girders through transverse rigidity in the structure.

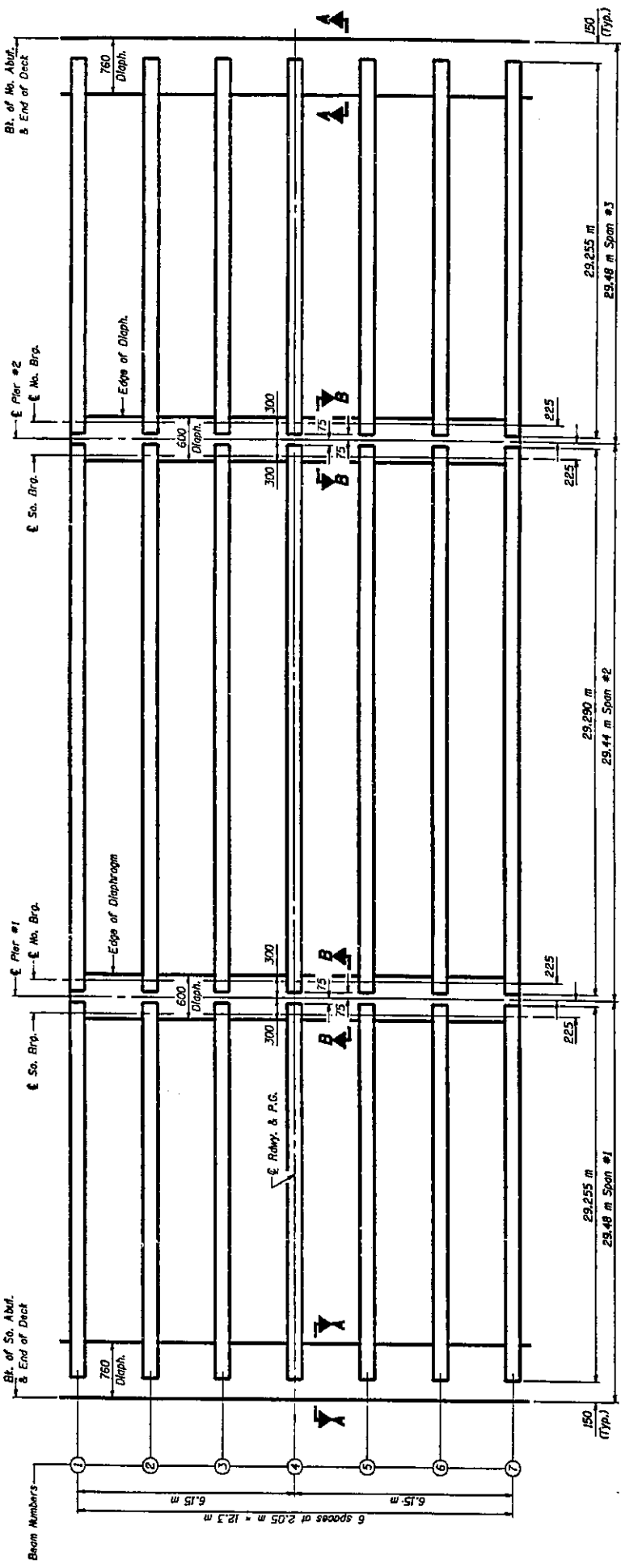
Until additional data becomes available on attached widenings, it would be advisable to construct all attached concrete and steel girder spans of over 18.3 and 22.9 m (60 and 75 ft) with at least an 18 in. closure pour between the deck sections of the widened and original. This closure pour should not be made on concrete structures until the falsework supporting the widening has been removed and a prescribed waiting period has passed. This pour should also be delayed a prescribed period on steel girders; diaphragms should not be attached until just prior to the pour.

The recommended type of damping depends on state practice, i.e., whether the State of Illinois allows its use.



CROSS SECTION
(Looking North)

Figure 7.4 Detailed cross section of steel bridge model



FRAMING PLAN

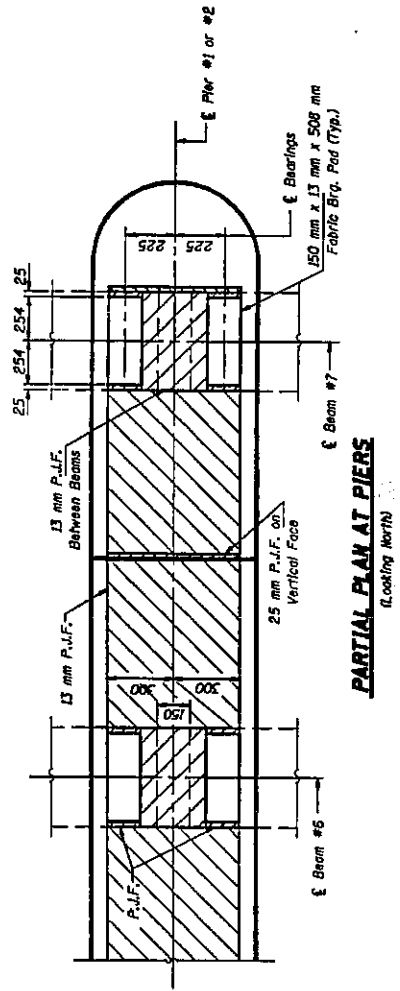


Figure 7.5 Detailed framing plan of concrete bridge model

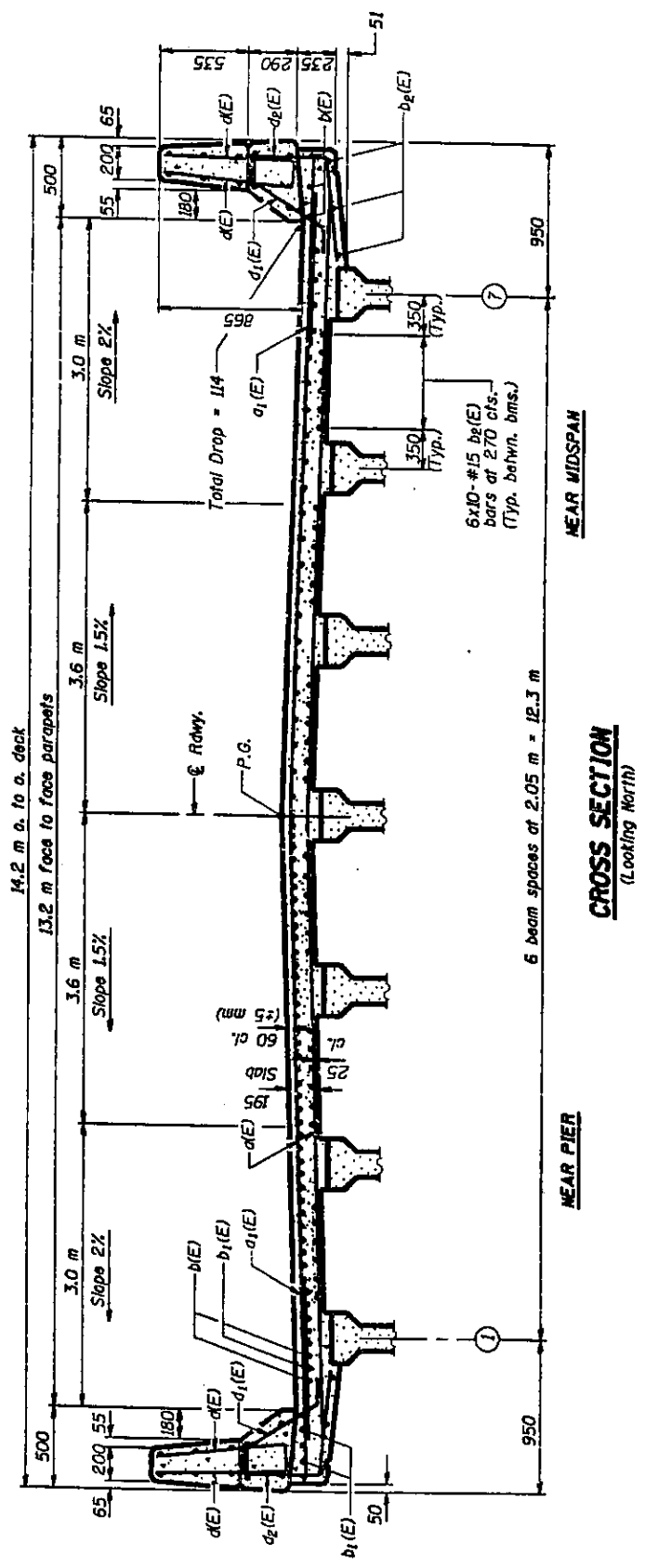


Figure 7.6 Detailed cross section of concrete bridge model

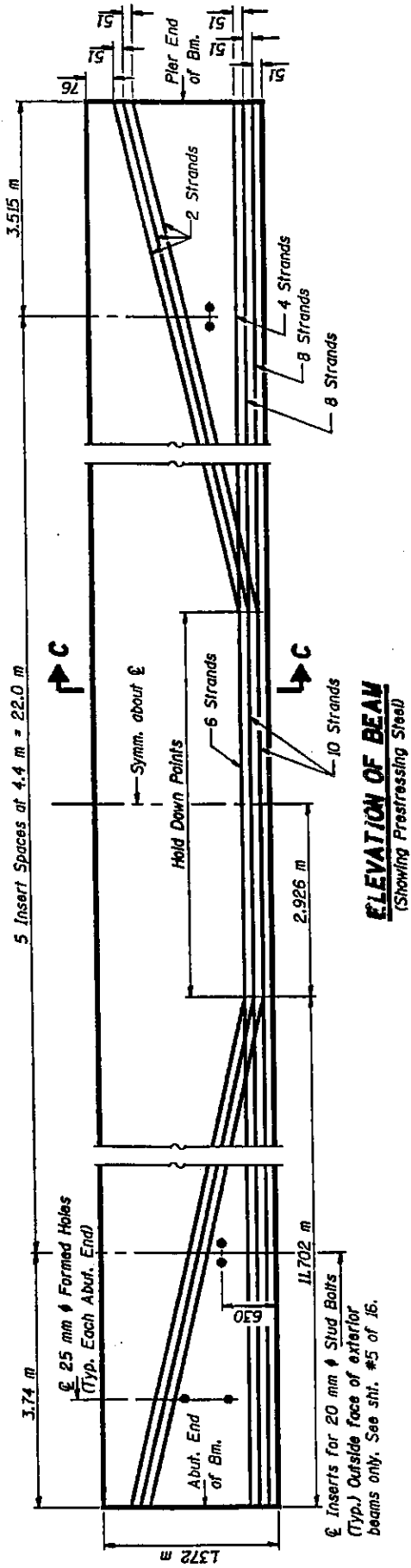
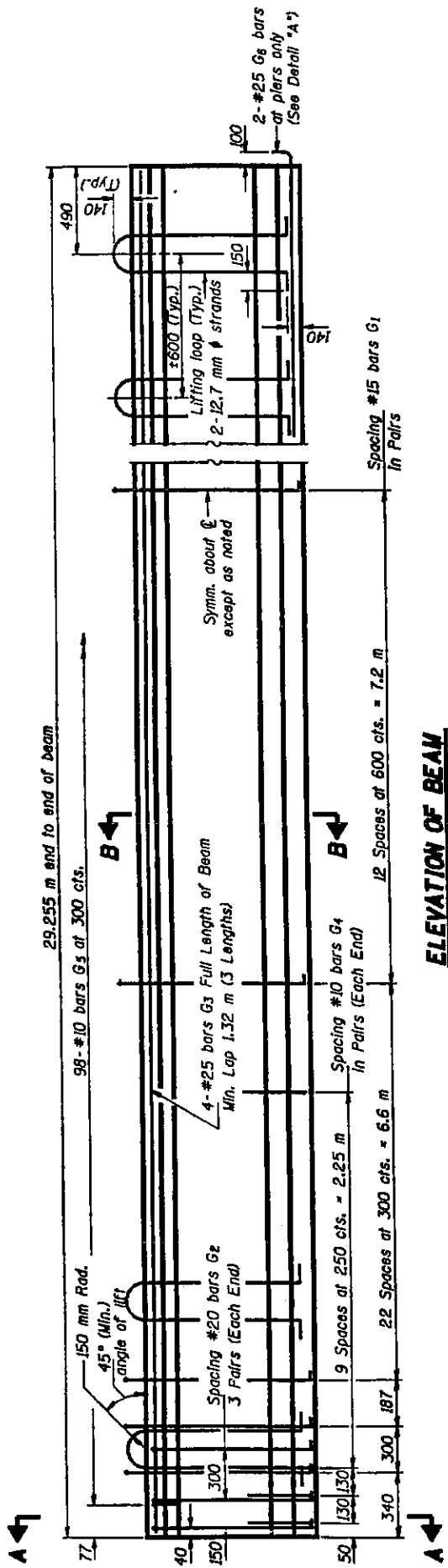


Figure 7.7 Prestressing details of concrete bridge girders

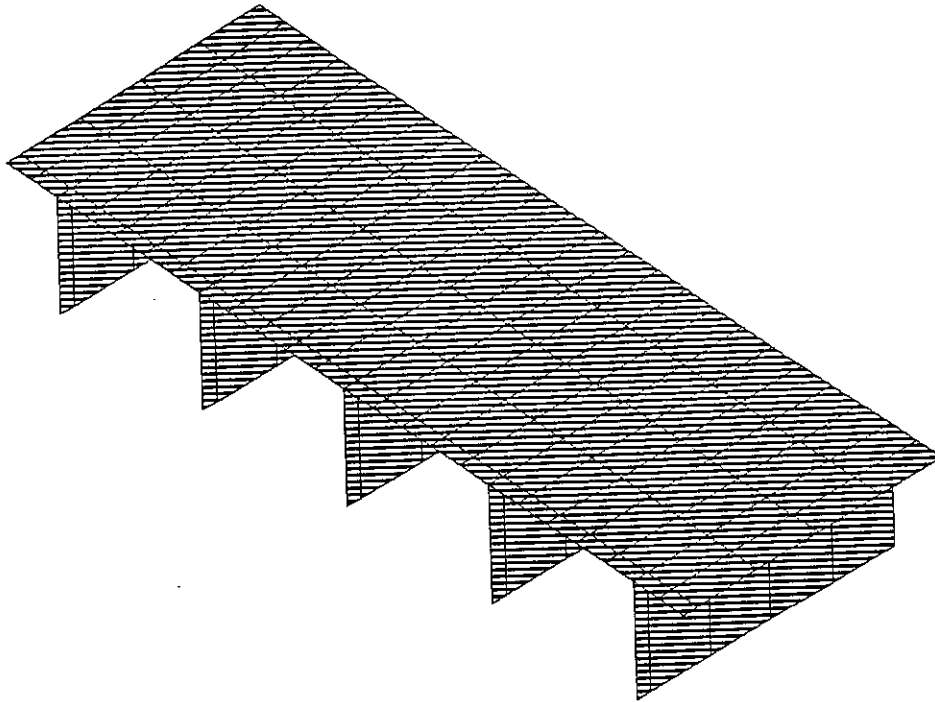


Figure 7.8 Closeup view of steel bridge model

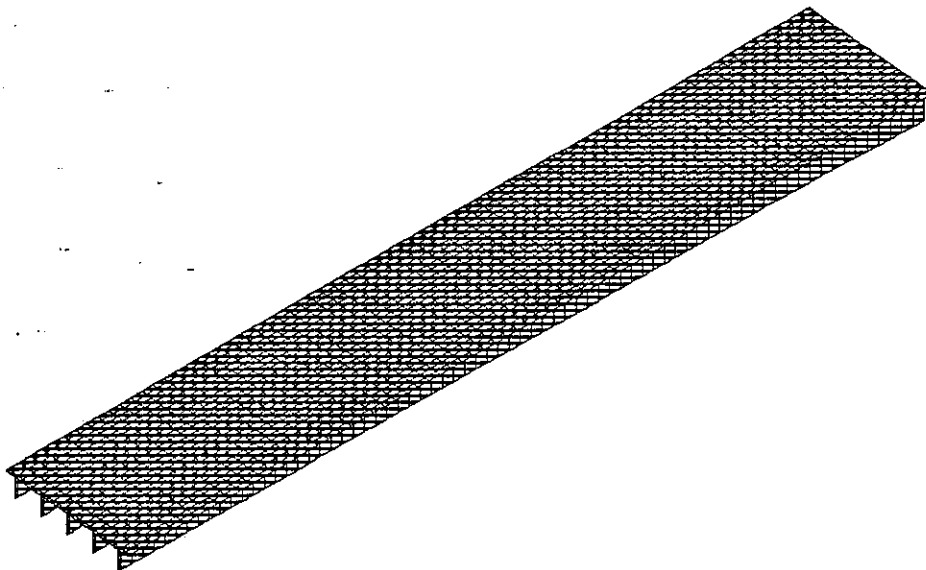


Figure 7.9 Steel bridge model

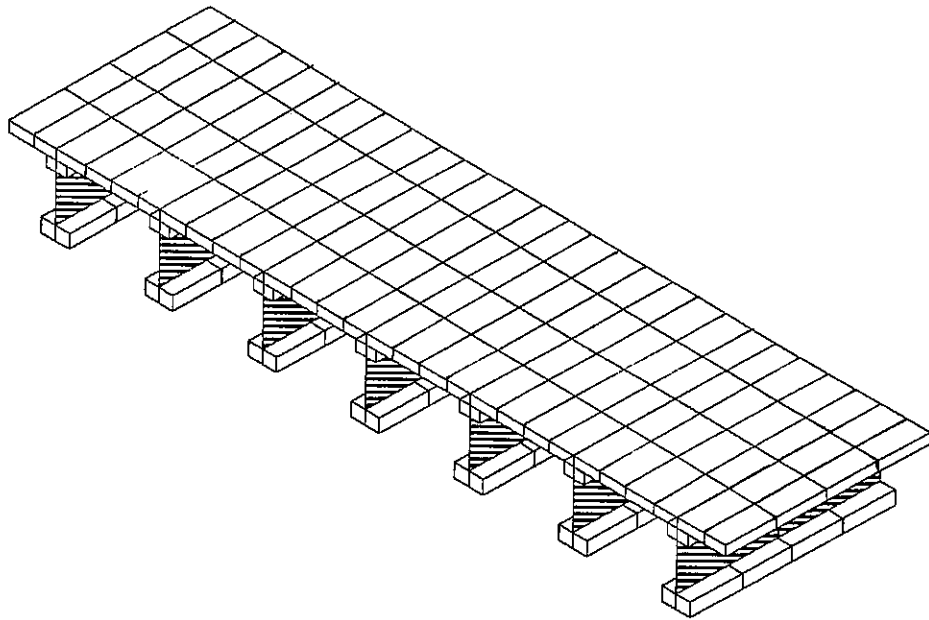


Figure 7.10 Closeup view of concrete bridge model

Load case #1 (front axle @ 8 m from end)
Maximum load = 18 kN
Minimum load = 4.5 kN

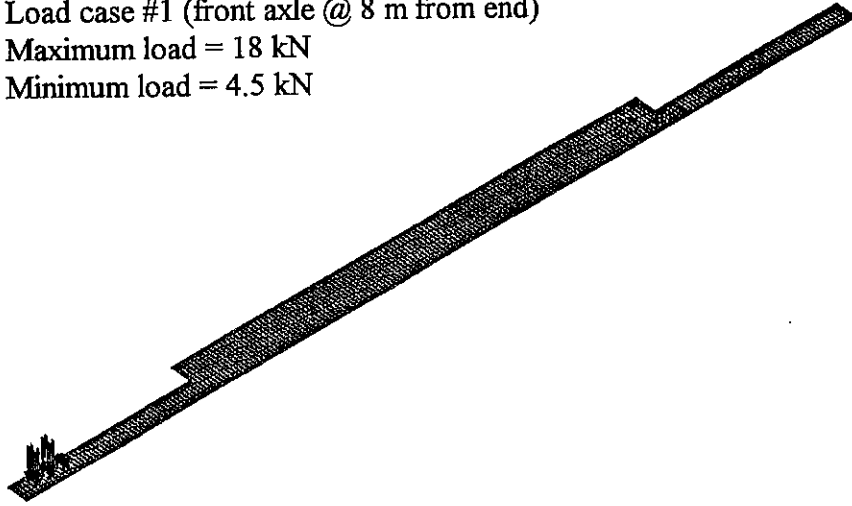


Figure 7.11 Loading condition No. 1

Load case #6 (front axle @ 70.5 m from end)
Maximum load = 18 kN
Minimum load = 4.5 kN

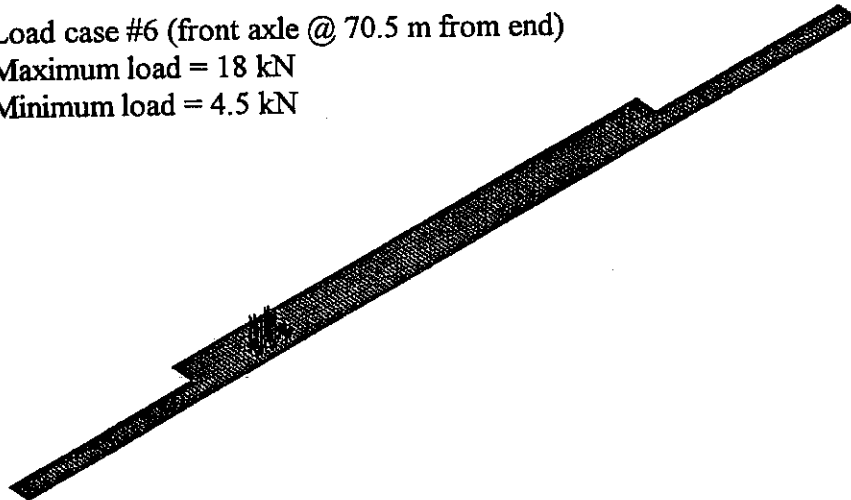


Figure 7.12 Loading condition No. 6

- Load case #10 (front axle @ 120.5 m from end)
Maximum load = 18 kN
Minimum load = 4.5 kN

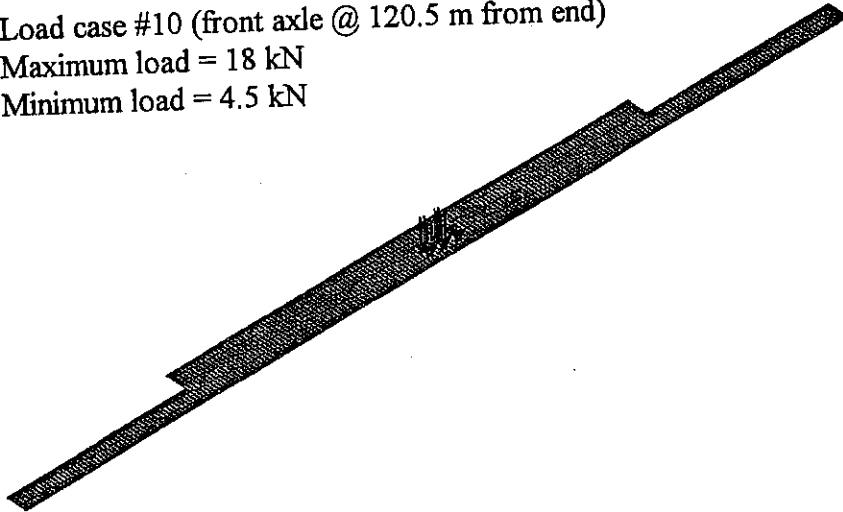


Figure 7.13 Loading condition No. 10

- Load case #19 (concrete mixer and pump loads)
Maximum load = 23 kN
Minimum load = 5.85 kN

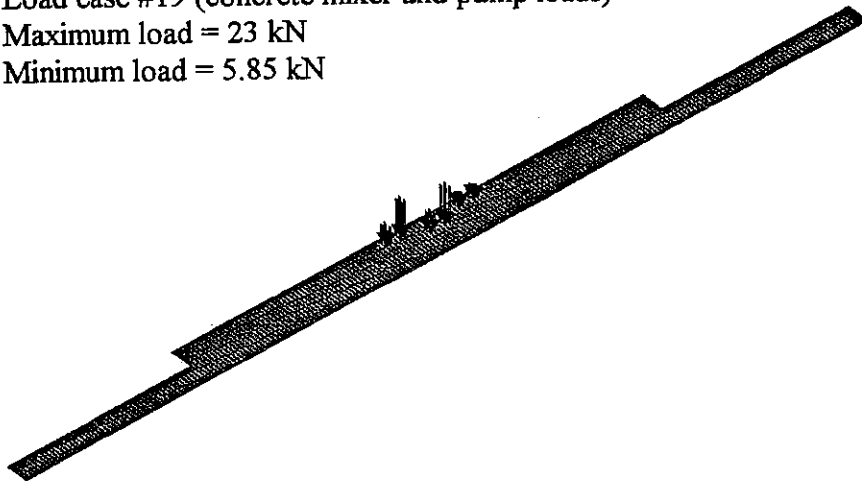


Figure 7.14 Loading condition No. 19

Nodal Loads

Maximum load = 18 kN

Minimum load = 4.5 kN

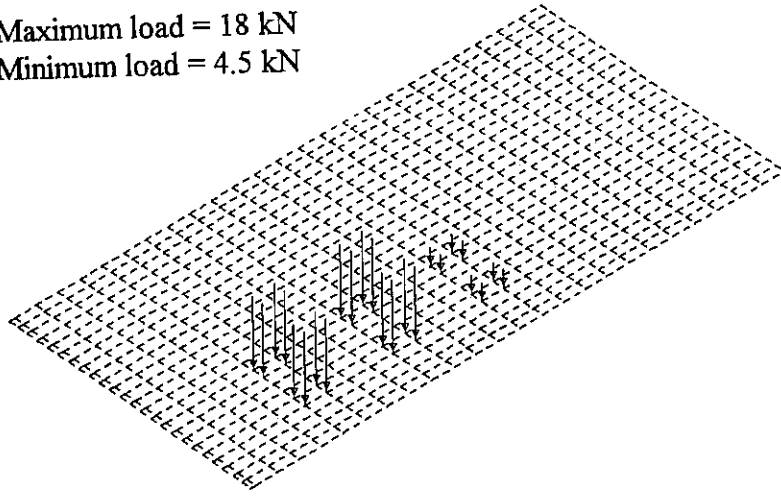


Figure 7.15 Closeup view of HS-20 truck

Nodal Loads

Maximum load = 23 kN

Minimum load = 5.85 kN

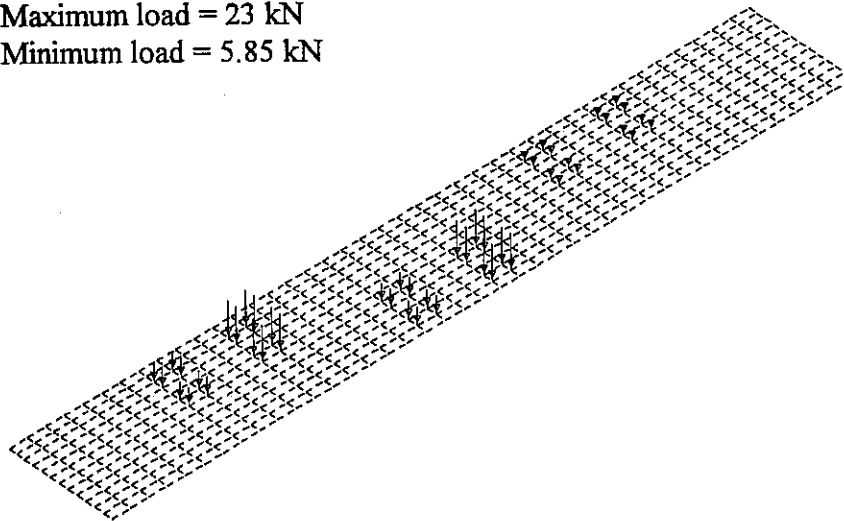


Figure 7.16 Closeup view of construction loads

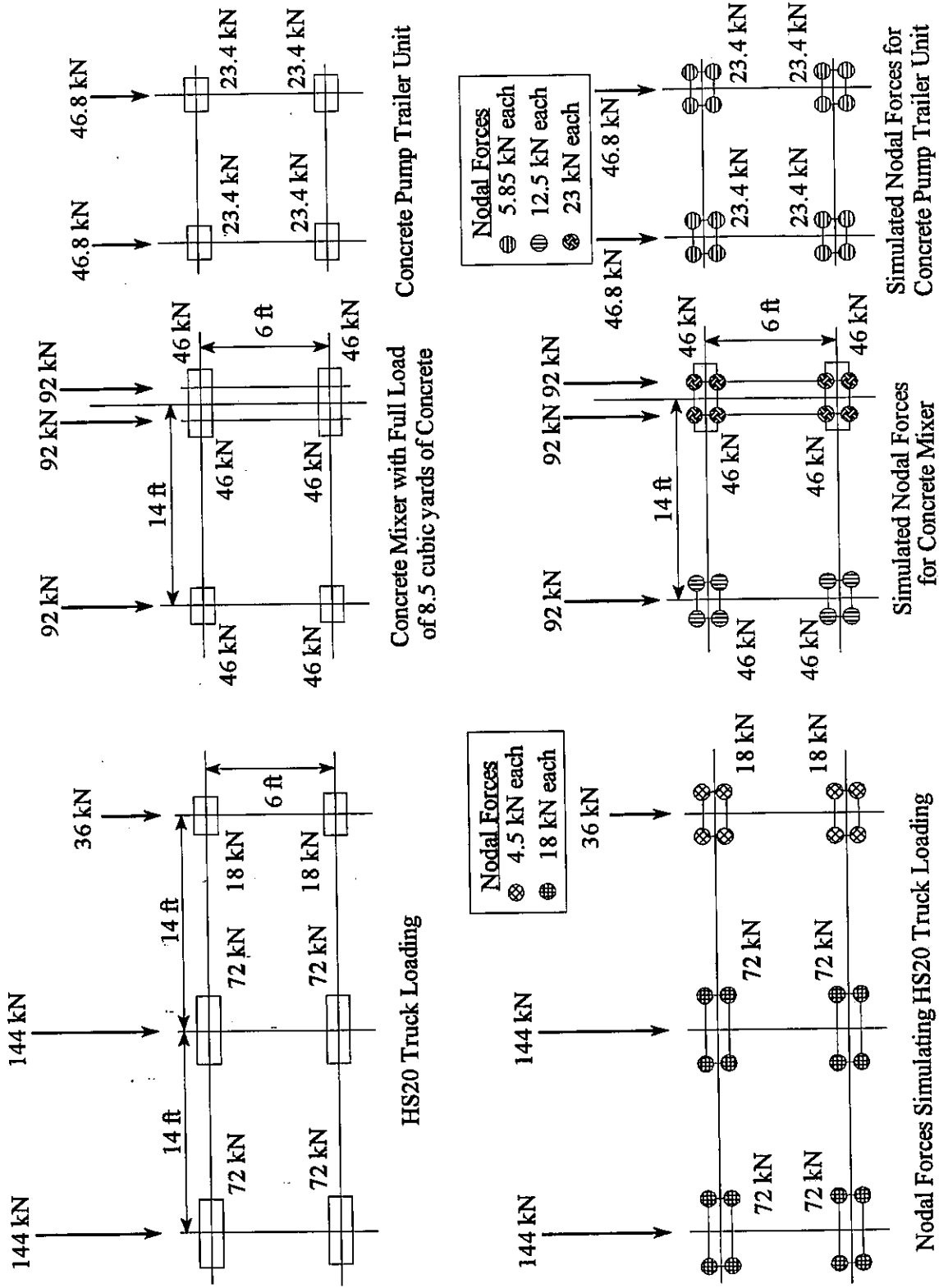


Figure 7.17 Loading patterns for HS20 truck loading and construction loads

Natural frequency = 1.21 Hz, 1st bending mode
Maximum upward displacement = 39.8 mm
Maximum downward displacement = 29.5 mm

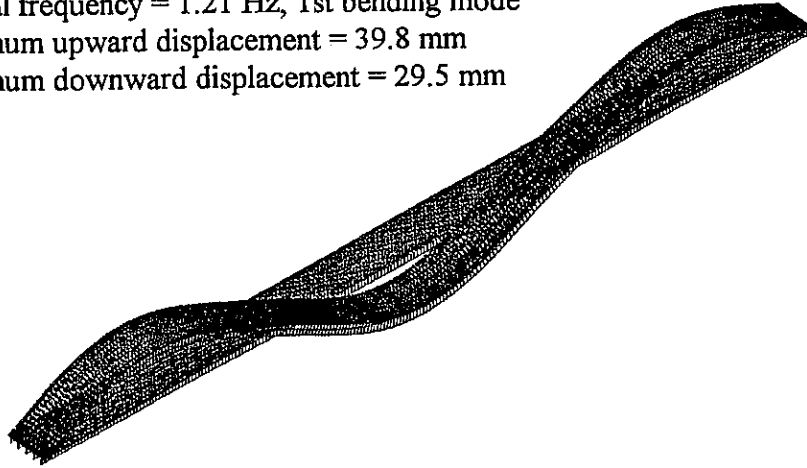


Figure 7.18 Mode shape 1 for steel bridge

Natural frequency = 1.41 Hz, 2nd bending mode
Maximum upward displacement = 40.8 mm
Maximum downward displacement = 40.1 mm

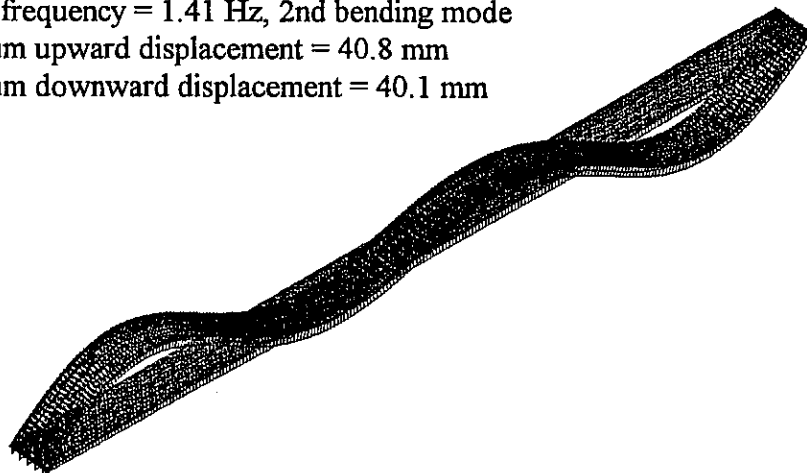


Figure 7.19 Mode shape 2 for steel bridge

Natural frequency = 1.86 Hz, 3rd bending mode
Maximum upward displacement = 0.6 mm
Maximum downward displacement = 37.8 mm

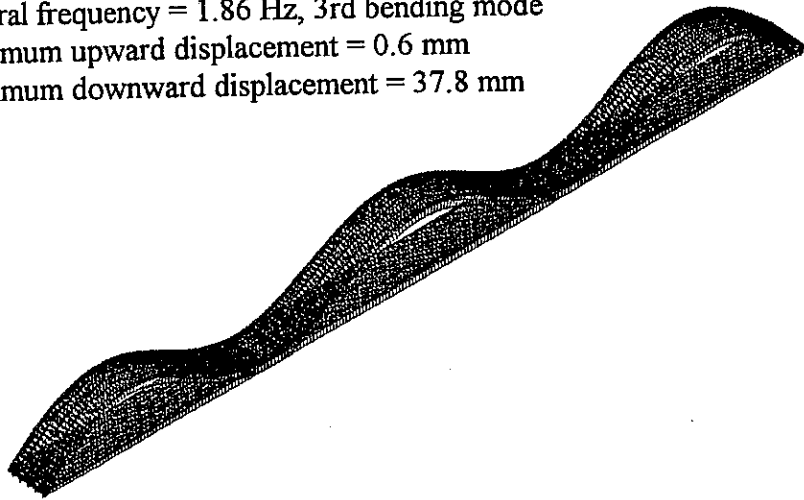


Figure 7.20 Mode shape 3 for steel bridge

Natural frequency = 2.22 Hz, 1st torsional mode
Maximum upward displacement = 104.7 mm
Maximum downward displacement = 104.3 mm

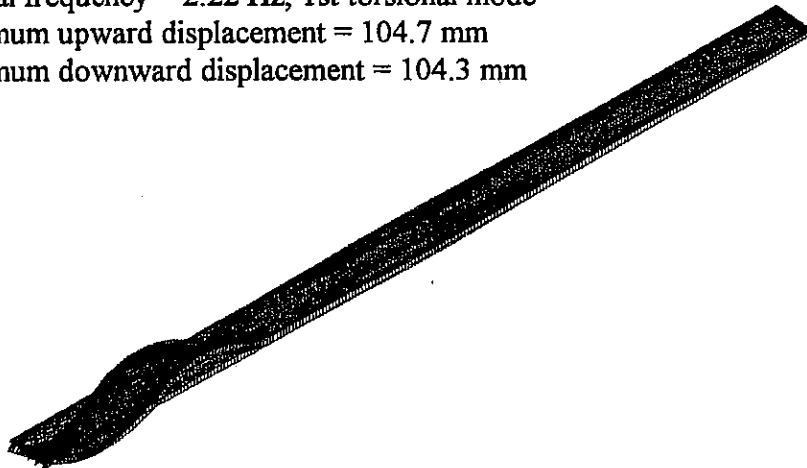


Figure 7.21 Mode shape 4 for steel bridge

Natural frequency = 2.28 Hz, 2nd torsional mode
Maximum upward displacement = 101.5 mm
Maximum downward displacement = 101.2 mm

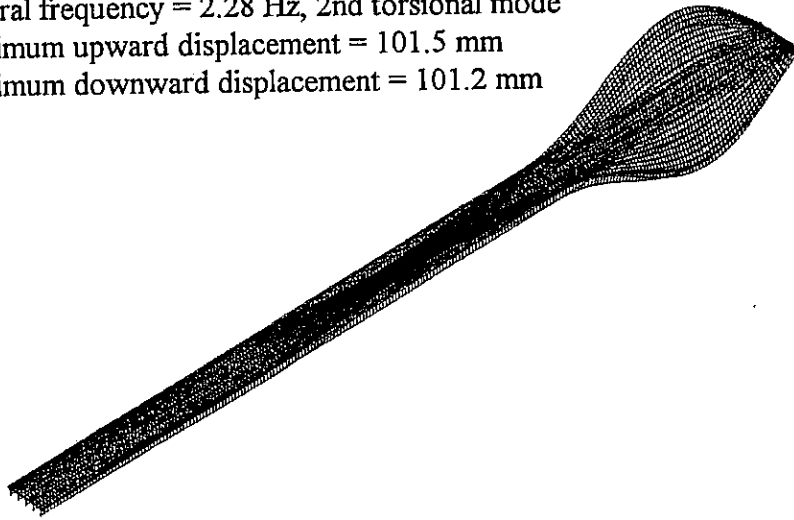


Figure 7.22 Mode shape 5 for steel bridge

Natural frequency = 2.30 Hz, 3rd torsional mode
Maximum upward displacement = 94.5 mm
Maximum downward displacement = 94.6 mm

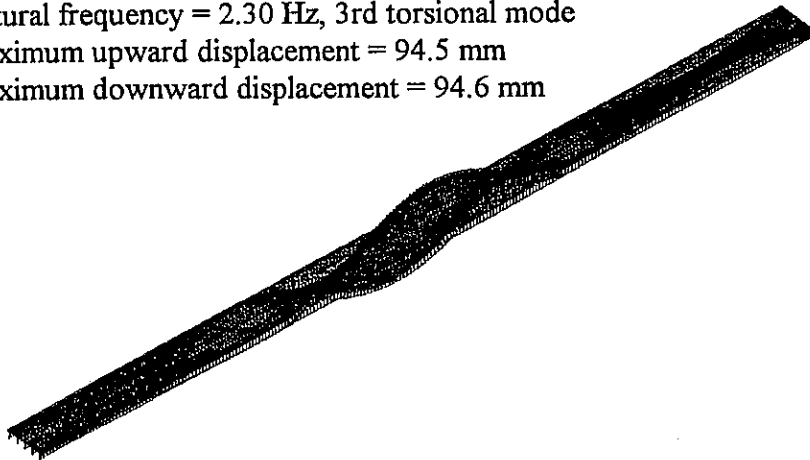


Figure 7.23 Mode shape 6 for steel bridge

Natural frequency = 3.49 Hz, 4th bending mode
Maximum upward displacement = 41.1 mm
Maximum downward displacement = 41.5 mm

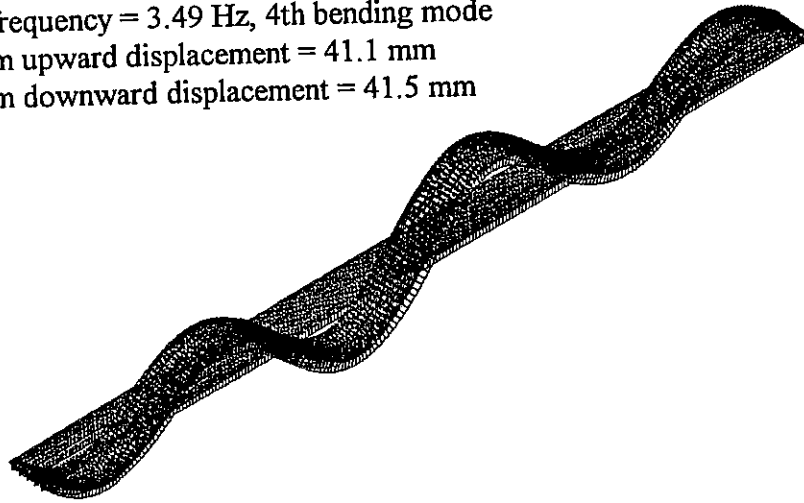


Figure 7.24 Mode shape 7 for steel bridge

Natural frequency = 4.36 Hz, 4th torsional mode
Maximum upward displacement = 62.2 mm
Maximum downward displacement = 94.2 mm

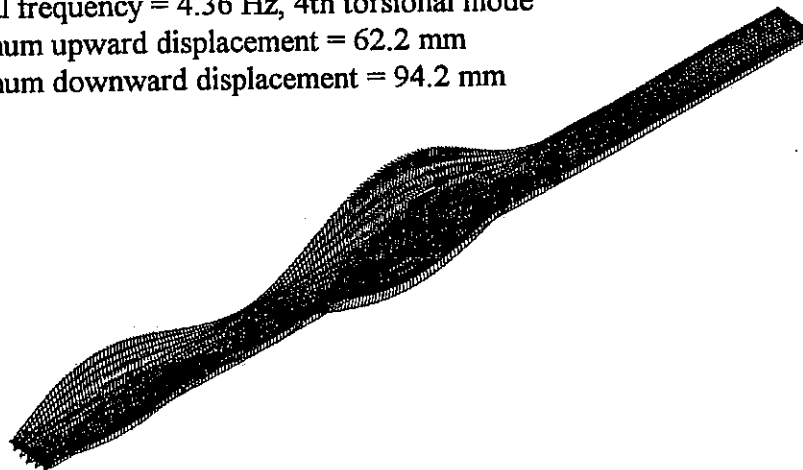


Figure 7.25 Mode shape 8 for steel bridge

Natural frequency = 4.36 Hz, 5th torsional mode
Maximum upward displacement = 102.0 mm
Maximum downward displacement = 67.2 mm

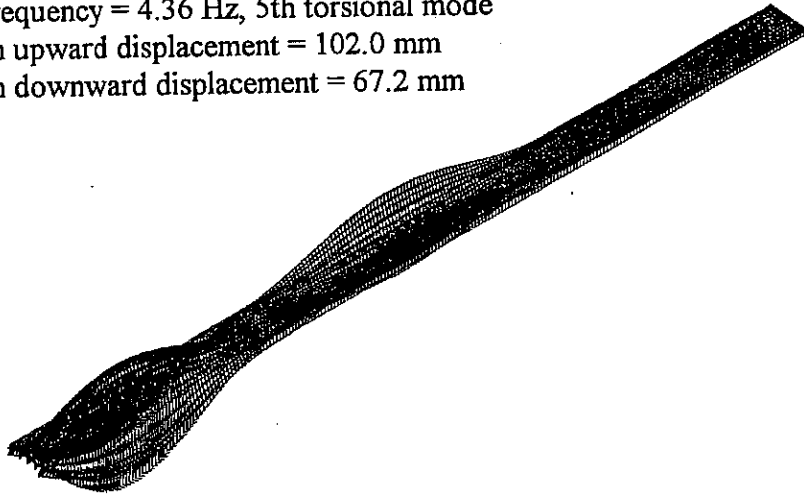


Figure 7.26 Mode shape 9 for steel bridge

Natural frequency = 4.38 Hz, 6th torsional mode
Maximum upward displacement = 76.8 mm
Maximum downward displacement = 117.1 mm

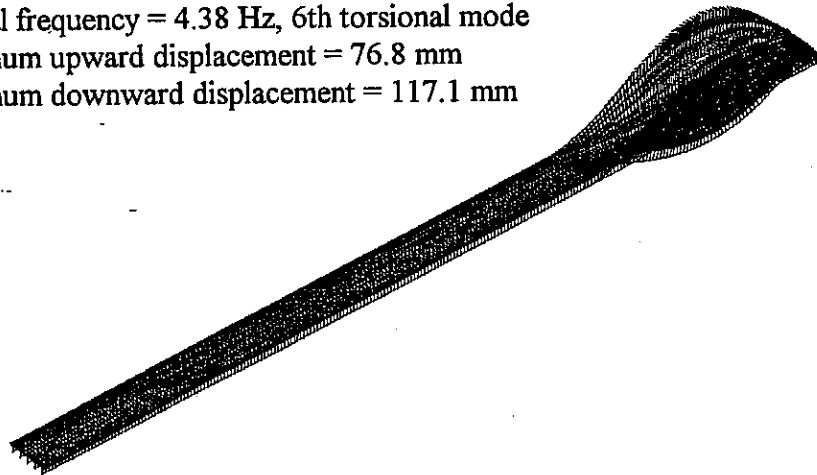


Figure 7.27 Mode shape 10 for steel bridge

Natural frequency = 2.01 Hz, 1st bending mode
Maximum upward displacement = 42.7 mm
Maximum downward displacement = 42.8 mm

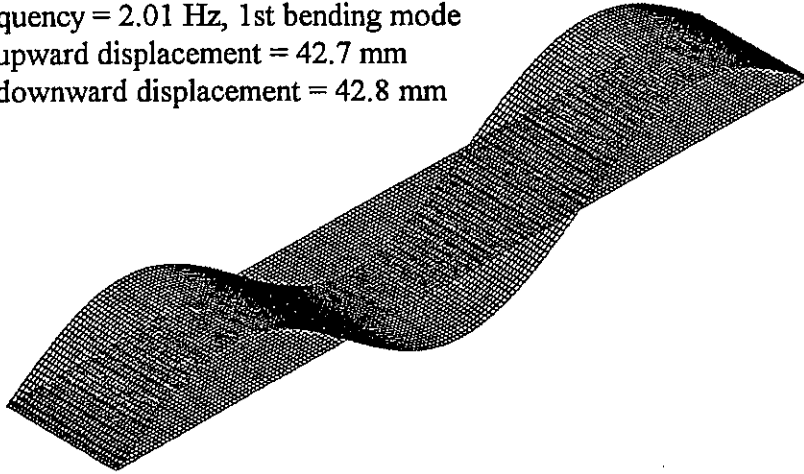


Figure 7.28 Mode shape 1 for concrete bridge

Natural frequency = 2.24 Hz, 1st torsional mode
Maximum upward displacement = 70.9 mm
Maximum downward displacement = 70.9 mm

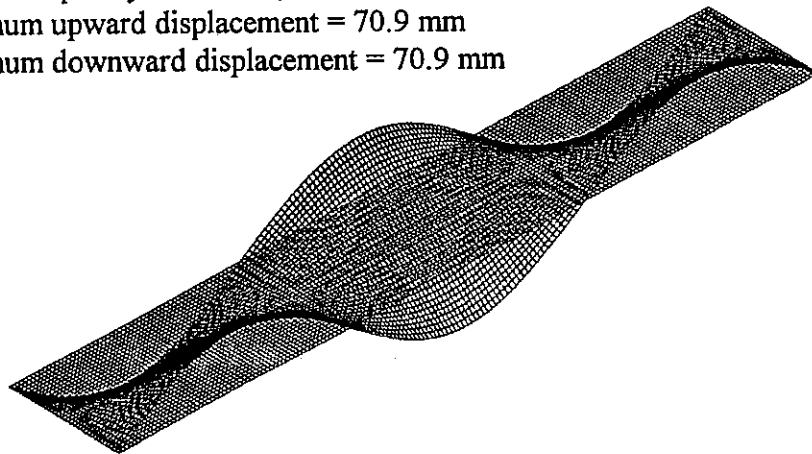


Figure 7.29 Mode shape 2 for concrete bridge

Natural frequency = 2.56 Hz, 2nd bending mode
Maximum upward displacement = 53.3 mm
Maximum downward displacement = 53.3 mm

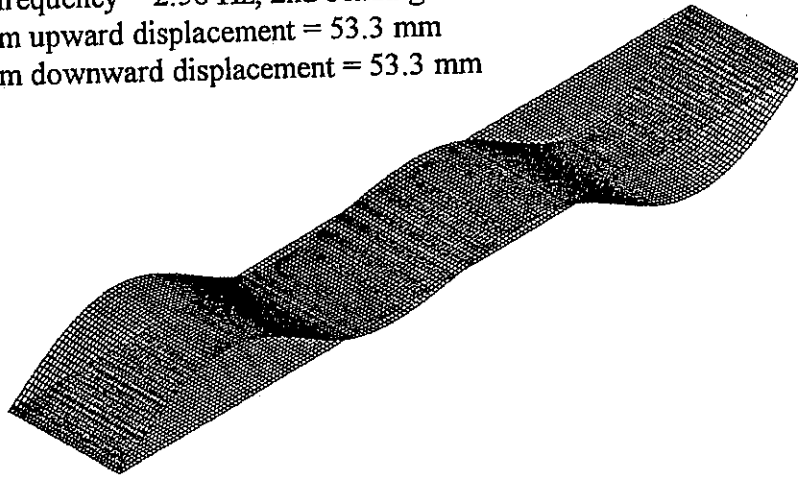


Figure 7.30 Mode shape 3 for concrete bridge

Natural frequency = 2.76 Hz, 2nd torsional mode
Maximum upward displacement = 88.3 mm
Maximum downward displacement = 88.3 mm

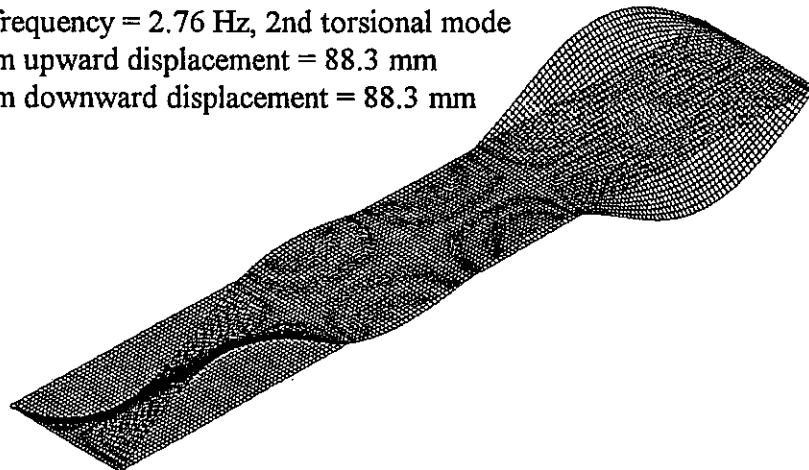


Figure 7.31 Mode shape 4 for concrete bridge

Natural frequency = 3.69 Hz, 1st bending/torsional mode
Maximum upward displacement = 81.6 mm
Maximum downward displacement = 82.2 mm

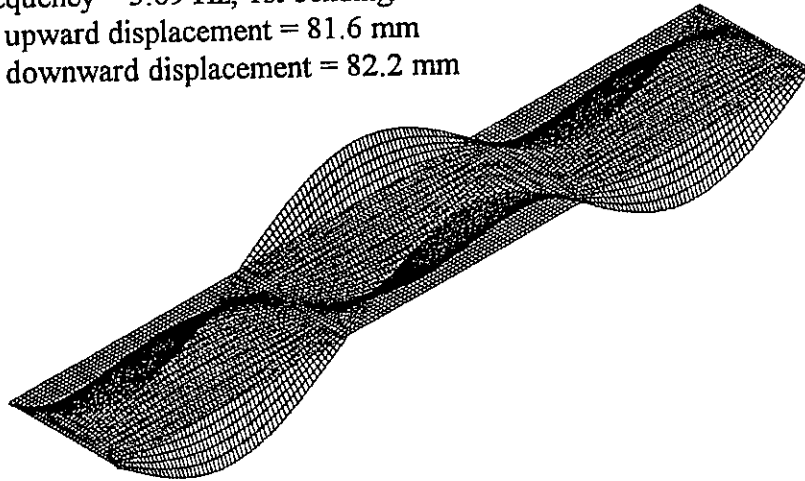


Figure 7.32 Mode shape 5 for concrete bridge

Natural frequency = 3.71 Hz, 3rd bending mode
Maximum upward displacement = 2.5 mm
Maximum downward displacement = 63.7 mm

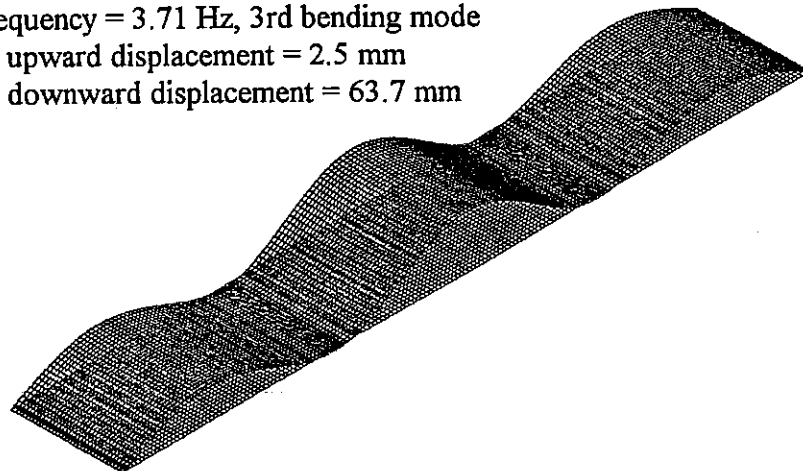


Figure 7.33 Mode shape 6 for concrete bridge

Natural frequency = 3.86 Hz, 3rd torsional mode
Maximum upward displacement = 105.2 mm
Maximum downward displacement = 105.2 mm

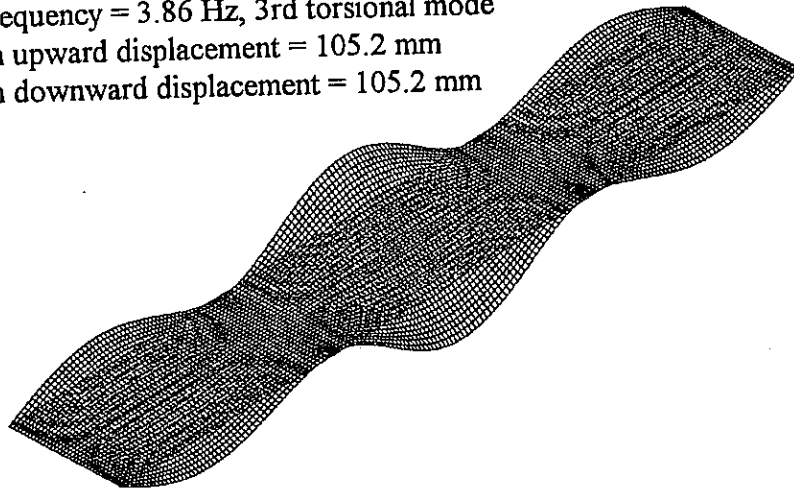


Figure 7.34 Mode shape 7 for concrete bridge

Natural frequency = 4.05 Hz, 2nd bending/torsional mode
Maximum upward displacement = 102.0 mm
Maximum downward displacement = 102.0 mm

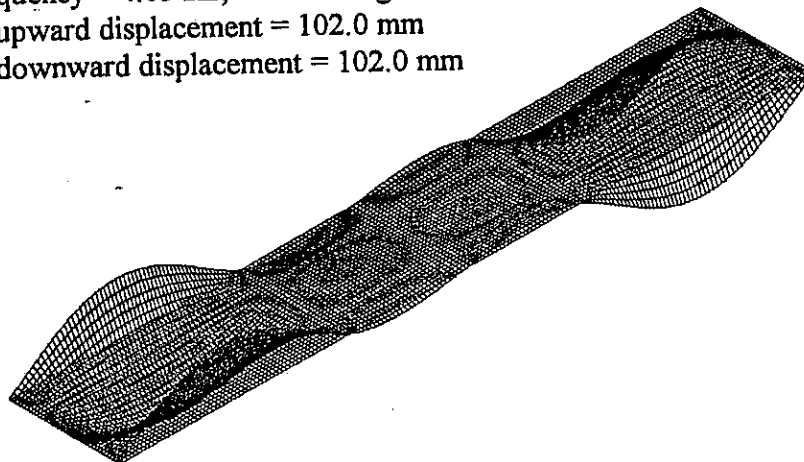


Figure 7.35 Mode shape 8 for concrete bridge

Natural frequency = 4.90 Hz, 3rd bending/torsional mode
Maximum upward displacement = 121.9 mm
Maximum downward displacement = 78.2 mm

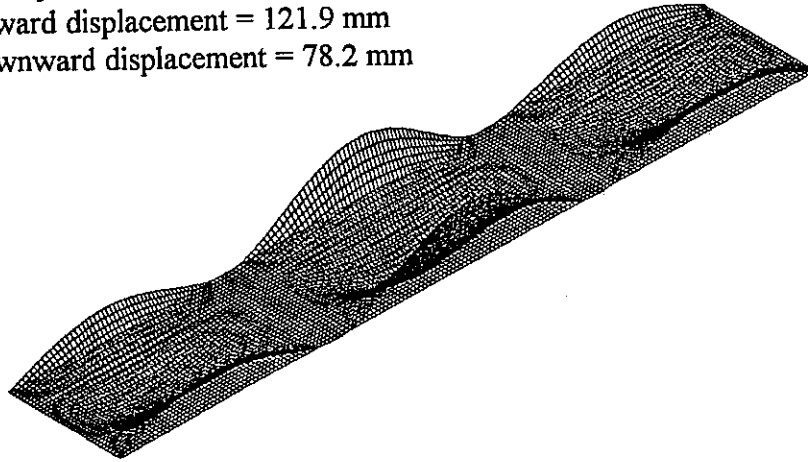


Figure 7.36 Mode shape 9 for concrete bridge

Natural frequency = 7.51 Hz, 4th bending/torsional mode
Maximum upward displacement = 84.8 mm
Maximum downward displacement = 84.7 mm

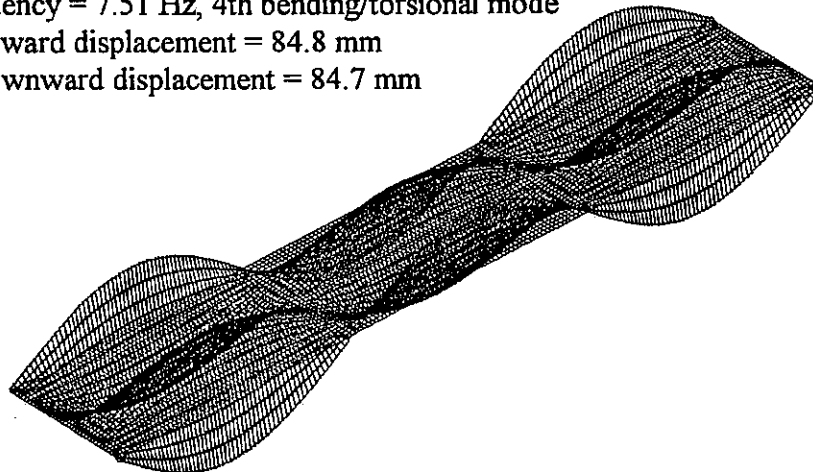


Figure 7.37 Mode shape 10 for concrete bridge

Frequencies for Various Bridges

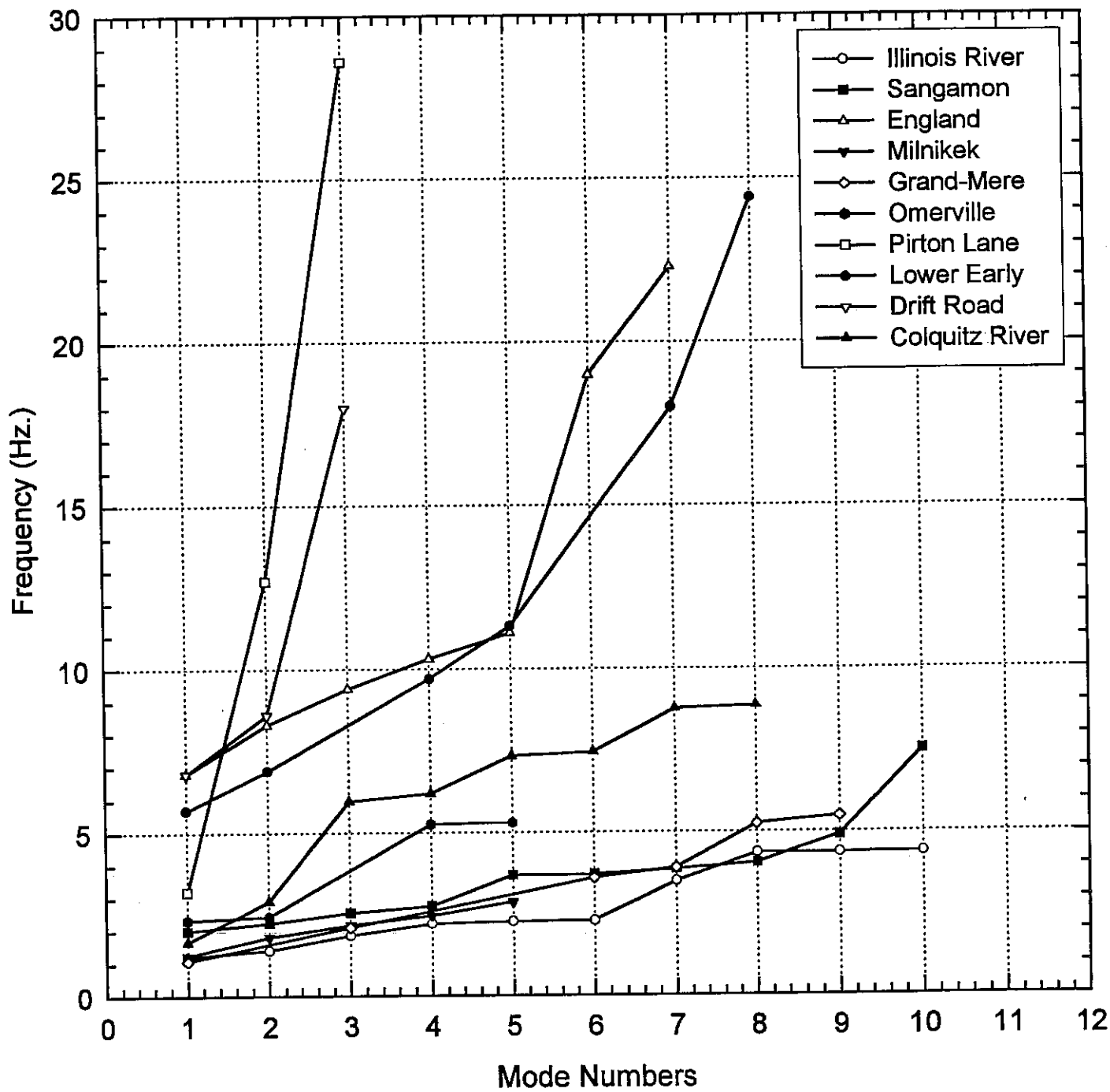


Figure 7.38 Frequencies vs mode shape numbers for various bridges

Frequencies for Various Bridges

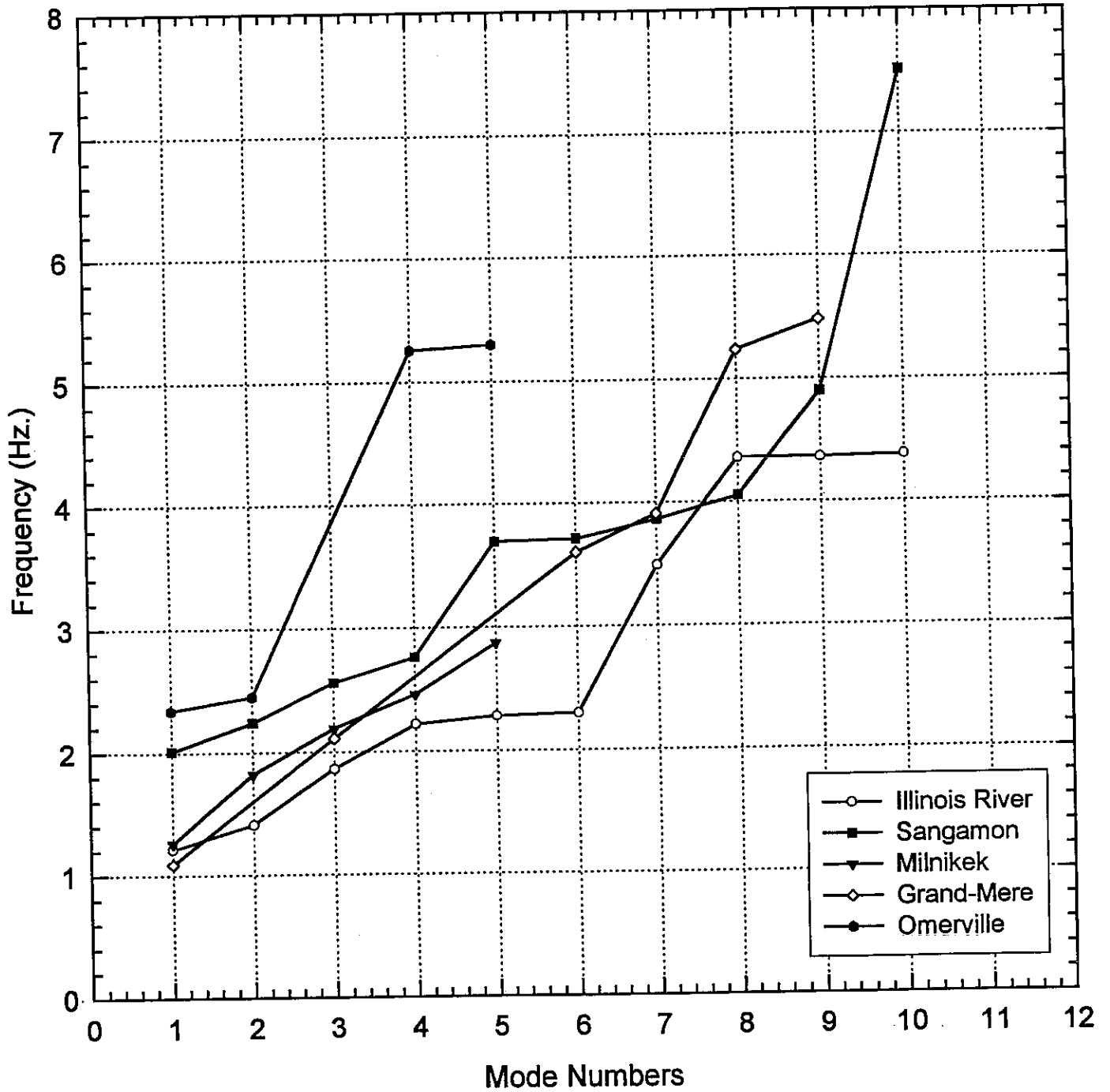


Figure 7.39 Low frequency bridges for various mode shapes

Frequency vs Span Length *Simply-Supported Bridges*

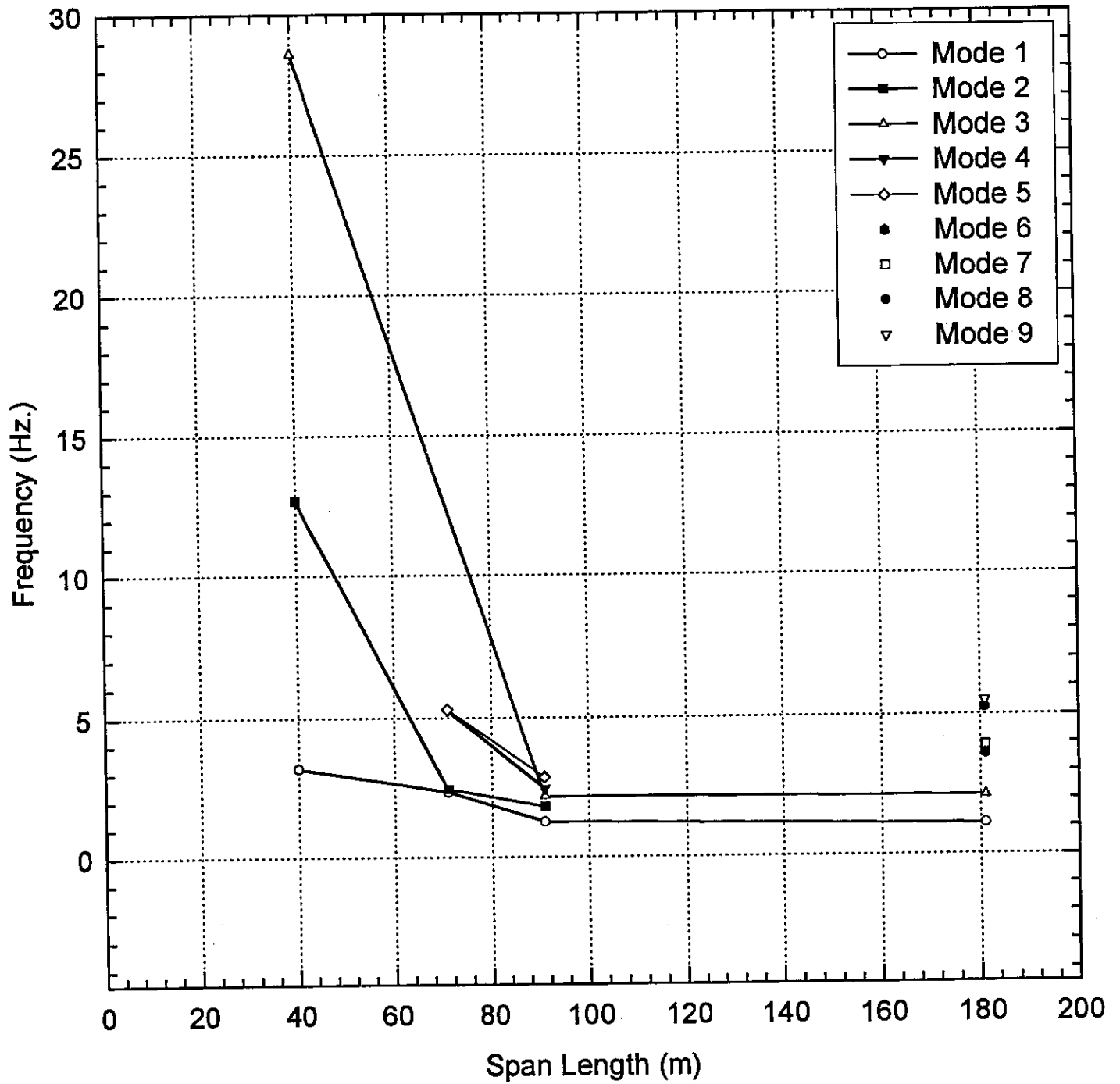


Figure 7.40 Frequencies vs span length for simply supported bridges

Frequency vs Span Length Continuous Bridges

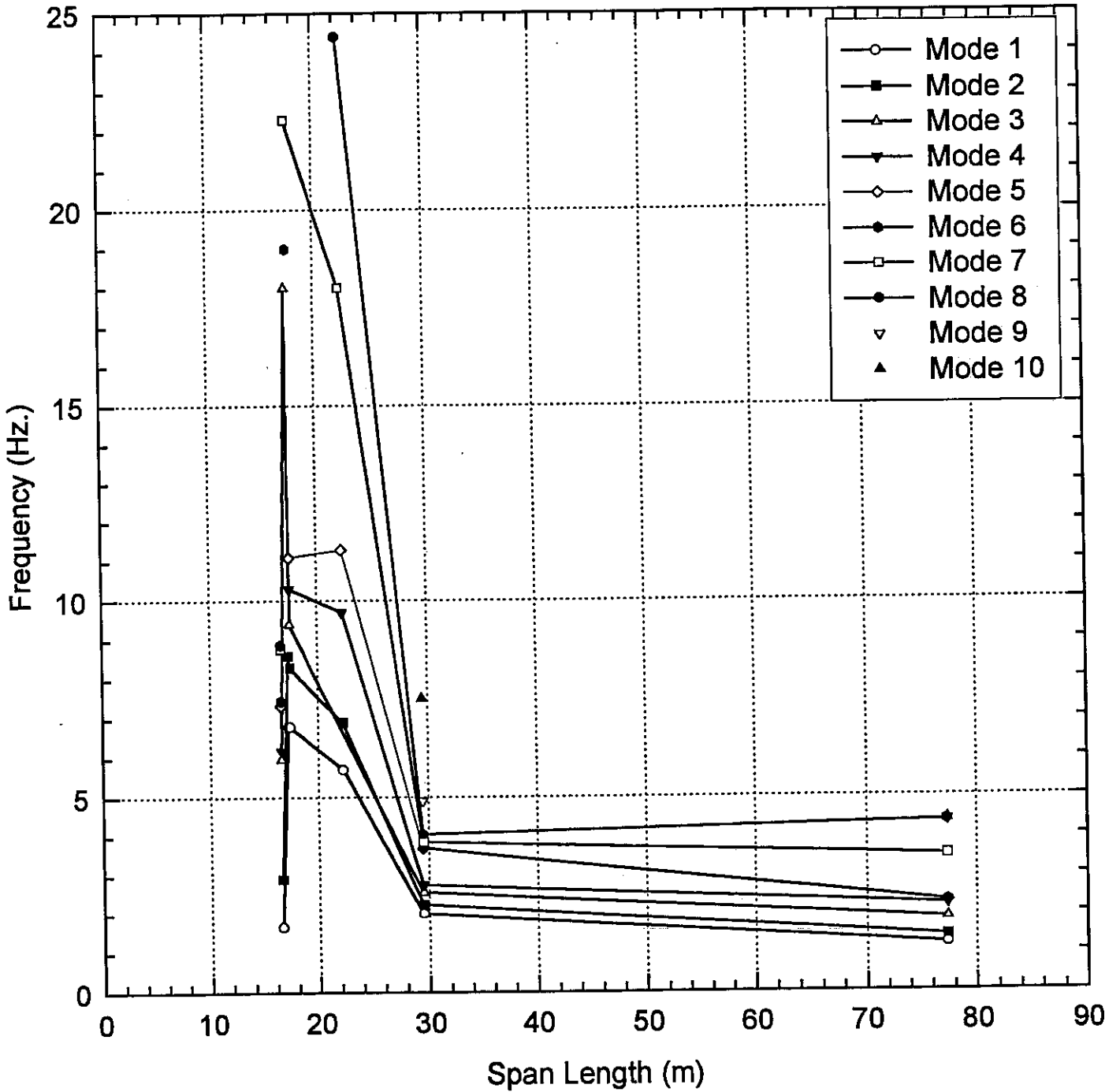


Figure 7.41 Frequencies vs span length for continuous bridges

Maximum displacement = 20.6 mm

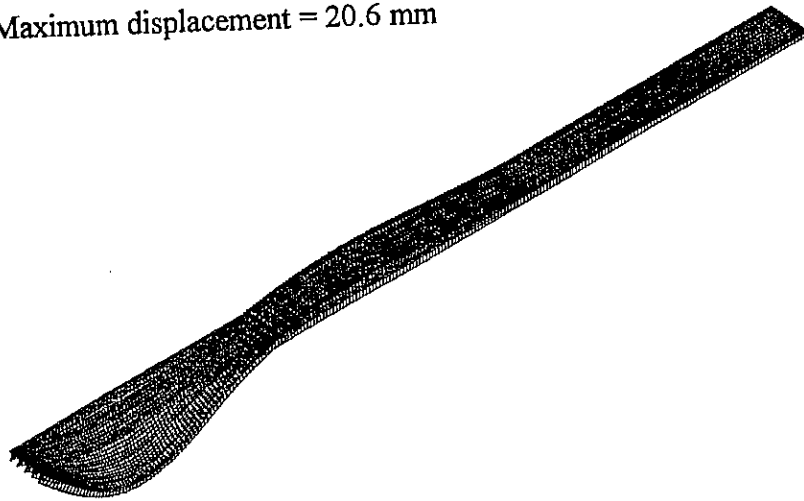


Figure 7.42 Maximum displacement in steel bridge due to moving vehicle

Maximum displacement = 17.1 mm

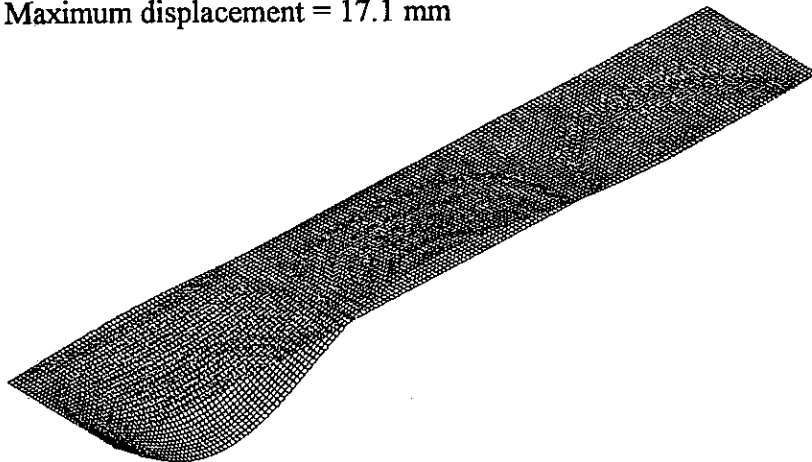


Figure 7.43 Maximum displacement in concrete bridge due to moving vehicle

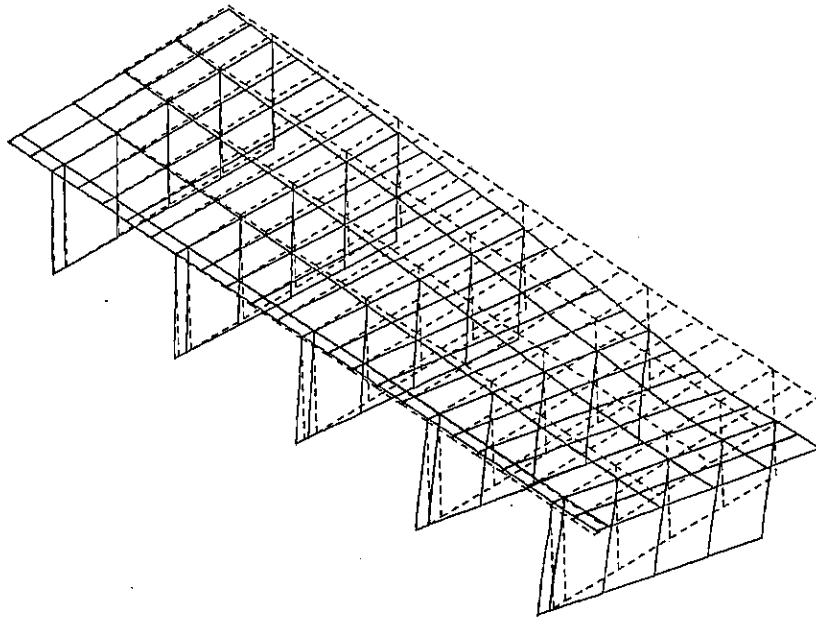


Figure 7.44 Typical deflection mode in steel bridge

Load case #19 (dead loads)
Maximum displacement = 102.3 mm

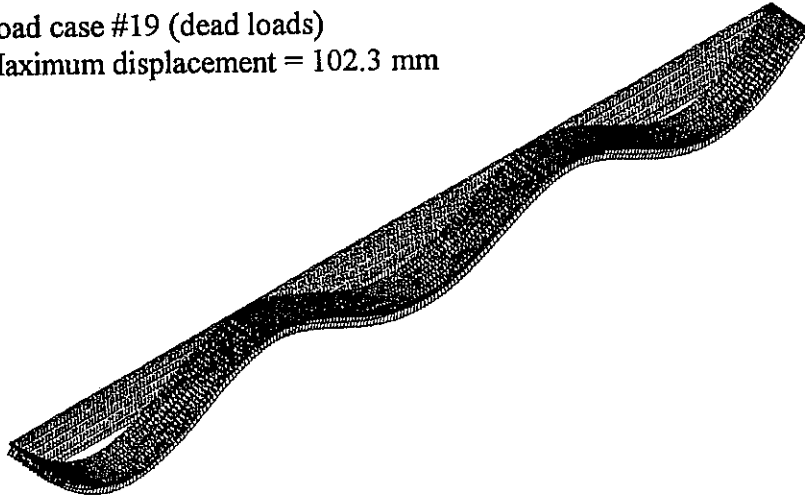


Figure 7.45 Displacement in steel bridge due to dead load

Load case #18 (dead loads)
Maximum displacement = 42.3 mm

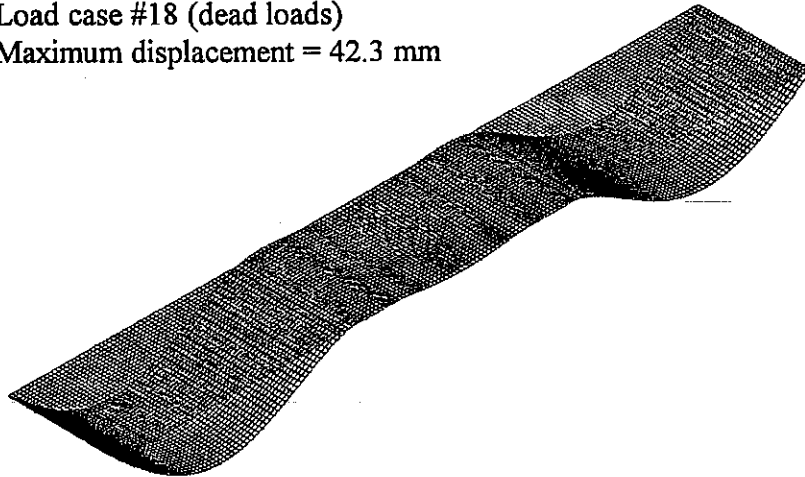


Figure 7.46 Displacement in concrete bridge due to dead load

Illinois River bridge Maximum Top & Bottom Stresses

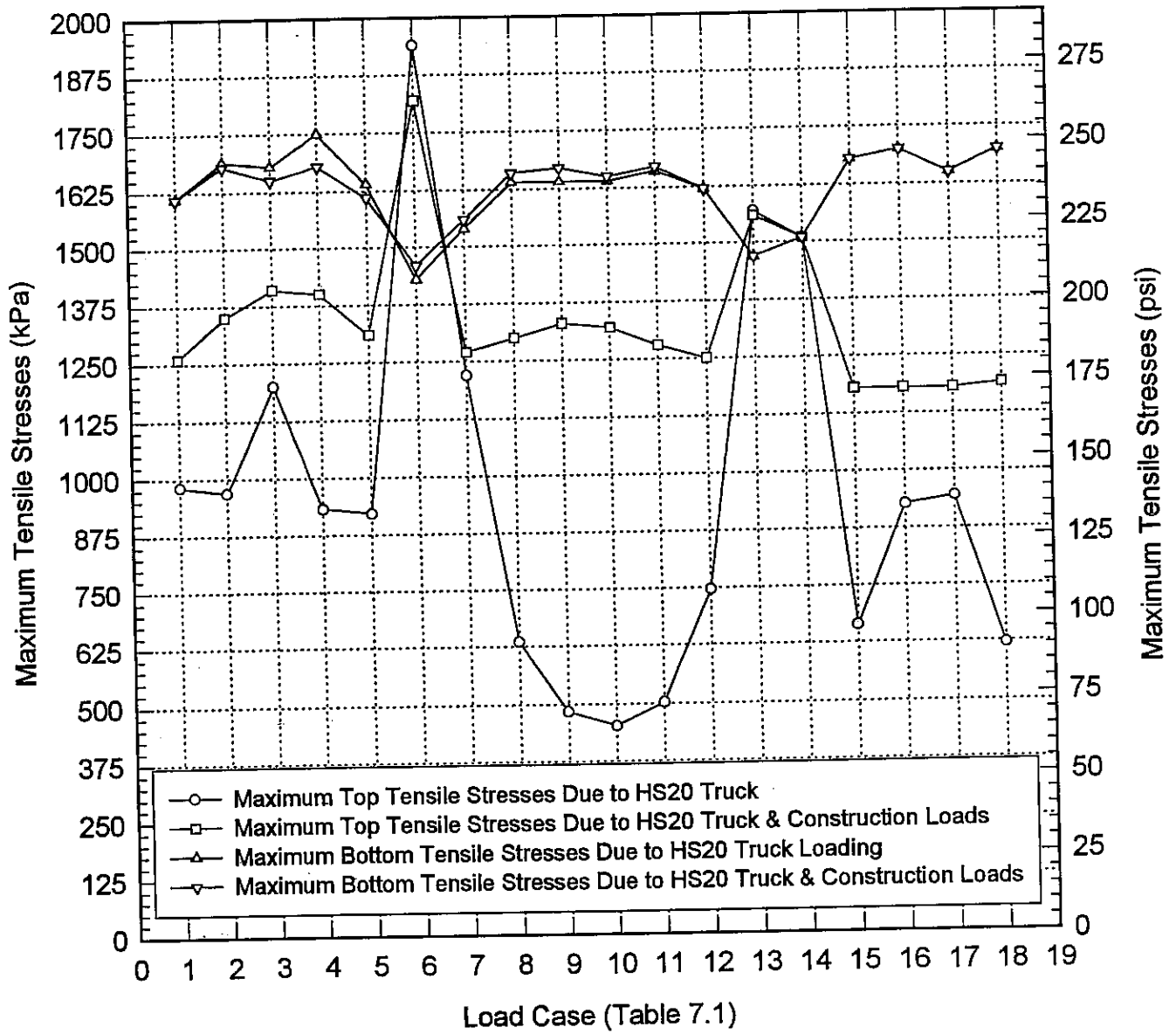


Figure 7.47 Maximum top & bottom stresses in slab

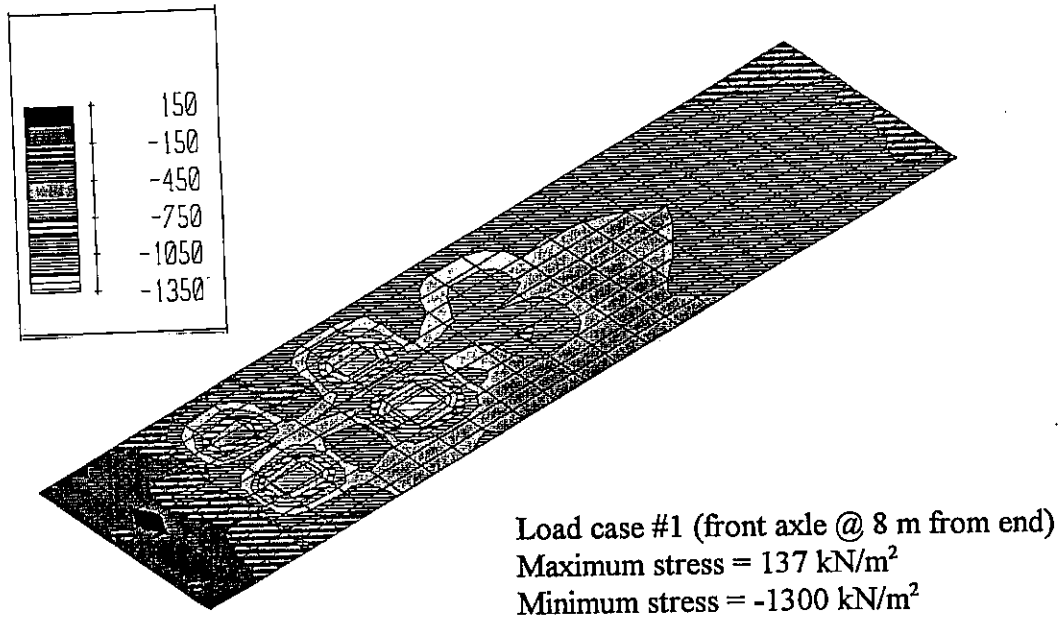


Figure 7.48 Normal stresses in longitudinal direction at top surface of slab (load case 1)

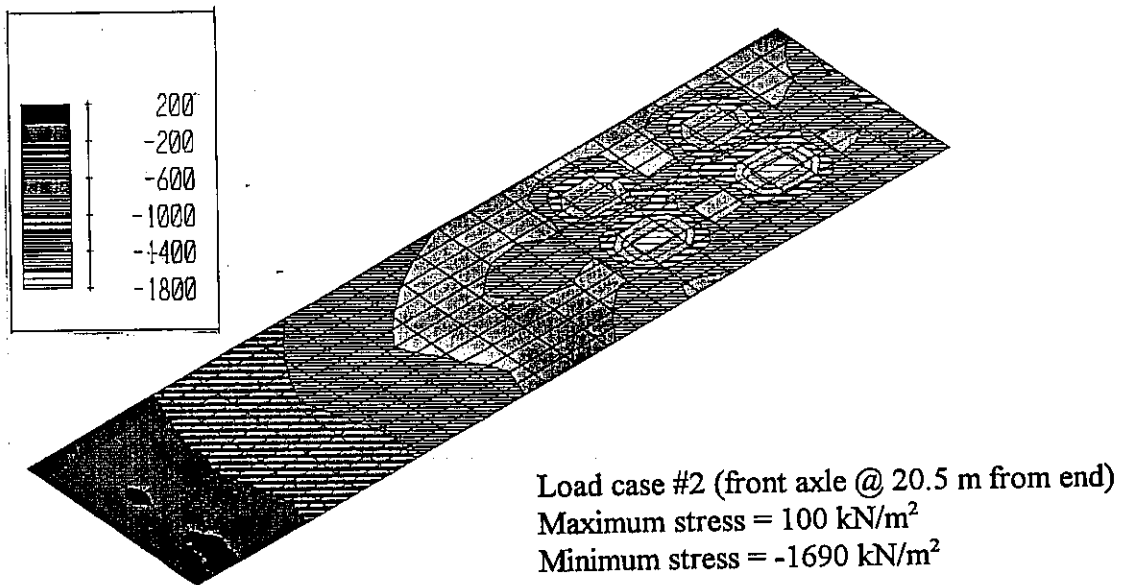


Figure 7.49 Normal stresses in longitudinal direction at top surface of slab (load case 2)

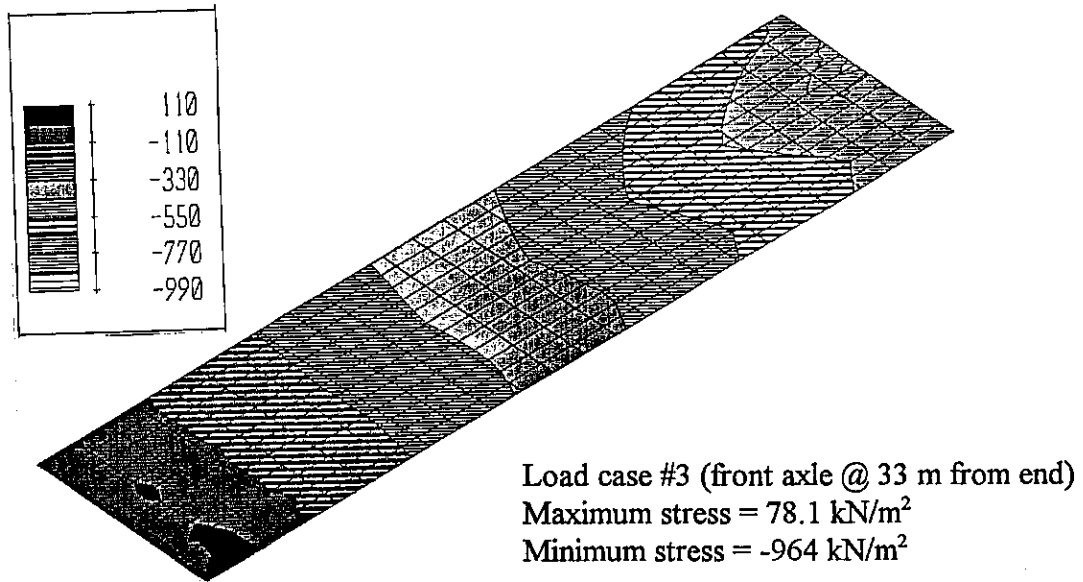


Figure 7.50 Normal stresses in longitudinal direction at top surface of slab (load case 3)

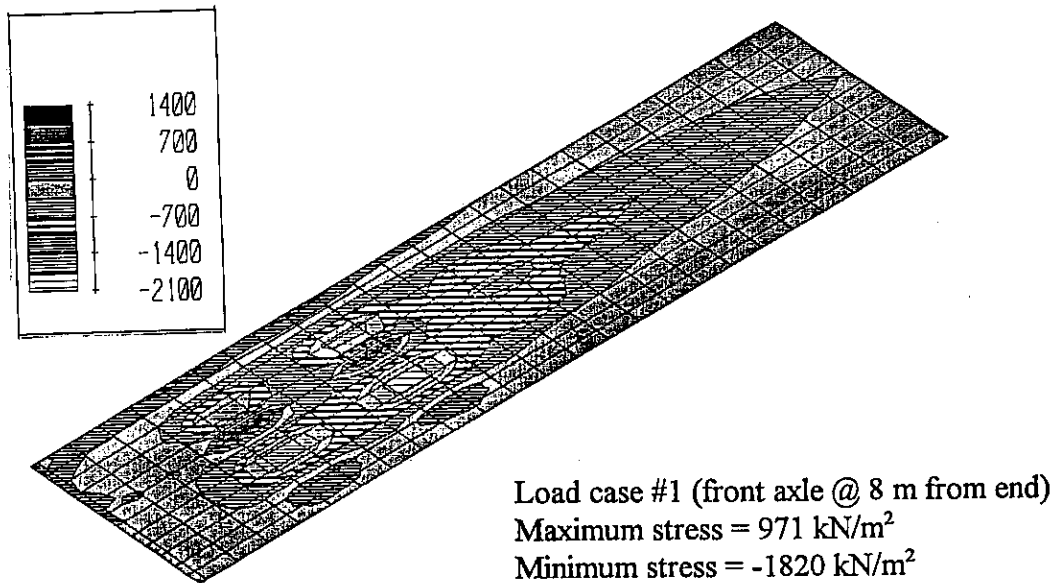


Figure 7.51 Normal stresses in transverse direction at top surface of slab (load case 1)

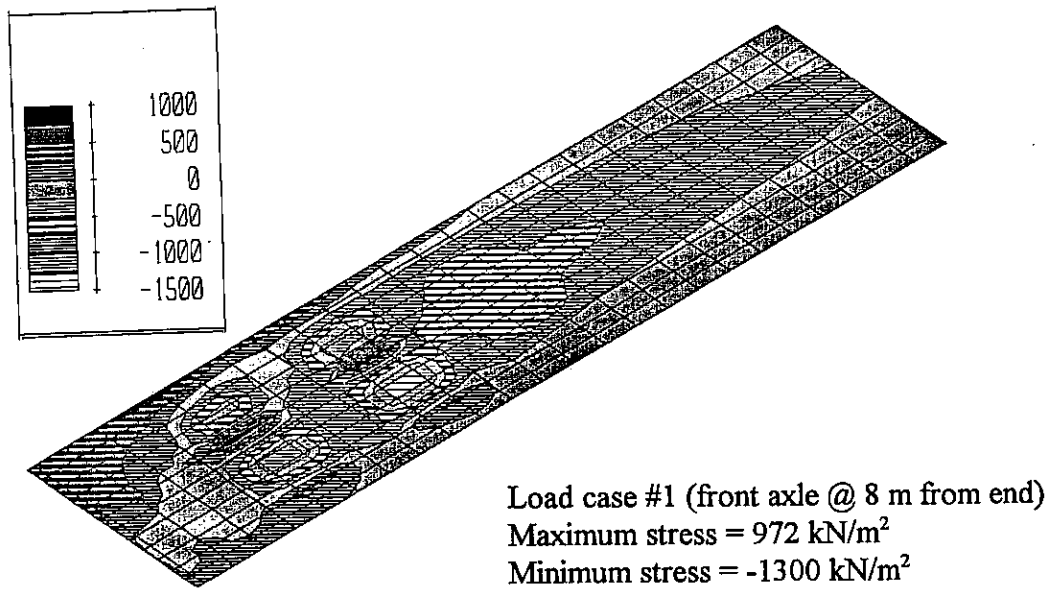


Figure 7.52 Maximum stresses at top surface of slab (load case 1)

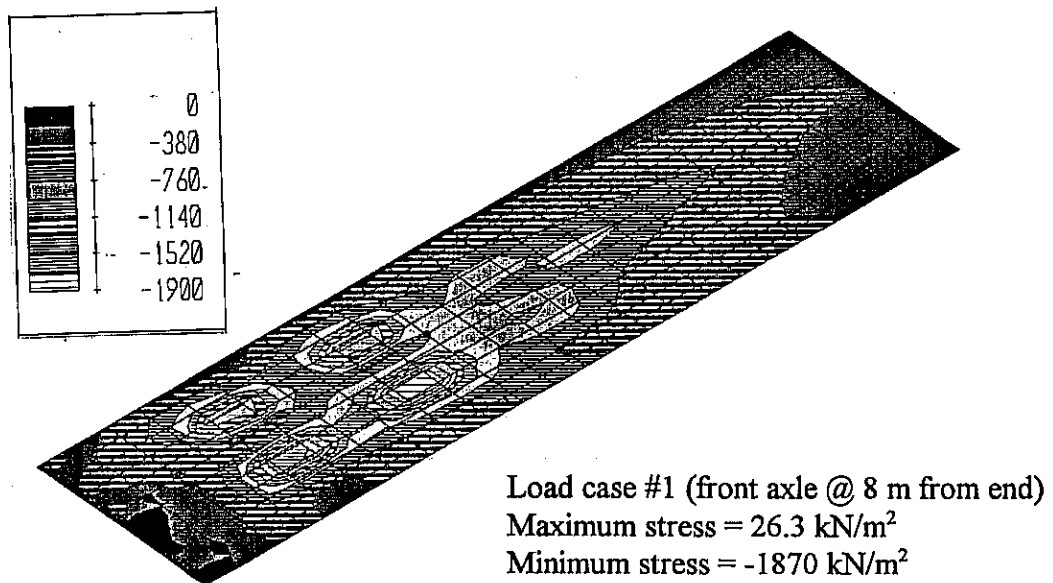


Figure 7.53 Minimum stresses at top surface of slab (load case 1)

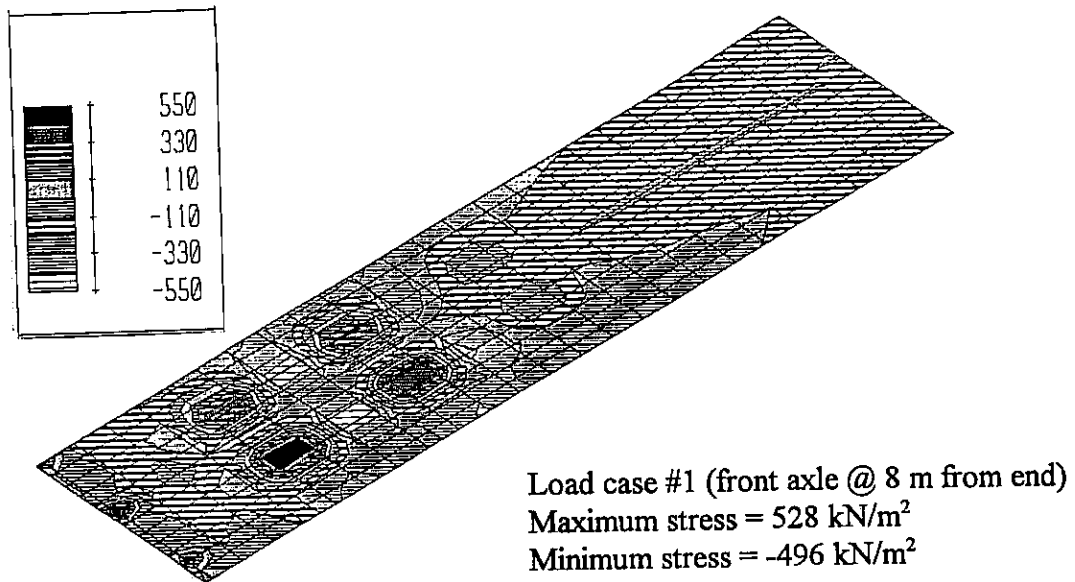


Figure 7.54 Normal stresses in longitudinal direction at bottom surface of slab (load case 1)

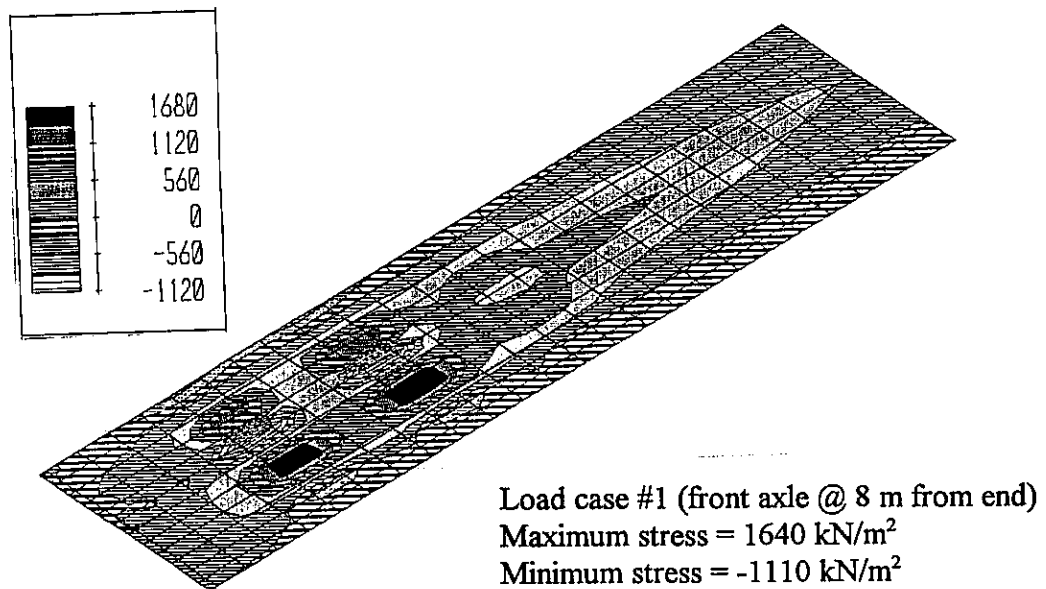


Figure 7.55 Normal stresses in transverse direction at bottom surface of slab (load case 1)

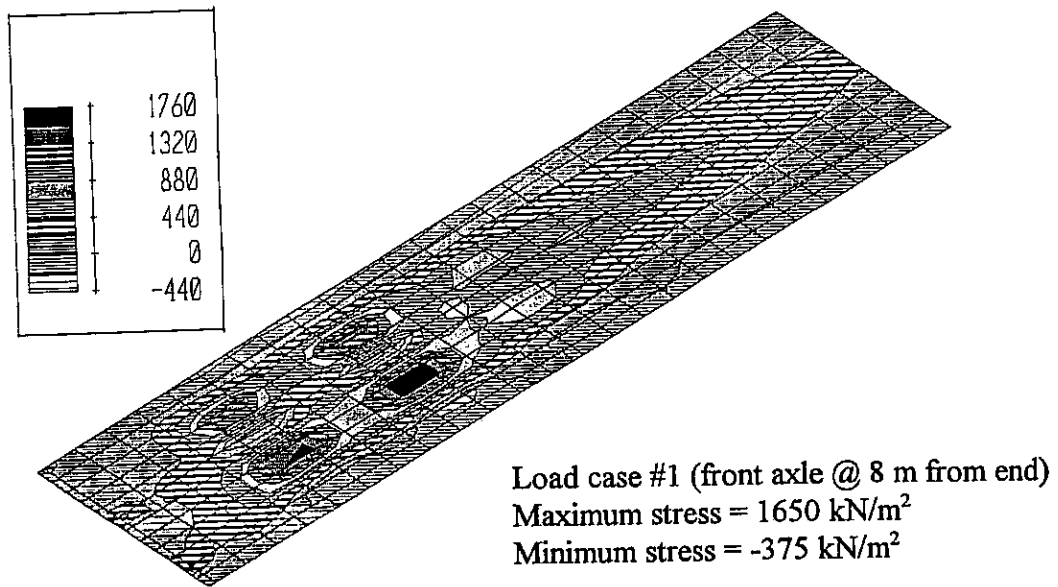


Figure 7.56 Maximum stresses at bottom surface of slab (load case 1)

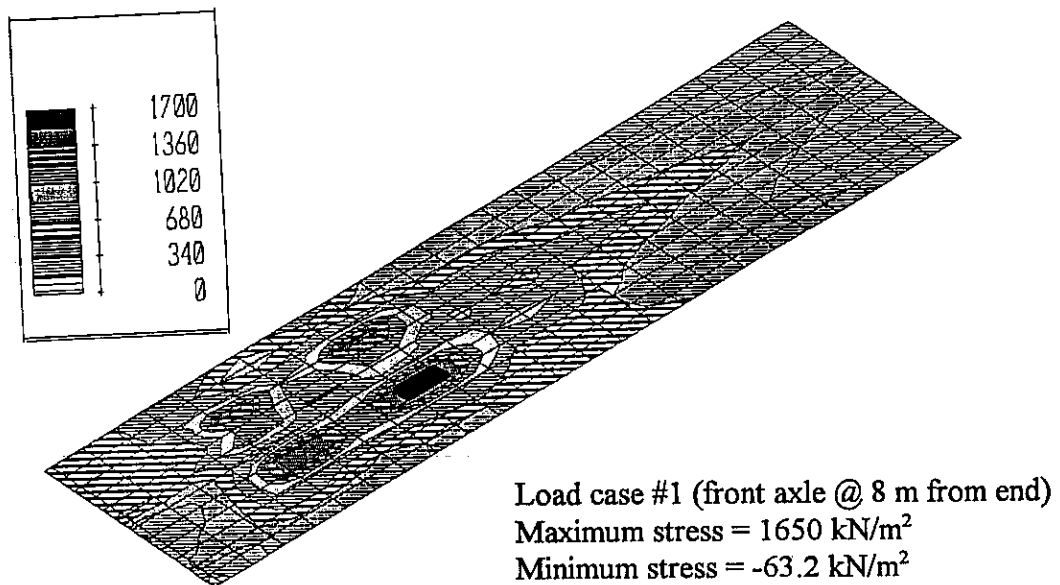


Figure 7.57 Von Mises stresses (load case 1)

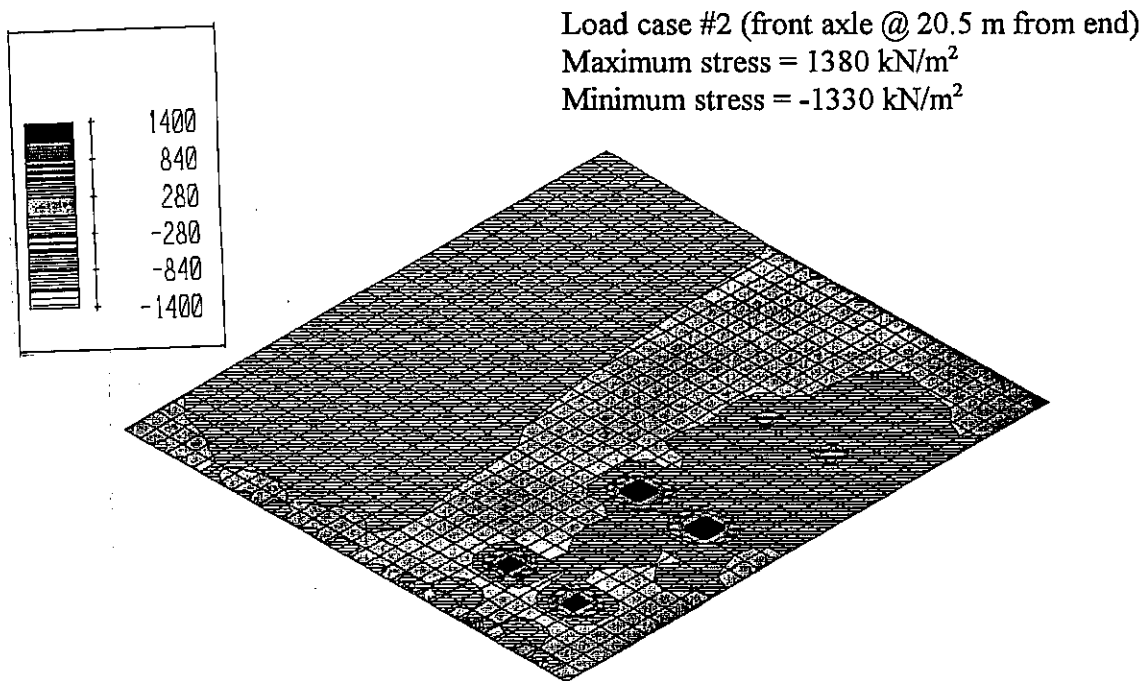


Figure 7.58 Normal stresses in longitudinal direction at bottom surface of slab (load case 2)

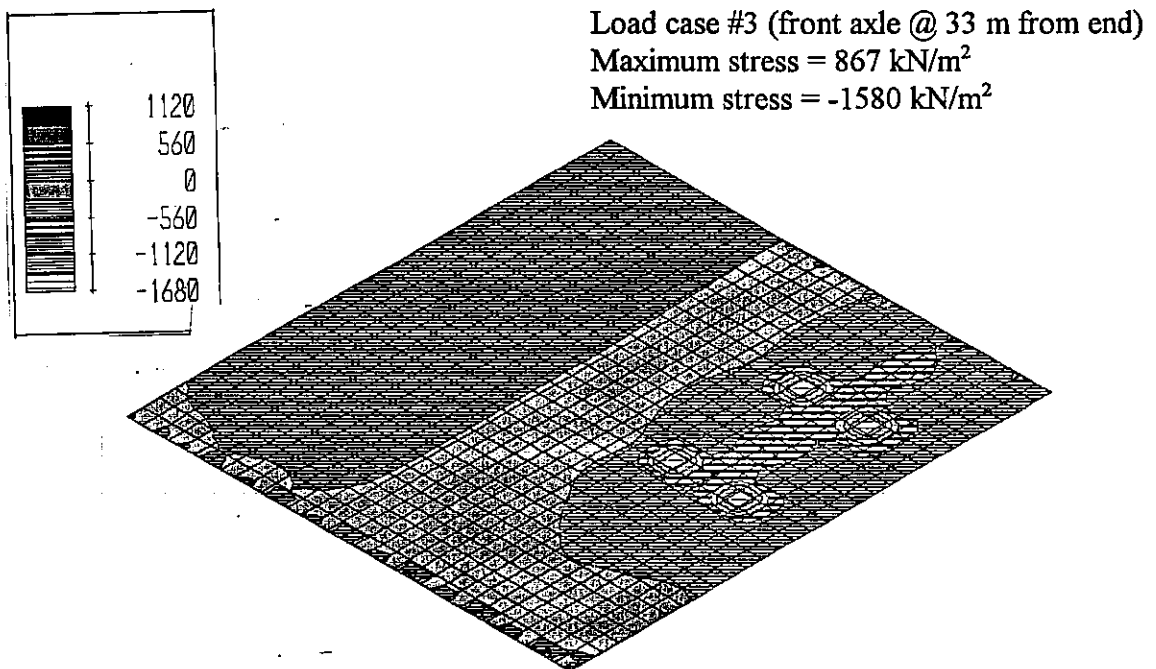
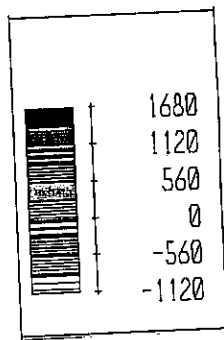


Figure 7.59 Normal stresses in longitudinal direction at top surface of slab (load case 3)



Load case #3 (front axle @ 33 m from end)
 Maximum stress = 1580 kN/m²
 Minimum stress = -867 kN/m²

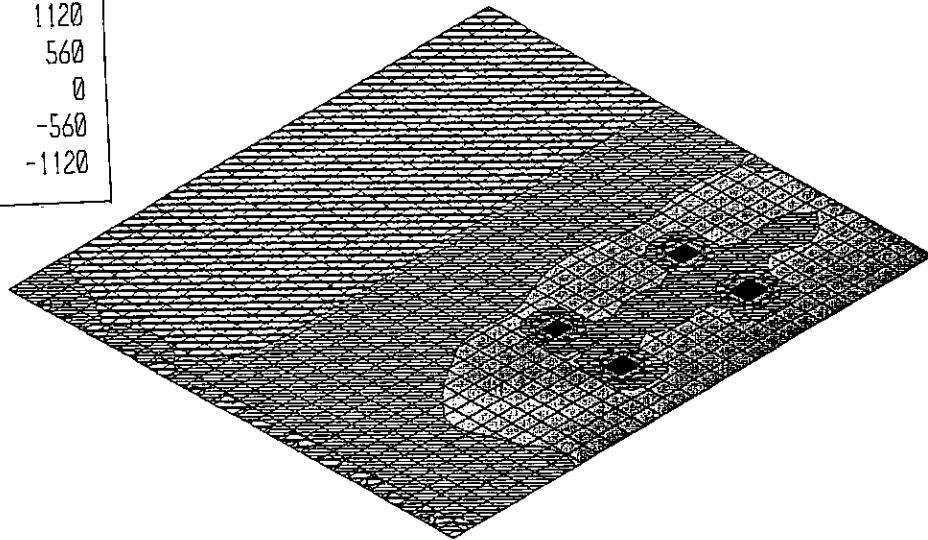
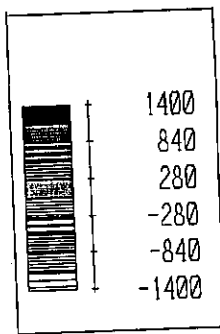


Figure 7.60 Normal stresses in longitudinal direction at bottom surface of slab (load case 3)



Load case #2 (front axle @ 20.5 m from end)
 Maximum stress = 1380 kN/m²
 Minimum stress = -1380 kN/m²

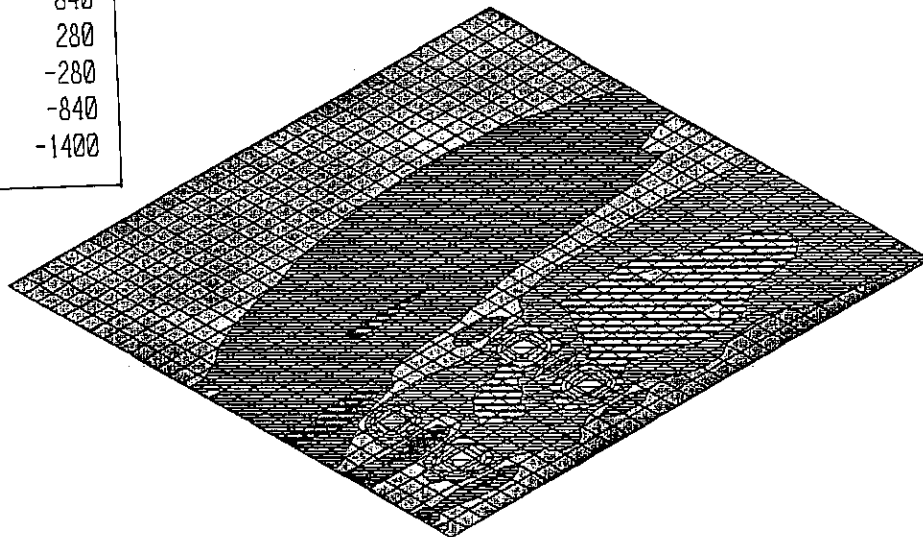


Figure 7.61 Maximum stresses at top surface of slab (load case 2)

1st bending mode
Maximum upward displacement = 43.6 mm
Maximum downward displacement = 32.5 mm

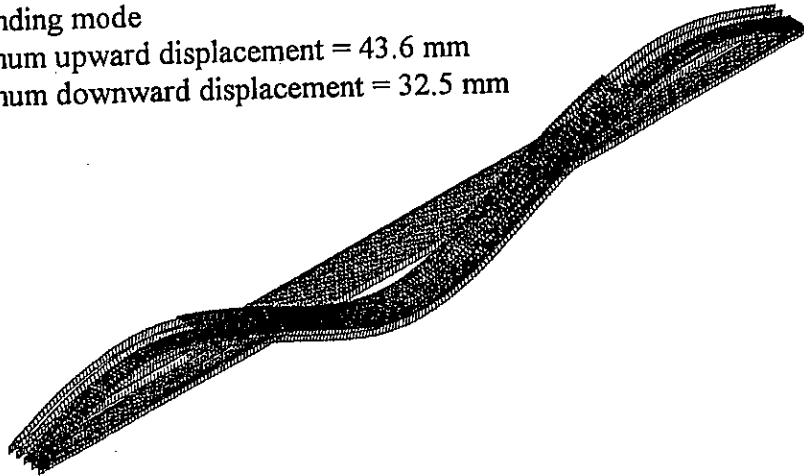


Figure 7.62 Mode shape 1 for steel bridge - stage construction

2nd bending mode
Maximum upward displacement = 55.3 mm
Maximum downward displacement = 60.0 mm

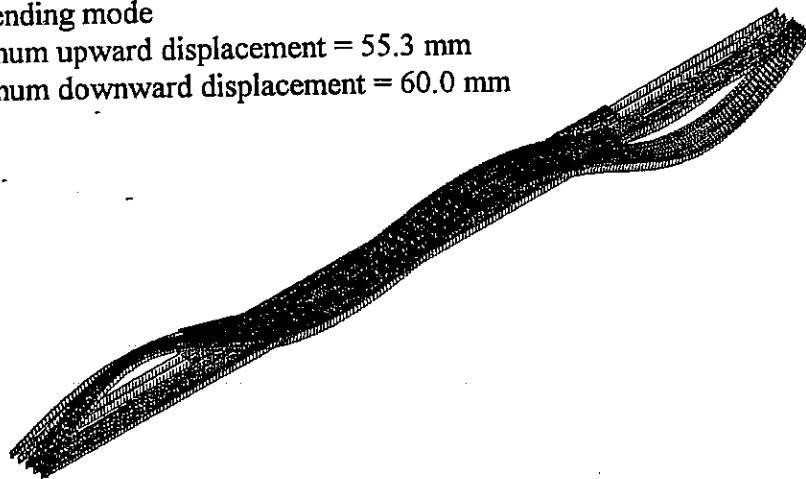


Figure 7.63 Mode shape 2 for steel bridge - stage construction

1st bending/torsional mode
Maximum upward displacement = 23.5 mm
Maximum downward displacement = 61.7 mm

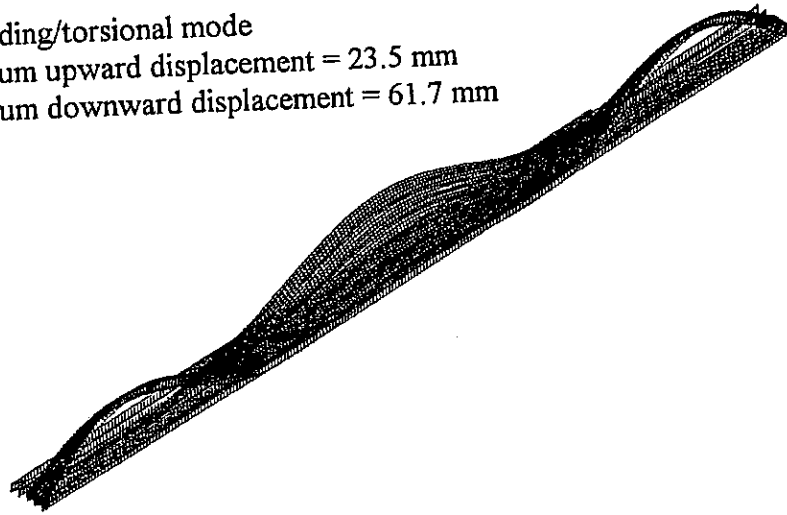


Figure 7.64 Mode shape 3 for steel bridge - stage construction

2nd bending/torsional mode
Maximum upward displacement = 93.0 mm
Maximum downward displacement = 68.1 mm

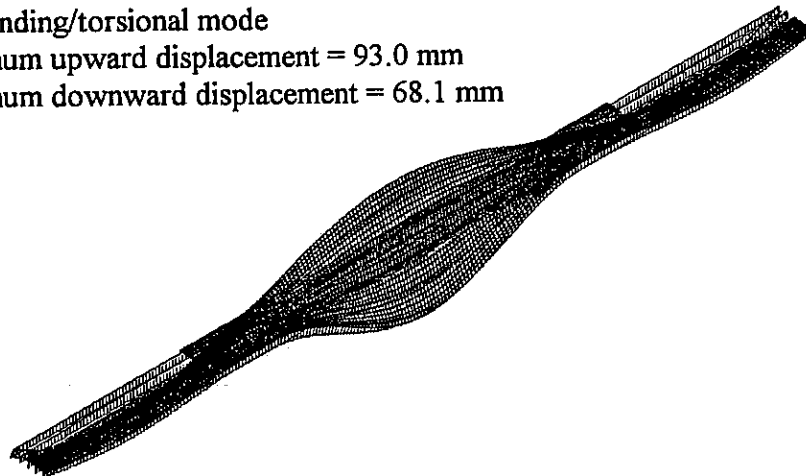


Figure 7.65 Mode shape 4 for steel bridge - stage construction

1st torsional mode
Maximum upward displacement = 139.1 mm
Maximum downward displacement = 110.0 mm

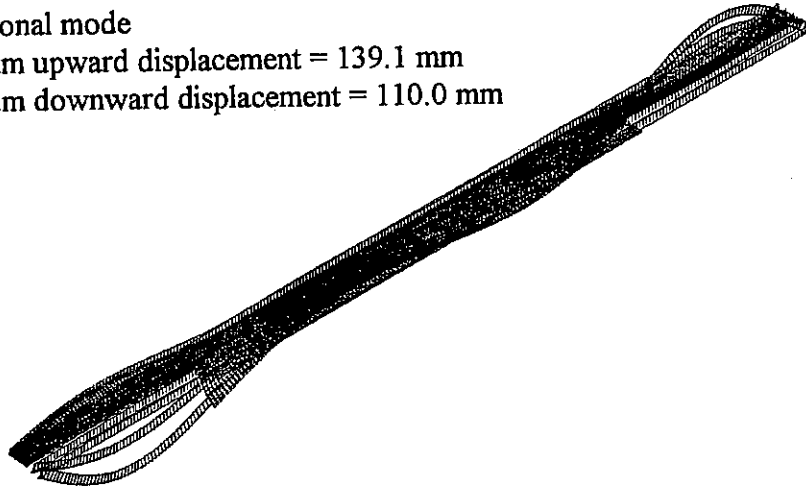


Figure 7.66 Mode shape 5 for steel bridge - stage construction

2nd torsional mode
Maximum upward displacement = 27.3 mm
Maximum downward displacement = 141.0 mm

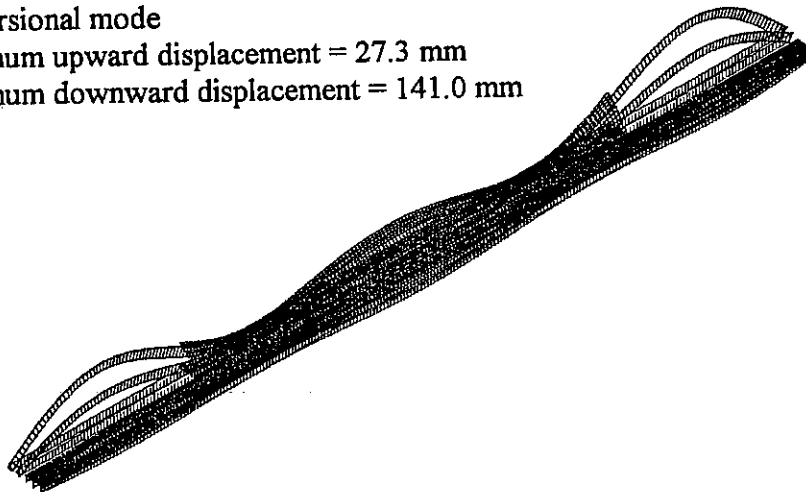


Figure 7.67 Mode shape 6 for steel bridge - stage construction

3rd torsional mode
Maximum upward displacement = 191.1 mm
Maximum downward displacement = 133.7 mm

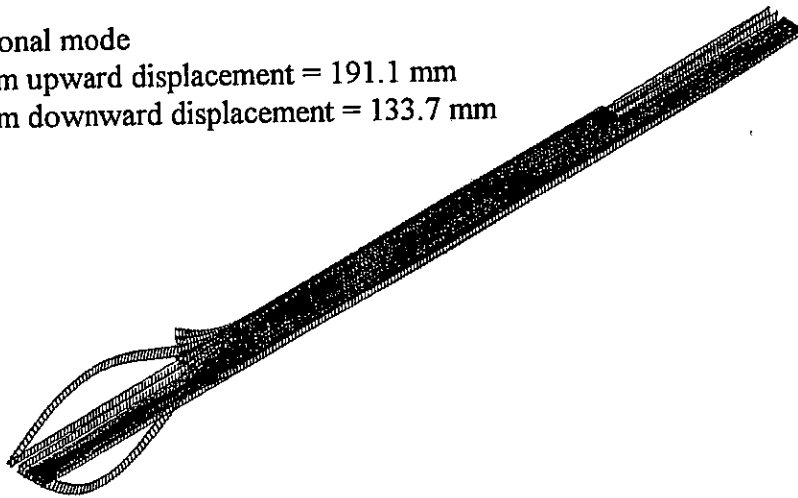


Figure 7.68 Mode shape 7 for steel bridge - stage construction

4th torsional mode
Maximum upward displacement = 187.3 mm
Maximum downward displacement = 130.2 mm

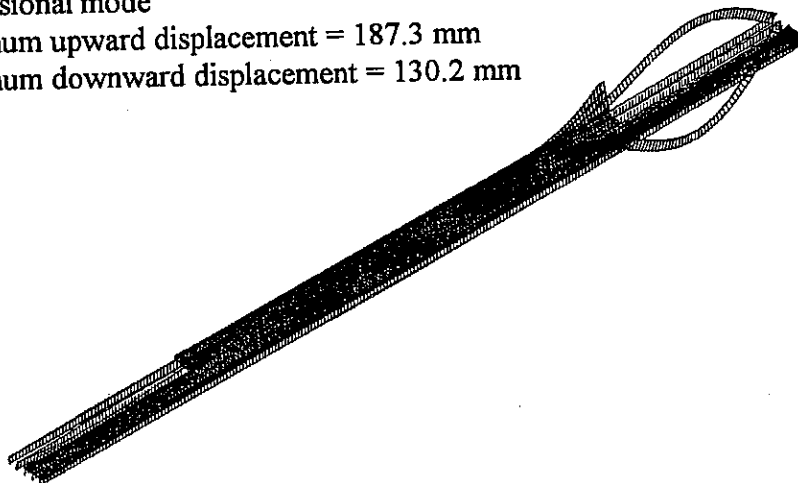


Figure 7.69 Mode shape 8 for steel bridge - stage construction

5th torsional mode
Maximum upward displacement = 120.5 mm
Maximum downward displacement = 126.8 mm

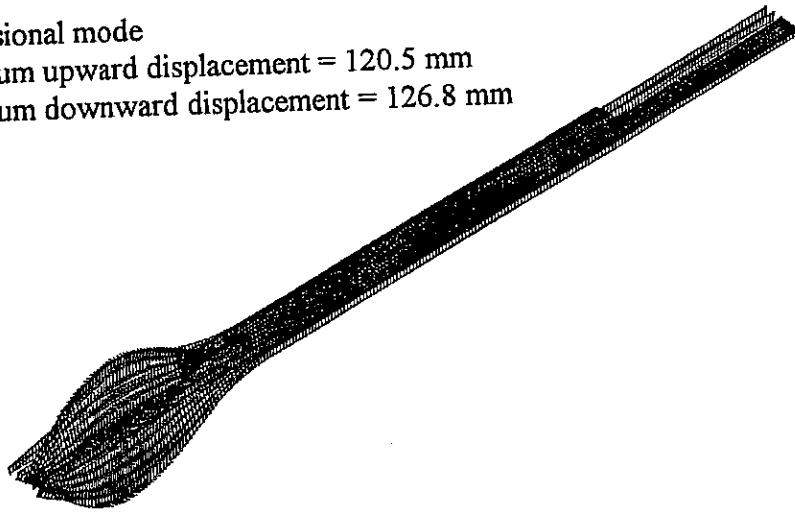


Figure 7.70 Mode shape 9 for steel bridge - stage construction

6th torsional mode
Maximum upward displacement = 119.2 mm
Maximum downward displacement = 125.3 mm

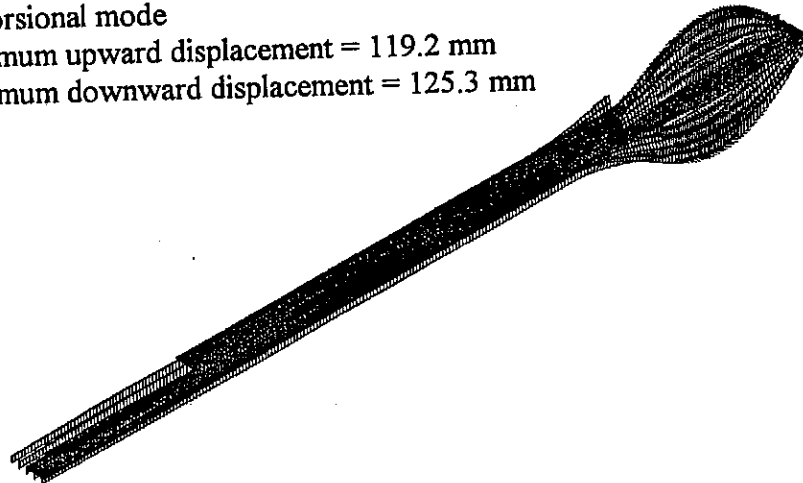


Figure 7.71 Mode shape 10 for steel bridge - stage construction

Load case #3 (front axle @ 33 m from end)
Maximum displacement = 23.5 mm

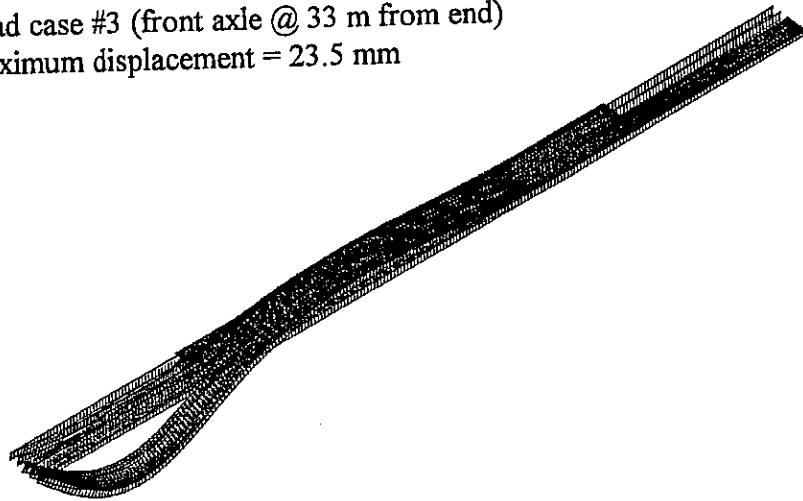


Figure 7.72 Maximum displacement in steel bridge due to moving vehicle - stage construction

Load case #37 (dead load)
Maximum displacement = 116.1 mm

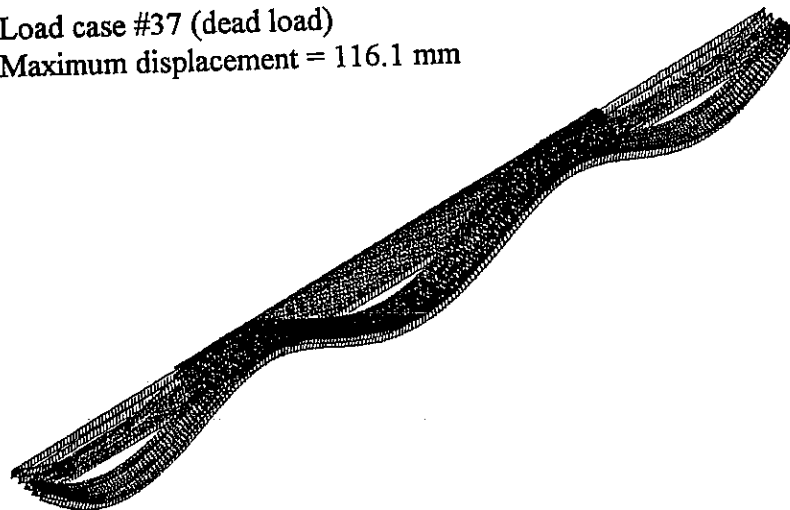


Figure 7.73 Displacement in steel bridge due to dead load - stage construction

Load case #37 (dead load)
Maximum displacement = 60.0 mm

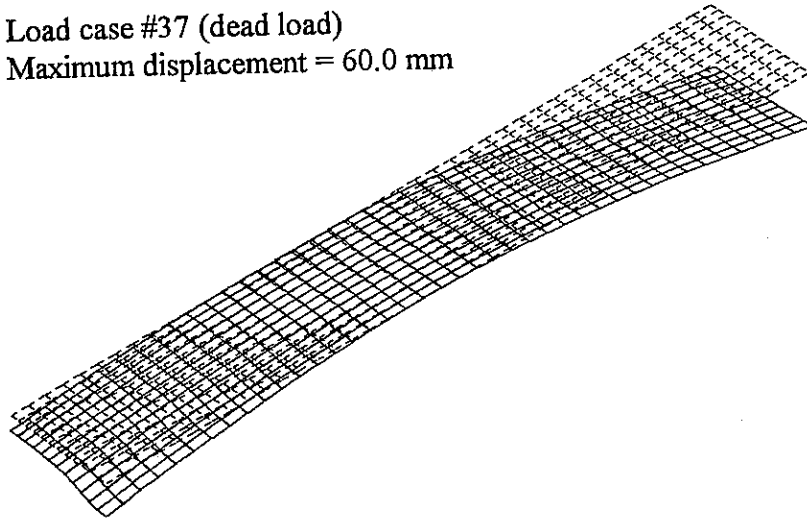


Figure 7.74 Displacement in wet concrete region due to dead load - stage construction

Load case #28 (HS 20 truck)
Maximum displacement = 23.5 mm

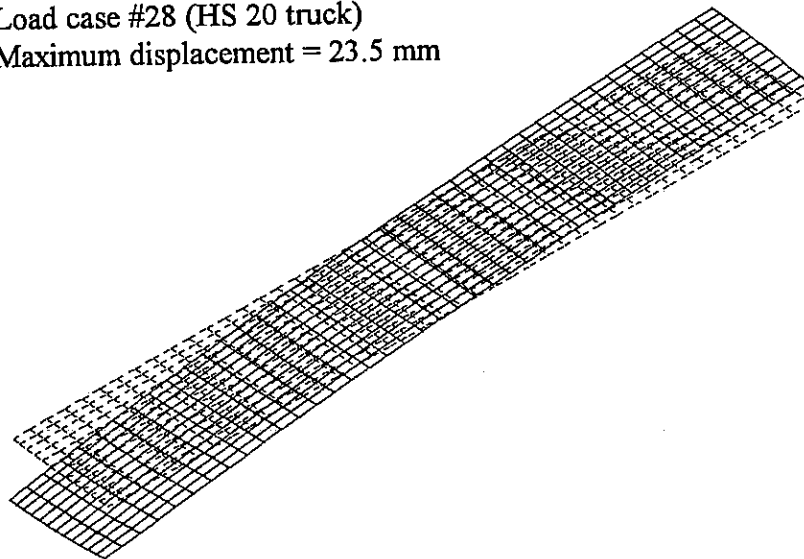


Figure 7.75 Displacement in wet concrete region due to live load - stage construction

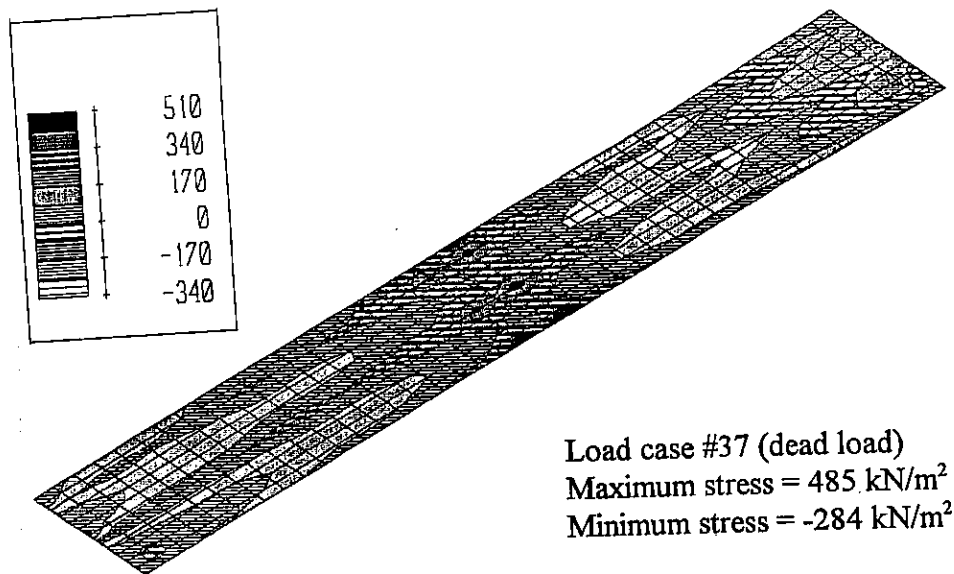


Figure 7.76 Normal stresses in longitudinal direction in wet concrete due to dead load

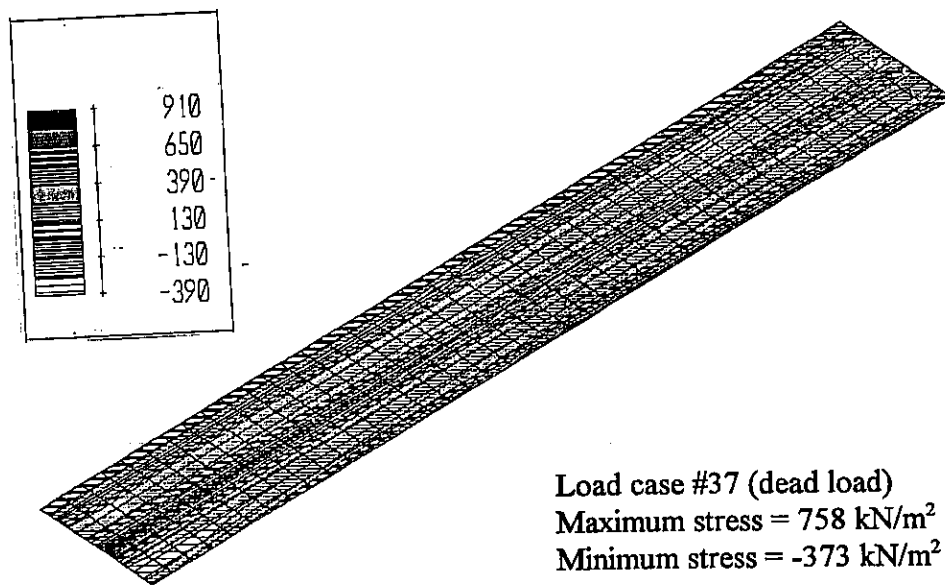


Figure 7.77 Normal stresses in transverse direction in wet concrete due to dead load

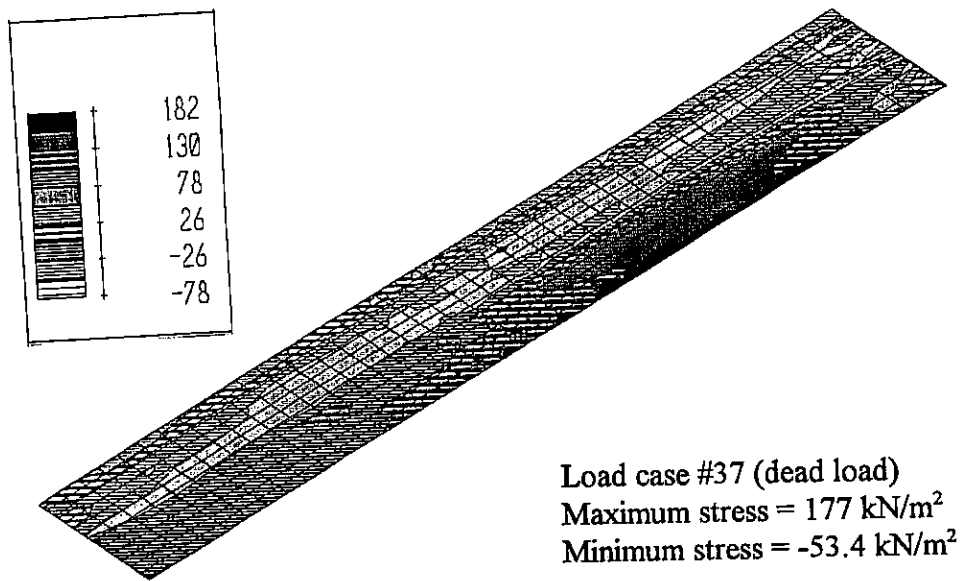


Figure 7.78 Shearing stresses in wet concrete due to dead load

Load case #3 (front axle @ 33 m from end)
 Maximum displacement = 32.5 mm

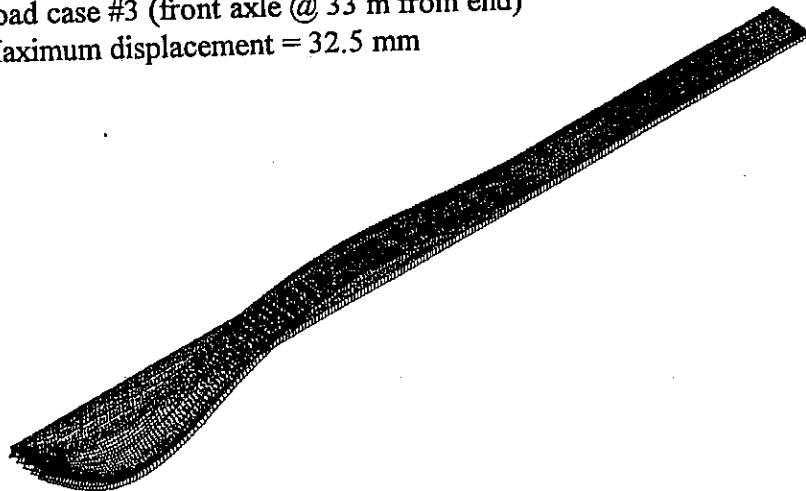


Figure 7.79 Maximum displacement in steel bridge due to two trucks

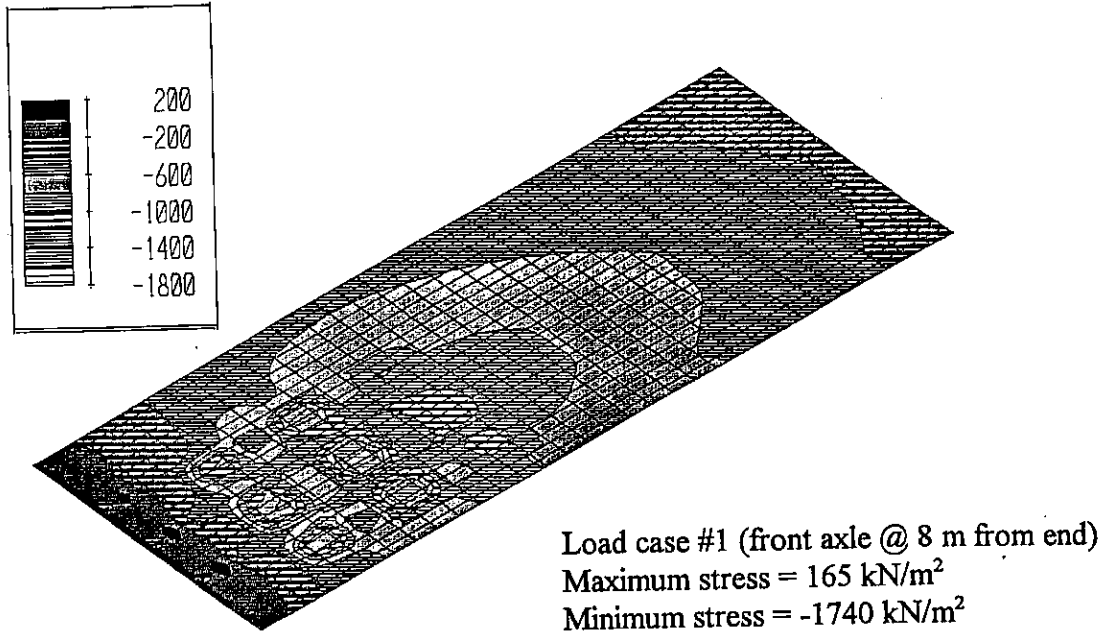


Figure 7.80 Normal stresses in longitudinal direction at top surface of slab (two trucks)

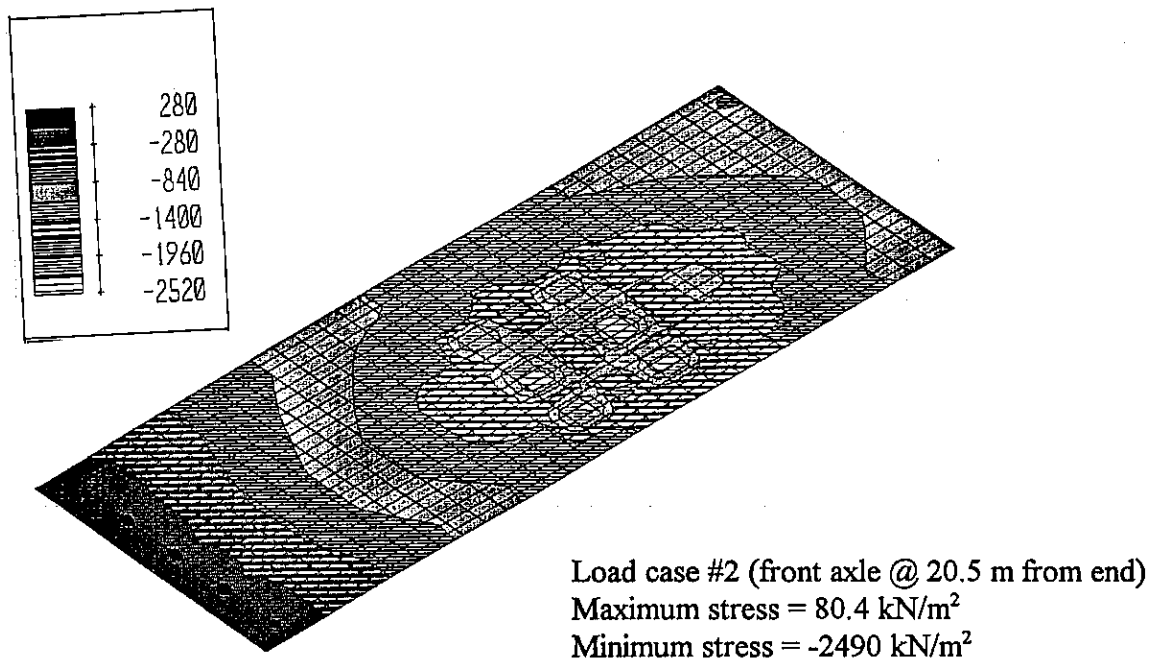


Figure 7.81 Normal stresses in longitudinal direction at top surface of slab (two trucks)

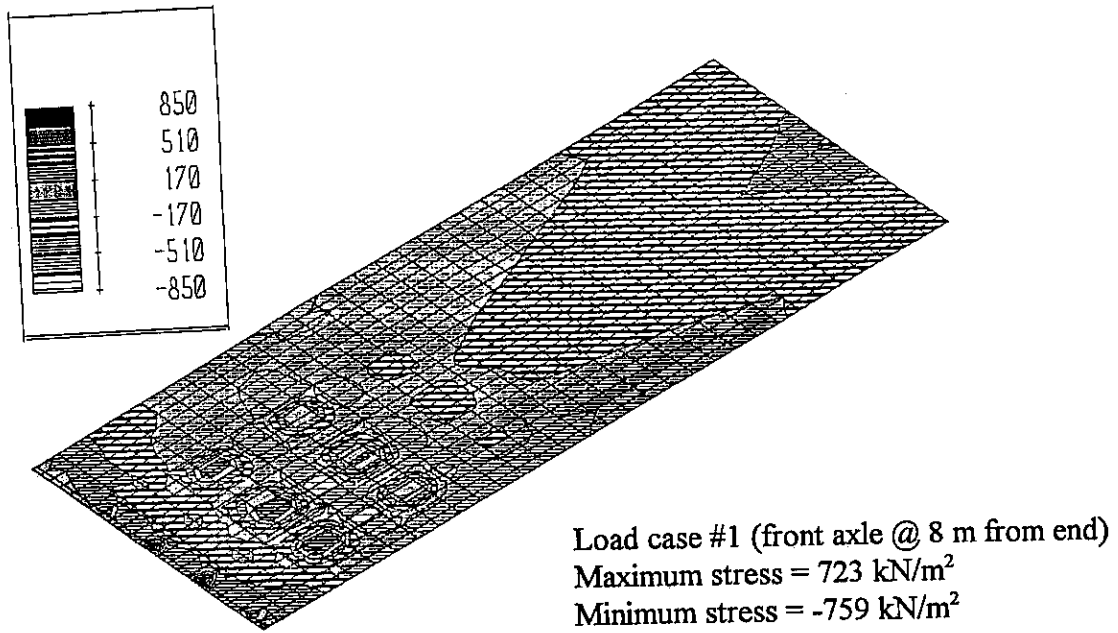


Figure 7.82 Normal stresses in longitudinal direction at bottom surface of slab (two trucks)

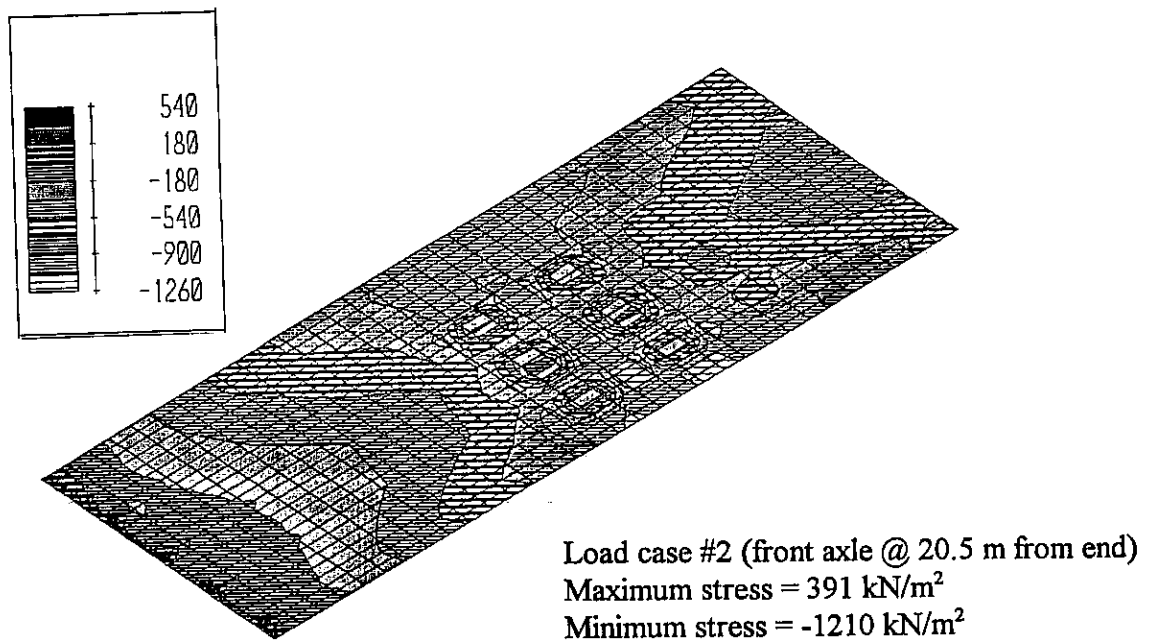


Figure 7.83 Normal stresses in longitudinal direction at bottom surface of slab (two trucks)

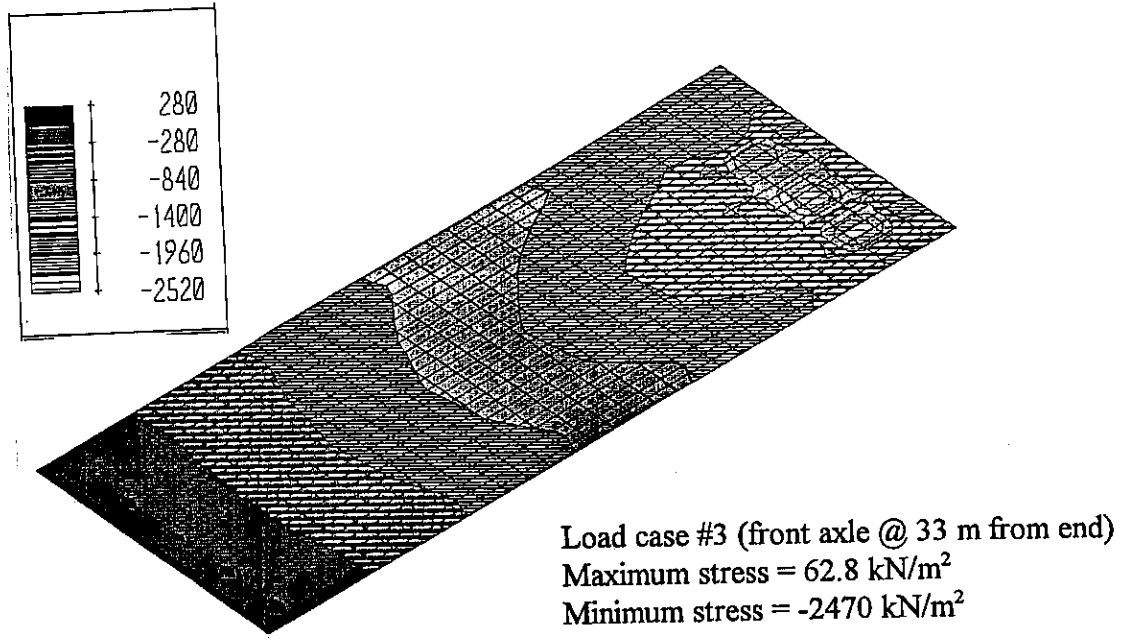


Figure 7.84 Normal stresses in longitudinal direction at top surface of slab (two trucks)

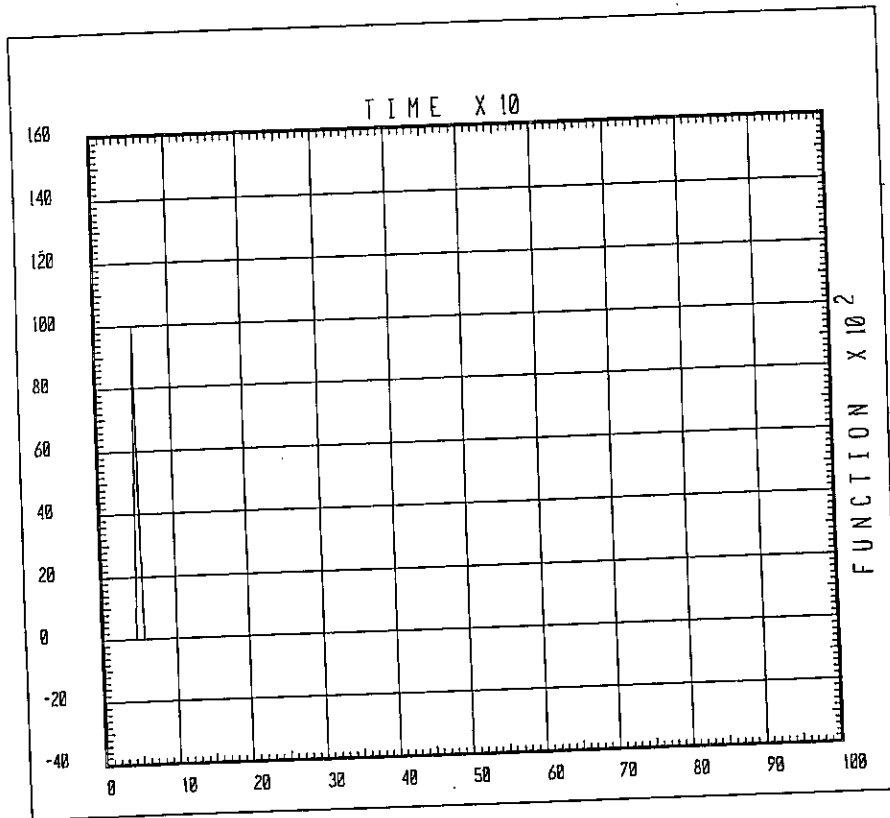


Figure 7.85 Time history function corresponding to vehicle location

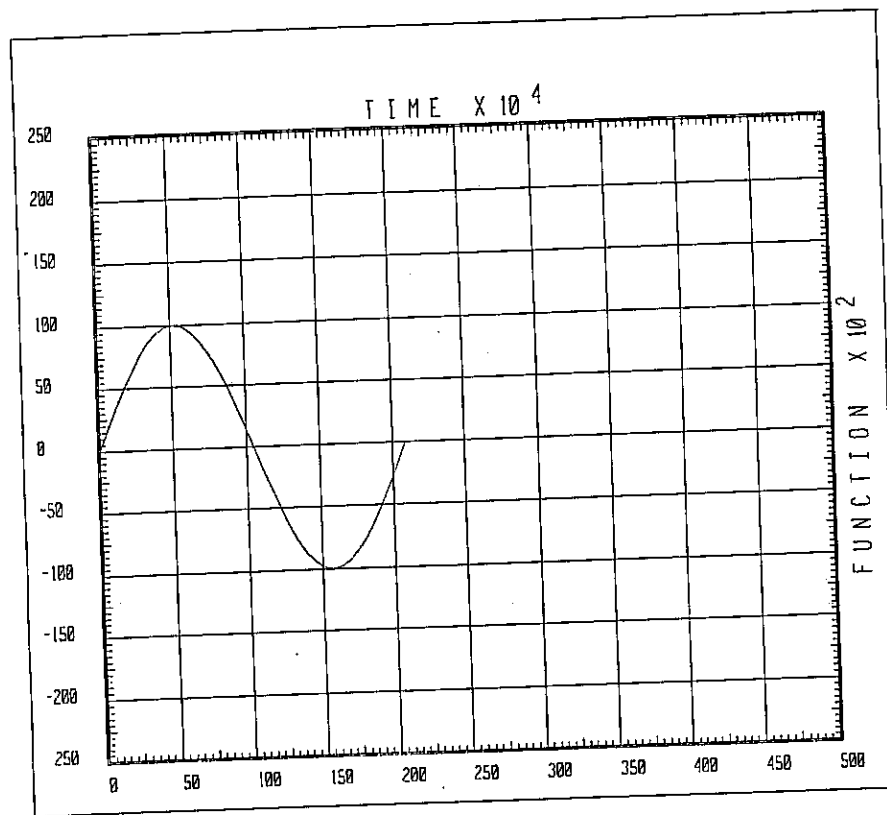


Figure 7.86 Sinusoidal time history function corresponding to vehicle location

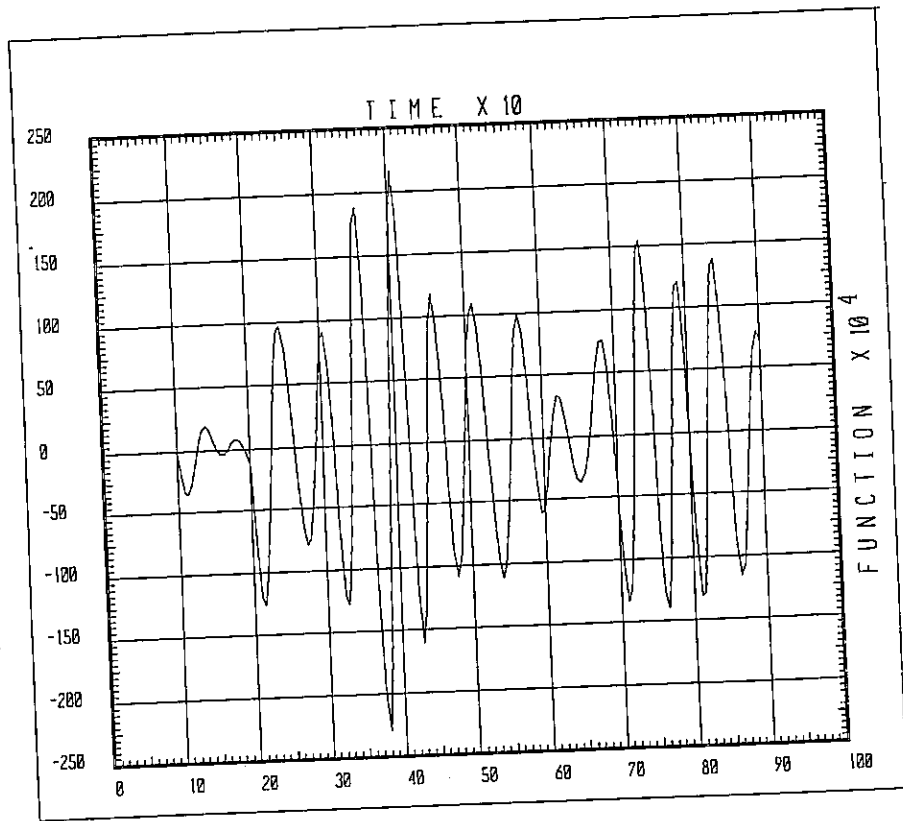


Figure 7.87 Time history, maximum displacement in z-direction as a function of time

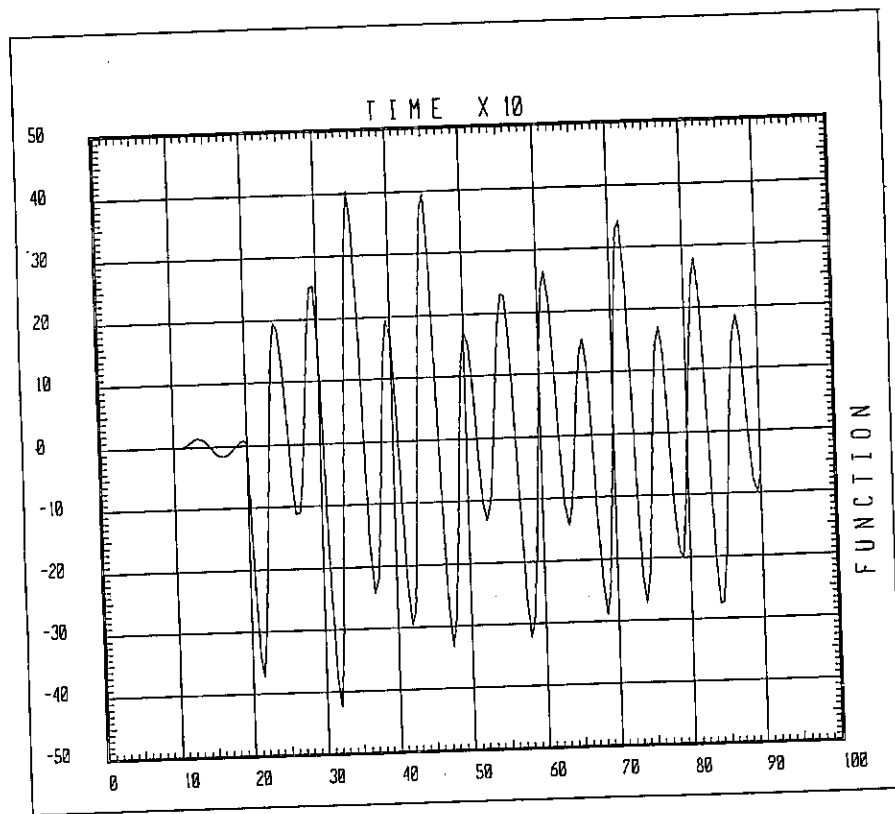


Figure 7.88 Time history plot for typical shell element in respect to σ_{11}

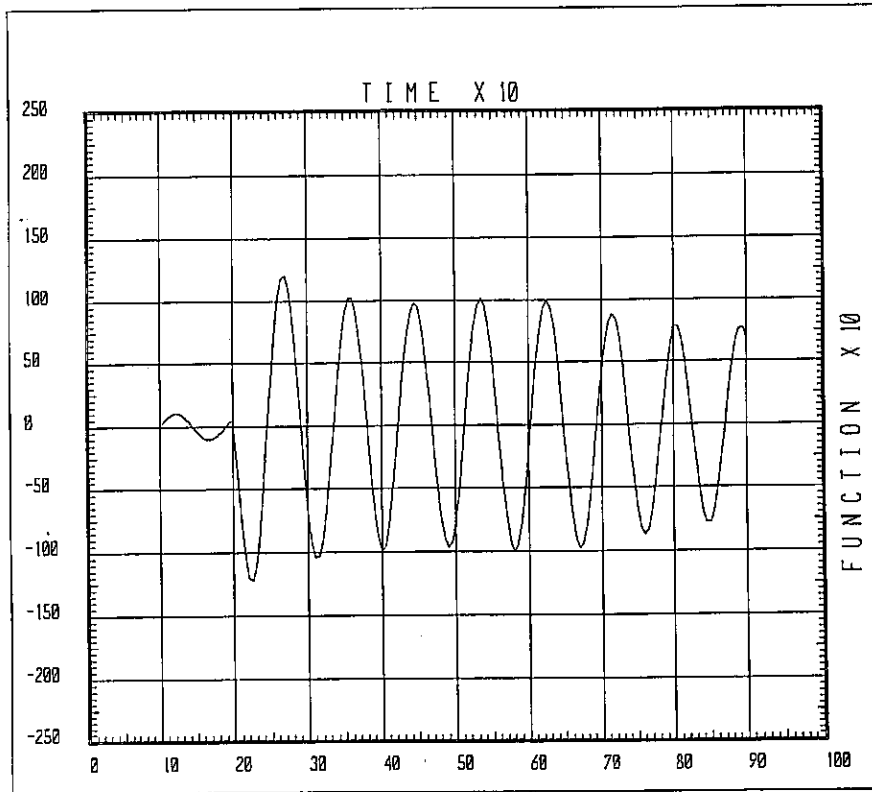


Figure 7.89 Time history plot for typical shell element in respect to σ_{11} (Mode 1)

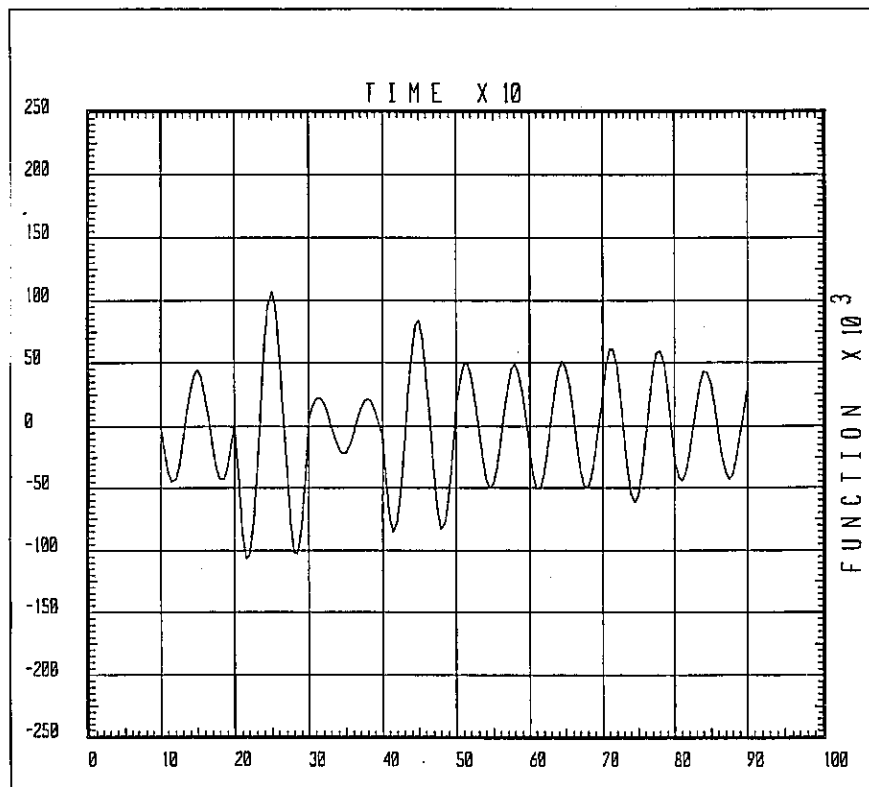


Figure 7.90 Time history plot for typical shell element in respect to σ_{11} (Mode 2)

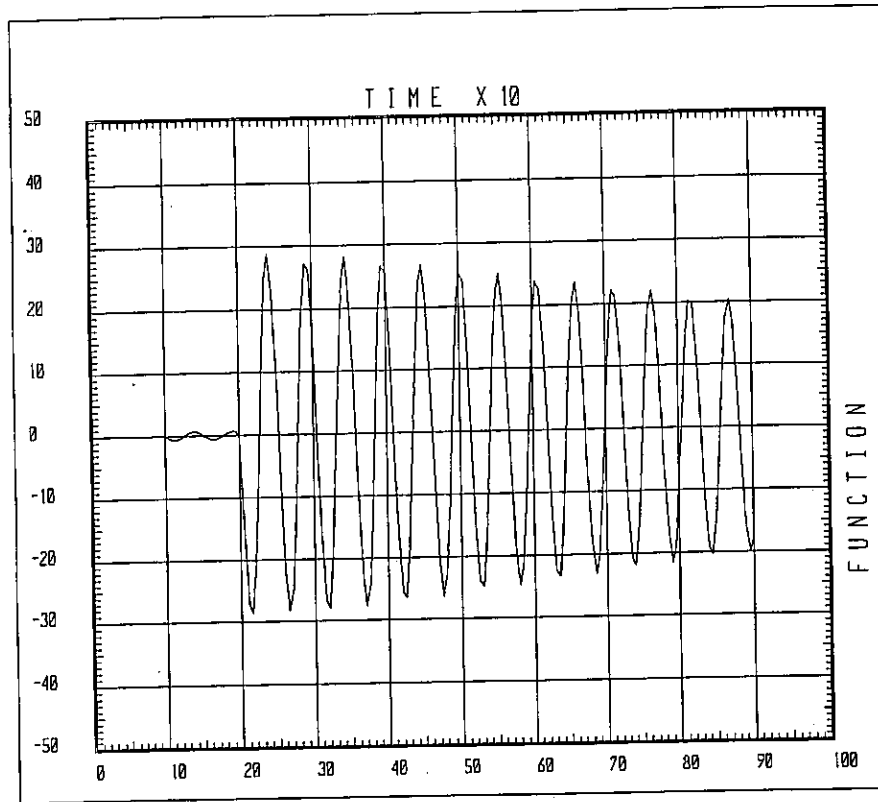


Figure 7.91 Time history plot for typical shell element in respect to σ_{11} (Mode 3)

8. DETAILED INSTRUMENTATION OF BRIDGES

During dynamic tests, various responses are measured with accelerometers, strain gages, and various displacement transducers. Typically, deformation and displacement data are used to obtain dynamic amplification factor values, while acceleration data are used to obtain dynamic properties. This instrumentation should be distributed on the main span and connected to a microcomputer-controlled data acquisition system. A layout of the dynamic testing and monitoring is depicted in Figure 8.1.

Vertical acceleration responses on a bridge are measured with low-frequency accelerometers. Each accelerometer has a resonant frequency of 50 Hz. with a frequency response fairly constant in the 0 to 20 Hz. range, which is usually well above the frequencies from the first five to ten vibration modes of modern highway bridges. The instruments are mounted on an aluminum plate and leveled on the surface with three adjustable screws and a bubble level. Accelerometer locations were selected to obtain as many mode shapes as possible. The finite element analysis performed earlier was used to determine points along the decks where motion is observed for most of the first 10 modes, and a reference point is chosen to compute frequency response functions.

Displacement transducers (LVDTs) are used to measure vertical displacement and are usually attached to one of the main girders and anchored to the ground or river bottom directly below. Strain gages are placed on bridge girders and slabs where maximum stress is expected. Displacement transducers are placed on the same sections on both sides of a bridge to observe torsional motions. Strain gages are much easier to install and are used more extensively, especially in cases where the

height of the bridge prevents the use of LVDTs. The strain gage signals are amplified and calibrated with a signal conditioning module.

Other researchers have achieved artificial forced vibration excitation of the bridge with an excitation system based on a hydraulic actuator mounted within a special frame. The force level can be varied by increasing or decreasing the dead mass mounted on top of the actuator piston rod. A load cell attached to the actuator allows measurement of the input load. However, this instrumentation setup would be an expensive form of monitoring. The proposed instrumentation layout if this manner of testing was chosen is shown in Figure 8.2.

The proposed form of excitation will be to limit the vibration to passing vehicles, vibration from construction equipment, and other environmental excitation transmitted through the supports. In the dynamic measurements, vertical acceleration response of the bridge deck will be measured and recorded via the data acquisition system. Therefore, the test would facilitate obtaining the structure's vibration response measurement.

During the tests, runs are made using the following patterns: (1) single truck; (2) single truck with trailer; and (3) two trucks side by side. For most bridges, a total of 30 to 40 vehicle runs are carried out at various speeds and positions on the deck. Most of the tests are performed at high speeds (90 to 100 km/h) along the centerline of the bridge and on one side of the bridge, near the barrier wall or curb. A few tests are also performed at crawling speed (15 km/h) to obtain quasi-static loading response, and data is also recorded with random traffic loading. The traffic control crew and drivers for all tests are kept in constant radio communication with the truck drivers, the data acquisition system operator, and test supervisor. The system operator signals the supervisor to begin a test. The supervisor then calls for traffic shut down, while the data acquisition system is initialized.

The supervisor signals the truck drivers to begin their run at a given speed and position on the bridge. The data acquisition is triggered before the vehicles reach the bridge. When the vehicles exit the bridge and the data collection is completed, the supervisor allows traffic to be released while the drivers are instructed to prepare for the following test.

The proposed testing will include the loads imposed by moving vehicles in adjacent lanes, construction equipment, concrete mix trucks, and concrete mixing pump. One of the most critical parameters to be studied is the sequence of pour, as a result, data collection of the various dynamic parameters will be related to the pouring sequence as well as construction loads. Monitoring will continue through the hardening of the concrete. Moving load tests will be limited to passing vehicles. Dynamic tests will also consist of monitoring the effects of construction equipment including concrete trucks and pumps. Data collection will consist of monitoring the dynamic parameters associated with the bridge using various instrumentation. LVDTs will be used to monitor the deflections, while accelerometers will be used to track the vibration imposed through moving and equipment loads. In addition, embedded and surface strain gages as well as vibrating wire strain gages will be used to monitor the strains in the concrete and steel. The data will be collected independently for all types of loading conditions and appropriately superimposed to determine the actual effects of construction loads and vibrations.

Proposed Measurement Locations

The relative locations of the accelerometers and LVDTs with respect to the deck cross section and support locations are shown in Figures 8.3-8.6 for the proposed testing of the two selected bridges. The dynamic response of the bridges will be measured at the locations identified to be

critical from the time history and dynamic finite element analysis of the two structures. One accelerometer will be stationed permanently at a reference point as noted in Figures 8.2-8.6. The other accelerometers will be moved from point to point until all the measurement locations are covered. This process will be repeated in order to cover the entire bridge length for data collection. A predetermined recording time will be adopted for each test.

The mode shapes obtained by the finite element analysis were used to optimize sensor locations for the dynamic field testing. Locations at the supports and along the two exterior girders of both bridges were selected for instrumentation based on the dynamic analysis results. The maximum displacements obtained from each mode shape were determined in order to locate the critical locations for the instrumentation. The instrumentation is necessary to measure the vertical and longitudinal movement of the bridge deck. The proposed instrumentation layout and cross-sections for the steel girder bridge and prestressed concrete bridge are shown in Figures 8.3-8.6, respectively. Additional instrumentation will be located as shown in the figures based on the critical deflections and rotations observed for each of the first ten mode shapes.

Refined Analytical Model

The dynamic analysis performed to optimize instrumentation locations is only a preliminary means of analysis. The analytical model will be refined after determining all the experimental frequencies and mode shapes of the structure. The main purpose of this refinement is to correlate the analytical frequencies as closely as possible to the results obtained from the experimental investigation. Several parameters may need modification including the increase in stiffness due to the composite action through the use of an effective moment of inertia of the beam elements. Other

modifications may include the addition of diaphragms and their composite action, the addition of the mass from the parapets, the increase of stiffness of the exterior composite girders due to the sidewalk assembly and the parapet, and the inclusion of the columns in order to allow transverse movement of the deck.

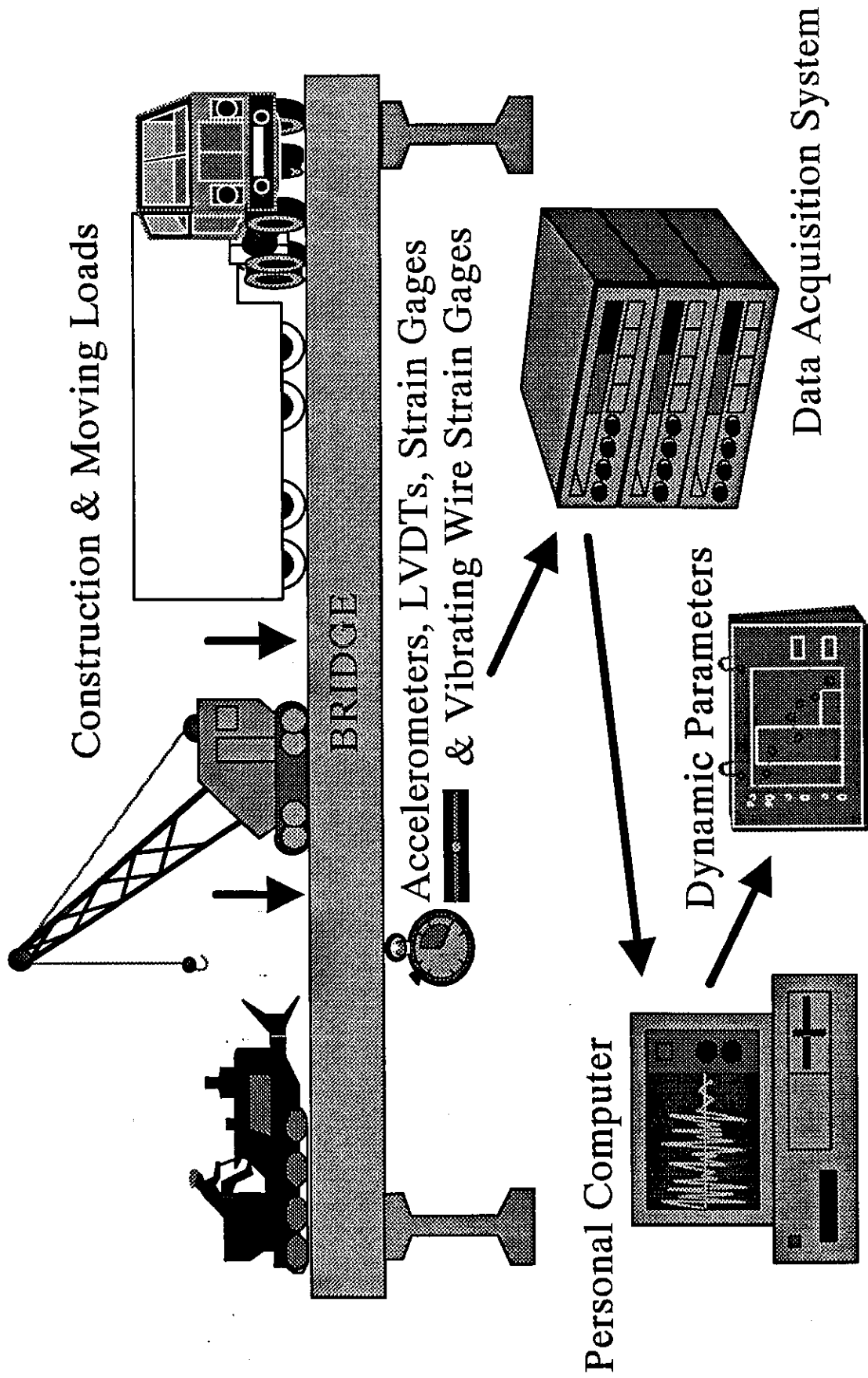
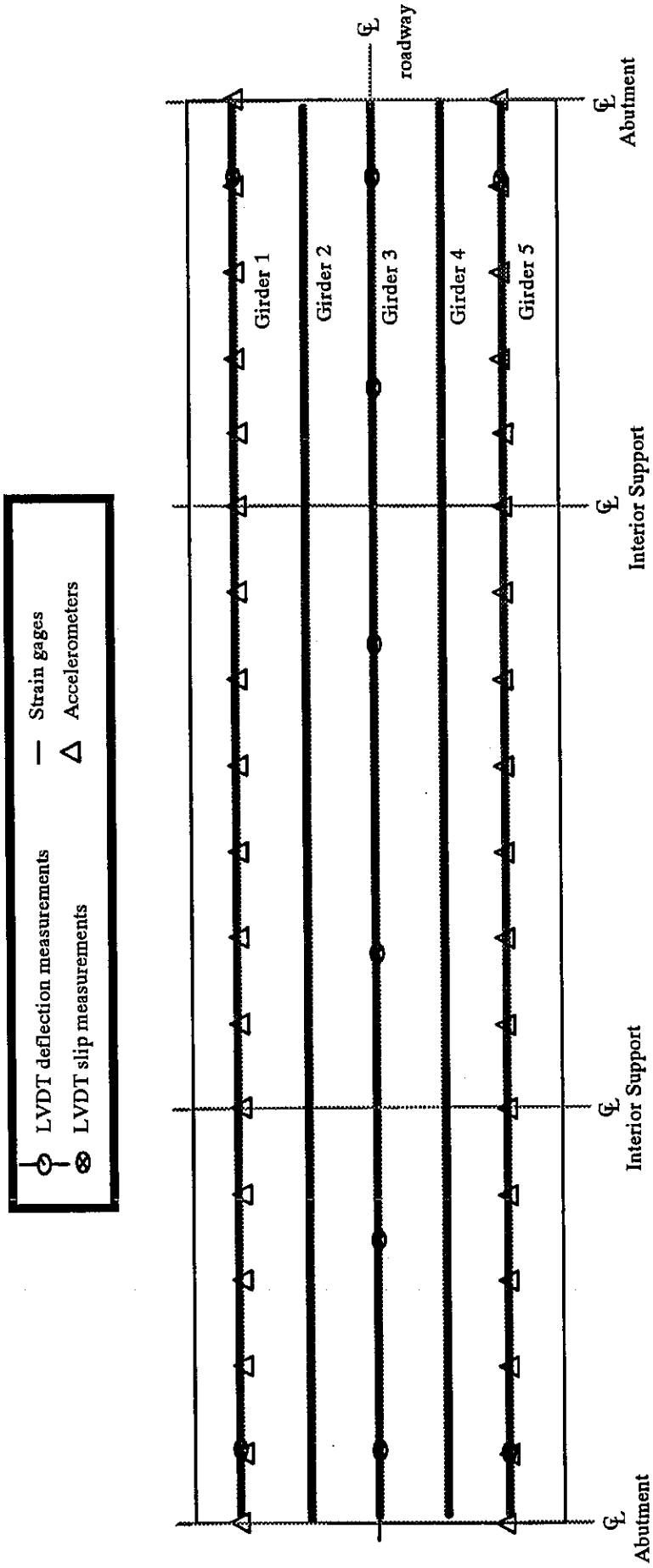
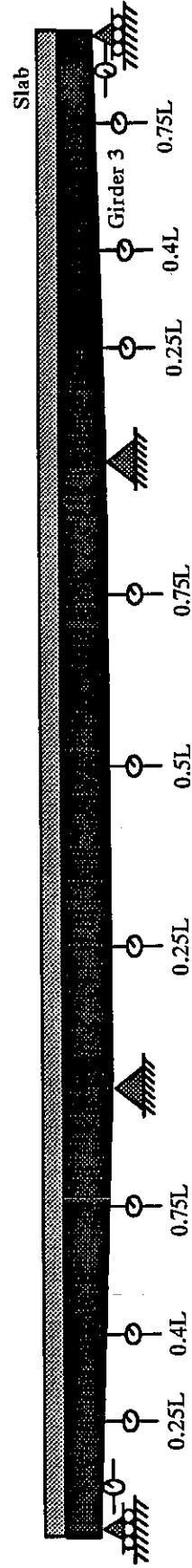


Figure 8.1 Instrumentation layout for dynamic test



(a) Plan view



(b) Instrumentation of a typical longitudinal critical girder (girder 3)

Figure 8.3 Plan view & instrumentation of steel girder bridge

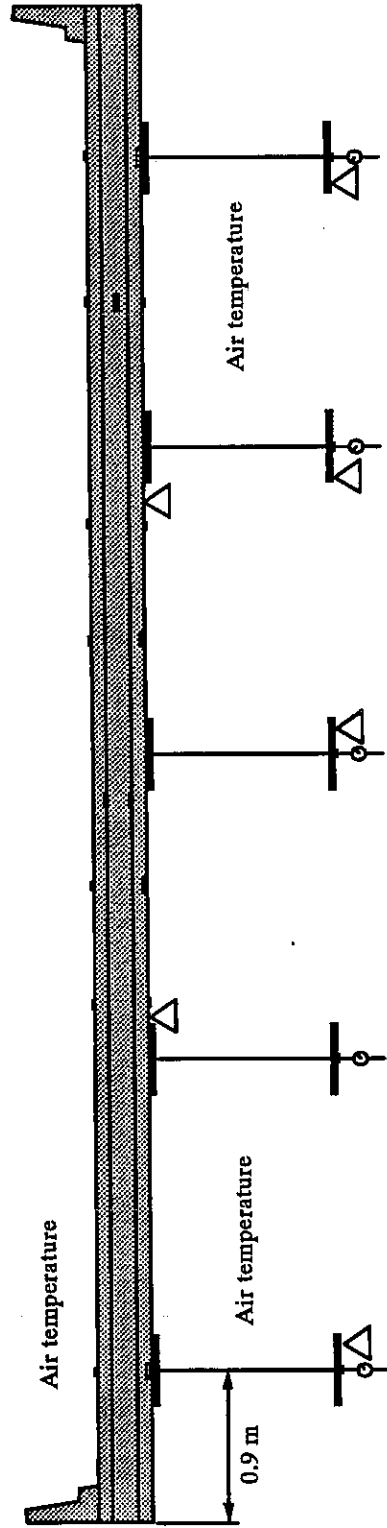
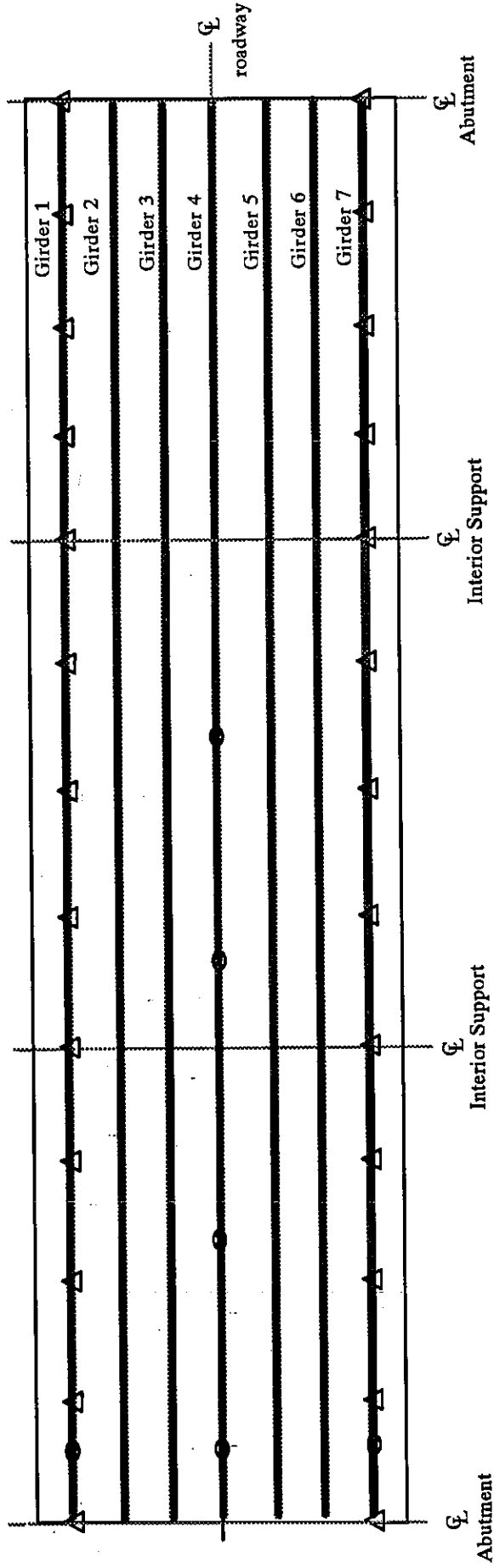
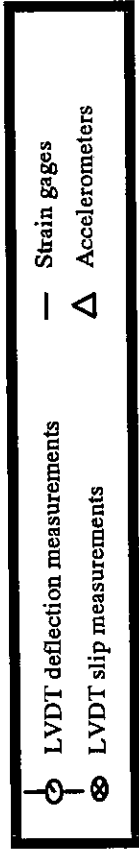
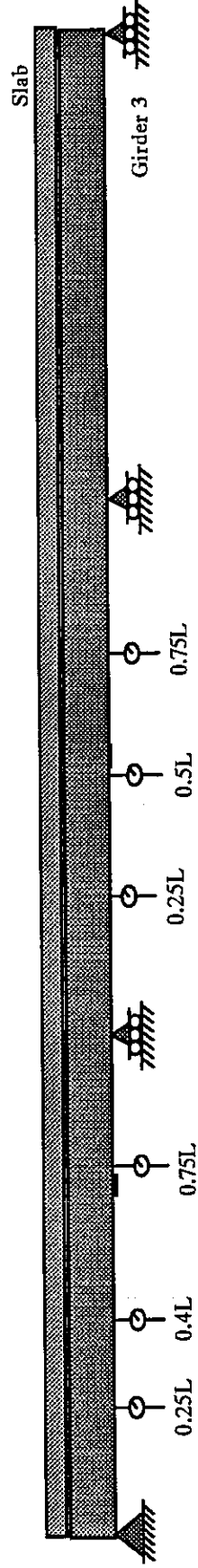


Figure 8.4 Instrumentation for typical transverse section



(a) Plan view



(b) Instrumentation of a typical longitudinal critical girder (girder 3)

Figure 8.5 Plan view & instrumentation of concrete girder bridge

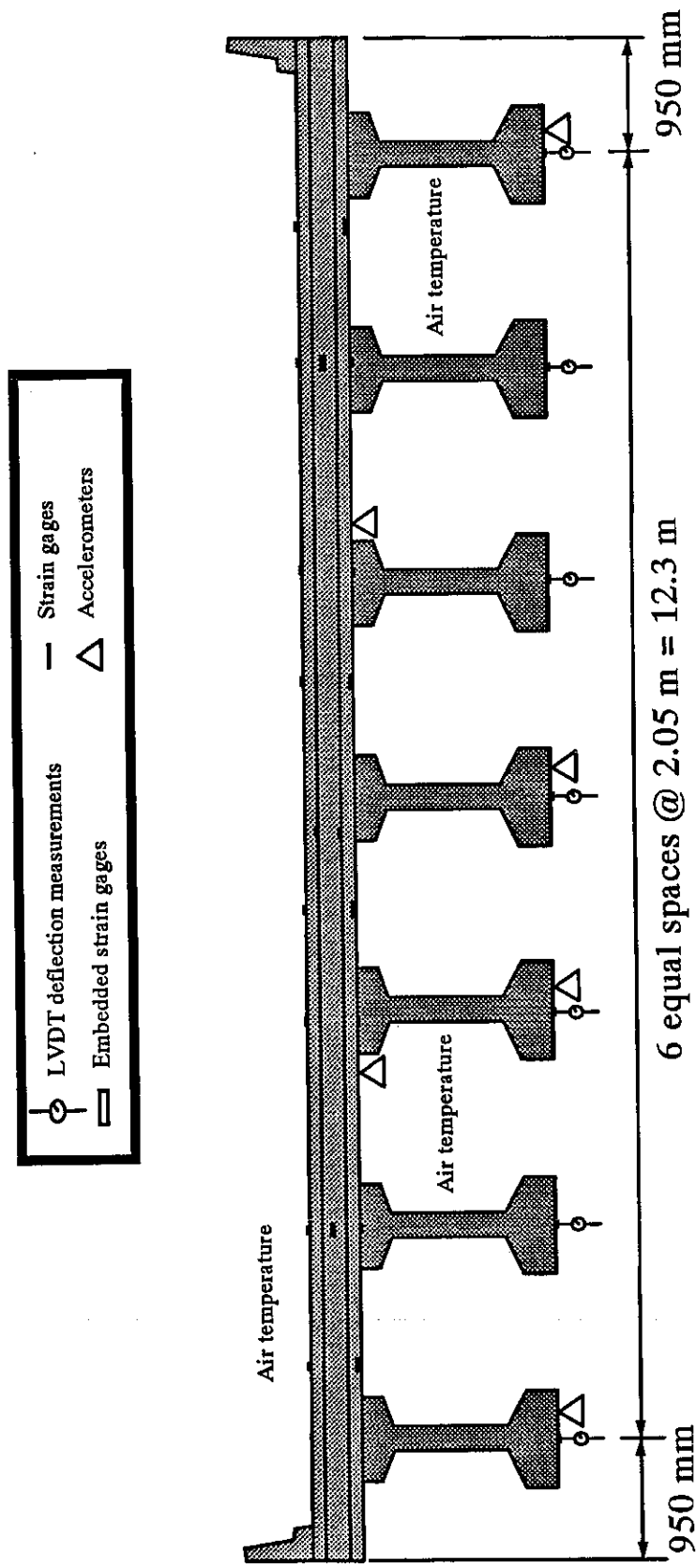


Figure 8.6 Instrumentation for transverse section

9. CONCLUSIONS

The conclusions from the research project are divided into several categories corresponding to each phase of the study.

9.1 Literature Review and Survey

As a result of the literature review and comprehensive survey, it may be concluded that vibrations due to adjacent traffic of bridge decks containing well-proportioned and well-compacted low slump concrete do not cause:

- decrease in concrete strength.
- decrease of bond strength between reinforcing steel and concrete.
- decrease of bond strength to existing structure.
- cracking of concrete.

However, additional vibrations due to adjacent traffic and construction equipment may increase cracking in the case of undervibrated, high slump concretes. The effect of adjacent traffic may be minimized by imposing speed limitations on the bridge, as well as restrictions of heavy truck traffic in lanes adjacent to the area under construction. However, this will have more effect on the eventual cracking of the joint between the newly poured and old concrete deck, and the bond strength between steel dowels and fresh concrete in the narrow zone close to the old concrete. Influence on cracking elsewhere in the concrete deck is insignificant.

Other factors influence the cracking of concrete bridge decks to a more significant degree. Although it is difficult to separate one factor from the other, it seems that in most cases cracking of concrete may be attributed to the following (in descending order of importance):

1. High evaporation rate, and by that high magnitude of shrinkage, as a result of inadequate concrete curing procedures during hot weather conditions, especially at very early concrete ages. This effect is attributed to:
 - lack of concrete protection.
 - inadequate uniform coverage with a curing compound.
 - delay of concrete protection application.
2. Use of high slump concrete.
3. Excessive amount of water in the concrete as a result of:
 - inadequate mixture proportions.
 - retempering of concrete.
4. Insufficient top reinforcement cover due to:
 - inadequate reinforcing detail plans.
 - improper placement of reinforcement.
 - insufficient deck depth due to deflections during construction.
5. Insufficient vibration of the concrete.
6. Inadequate reinforcing details of the joint between the new and old deck.
7. Sequence of pour.
8. Weight and vibration of machinery.
9. Weight of the forms.

10. Deflection of forms.

Note that lack of concrete protection at early ages is of much more importance than at later ages. Proper care at later ages will not compensate for the lack of the protection in the very early ages. As it may be noticed, creep and particularly shrinkage are not mentioned as separate categories. These effects are closely related to protection and curing of concrete and as such are impossible to separate since they are highly dependent on curing procedures.

Note that although vibrations due to different sources are not directly included in the previous list, their influence is given through other categories such as slump and reinforcement cover. Due to insufficient data with respect to the influence of sequence of pour and construction procedures, a feasible determination of realistic importance is not possible. However, high differences in curvatures for various sequences of pour, as well as reported cracking of continuous concrete bridge decks at the regions over the supports, deserve further analysis.

The comprehensive survey of state DOT's suggested that cracking of full depth concrete bridge decks is not believed to be related to vibrations and loads imposed by adjacent traffic. However, experience with concrete bridge deck overlays indicates that the significance of these effects on this particular type of rehabilitation is more prominent. In addition, the conclusions from the survey are not substantial due to the lack of information in this field. Adjacent traffic as well as other factors that were addressed in the survey such as construction loads and equipment (concrete mixer trucks and concrete pump trailer units) disturb the setting of concrete at early ages.

9.2 Dynamic and Vibration Analysis

The time history and dynamic analysis indicated that the sequence of pour has a significant effect on the deformation of the concrete at early ages. The deflections in the case when negative moment regions, i.e., over the interior supports, were poured first were twice as great as those obtained if the positive moment regions were poured prior to the negative moment regions. The deflections and stresses observed in the fresh concrete due to the construction loads and equipment were somewhat significant. However, the largest contribution was observed to be as a result of the dead weight of the superstructure. This was prominent due to the fact that the span lengths were significantly long, especially in the case of the steel girder bridge.

The dynamic and vibration analysis indicated that the simulated moving loads in adjacent lanes, as well as construction loads and vibrations, have a significant effect on the behavior of concrete at early ages. Significant deflections were observed as a result of the various mode shapes as well as the effects of the imposed dynamic and vibration loads. These deformations would be harmful to concrete at early ages, where settlement and loss of concrete cover are of major concern. There are other critical factors that were not addressed in the finite element analysis, which include the effect of the protruding steel reinforcement from finished decks into the deck under construction. The vibration and movement imposed on the extended reinforcement is a major source of crack initiation in the concrete deck.

9.3 Phase II of Study

Following the successful completion of the previous tasks, i.e., reviewing and identifying the various types of loads and vibrations affecting the concrete during construction, the findings will be

discussed with the project Technical Review Panel. As a result of the study, the instrumentation and monitoring of structures for construction loads and vibrations is vital. Specific methodologies and schemes will be developed with respect to the instrumentation and monitoring of the two proposed structures through discussions with the Technical Review Panel.

A detailed instrumentation plan is provided in Chapter eight along with the data collection and construction monitoring procedures. The conclusions from the study as well as the instrumentation and monitoring plan will be discussed with the Technical Review Panel in order to verify the feasibility of proceeding with Phase II of the study encompassing field investigations on two types of structures: continuous plate girder bridge and continuous prestressed concrete beam bridge. The collected data from the field investigation will mainly be used to support the following goals:

1. Verification of the finite element models and allow refinement of the models.
2. Determination of the dynamic effects experienced by the bridges during construction due to any detrimental factors.

The factors influencing the performance of the structure in the field include:

- Monitoring the supporting system (e.g., steel girders) during construction prior to deck curing for: (1) vertical and lateral movement, (2) compression flange buckling, and (3) web buckling. There have been instances where the weight of the wet concrete in the overhangs has caused the form support brackets to dent the web.
- Monitoring the structure for movement and placement of construction equipment.
- Observing any cracking in the concrete deck.
- Analyzing the data collected to determine the impact of construction loads and vibrations.

- Evaluating the pouring sequence program that is developed by the research team to determine the actual tensile stresses in the concrete.
- Evaluating construction sequence to determine whether the stiffness of the structure can be improved to reduce potential deflections at critical locations during the construction period.

Future work could also focus on more experimental work to observe the behavior of concrete at 12 hours, 24 hours, and 3 days, and to obtain the stress-strain relationships at these ages in an effort to verify the previous results and to be able to compare with the results obtained by previous research and code limitations. The computer program which determines the effect of sequence of pours on concrete curvatures will be refined as a result of the experimental program and other significant developments.

10. REFERENCES

1. Prenger, H.B., "Bridge Deck Cracking," Research Report, MD-93-04, Maryland DOT, State Highway Administration, 1993, 19 pp.
2. Fouad, F.H. and Furr, H.L., "Behavior of Portland Cement Mortar in Flexure at Early Ages," ACI, SP 95-6.
3. Dakhil, F.H., Cady, P.D., and Carrier, E., "Cracking of Fresh Concrete as Related to Reinforcement," ACI Structural Journal, 1975, V. 72, No. 8, pp. 421-428.
4. Halvorsen, G.T., "Troubleshooting Concrete Cracking During Construction," Aberdeen's Concrete Construction, 1991, V. 36, No. 11, pp. 811-816.
5. Hadje-Ghaffari, H., Choi, O.C., Darwin, D., and McCabe, S.L., "Bond of Epoxy Coated Reinforcement: Cover, Casting Position, Slump and Consolidation," ACI Structural Journal, 1994, V. 91, No. 1, pp. 59-68.
6. Hughes, B.P. and Videla, C., "Design Criteria for Early Age Bond Strength of Reinforced Concrete," Materials and Structures, 1992, V. 25, pp. 445-463.
7. ACI Committee 345, "Recommended Practice for Concrete Highway Bridge Deck Construction," Journal of ACI, 1973, V. 70, No. 6, pp. 381-415.
8. Ayaub, H. and Karshenas, S., "Survey Results for Concrete Construction Live Loads on Newly Poured Slabs," Journal of Structural Engineering, ASCE, 1994, V. 120, No. 5, pp. 1543-1563.
9. Gardner, N.J., "Effect of Temperature on the Early-Age Properties of Type I, Type III, and Type I/Fly Ash Concretes," ACI Materials Journal, 1990, V. 87, No. 1, pp. 68-78.

10. Harsh, S. and Darwin, D., "Effect of Traffic Induced Vibration on Bridge Deck Repairs," University of Kansas, Center for Research, June 1983.
11. Manning, D.G., "Effects of Traffic Induced Vibrations on Bridge-deck Repairs," Highway Practice, 1981, V. , 86-, pp. 40, Highway Engineering.
12. Manning, D.G., "Effects of Traffic Induced Vibrations on Bridge-deck Repairs," Synthesis of Highway Practice, No. 86, December 1991.
13. Huang, D., Wang, T.L., and Shahawy, M., "Impact Studies of Multigirder Concrete Bridges," Journal of Structural Engineering, ASCE, 1993, V. 119, No. 8, pp. 2387-2402.
14. Furr, H.L. and Fouad, F.H., "Bridge Slab Concrete Placed Adjacent to Moving Live Loads," Research Report 266-1F, Texas Transportation Institute, State Department of Highways and Public Transportation, 1981, 131 pp.
15. Hearn, G. and Ghia, R., "Vibration Response of Highway Bridges Under Normal Traffic," January 1993, Transportation Research Board, 72nd Annual Meeting, Washington, pp. 12.
16. Inbanathan, M.J. and Wieland, M., "Bridge Vibration Due to Vehicle Moving Over Rough Surface," Journal of Structural Engineering, ASCE, 1987, V. 113, No. 9, pp. 1994-2008.
17. Chang, D and Lee, H., "Impact Factors for Simple Span Highway Girder Bridges," Journal of Structural Engineering, ASCE, 1994, V. 120, No. 3, pp. 704-715.
18. Gaunt, J.T., Aramraks, T., Gutzwiller, M., and Lee, R.H., "Highway Bridge Vibration Studies," Transportation Research Record, #645, pp. 15-20.
19. Dusseau, R.A. and Dubaisi, H.N., "Natural Frequencies of Concrete Bridges in the Pacific Northwest," Transportation Research Record, 1993, No. 1393, pp. 119-132.

20. Dusseau, R.A., "USGS-sponsored Bridge Research in the Pacific Northwest," Fifth US National Conference on Earthquake Engineering-Proceedings, July 94, pp. 491-500.
21. Hilsdorf, H.K. and Lott, J.L., "Revibration of Retarded Concrete for Continuous Bridge Decks," NCHRP Report 106, Highway Research Board, Washington, D.C.
22. Karakouziyam, M., Boehm, R.F., Hudyma, N., and Harris, D.D., "Effects of Reinforcement Temperature on Shrinkage Cracking of PC," Concrete International, 1994, pp. 67-67.
23. Ryell, J. and Bowering, L., "Quality Assurance in Bridge Construction in Canada: A Study of Inspection and Testing Programs," Transportation and Research Record #652, 1977, pp. 42-51.
24. Kostem, C.N., "Dynamic Properties of Beam-slab Highway Bridges," Transportation Research Record, #645, 23 pp.
25. Lane, D.S., Investigation of Bridge Deck Cracking on I-95 Northbound over Powell Creek, Virginia Transportation and Research Council, 1994, 11 pp.
26. Cheong, H.K. and Lee, S.C., "Strength of Retempered Concrete," ACI Materials Journal, 1993, V. 90, No. 3, pp. 203.
27. Tam, K.S.S. and Scanlon, A., "Analysis of Cracking Due to Drying Shrinkage in Reinforced Concrete Members," A paper submitted for publication to the ACI, September 1984.
28. Ravina, D. and Soroka, I., "Slump Loss and Compressive Strength of Concrete Made with WRR and HRWR Admixtures and Subjected to Prolonged Mixing," Cement and Concrete Research, 1994, V. 24, No. 8, pp. 1455-1462.
29. De Schutter, G. and Taerwe, L., "General Hydration Model for Portland Cement and Blast Furnace Slag Cement," Cement and Concrete Research, 1995, V. 25, No. 3, pp. 593-604.

30. Branco, F.A., Mendes, P.A., and Mirambell, E., "Heat of Hydration Effect in Concrete Structures," *ACI Materials Journal*, 1992, V. 89, No. 2, pp. 139-145.
31. Sanchez de Rojas, M.I., Luxan, M.P., Frias, M., and Garcia, N., "The Influence of Different Additions on Portland Cement Hydration Heat," *Cement and Concrete Research*, 1993, V. 23, pp. 46-54.
32. Emborg, M. and Bernander, S., "Assessment of Risk of Thermal Cracking in Hardening Concrete," *Journal of Structural Engineering*, 1994, V. 120, No. 10, pp. 2893-2912.
33. Elbadry, M.M. and Ghali, A., "Temperature Variations in Concrete Bridges," *Journal of Structural Engineering*, ASCE, 1983, V. 109, No. 10, pp. 2355-2374.
34. Hilton, M.H., "Factors Affecting Girder Deflections During Bridge Deck Construction," *Virginia Highway Research Council, Highway Research Record*, 1972, No. 400, pp. 55-68.
35. Dutt, A.J., Roy, S.K., and Chew, M.Y.L., "Effect on Wind Flow on Freshly Poured Concrete," *Journal of Wind Engineering and Industrial Aerodynamics*, 1992, V. 44, No. 2, pp. 2629-2630.
36. Alsayed, S.H. and Amjad, M.A., "Effect of Curing Conditions on Strength, Porosity, Absorptivity, and Shrinkage of Concrete in Hot and Dry Climate," *Cement and Concrete Research*, 1994, V. 24, No. 7, pp. 1390-1398.
37. Ho, D.W.S., Cui, Q.Y., and Ritchie, D.J., "The Influence of Humidity and Curing Time on the Quality of Concrete," *Cement and Concrete Research*, 1989, V. 19, pp. 457-464.
38. Schmitt, T.R. and Darwin, D. "Cracking in Concrete Bridge Decks," Report K-TRAN, KU-94-1, A Cooperative Transportation Research Program Between Kansas DOT, the Kansas State University, and the University of Kansas, 1995, 151 pp.

39. Jackson, M., "Durability of Bridge Decks," Interim Report TRC-9210, Arkansas State Highway and Transportation Department in Cooperation with Federal Highway Administration, 1992, 46 pp.
40. Babaei, K., "Evaluation of Concrete Overlays for Bridge Applications," Final Report, WA-RD 137.1, Washington State DOT in Cooperation with the United States Department of Transportation Federal Highway Administration, 1987, 72 pp.
41. Construction Technology Laboratories, Inc., "Petrographic Examination of Three Concrete Cores Taken from Two Bridge Decks in Rock Island County, Illinois," Submitted by Illinois Department of Transportation, April 1994, 20 pp.
42. Steward, C.F., McMahon, J.E., and Womack, J.C., "Bridge Widening Problems," Report HPR-1(2) D0422, State of California Highway Transportation Agency, Department of Public Works, Division of Highways, Bridge Department, 1965, 10 pp.
43. Lambe, T.W. and Whitman, R.V., Soil Mechanics, Series in Soil Engineering, John Wiley & Sons, New York, 1968, 553 pp.
44. Dowding, C.H., Construction Vibrations, Prentice-Hall, Inc., 1996, 610 pp.
45. Roberts, A., Applied Geotechnology, Pergamon Press, 1981, 344 pp.
46. Horn, M.W., Stewart, C.F., and Boulware, R.L., Factors Affecting the Durability of Concrete Bridge Decks: Construction Practices, Interim Report No. 4, Bridge Department, California Division of Highways, CA-DOT-ST-4104-4-75-3, March 1975.
47. Stewart, C.F. and Gunderson, B.J., Factors Affecting the Durability of Concrete Bridge Decks, Interim Report No. 2, Research and Development Section of the Bridge Department, State of California, November 1969.

48. Cheng, T.T. and Johnston, D.W., Incidence Assessment of Transverse Cracking in Bridge Decks: Construction and Material Considerations, FHWA A/NC/85-002, Vol. 1, North Carolina State University, Department of Civil Engineering, Raleigh, North Carolina, June 1985.
49. Gardner, N.J. and Zhao, J.W., "Creep and Shrinkage Revisited," ACI Materials Journal, 1993, V. 90, No.38, pp. 236-246.
50. Humar, J.L. and Kashif, A.H., "Dynamic Response Analysis of Slab-Type Bridges," Journal of Structural Engineering, ASCE, V. 121, No. 1, January 1995, pp. 48-62.
51. Yang, Y.-B., Liao, S.-S., and Lin, B.-H., "Impact Formulas for Vehicles Moving Over Simple and Continuous Beams," Journal of Structural Engineering, ASCE, V. 121, No. 11, November 1995, pp. 1644-1650.
52. Chen, H.L., Spyrakos, C.C., and Venkatesh, G., "Evaluating Structural Deterioration by Dynamic Response," Journal of Structural Engineering, ASCE, V. 121, No. 8, August 1995, pp. 1197-1204.
53. Memory, T.J., Thambiratnam, D.P., and Brameld, G.H., "Free Vibration Analysis of Bridges," Engineering Structures, V. 17, No. 10, 1995, pp. 705-713.
54. Saadeghvaziri, M.A., "Finite Element Analysis of Highway Bridges Subjected to Moving Loads," Computers and Structures, V. 49, No. 5, 1993, pp. 837-842.
55. Salawu, O.S. and Williams, C., "Bridge Assessment Using Forced-Vibration Testing," Journal of Structural Engineering, ASCE, V. 121, No. 2, February 1995, pp. 161-173.
56. Casas, J.R. and Aparicio, A.C., "Structural Damage Identification from Dynamic-Test Data," Journal of Structural Engineering, ASCE, V. 120, No. 8, August 1994, pp. 2437-2450.

57. Law, S.S., Ward, H.S., Shi, G.B., Chen, R.Z., Waldron, P., and Taylor C., "Dynamic Assessment of Bridge Load-Carrying Capacities. I," *Journal of Structural Engineering*, ASCE, V. 121, No. 3, March 1995, pp. 478-487.
58. Paultre, P., Proulx, J., and Talbot, M., "Dynamic Testing Procedures for Highway Bridges Using Traffic Loads," *Journal of Structural Engineering*, ASCE, V. 121, No. 2, February 1995, pp. 362-376.
59. Cebon, D., "Vehicle-Generated Road Damage: A Review," *Vehicle System Dynamics*, V. 18, 1989, pp. 107-150.
60. Green, M.F., Cebon, D., and Cole, D.J., "Effects of Vehicle Suspension Design on Dynamics of Highway Bridges," *Journal of Structural Engineering*, ASCE, V. 121, No. 2, February 1995, pp. 272-282.
61. Law, S.S., Ward, H.S., Shi, G.B., and Chen, R.Z., "Study of Vibrational Parameters of Twenty-Nine Reinforced Concrete Bridge Deck as Indicator of Structural Integrity," Research Report, Civil and Structural Engineering Department, Hong Kong Polytechnic, Hung Hom, Kowloon, Hong Kong.
62. Moody, J.R. and Mansell, D.S., "Dynamic Interaction of Bridge Bearings, Superstructure and Loads," *Proceedings of Australian Conference on the Mechanics of Structures and Materials*, 1980, pp. 80-84.
63. Law, S.S., "Finite Element Modelling and Parameter Study on the Effect of Boundary Conditions on the Vibrational Response of Bridge Deck," Research Report, Civil and Structural Engineering Department, Hong Kong Polytechnic, Hung Hom, Kowloon, Hong Kong.

64. Kawashima, K. and Unjoh, S., "Seismic Response Control of Bridges by Variable Dampers," *Journal of Structural Engineering, ASCE*, V. 120, No. 9, September 1994, pp. 2583-2601.
65. Ventura, C.E., Felber, A.J., and Stierner, S.F., "Determination of the Dynamic Characteristics of the Colquitz River Bridge by Full-Scale Testing," *Canadian Journal of Civil Engineering*, V. 23, No. 2, April 1996, pp. 536-548.



APPENDICES



APPENDIX A



**SURVEY ON CAST-IN-PLACE CONSTRUCTION
OF BRIDGE DECKS**

State: _____

1. Does your agency permit regular vehicular traffic to continue using one or more lanes of a bridge when concrete is being placed on the same structure using:

- | | | | | |
|--------------------------|-----|--------------------------|----|--------------------------|
| a) full deck replacement | Yes | <input type="checkbox"/> | No | <input type="checkbox"/> |
| b) bridge deck overlay | Yes | <input type="checkbox"/> | No | <input type="checkbox"/> |

2. Do you impose any restrictions on the traffic related to construction loads, e.g., limit on speed or truck weight, or the concreting operation, e.g., time of day, using:

- | | | | | |
|--------------------------|-----|--------------------------|----|--------------------------|
| a) full deck replacement | Yes | <input type="checkbox"/> | No | <input type="checkbox"/> |
| b) bridge deck overlay | Yes | <input type="checkbox"/> | No | <input type="checkbox"/> |

If yes, please specify _____

3. What is the rationale behind your agency's policy of either permitting or prohibiting traffic to continue in adjacent lanes?

4. Does your agency conduct research or field studies on the factors most likely to inflict any damage on newly poured concrete during construction, and if so, could you provide us with your own specifications for these construction techniques, or any published reports?

5. Have you experienced a significant premature occurrences of any of the following defects in bridge deck concrete that had been *subjected to construction loads and vibrations* during construction, rehabilitation, widening or overlaying of the deck? If applicable, check the appropriate boxes and indicate prevailing conditions at the job sites involving deck construction or repair by indicating the corresponding letter from the list provided below the table. We would appreciate if you could send us a copy of any published reports.

Defect	On Full Depth Concrete	On Overlay (If so, indicate type of overlay)	Letter for condition
Longitudinal cracks			
Transverse cracks			
Random cracks			
Cracking over supports			
Cracking at midspan			
Bond failure at overlay-deck interface			
Delamination at rebar level			
Inadequate concrete strength			
Other, specify			

- a - Traffic-induced vibrations during placement of concrete
- b - Vibrations caused by construction equipment
- c - Adjacent pile driving
- d - Deflections caused by moving equipment
- e - Clean concrete cover
- f - Concrete age associated with pour stages
- g - Sequence of pours
- h - Curing procedures
- I - Thermal changes
- j - Heat of hydration
- k - Type of concrete
- l - Time of year and conditions prevalent at pour stages
- m - Type of paving and/or finishing equipment used
- n - Adjacent railroad traffic
- o - Shear connector design
- p - Other

If so, please specify _____

6. What type of concrete and cement type (if known) was used?

7. Do you have any bridge deck construction, rehabilitation, widening or overlay projects scheduled for the 1996 construction season?

Yes No

If yes, please provide a contact regarding this work:

Name: _____ Phone: _____

Name of respondent: _____

Title: _____

Phone: _____ Fax _____ E-mail _____

Address: _____

If you are interested in a copy of the survey results, please indicate,

Yes No

Please mail completed survey to:

Dr. Mohsen A. Issa
University of Illinois at Chicago
Department of Civil and Materials Engineering
Room 2095 ERF, (M/C 246)
842 West Taylor Street
Chicago, Illinois 60607

TABLE A.1

SUMMARY OF ANSWERS BY STATE

State	1 a	1b	2a	2 b	Question 2 comment	3	4	5	6	7
Alaska	Y	Y	N	N		Allows highway to remain open	N	l, l, p, o ^{††}	Class AA (Full depth), Micro silica (overlay)	Y
Arkansas	Y	Y	N	N		Economics; cracking when there are no construction loads on bridge	Y	q ^{**}	AASHTO M85 Type I	Y
California	Y	Y	N	N	Closure pours	Research on widening	Y	p	Type II low alkali cement	Y
Colorado	Y	N	N	N		Vibrations are not a problem	N	No to all questions	4500psi/Type I or II cement	Y
Columbia	Y	Y	N	N		Inconvenience to traveling public	N	g, h, I	4500psi/Type I/Air Entrained	Y
Delaware	Y	Y	Y	N	Speed limit, sometimes truck traffic prohibited	Opinion that there is no relationship between vibrations and cracking	A	NA	4500psi/Type I or II cement	Y
Florida	Y	Y	Y	Y	Speed Limit for Safety	Past experience and research reports	Y	e, f, g, h, I, k, l	Type I or II cement with fly ash	Y
Georgia: Bridge Engineer	Y	Y	N	N		Use close pour strips to minimize vibrations for continuous bridges	A	No to all questions	Does not apply	N
Georgia: State Construction Engineer	Y	Y	N	N		Inconvenience to traveling public	N	N	NA	Y
Hawaii	N A	Y	N A	Y		No full deck replacement. Overlay limited to patching of spalled areas	N	NA	NA	N
Idaho	Y	Y	Y	Y	Speed Limit, for small clearance close traffic	Each project considered individually	N	z	NA	Y
Iowa	Y	Y	Y	Y	Traffic lights, so traffic speed is slow	Did not notice detrimental effect of adjacent traffic	Y [†]	NA	P.C. concrete, Type I cement	Y
Kansas	Y	Y	Y	Y	Detailed specification attached	Inconvenience and unavailability of detour routes	Y	d, f, j	Unknown, Probably cement Type I or II	Y
Kentucky	Y	Y	Y	Y	Speed Limit	Inconvenience to traveling public	N A	NA	4000psi/Type III/High Early Strength	Y
Louisiana	Y	Y	Y	Y	Speed Limit 45 mph	Economics, Safety, Detour routes	N A	f, g	3200 psi Type I or II cement	Y

TABLE A.1- Continued

SUMMARY OF ANSWERS BY STATE

State	1a	1b	2a	2b	Question 2 comment	3	4	5	6	7
Maryland	Y	Y	N	N	Speed Limit	Study found that deflection and vibration effects are not significant	Y	d, g, h, I, I [†]	Standard Mix #6, 4500 psi Type I cement	Y
Massachusetts	Y	Y	N	N	Speed Limit as part of traffic management plan	No definitive basis for not permitting traffic	N	a ^{EE}	115 pcf lightweight concrete, 4000 psi, 3/4" aggregate, 658lb Type I cement per cubic yard	Y
Michigan	Y	Y	Y	N	Heavy traffic, mixers, slip form machines prohibited	1. No evidence that adjacent traffic has detrimental effect 2. Inconvenience	N	h, I, j, l	≥4000 psi @ 28 days, Type I or IA cement	Y
Minnesota	Y	Y	N	N		No alternative route and experience shows no damage	N	d, f, g, h, I, j, l	Mn DOT standard using Type I cement	Y
Mississippi	Y	Y	Y	Y	Speed, Weight, Time of day	Research indicates it is not harmful	N	NA*	Type I Portland cement	Y
Missouri	Y	Y	Y	Y	Load and Speed Limits	Inconvenience to traveling public	N	a,h	7.75 Sacks, 2.5" Slump, W/C ≤ .4, Type I or II cement	Y
Nebraska	N	N	N	N		Allow traffic if portion of the bridge is not structurally connected	N	NA	Fill depth 4000 psi, Overlay - High density & silica fume	Y
Nevada	Y	Y	N	N		Problems not attributed to adjacent traffic	N	NA*	Specification Given	Y
New Jersey	Y	Y	N	N		NA	N	j,l,p	Full Depth - P Cement Type I or II, Overlay - Latex Modified Concrete	Y
New Jersey Turnpike Authority	Y	Y	N	N	NA	NA	N	j,l,p	PC concrete Type I Cement, Latex overlay	Y
New Mexico	Y	Y	Y	Y	Speed Limit 10 mph, project specific	Believe that vibrations are harmful but have no choice but to maintain traffic	N	a	7 sack mix, Type II cement	Y
New York State	Y	Y	Y	Y	Speed Limit	Maintaining acceptable traffic thru the bridge site	N	no significant occurrence	NA	Y

TABLE A.1- Continued

SUMMARY OF ANSWERS BY STATE

State	1 a	1b	2a	2 b	Question 2 comment	3	4	5	6	7
North Carolina	Y	Y	N	N		Did not have any problems due to adjacent traffic	N	NA	4500 psi normal weight	Y
North Dakota	Y	Y	Y	Y	Full deck 70% of design strength, Overlay 5 day curing period	Not aware of negative effects of adjacent traffic vibration	N	NA	Unknown	Y
Northern Mariana Islands*	N A	N A	N A	N A	NA	NA	N A	NA	NA	Y
Ohio	Y	Y	N	N	NA	Availability of adequate detour	Y	h,l,p	Micro silica, latex, superplasticized dense	Y
Oklahoma	N	Y	N	Y	Speed Limit 15 - 20 mph	To reduce vibrations to a tolerable level during adjacent overlay construction	N	a	Not known	N
Oregon	Y	Y	Y	Y	Speed limit often, load restriction seldom	Cost, no serious effects of adjacent traffic	N A	NA	NA	Y
Pennsylvania	Y	Y	Y	Y	Partial width construction avoided	Belief that on less rigid structure traffic can cause cracking	Y [†]	NA	NA	Y
Rhode Island	Y	Y	N	N		Availability of detour route	N	NA	NA	Y
South Carolina	Y	Y	Y	Y	Speed Limit	Must provide for traffic, no good detour available	N	NA	Attached "Special provisions for bridge deck rehabilitation"	Y
South Dakota	Y	Y	Y	Y	Speed Limit	Past history not indicated significant problems due to adjacent traffic.	N	NA	Class A45, 4500 psi, Type II Cement	Y
Tennessee	Y	Y	Y	Y	Speed Limit in Selected Cases	Traffic volumes dictate minimum service requirements	A	g, h, I, l	3000psi Class A or 4000psi Class D Type I cement	Y
Utah	Y	N U	N	N U		Found no correlation between traffic and cracking	Y	'	Type II cement	Y
Vermont	Y	Y	Y	Y	Speed Limit	Only when alternate traffic maintenance is not feasible	N	None to all questions	NA	Y

TABLE A.1- Continued

SUMMARY OF ANSWERS BY STATE

State	1 a	1b	2a	2 b	Question 2 comment	3	4	5	6	7
Virginia	Y	Y	N	N		No rationale	N	NA	3500 to 4500 psi Type I, II and III cement	Y
Washington	Y	Y	Y	Y	Speed Limit	No proof that adjacent traffic will cause harm	Y	h, l	Type II cement	Y
West Virginia - Division of Highways, Materials Control, Soil, and Testing	Y	Y	Y	Y	Speed Limit 50 mph	Investigations have not shown relationship between vibrations and cracking	N A	NA	NA	Y
West Virginia - Highway Division	Y	Y	Y	Y	Speed Limit 50 mph	Inconvenience to traveling public	A	b, h, k, l	Type I cement	Y
Wisconsin	N	N	N	N		Traffic prohibited and day of pour to allow concrete to take initial set	N	a	7 bag on decks, 9 bag on overlay	Y
Wyoming	Y	Y	Y	Y	Speed Limit 10 during pour and 8 h after	No feasible way to close bridge	N A	a, b	NA	Y

* Problems attributed to environmental factors. No data exists

** Cracking not related to any prevailing condition at the job site

† Suspected causes - not proven

†† Seismic activity

‡ Results not available at the time

‡ Not related to construction loads and vibrations

‡ Premature cracking found as much on jobs with and without adjacent traffic

‡ Concrete settled outside main deck reinforcement, lightweight concrete

*There are no bridge constructions in this state

TABLE A.2

SUMMARY OF ANSWERS BY ILLINOIS DISTRICT

District	1a	1b	2a	2b	Question 2 comment	3	4	5	6	7
1 District Engineer	Y	Y	N	N	NA	Public Convenience	N	a,d	Type I cement	Y
1 Area Construction Supervisor	Y	Y	N	N	NA	Traffic volume w/o sufficient detour routes	N	a,p	Type I cement, High range water reducer, Air entr., w/c 0.44...	Y
2	Y	Y	Y	Y	Speed restriction	Economics and inconvenience	Y	NA	Microsilica 600 lb Type I Cement for overlay	
3	Y	Y	N	N	NA	Traffic not harmful	N	N	Class SI (Class X)	Y
4										
5	Y	Y	Y	N	Sequence of pour determined, time between pours	Cost, Inconvenience	Y	a,b,f,g,h,i,k,l,p	NA	Y
6	Y	Y	N	N	NA	NA	NA	p	NA	Y
7	Y	Y	N	N	NA	NA	N	a,h,i,j,p	Vary	Y
8	Y	Y	N	N	NA	No problems	N	NA	Vary	Y

APPENDIX B

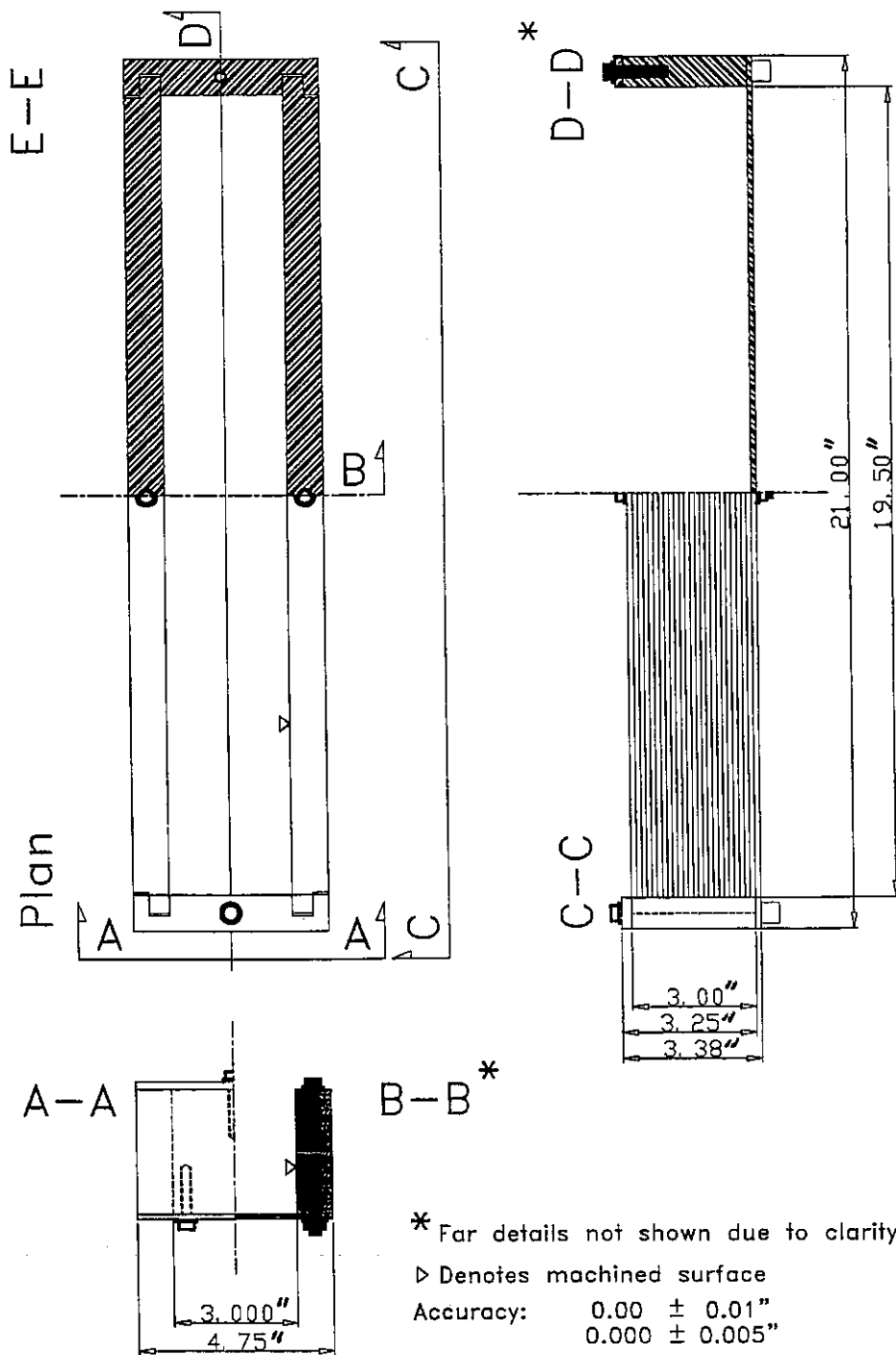


Figure B.1 Flexible mold

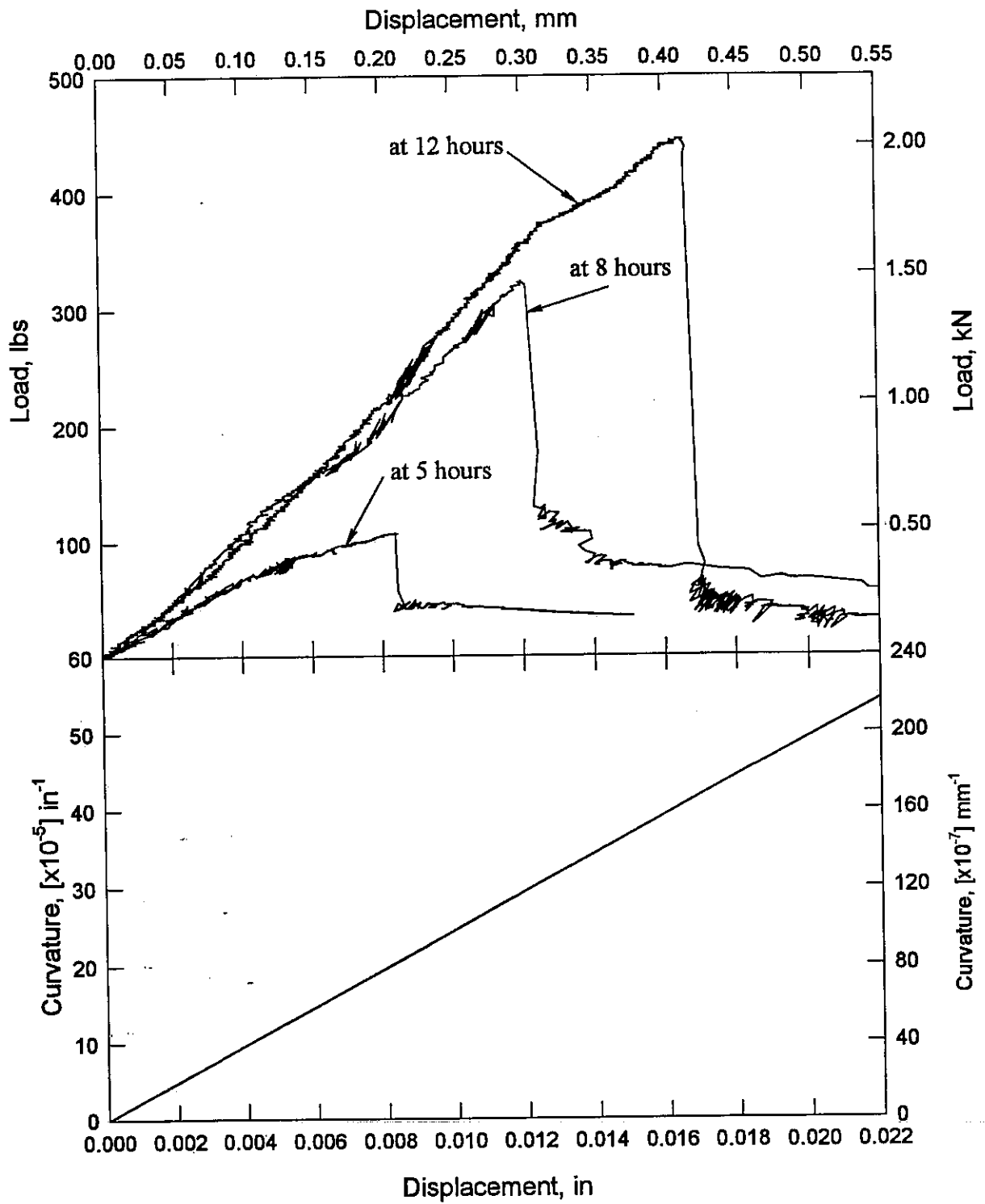


Figure B.2 Load-displacement-curvature diagrams for specimens set 1, concrete without additives

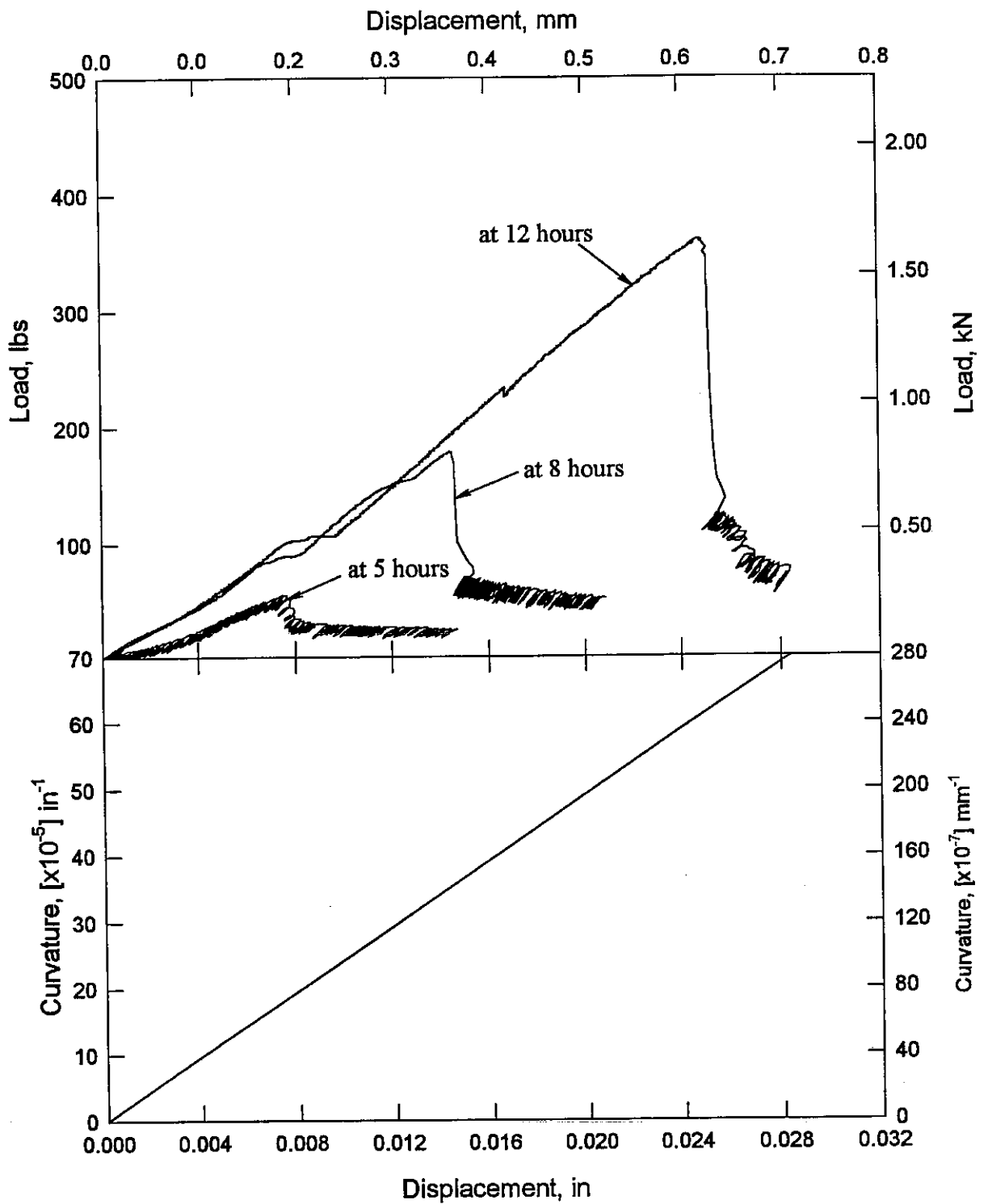


Figure B.3 Load-displacement-curvature diagrams for specimens set 1, concrete with superplasticizer

APPENDIX C

PROGRAM MANUAL

The program contains an executable file "BCL.EXE" and three additional files, "EDIT.BAT", "DOSXMSF.EXE" and "DOSXNT.386". "EDIT.BAT" is a batch file that defines the editor used for viewing data. The last two files are support files needed to run 32-bit programs under DOS or Windows 3.1x environment, respectively. All files, except "EDIT.BAT", should be copied into the desired directory (e.g., C:\BCL). However, file "EDIT.BAT" should be copied into any directory that is listed under the "PATH" command in your "AUTOEXEC.BAT" file. The user should edit the "EDIT.BAT" file and type the command that will start preferred editor (e.g. "EDIT.COM %1"). To use this program under Windows, the "SYSTEM.INI" file in your Windows directory should be edited. Assuming that the programs are installed in the C:\BCL directory, the following line should be added in the [386enh] section:

```
device=c:\bcl\dosxnt.386
```

After starting the program, the main menu will appear (Figure C.1). Selection can be made by typing the number or highlighted letter, corresponding to the desired task.

First, the name of the file has to be set up by choosing "1" or "f". A screen similar to Figure C.2 will appear. Type the desired name, which may contain the full path and press "Enter". Note that the current filename will appear at the top of the screen. If this is a new file, you have to create it choosing "2". If the file already exists, a message similar to Figure C.3 will appear. Furthermore, the user must provide the necessary data interactively by responding to several questions (Figures C.4 to C.8). Logical controls are used to avoid as many mistakes as possible (e.g., concrete deck overlap between sequences, overwriting data, negative values for section properties,

etc.). If, however, a mistake was made, the user may change each parameter in a separate section from the existing input file (except number of spans), again with the same logical controls as in the input section.

After creating the input file, the system can be solved by choosing "3" or "s". After the problem is solved, the program will return to the main menu (Figure C.9).

The output file may be viewed by pressing "4" or "e". Note that this option will call "EDIT.BAT". To use the editor of your choice edit "EDIT.BAT" so that it calls the desired editor. The output file consists of two sections. The first section contains formatted output of the input data as given by the user. It provides opportunity to check if the data are correctly specified. The second section contains the calculated data for the self weight of the girder and thereafter for each step. For each sequence of pour, initial data given are due to the loads acting during a particular sequence only, followed by the combined data, this data is added to all previously calculated loads.

Furthermore, you may change the existing data for the currently chosen filename by selecting "5" or "c". A screen similar to Figure C.10 will appear. You may opt to save the changed data to a new filename, or replace the existing data. A new menu offering different choices will then appear (Figure C.11). Most of the data available in the second selection screen are available, except number of spans. Select any number or letter accordingly with the data you want to change. This will lead to the input screen where proper data can interactively be entered, same as selection "2" or "I" from the main menu.

Units may be changed choosing option "6" or "u" from the main menu (Figure C.12). Note that this option is valid only for the newly created file. Existing files are not affected by this choice.

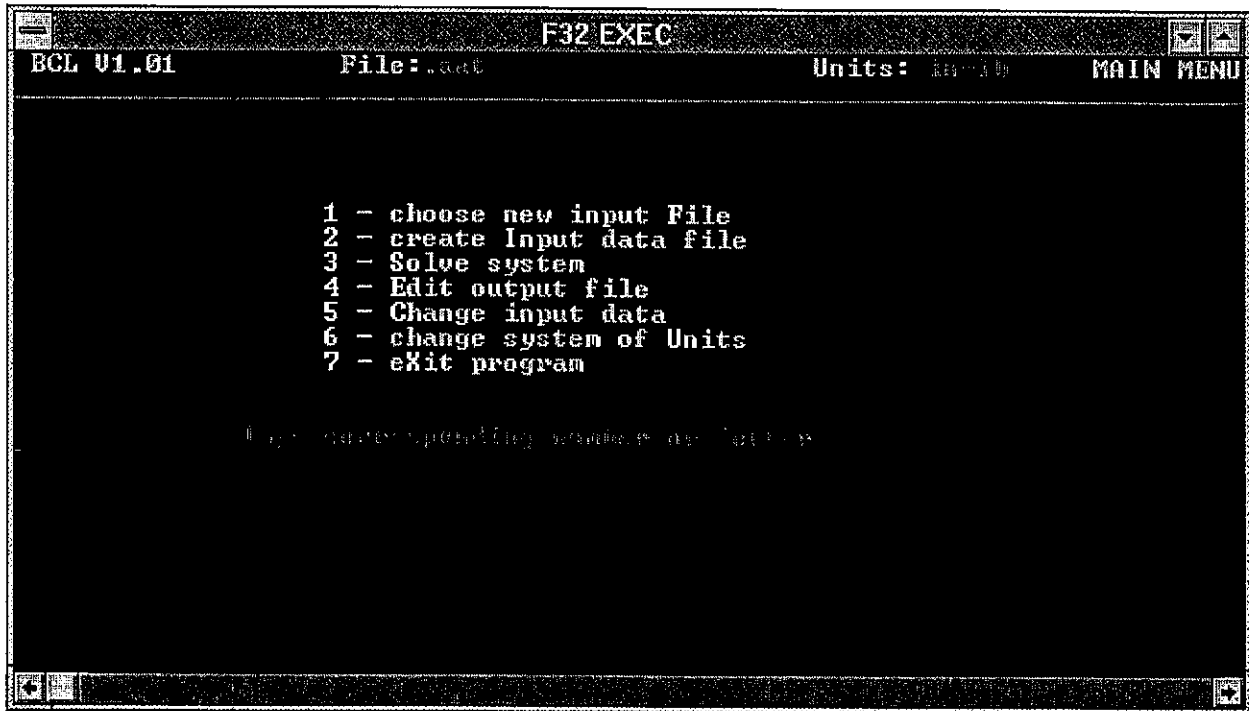


Figure C.1 Main menu screen

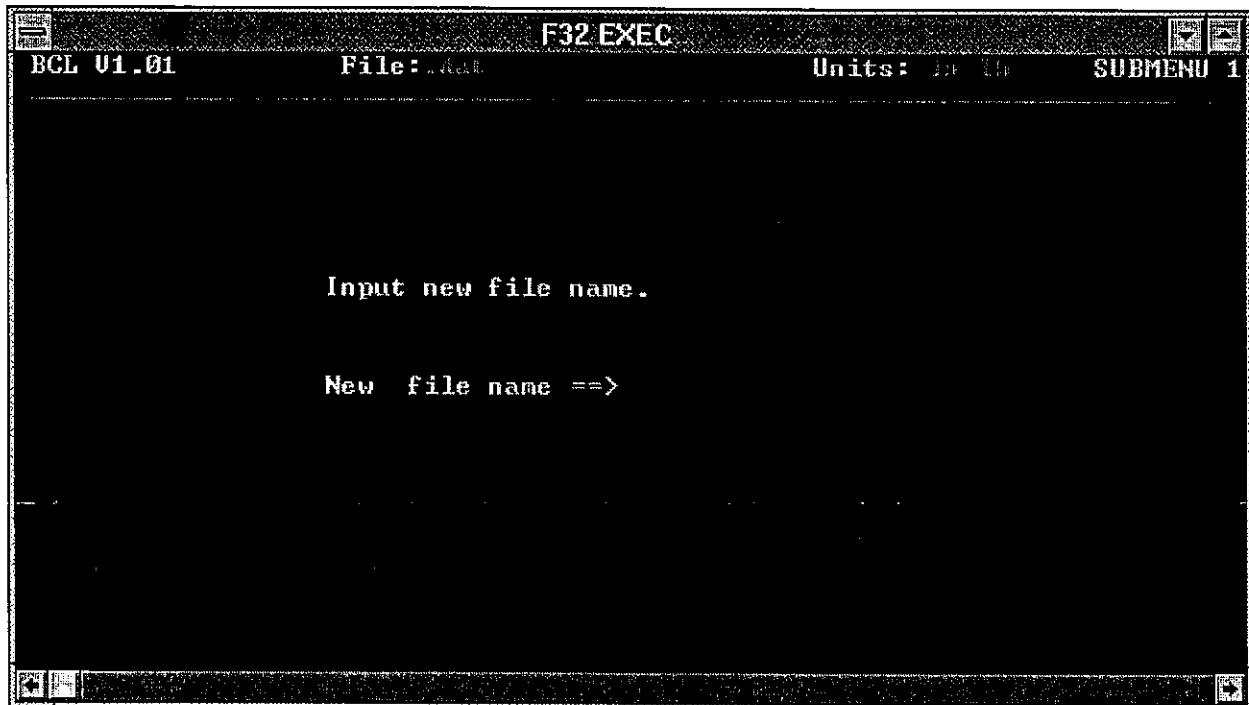


Figure C.2 New input filename screen

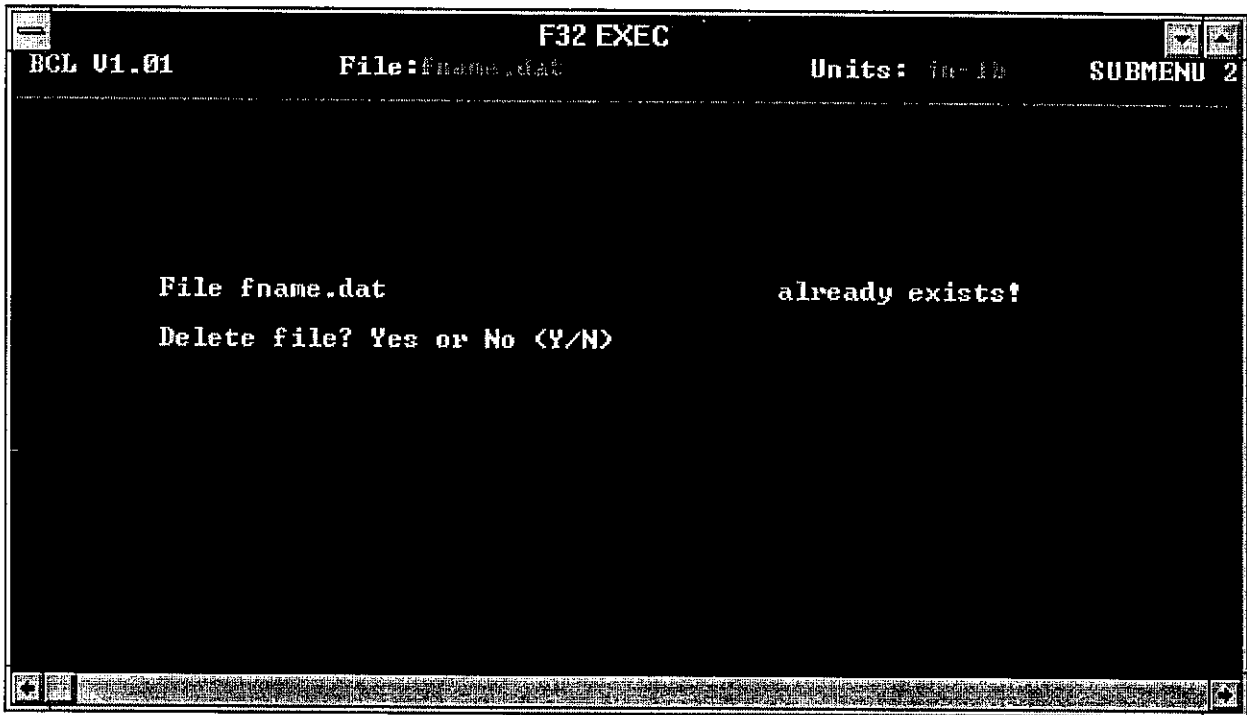


Figure C.3 File overwrite warning screen

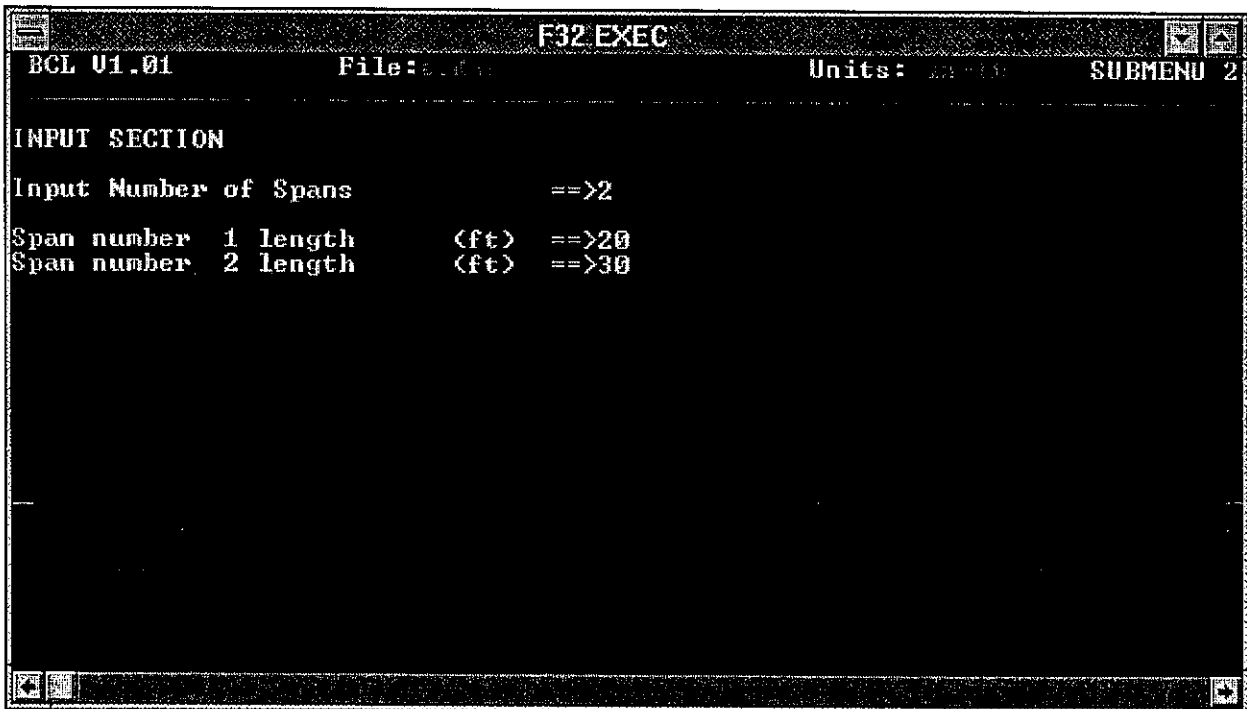


Figure C.4 Span data screen

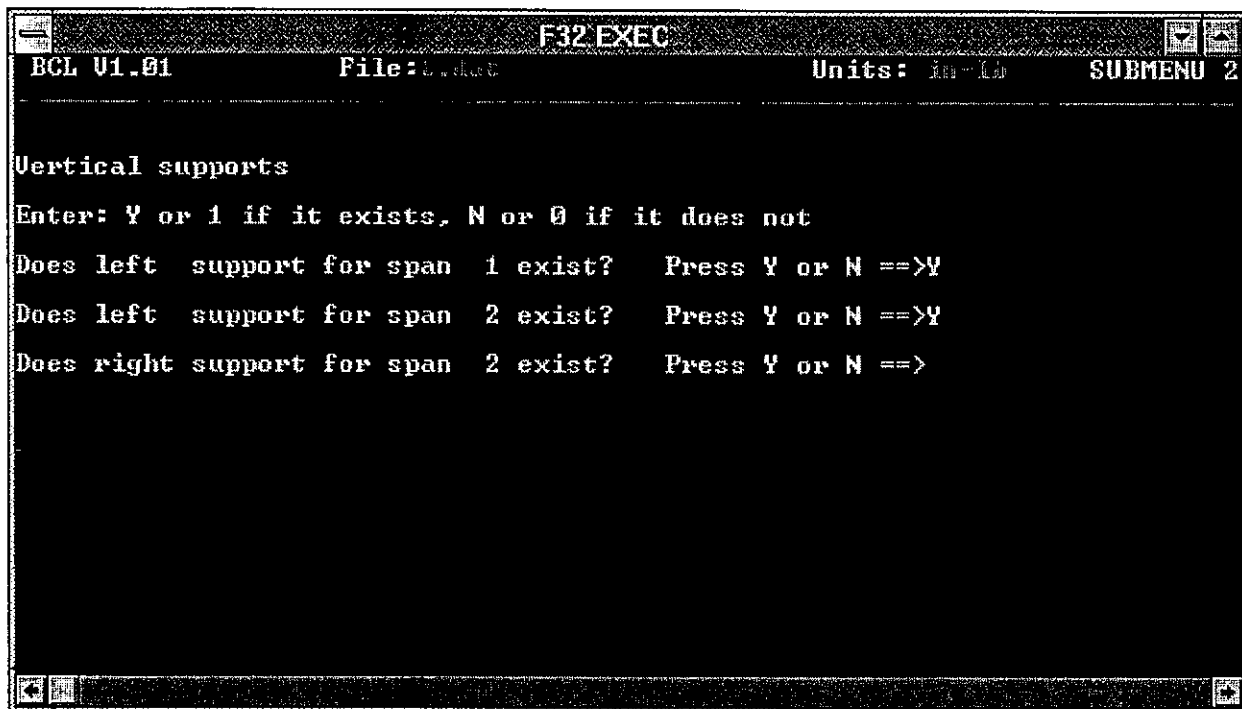


Figure C.5 Vertical supports screen

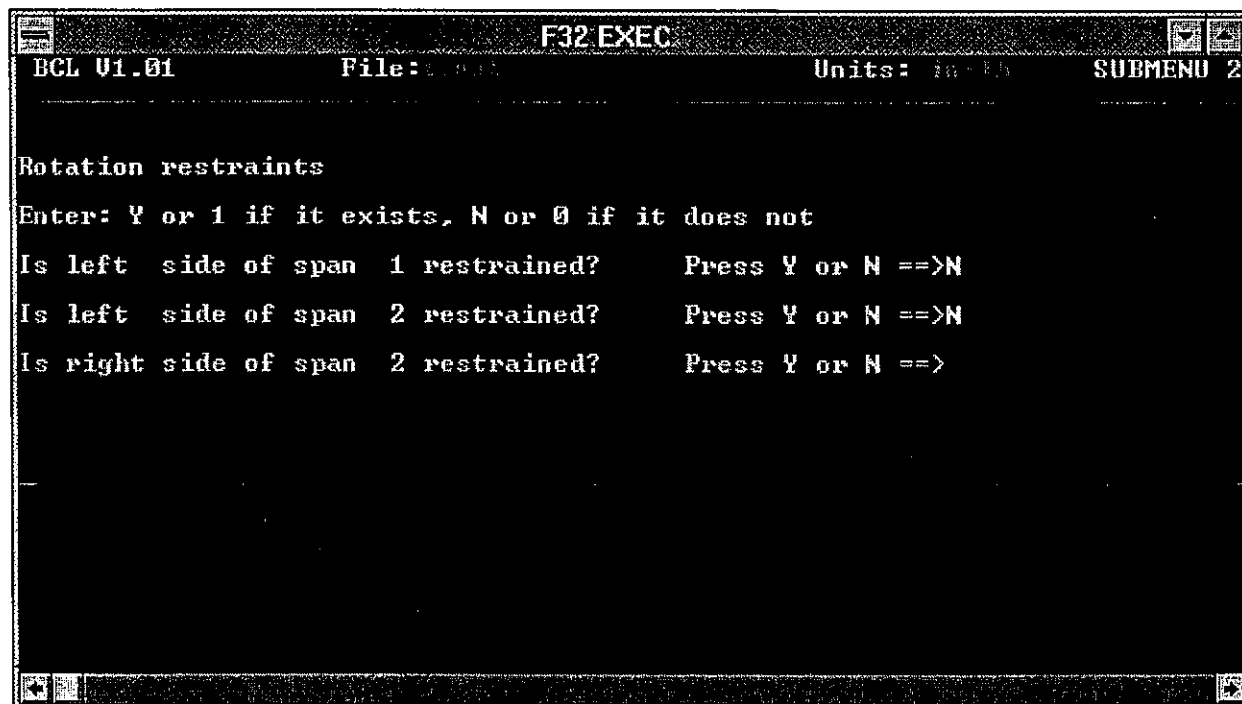


Figure C.6 Rotational supports screen

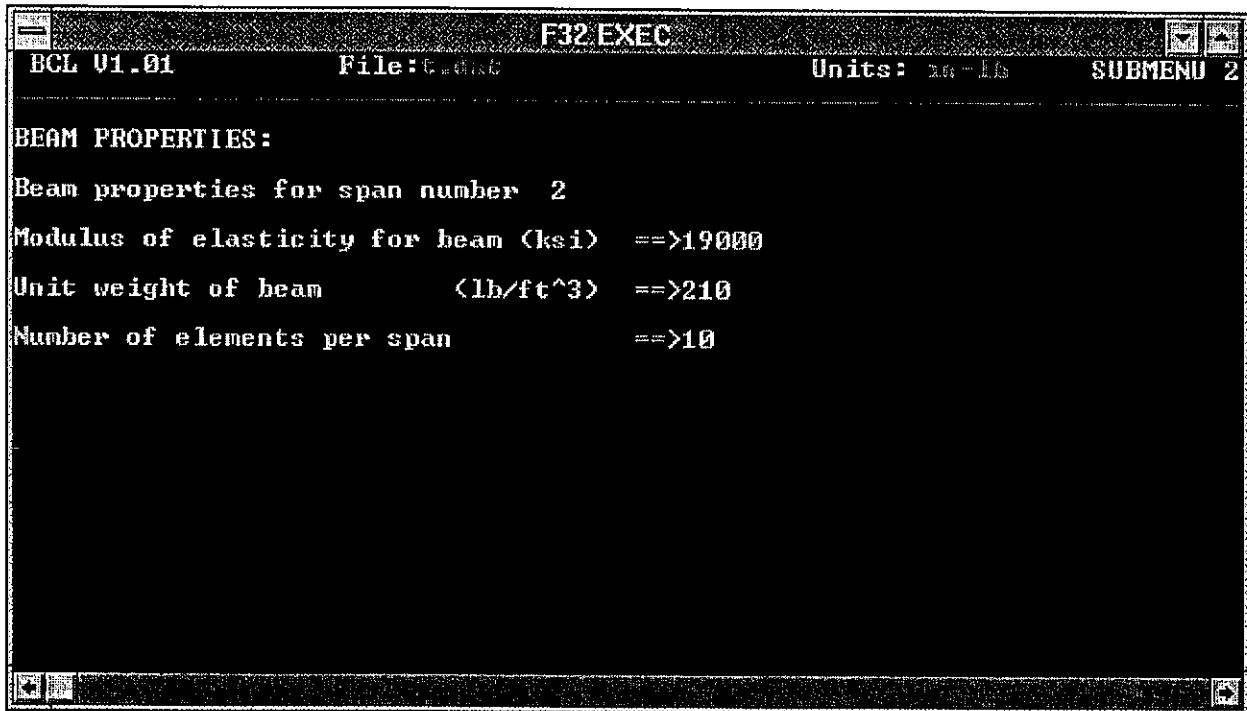


Figure C.7 Beam properties screen

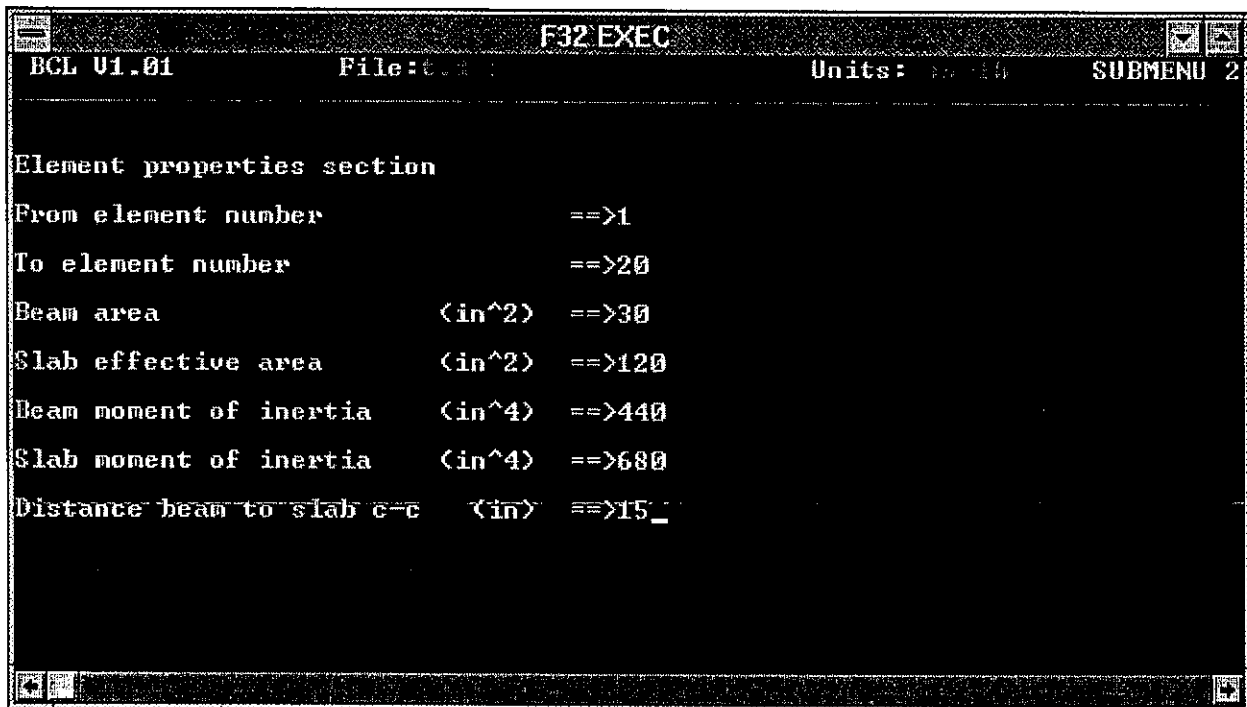


Figure C.8 Element properties data screen

```

BCL U1.01                               F32 EXEC                               Units: in-lb  SUBMENU 3
-----
OPENING FILES
PREPROCESSING DATA
Calculated E for slab (current units):    1871.
PRINTING INPUT DATA SECTION
READING PREPROCESOR DATA
ALLOCATING MEMORY
WORKING ON GIRDER LOADS
WORKING ON SEQUENCE Number:              1
WORKING ON SEQUENCE Number:              2
CLOSING FILES
Press any key to continue?

```

Figure C.9 Program trace screen

```

BCL U1.01                               F32 EXEC                               Units: in-lb  SUBMENU 5
-----
New data can be save in to a current file or new file
Do you want to save it in to a new file?  Press Y or N ==>_

WARNING? If you choose N data in curent file
will be replaced with new one

```

Figure C.10 Choosing output file name for changed data

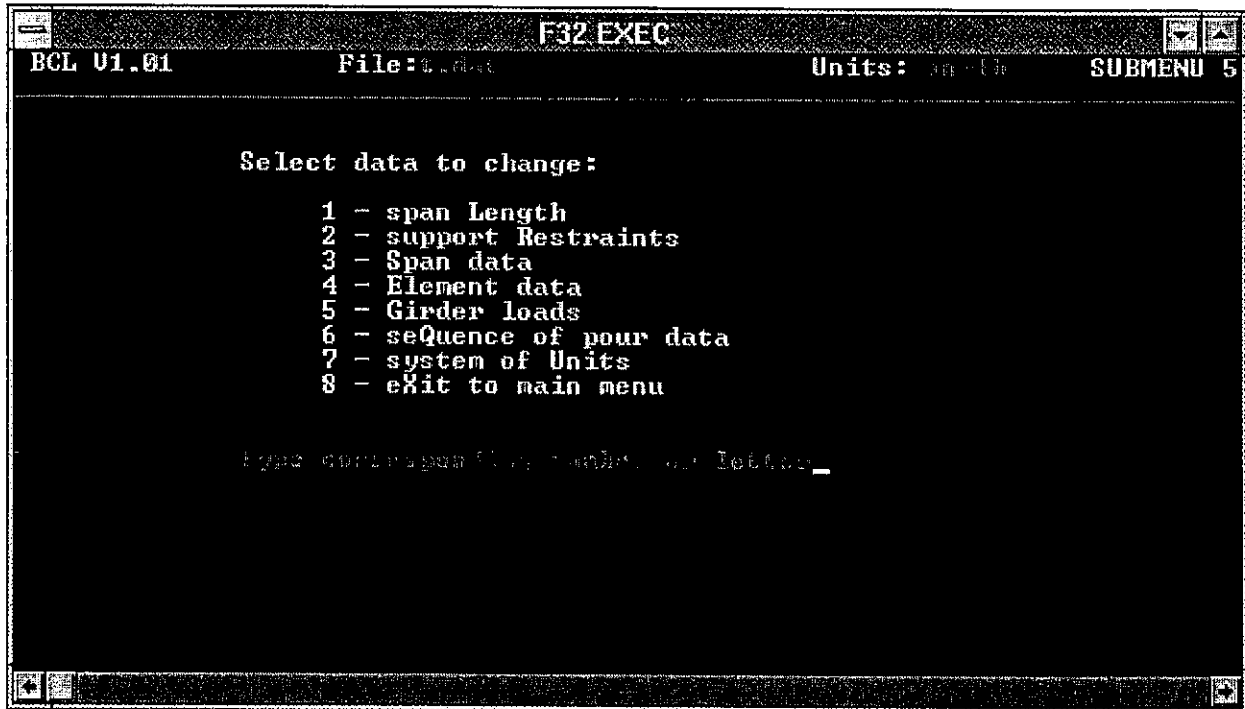


Figure C.11 Change input data submenu

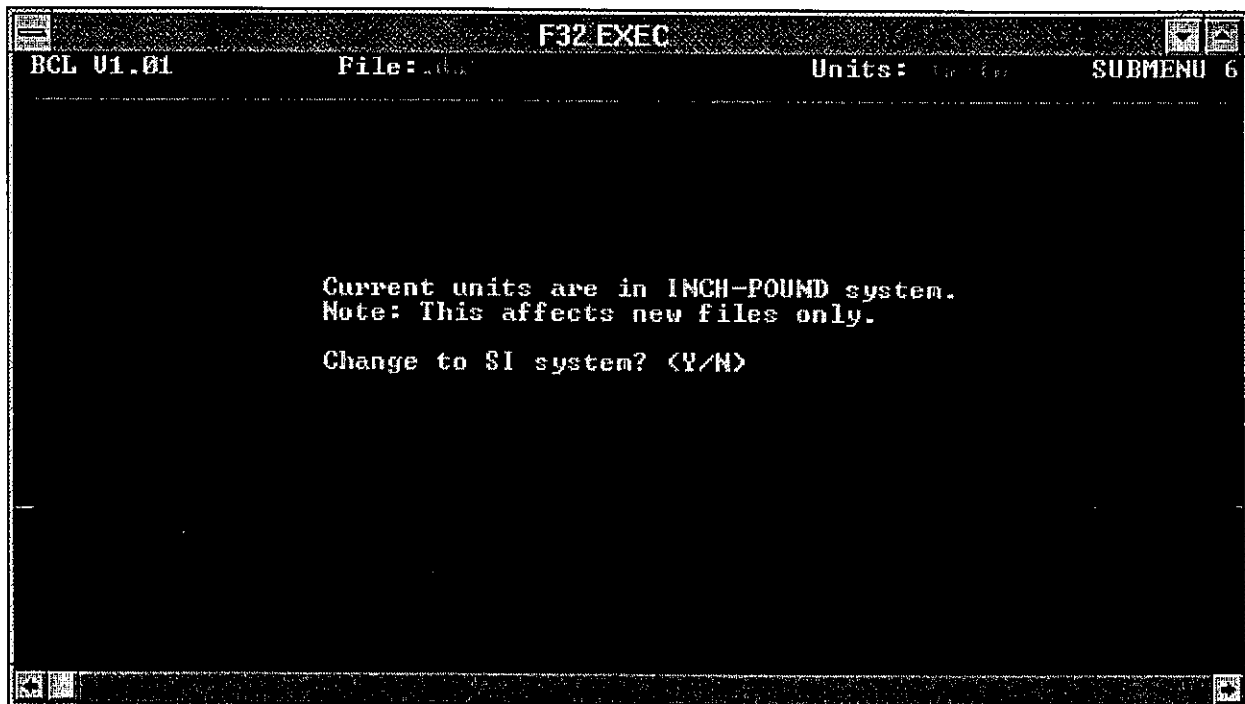
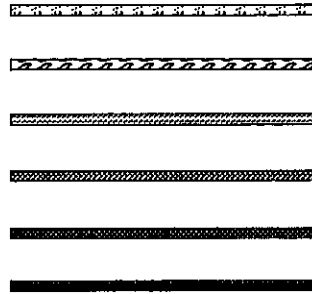


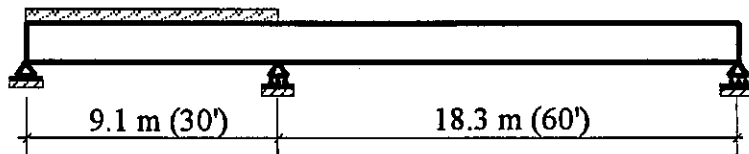
Figure C.12 Change system of units screen

Current (The Latest) Sequence

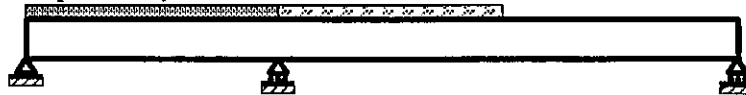


The Oldest Sequence

Sequence 1; $t = 0$



Sequence 2; $t = 24$ hours



Sequence 3; $t = 48$ hours



Figure C.13 Sequence of pour for bridge AL-2 Case "a"

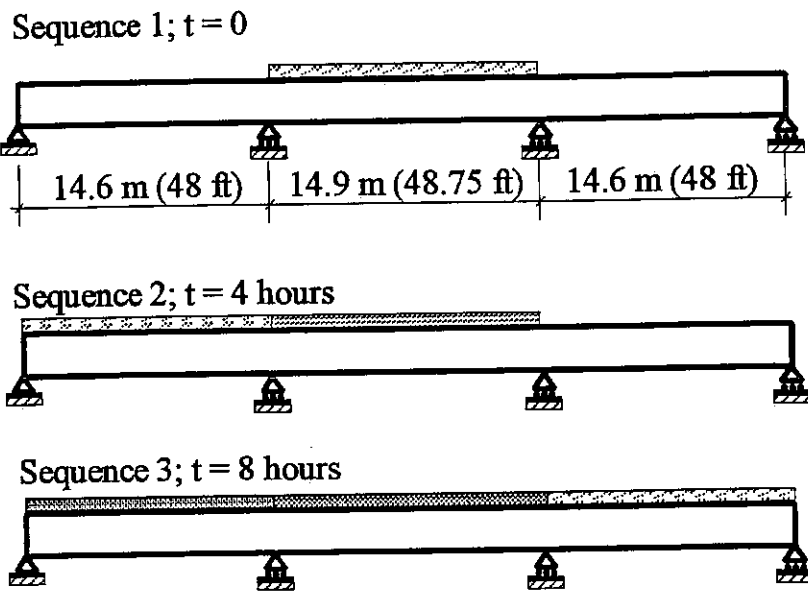


Figure C.14 Sequence of pour for bridge OT-3 Case "c"

AL 2 - a

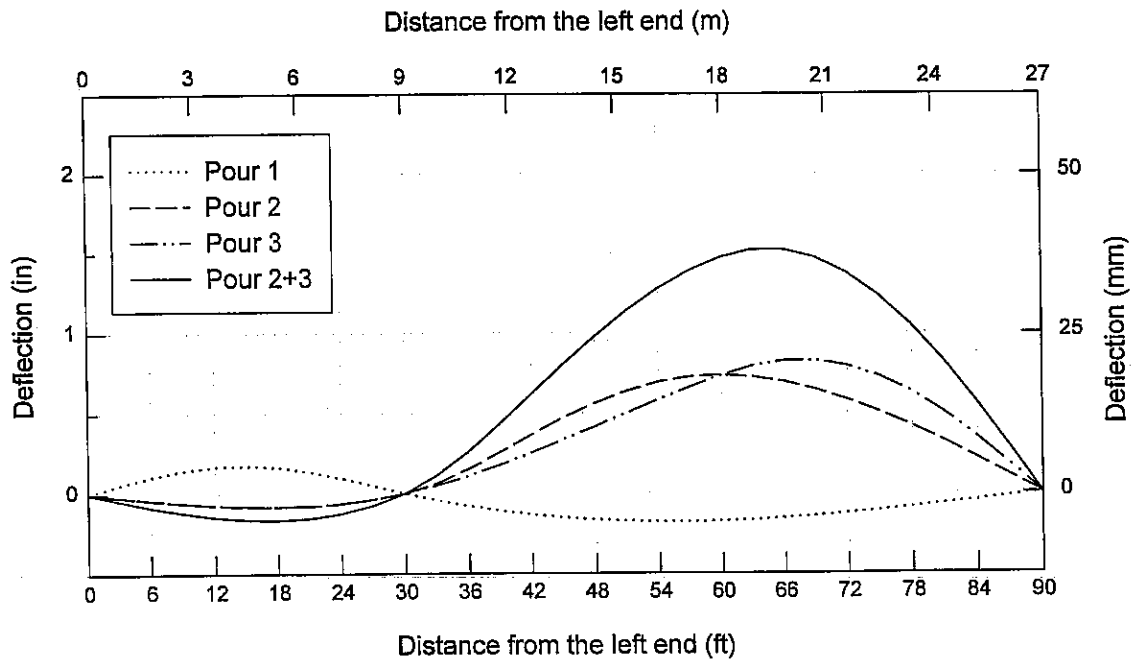
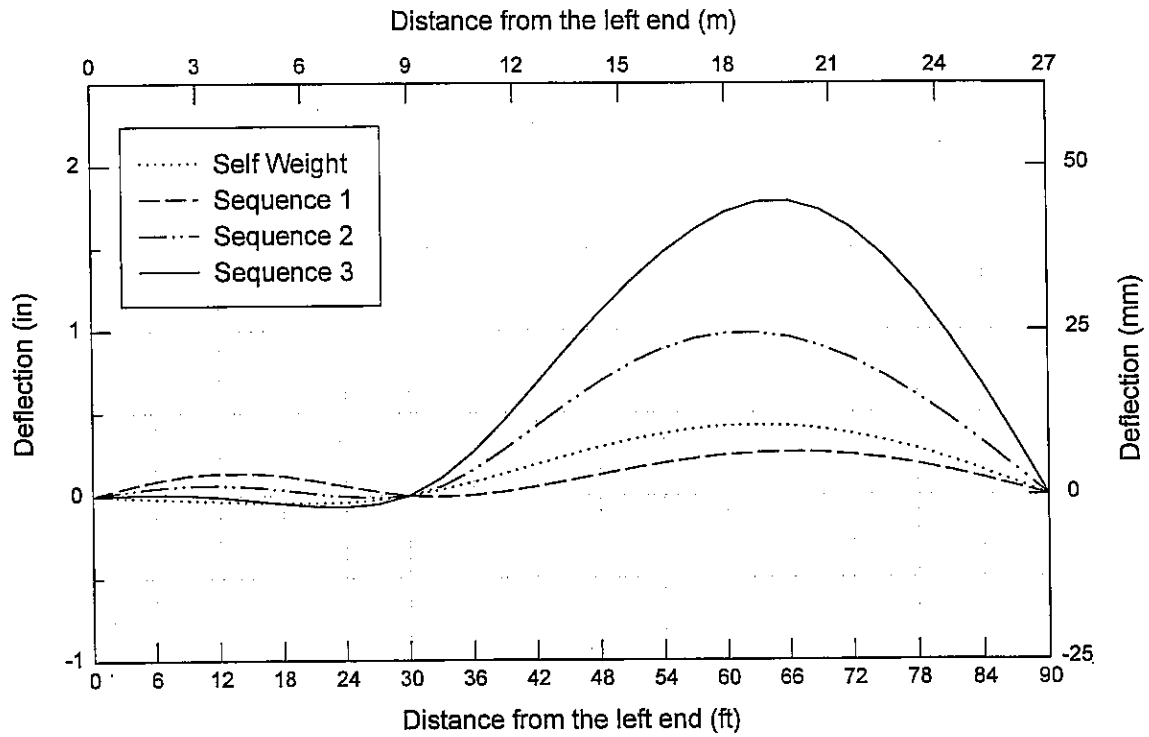


Figure C.15 Bridge AL-2 deflections for sequence of pour Case "a"

AL 2 - a

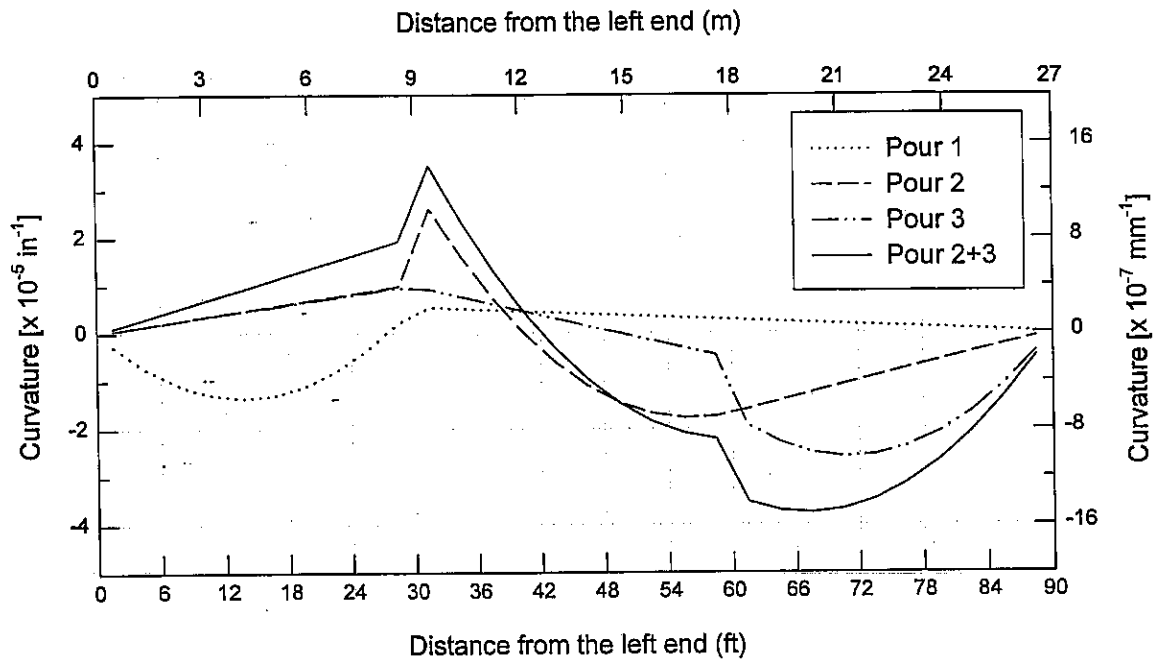
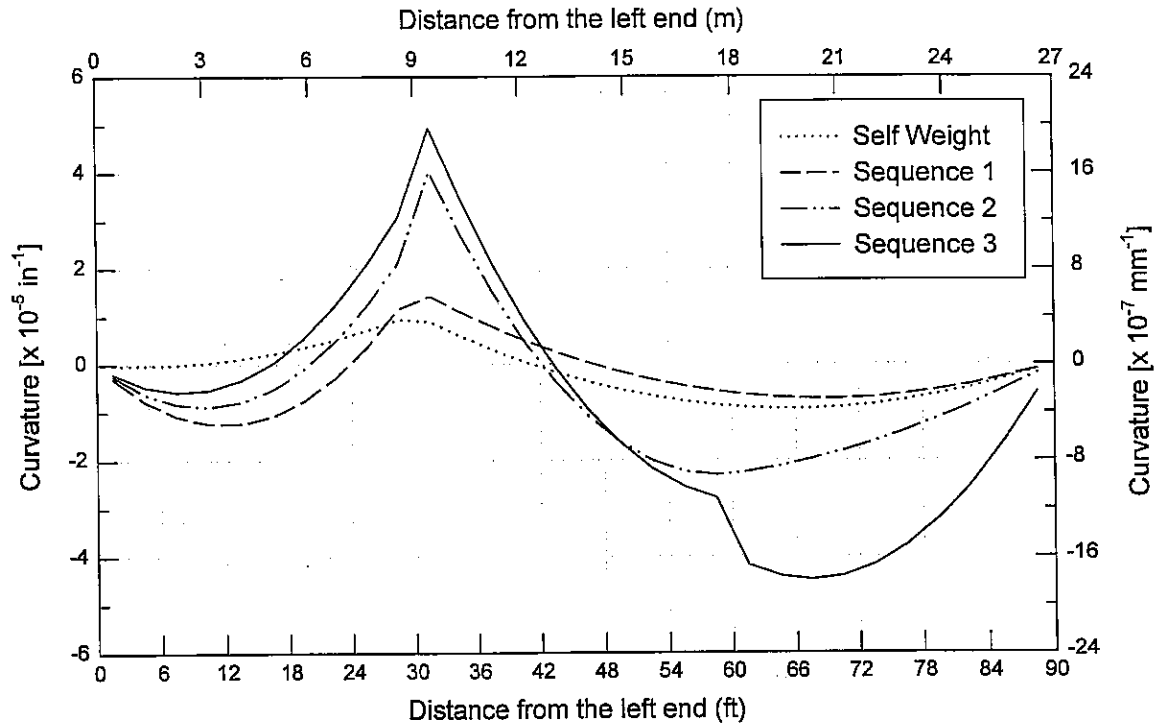
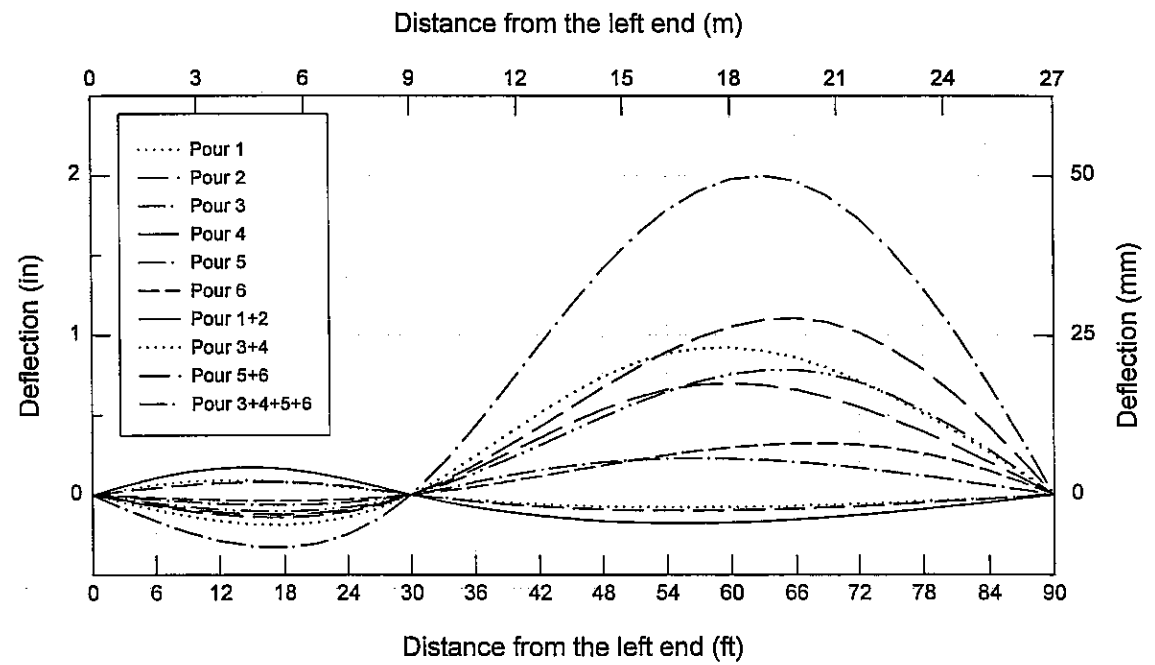
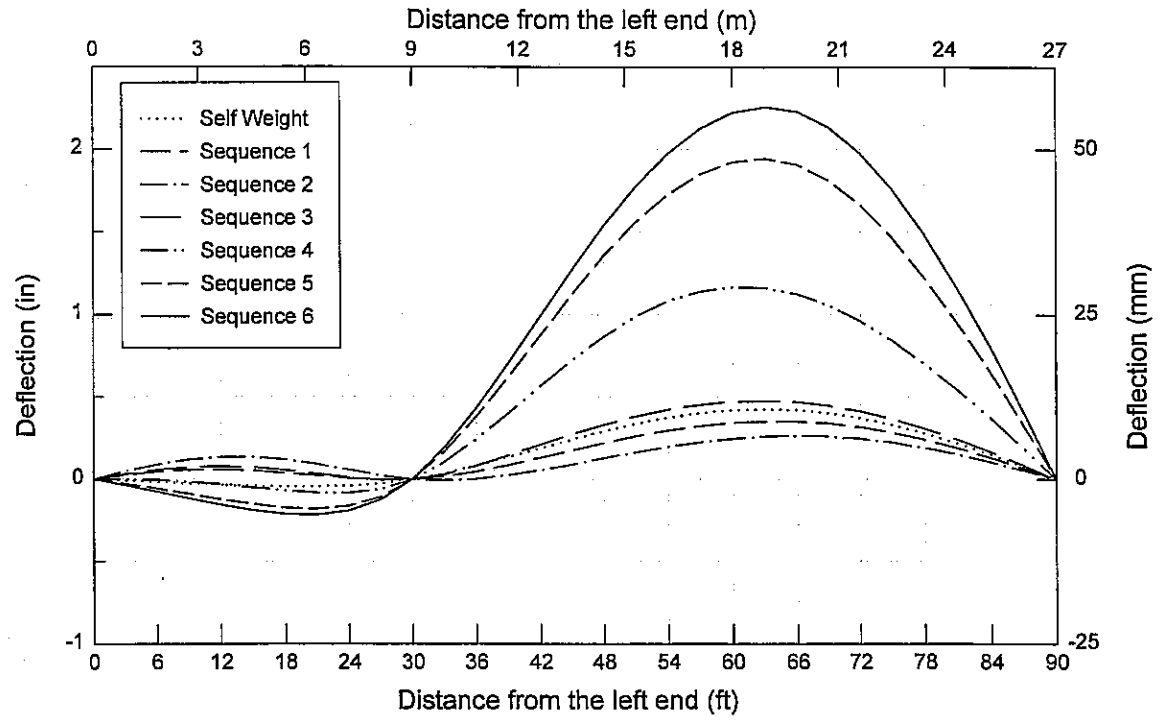


Figure C.16 Bridge AL-2 curvatures for sequence of pour Case "a"

AL 2 - aa



F

Figure C.17 Bridge AL-2 deflections for sequence of pour Case "aa"

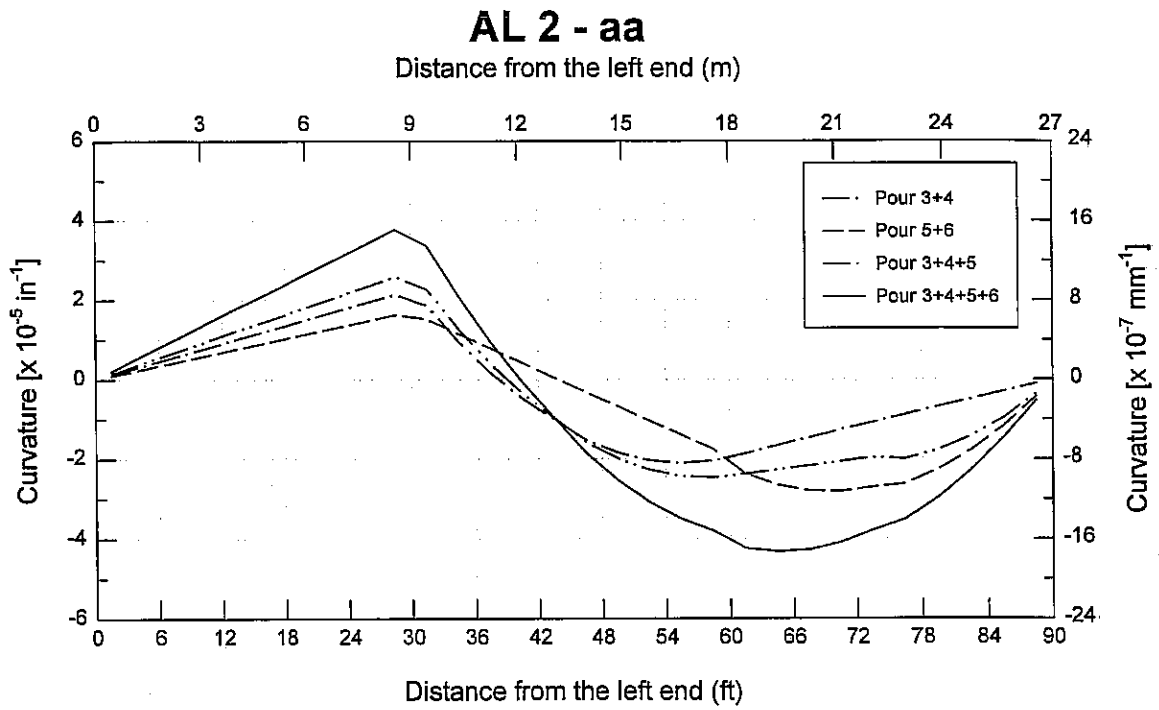


Figure C.19 Bridge AL-2 curvatures for sequence of pour Case "aa", last two sequences

AL 2 - b

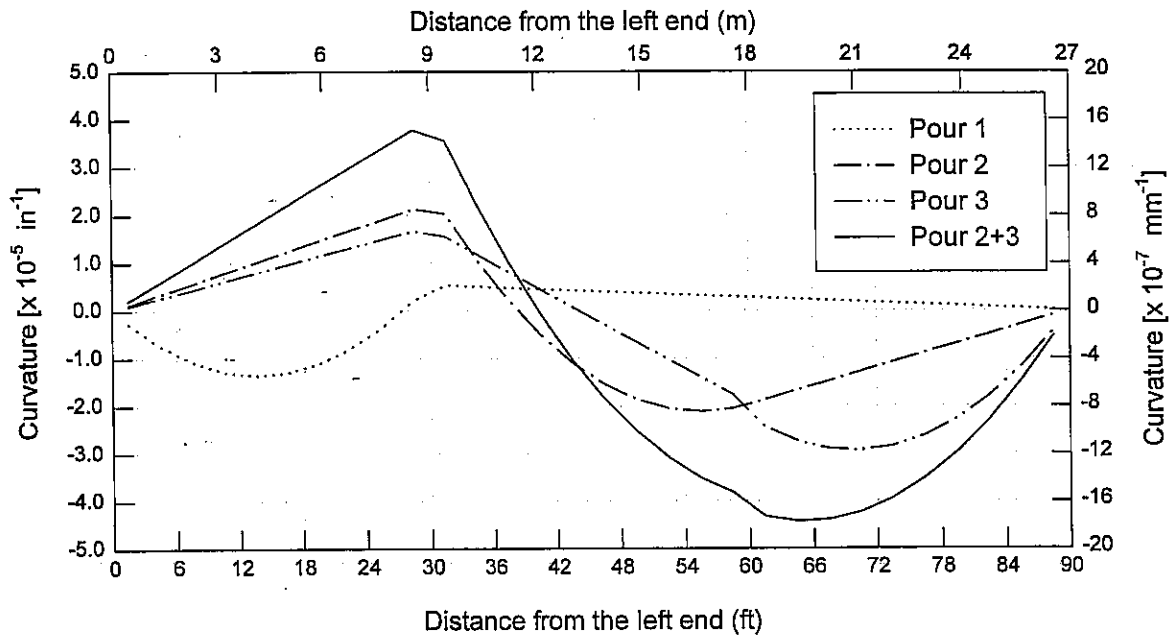
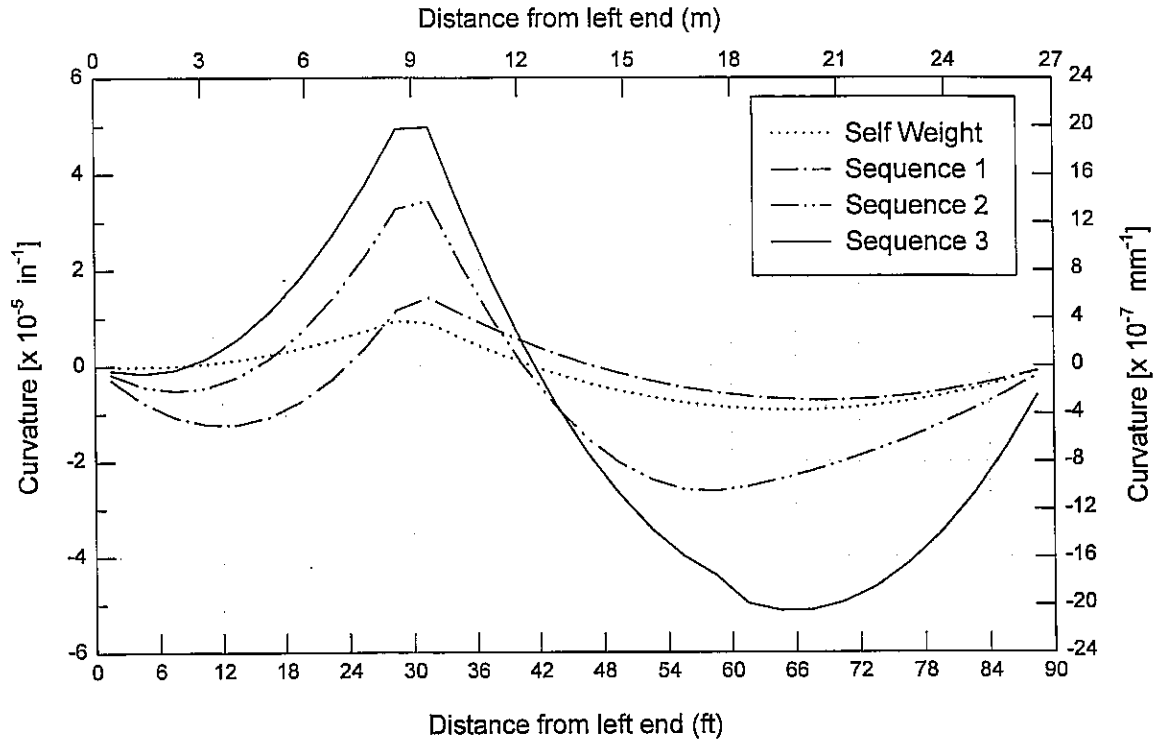


Figure C.20 Bridge AL-2 curvatures for sequence of pour Case "b"

AL 2 - c

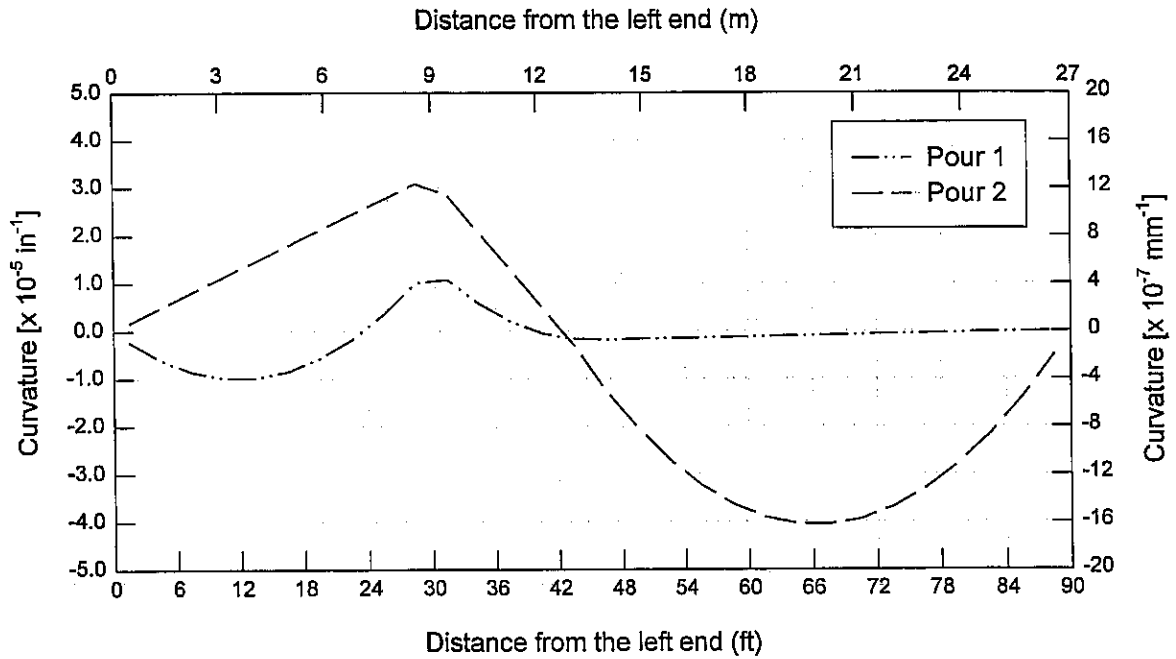
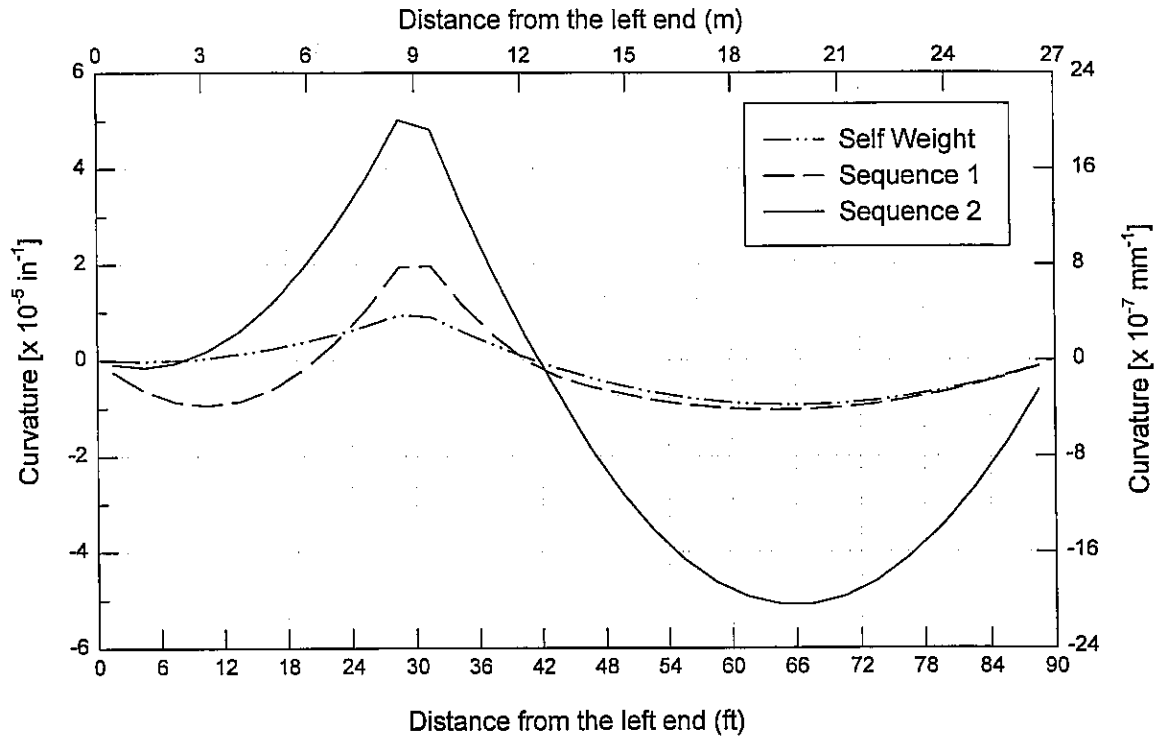


Figure C.21 Bridge AL-2 curvatures for sequence of pour Case "c"

AL 2 - cc

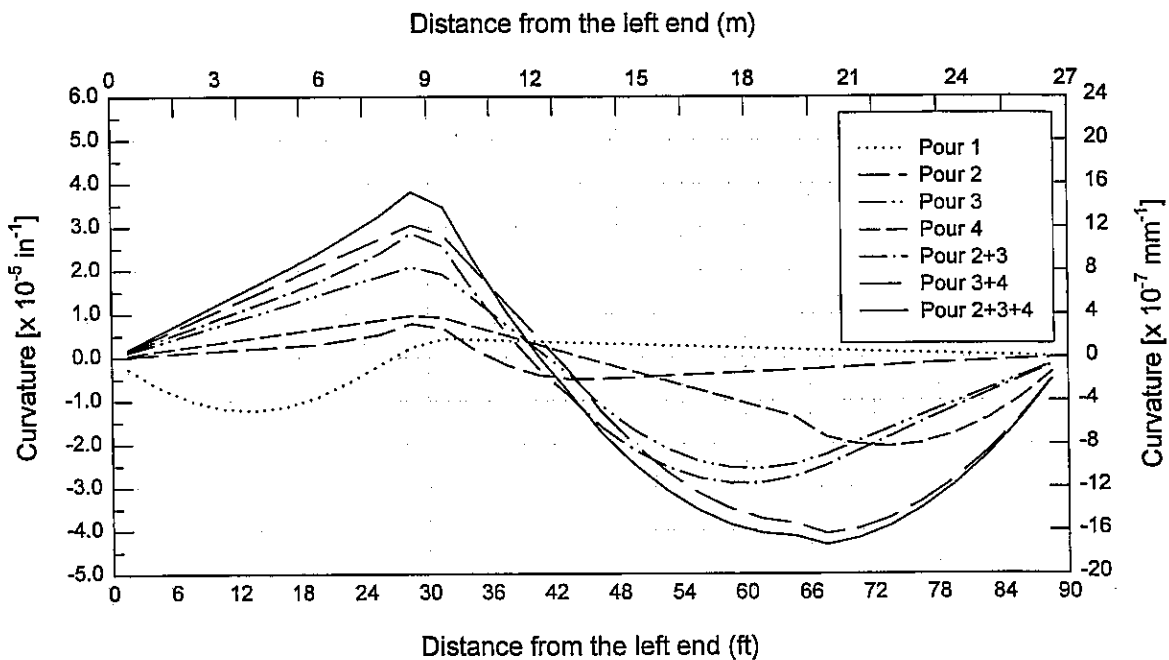
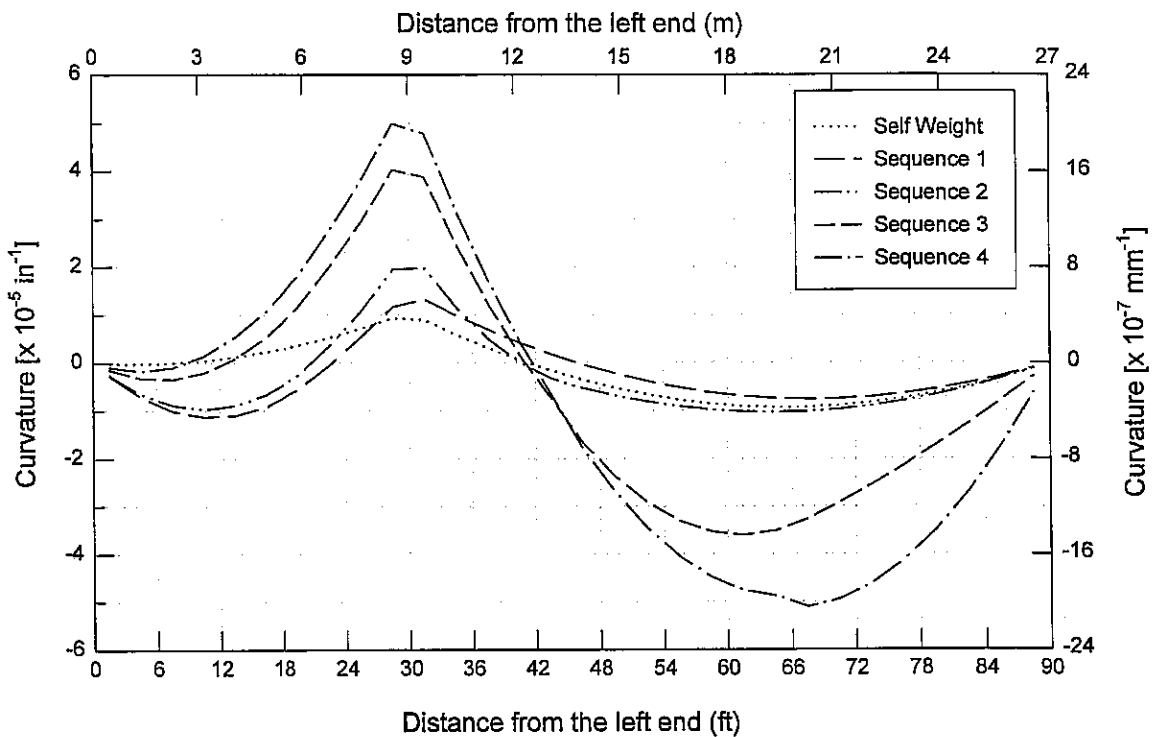


Figure C.22 Bridge AL-2 curvatures for sequence of pour Case "cc"

AL 2 - d

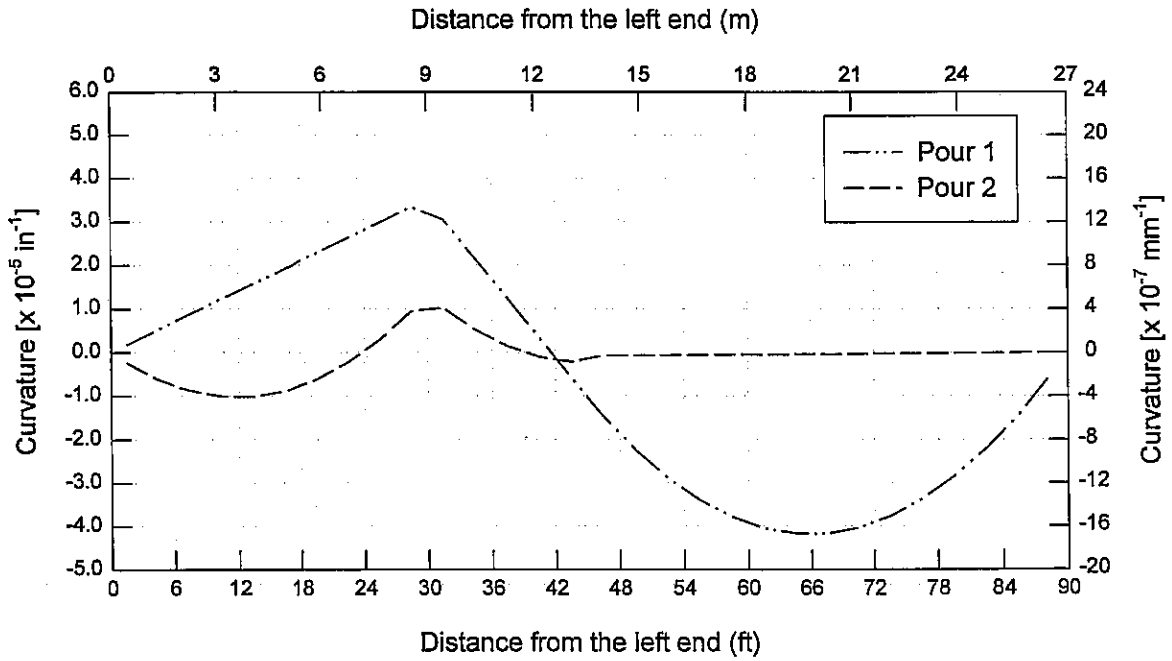
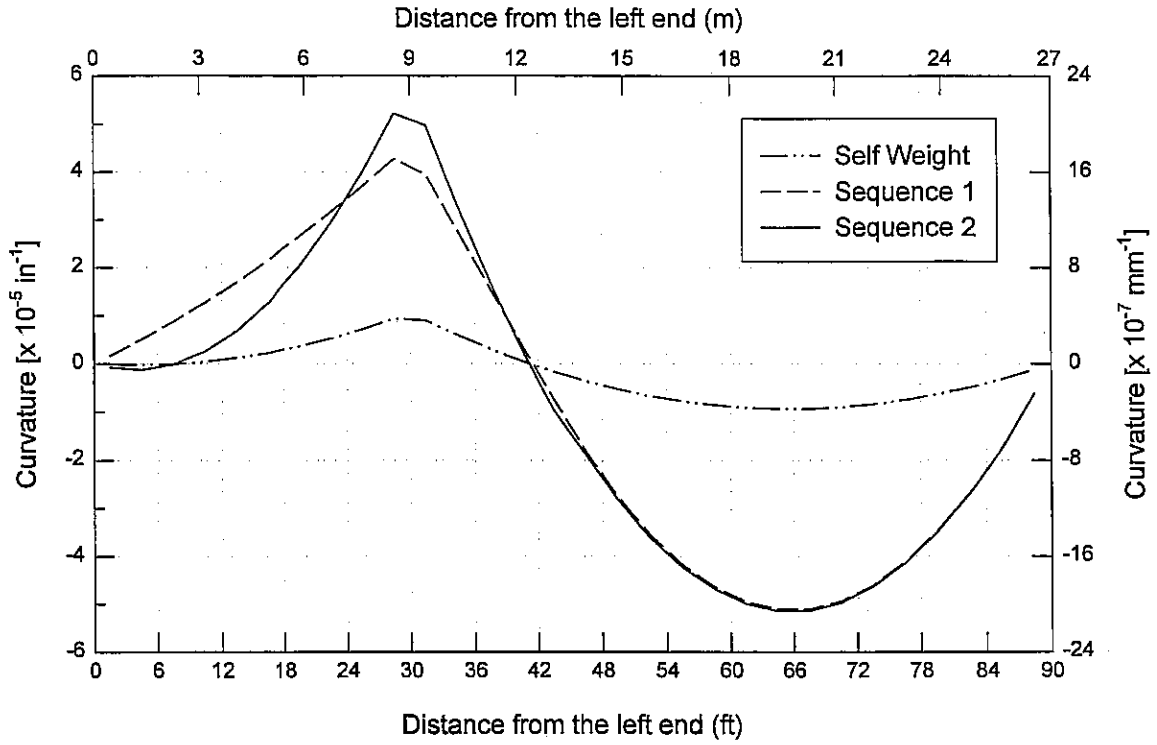


Figure C.23 Bridge AL-2 curvatures for sequence of pour Case "d"

SYMBOLS USED IN FIGURES C.24 TO C.25

A_{bm}	Beam area
$A_{tr}(t)$	Area of transformed concrete slab at time t
A_{sl}	Effective area of concrete slab
$A_{sl}(t)$	Effective area of concrete slab at time t
b_{tr}	Width of transformed concrete slab at time t
b_{sl}	Width of concrete slab
$b_{sl}(t)$	Width of concrete slab at time t
$cg_{sl} - cg_{bm}$	Distance between concrete slab and beam center of gravity
E_{bm}	Beam modulus of elasticity
$E_c(t)$	Concrete modulus of elasticity at time t
f_{sl}'	Nominal concrete compressive strength
$f_{sl}'(t)$	Nominal concrete compressive strength at time t
I_{bm}	Beam moment of inertia
I_{sl}	Moment of inertia of concrete slab
$I_{sl}(t)$	Moment of inertia of concrete slab at time t
$I_{tr}(t)$	Moment of inertia of transformed concrete slab at time t
γ_{bm}	Specific gravity of beam
γ_{sl}	Specific gravity of concrete slab

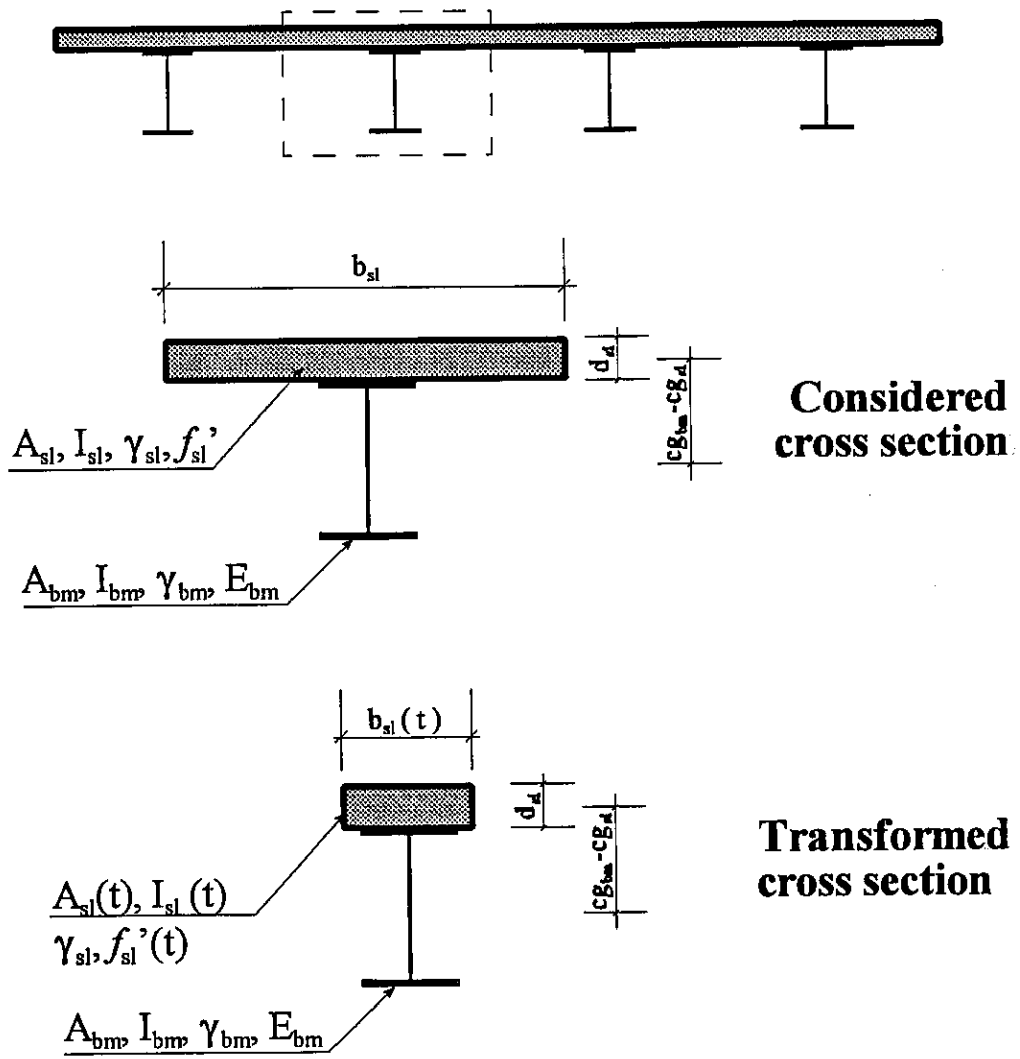


Figure C.24 Typical cross section

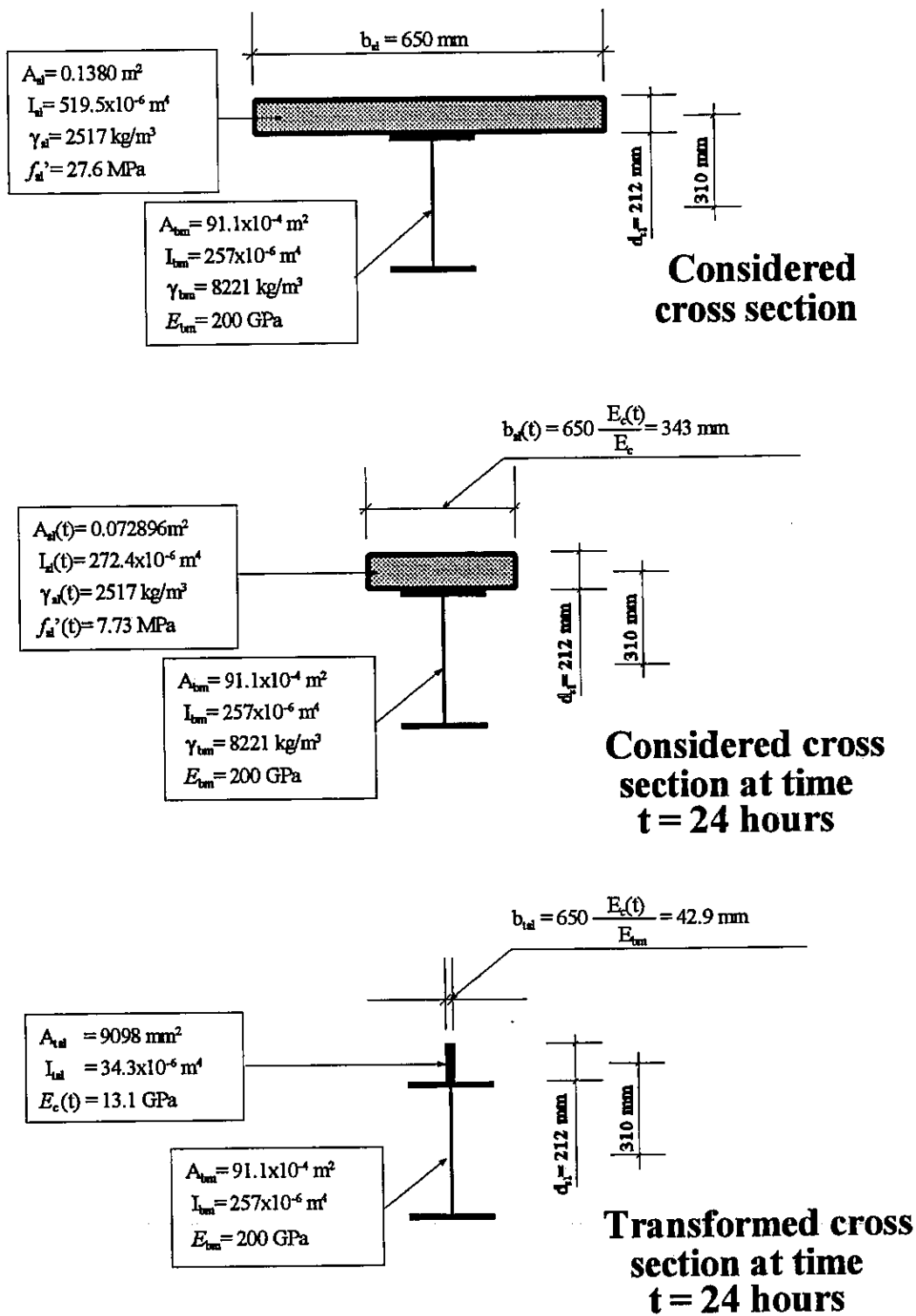
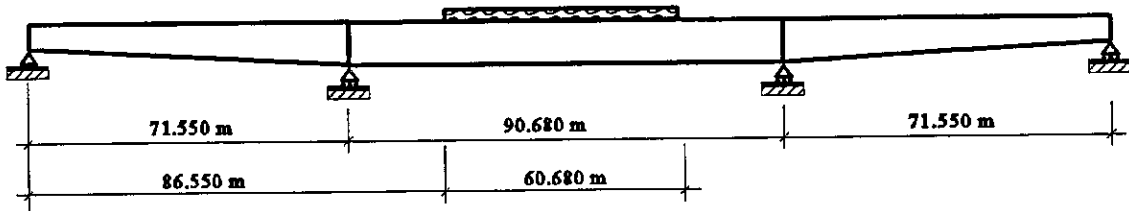
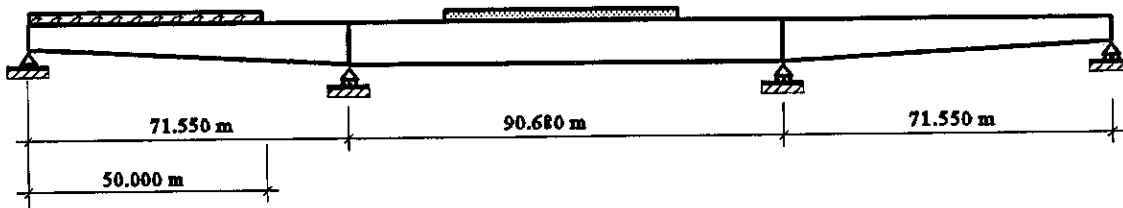


Figure C.25 Cross section for bridge Al-2

Sequence 1; t = 0



Sequence 2; t = 6



Sequence 3; t = 72

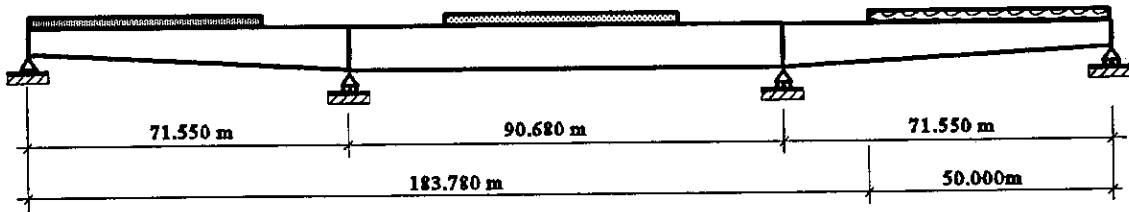
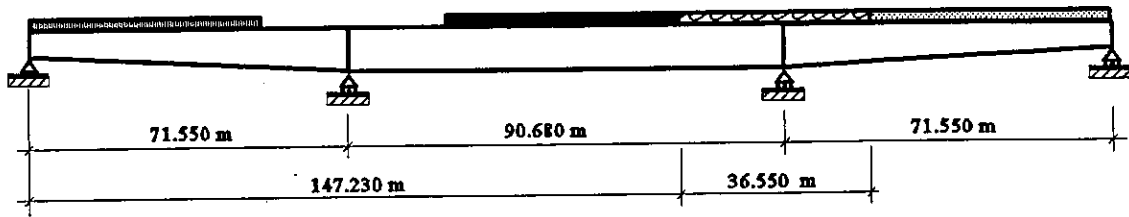


Figure C.26 Three span steel bridge - span sections cast prior to support sections

Sequence 4; t = 76



Sequence 5; t = 80

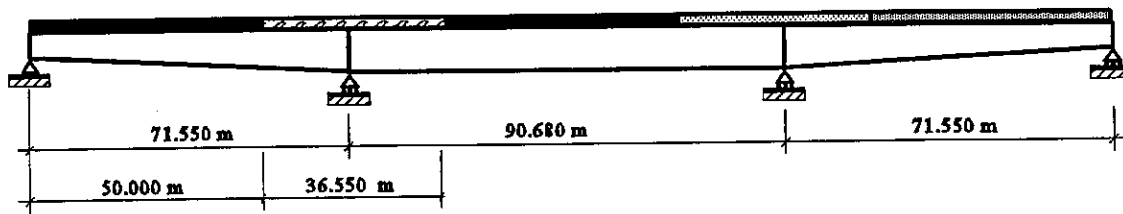


Figure C.27 Three span steel bridge - span sections cast prior to support sections (continued)

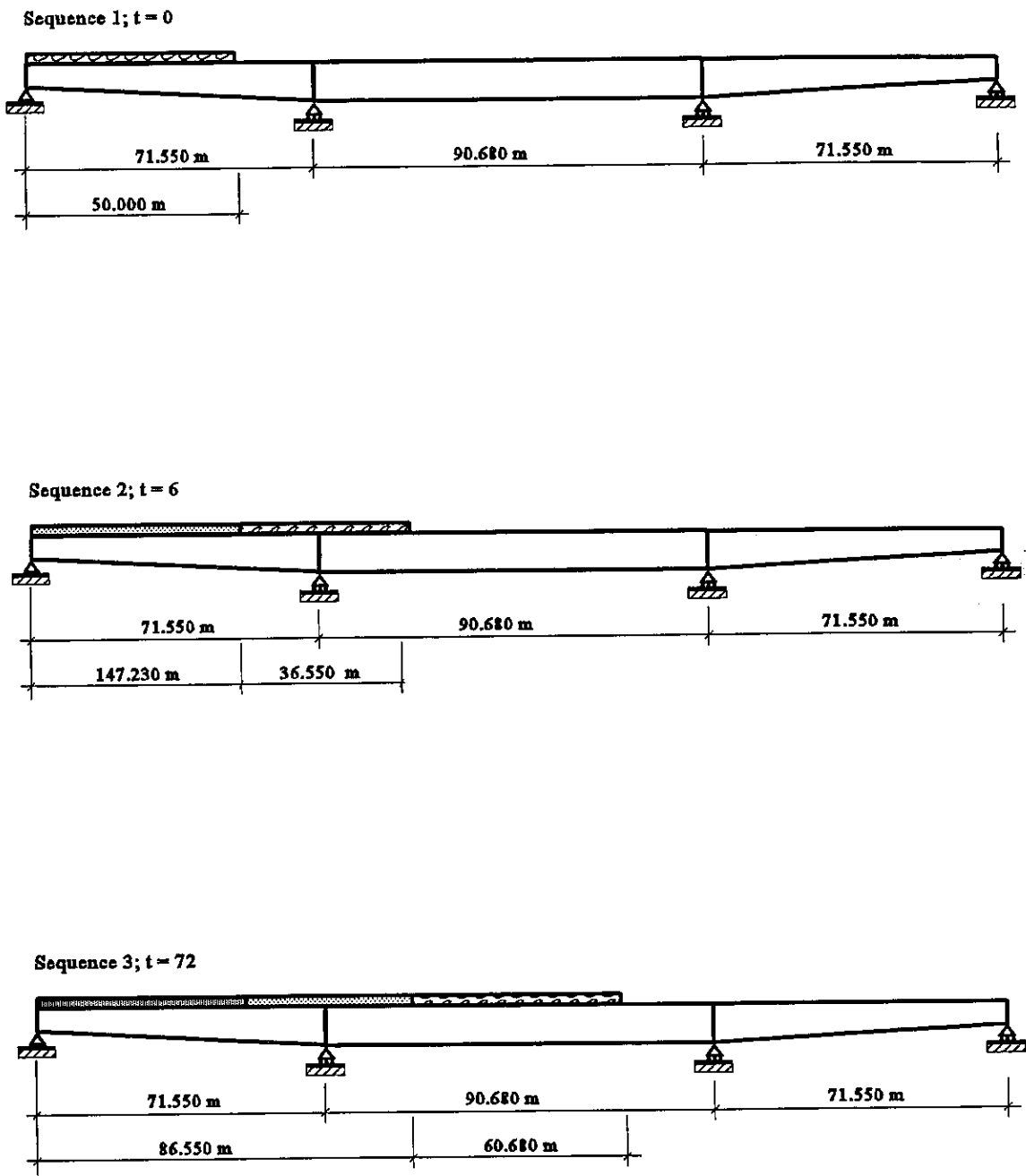
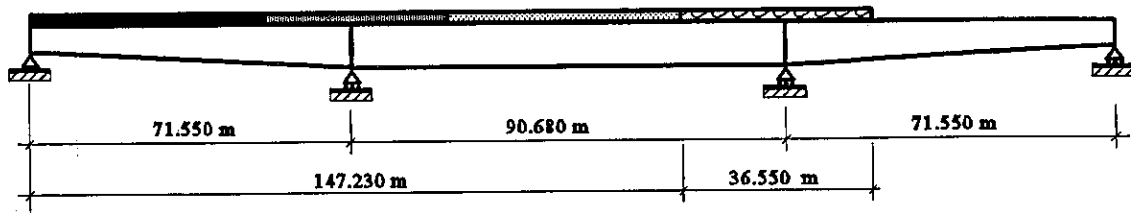


Figure C.28 Three span steel bridge - slab cast from the left end sections

Sequence 4; t = 76



Sequence 5; t = 80

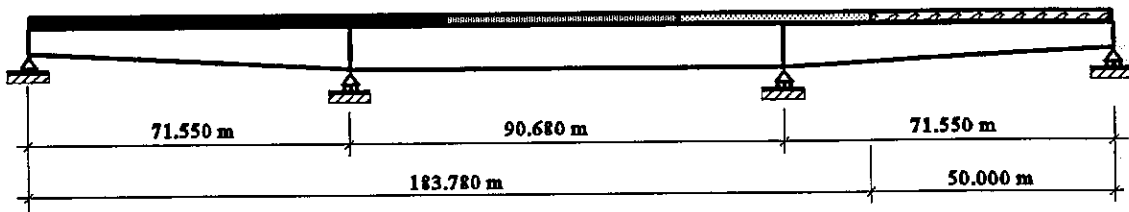
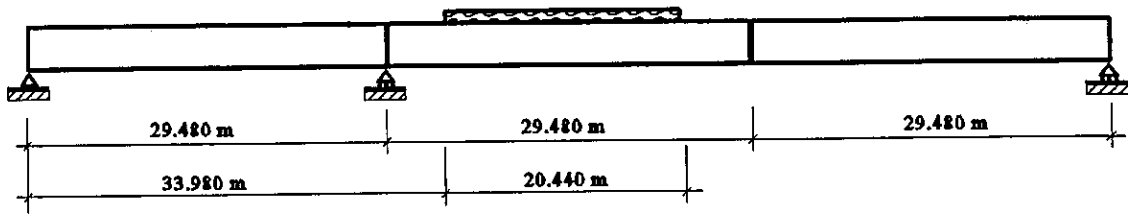
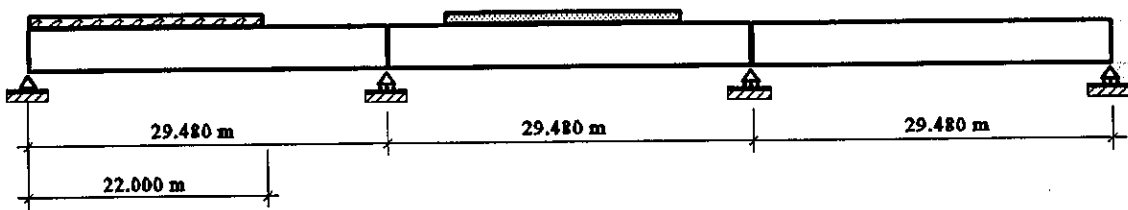


Figure C.29 Three span steel bridge - slab cast from the left end sections (continued)

Sequence 1; $t = 0$



Sequence 2; $t = 6$



Sequence 3; $t = 72$

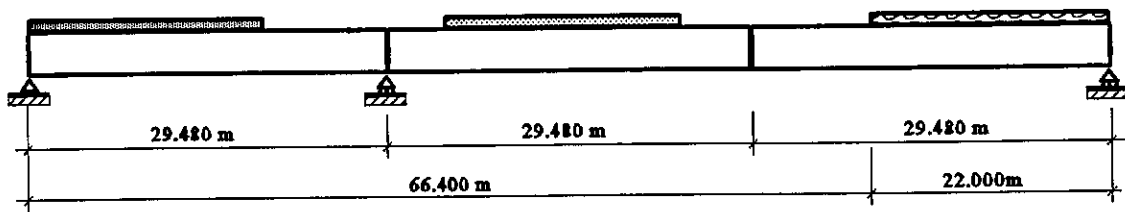
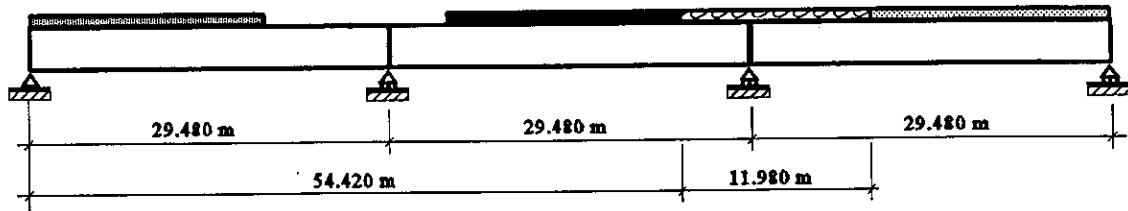


Figure C.30 Three span prestressed concrete bridge - span sections cast prior to support sections

Sequence 4; t = 76



Sequence 5; t = 80

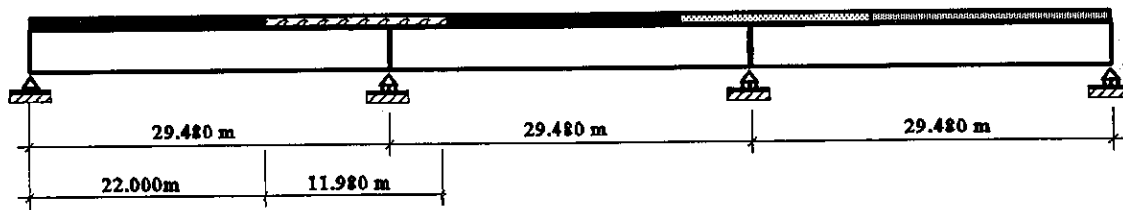
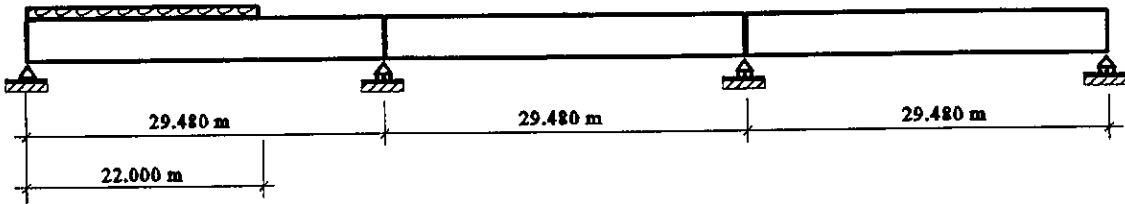
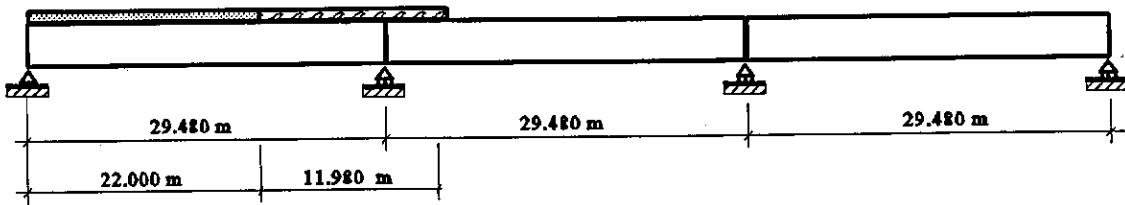


Figure C.31 Three span prestressed concrete bridge - span sections cast prior to support sections
(continued)

Sequence 1; t = 0



Sequence 2; t = 6



Sequence 3; t = 72

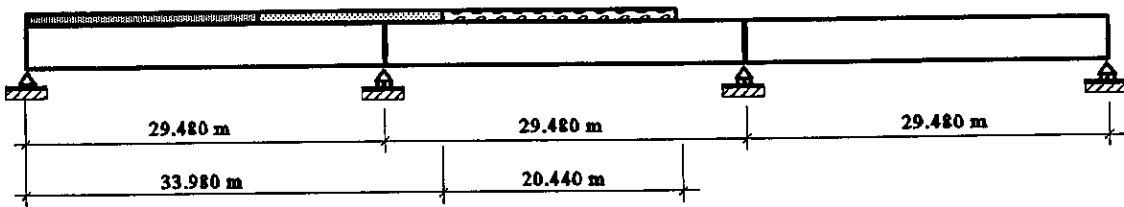
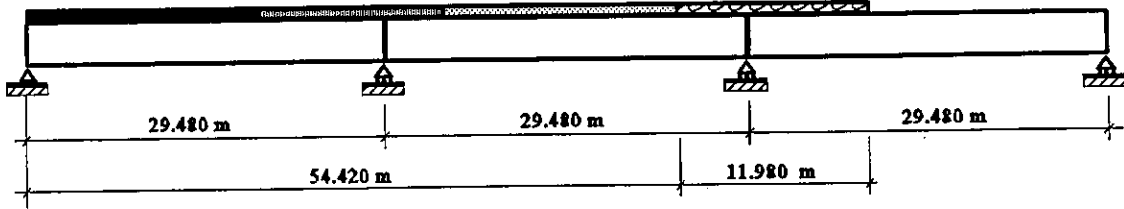


Figure C.32 Three span prestressed concrete bridge - slab cast from the left end sections

Sequence 4; t = 76



Sequence 5; t = 144

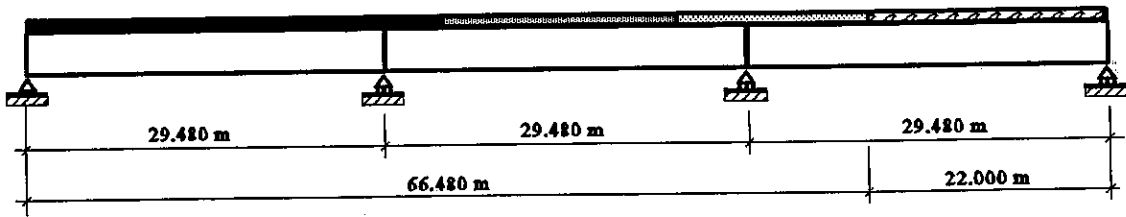


Figure C.33 Three span prestressed concrete bridge - slab cast from the left end sections (continued)

Three Span Steel Bridge Spans cast prior to supports

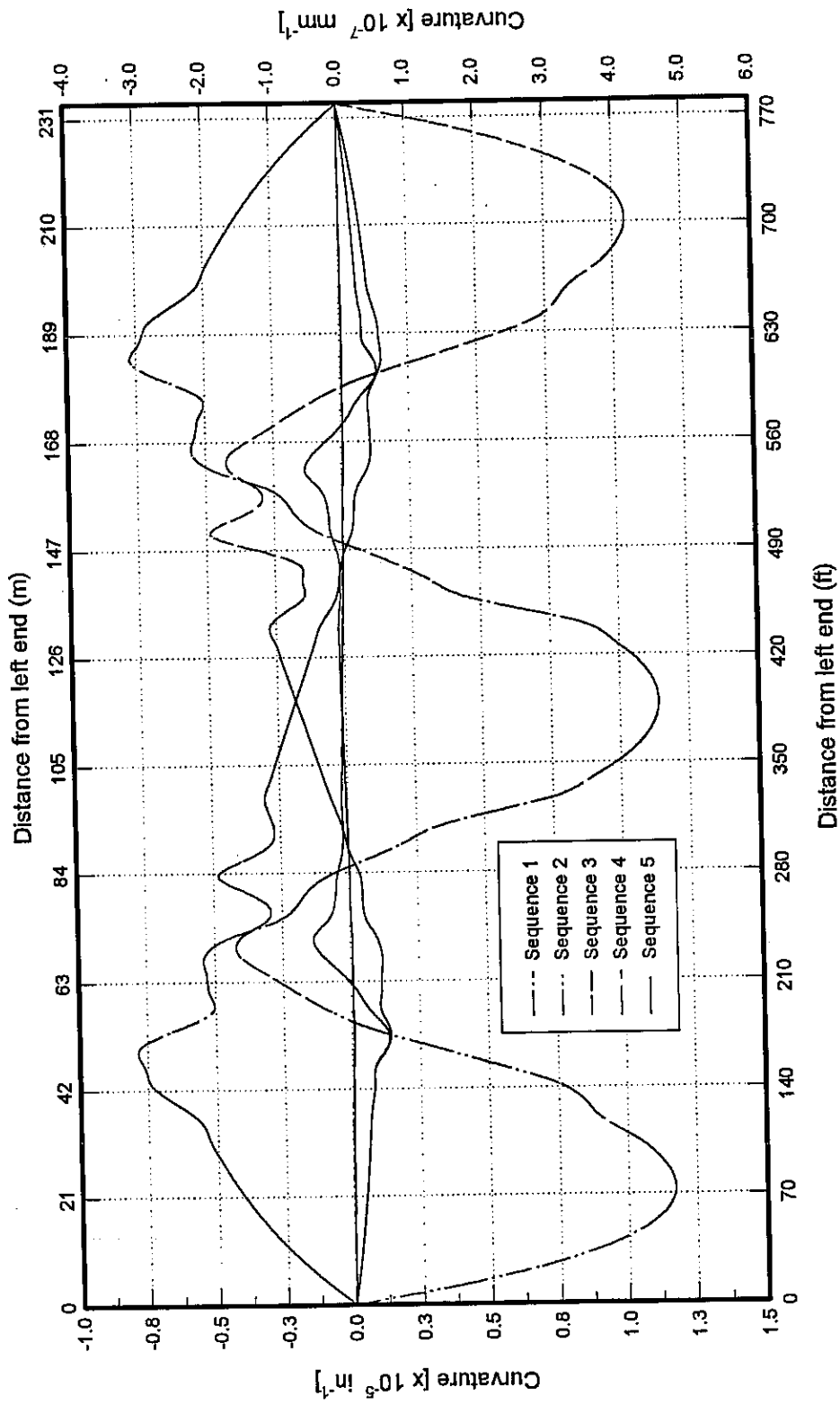


Figure C.34

Three Span Steel Bridge

Spans cast prior to supports

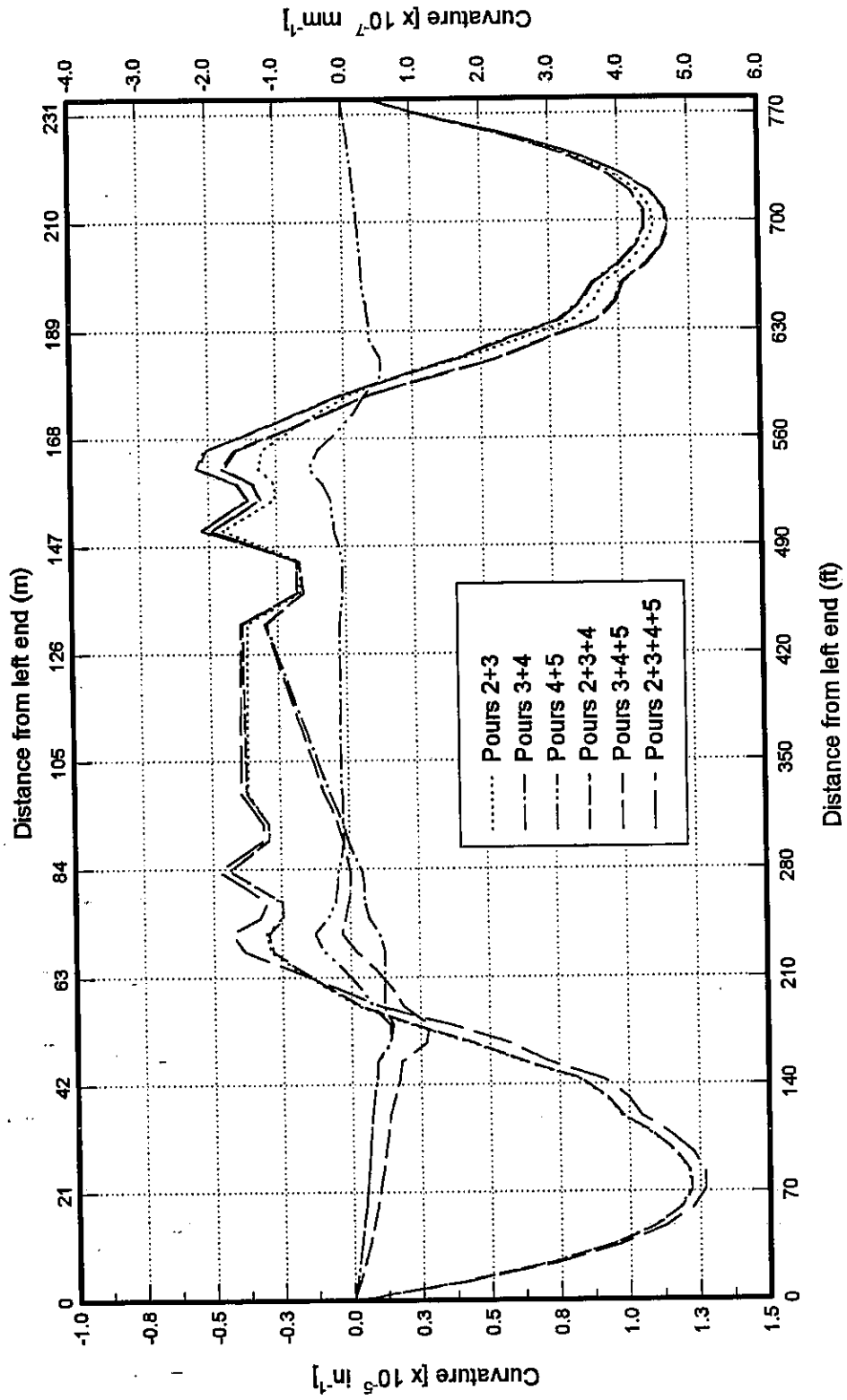


Figure C.35

Three Span Steel Bridge

Slab cast from the left end

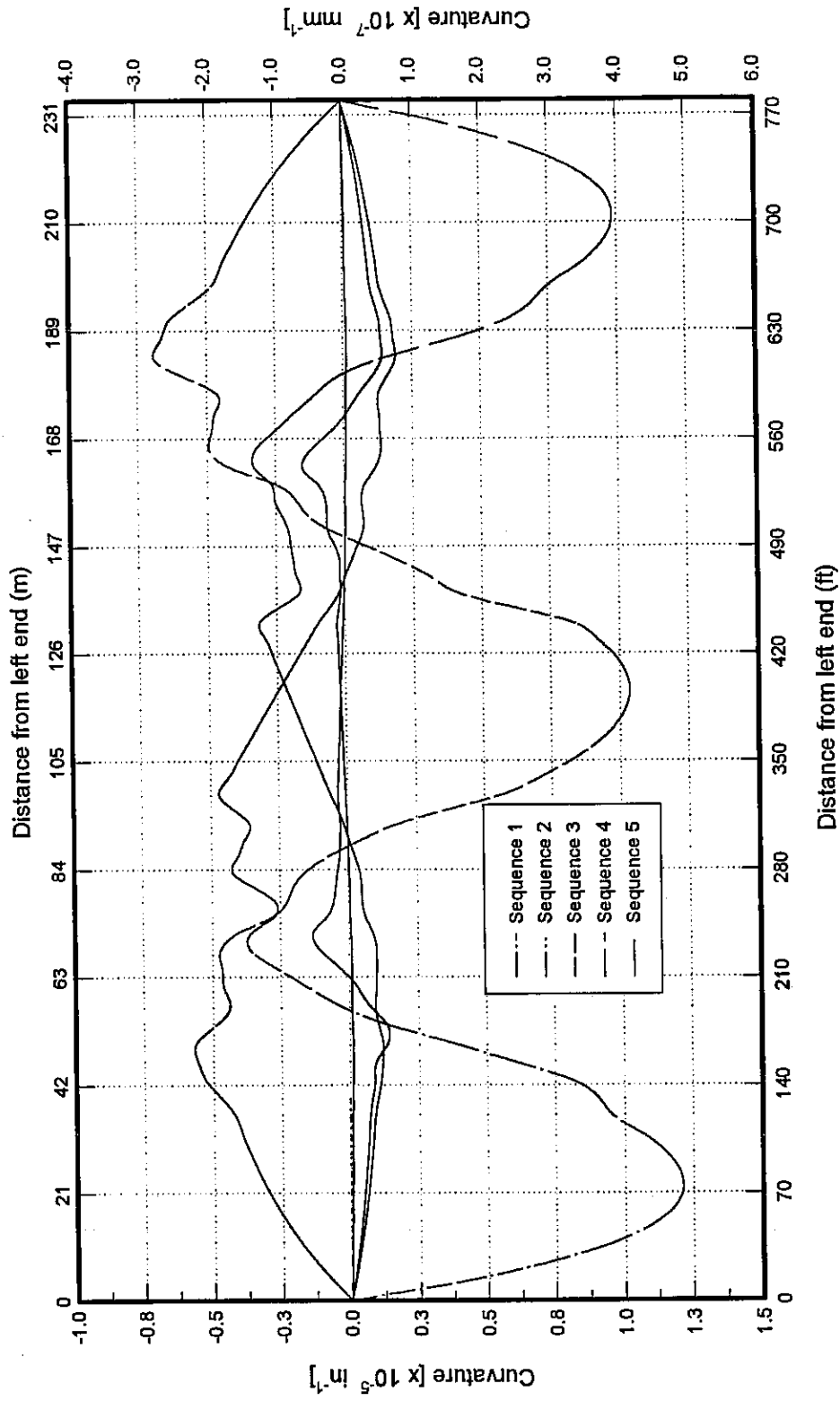


Figure C.36

Three Span Steel Bridge

Slab cast from the left end

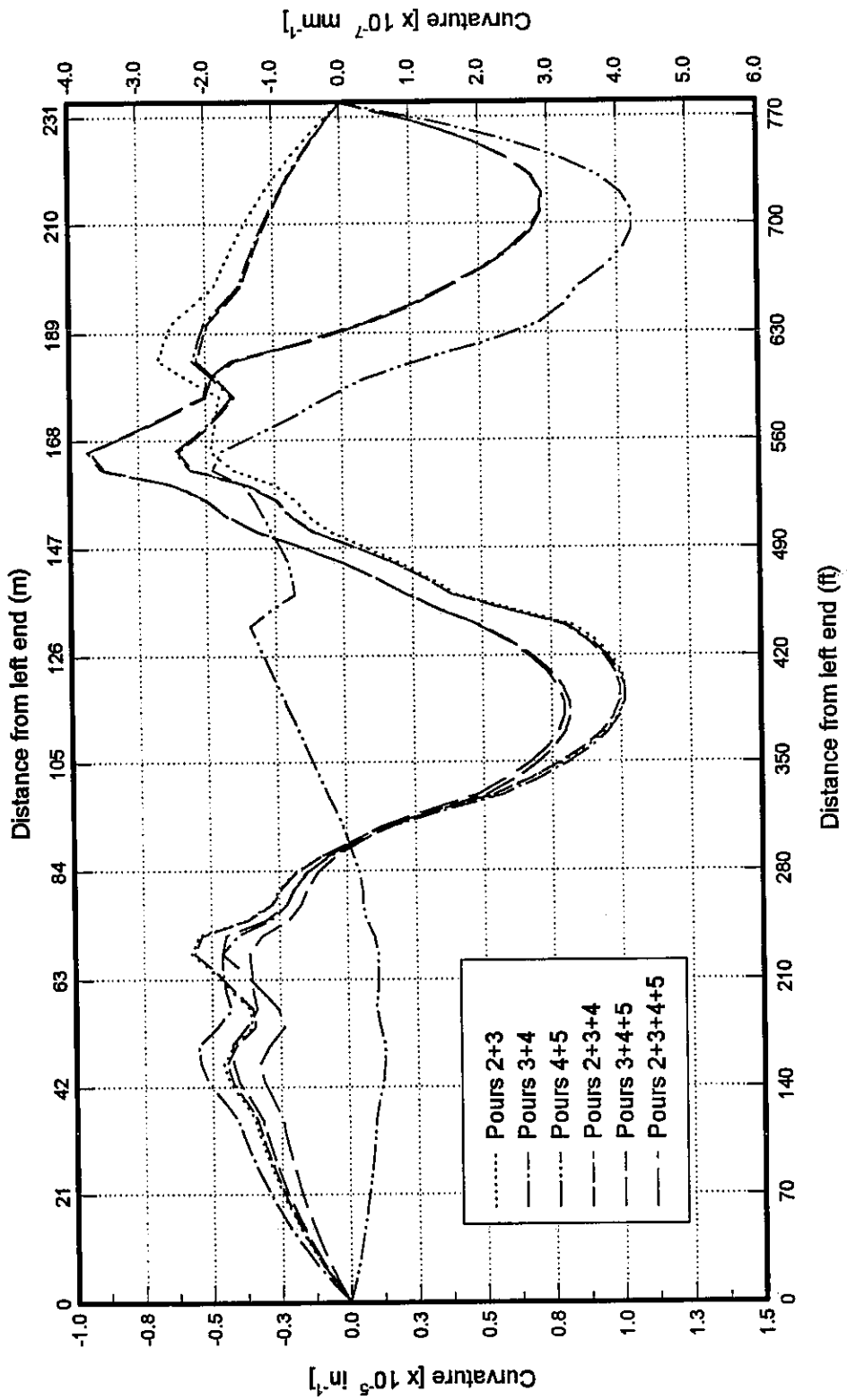


Figure C.37

Three Span Prestressed Concrete Bridge

Spans cast prior to supports

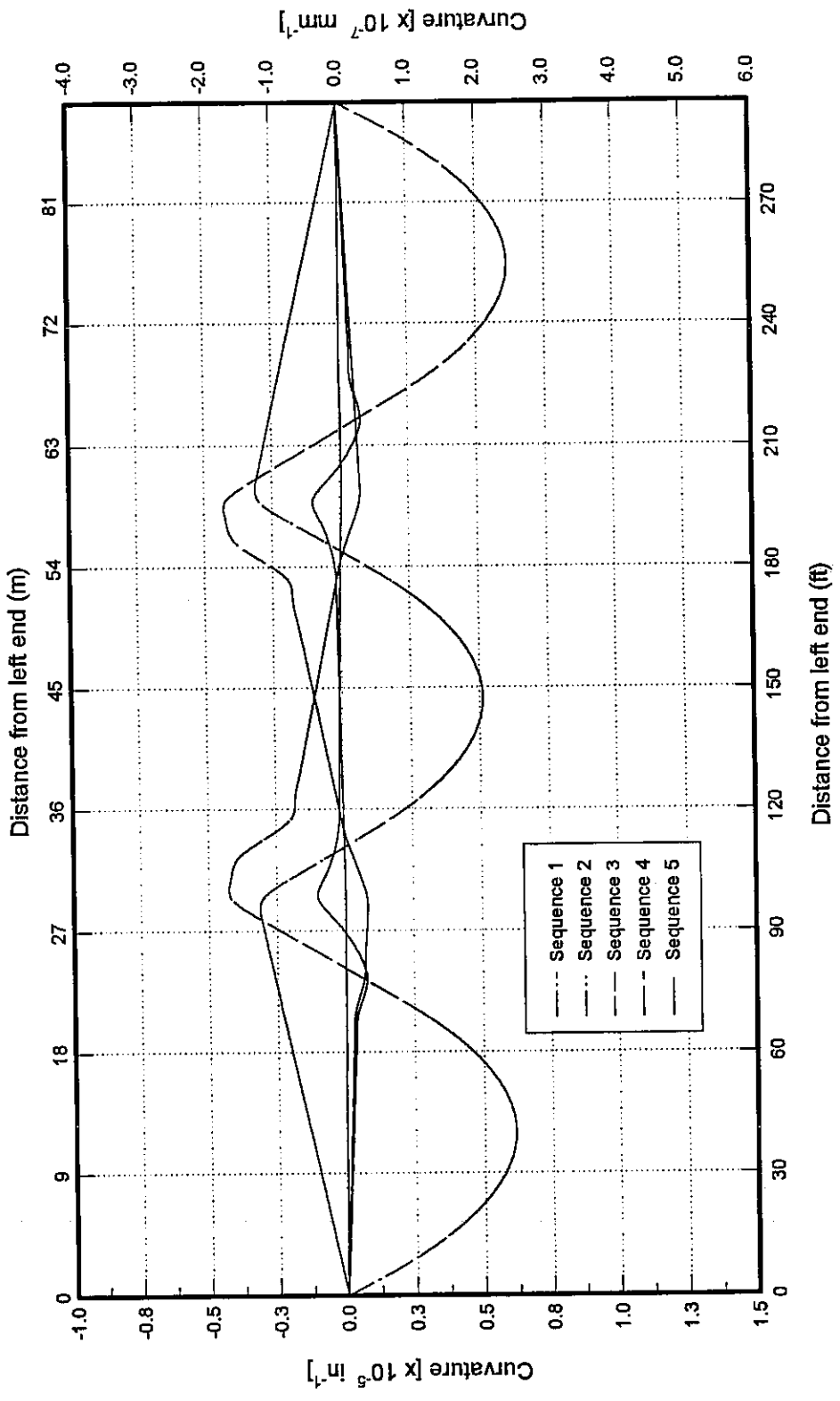


Figure C.38

Three Span Prestressed Concrete Bridge

Spans cast prior to supports

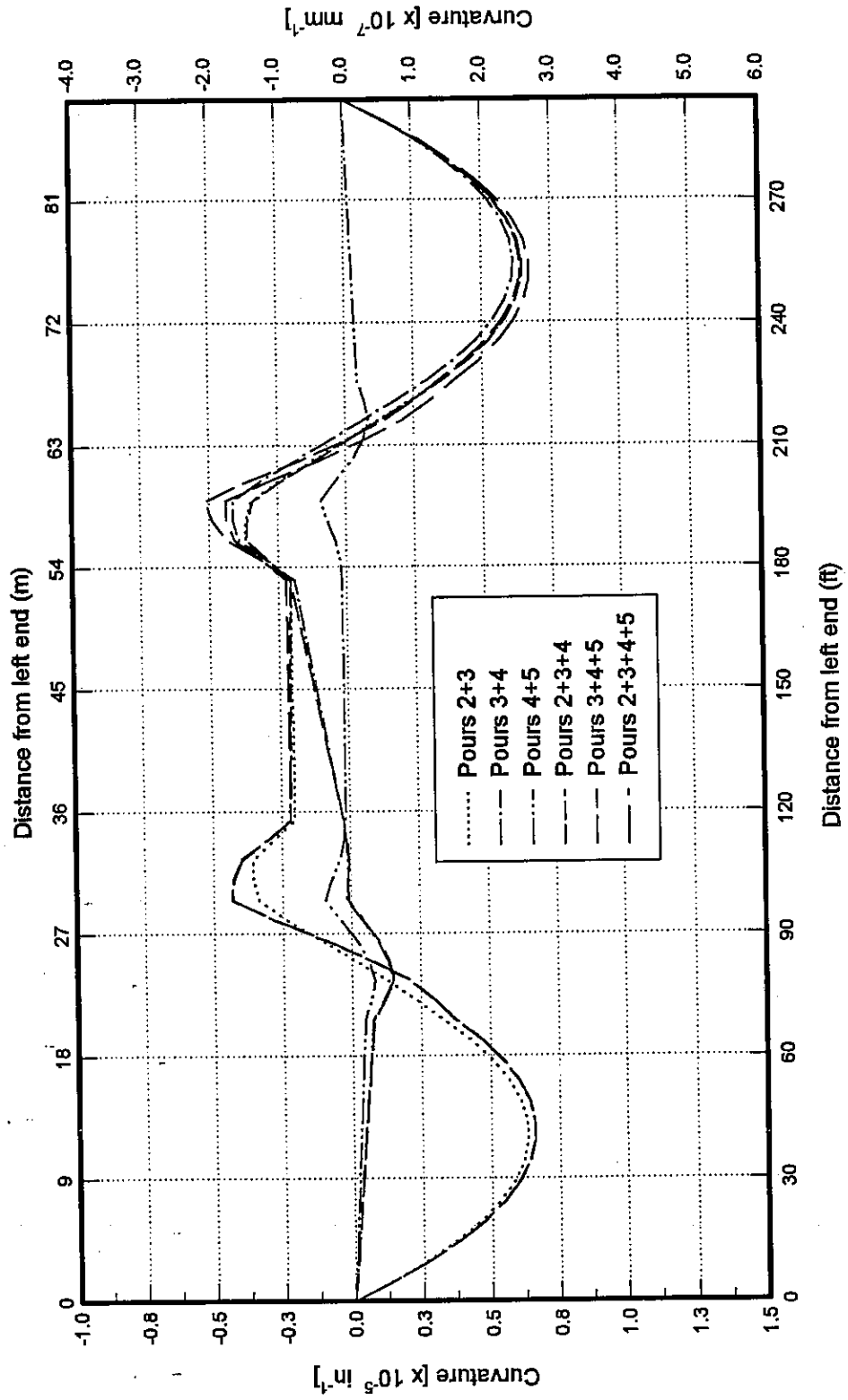


Figure C.39

Three Span Prestressed Concrete Bridge

Slab cast from the left end

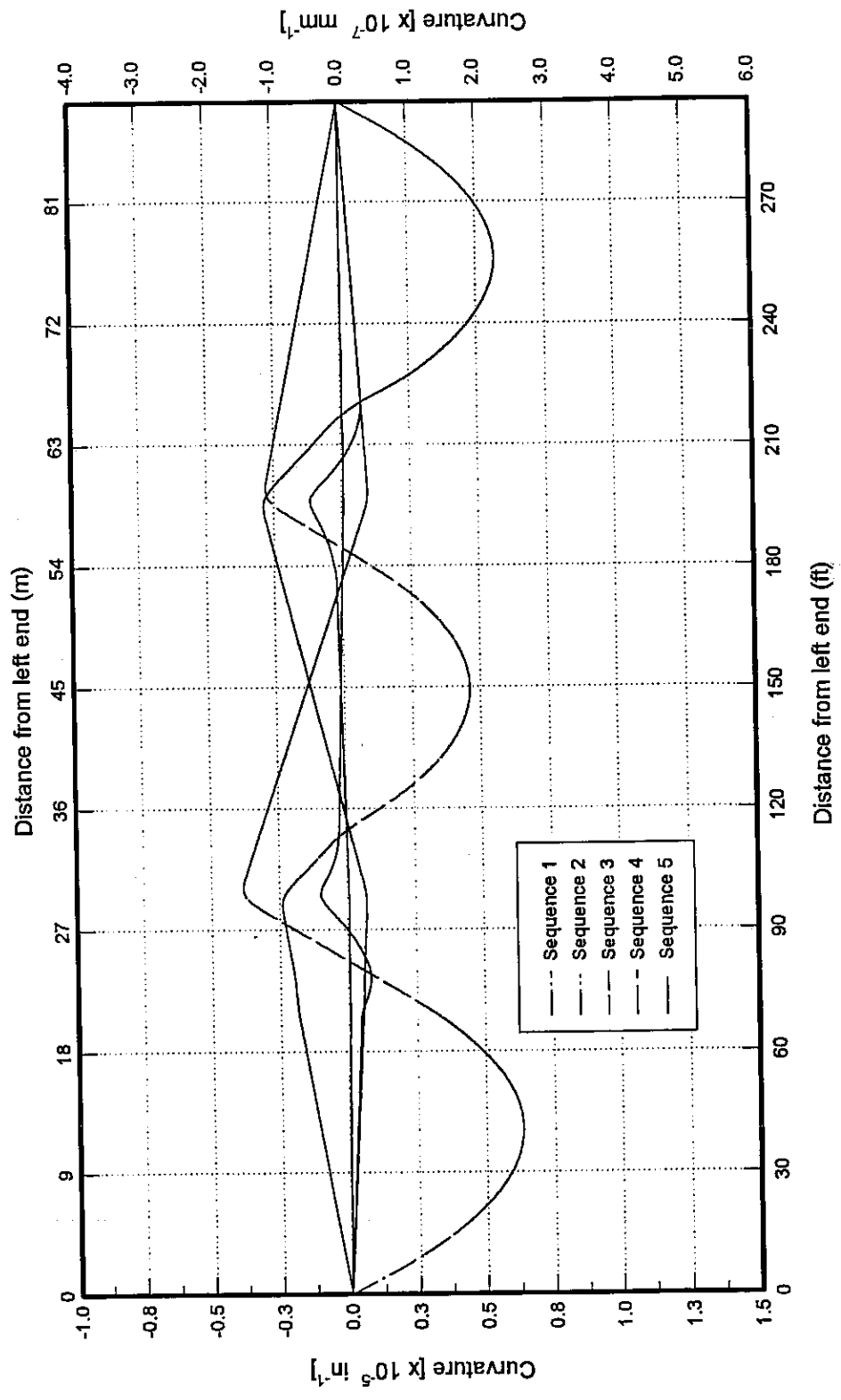


Figure C.40

Three Span Prestressed Concrete Bridge

Slab cast from the left end

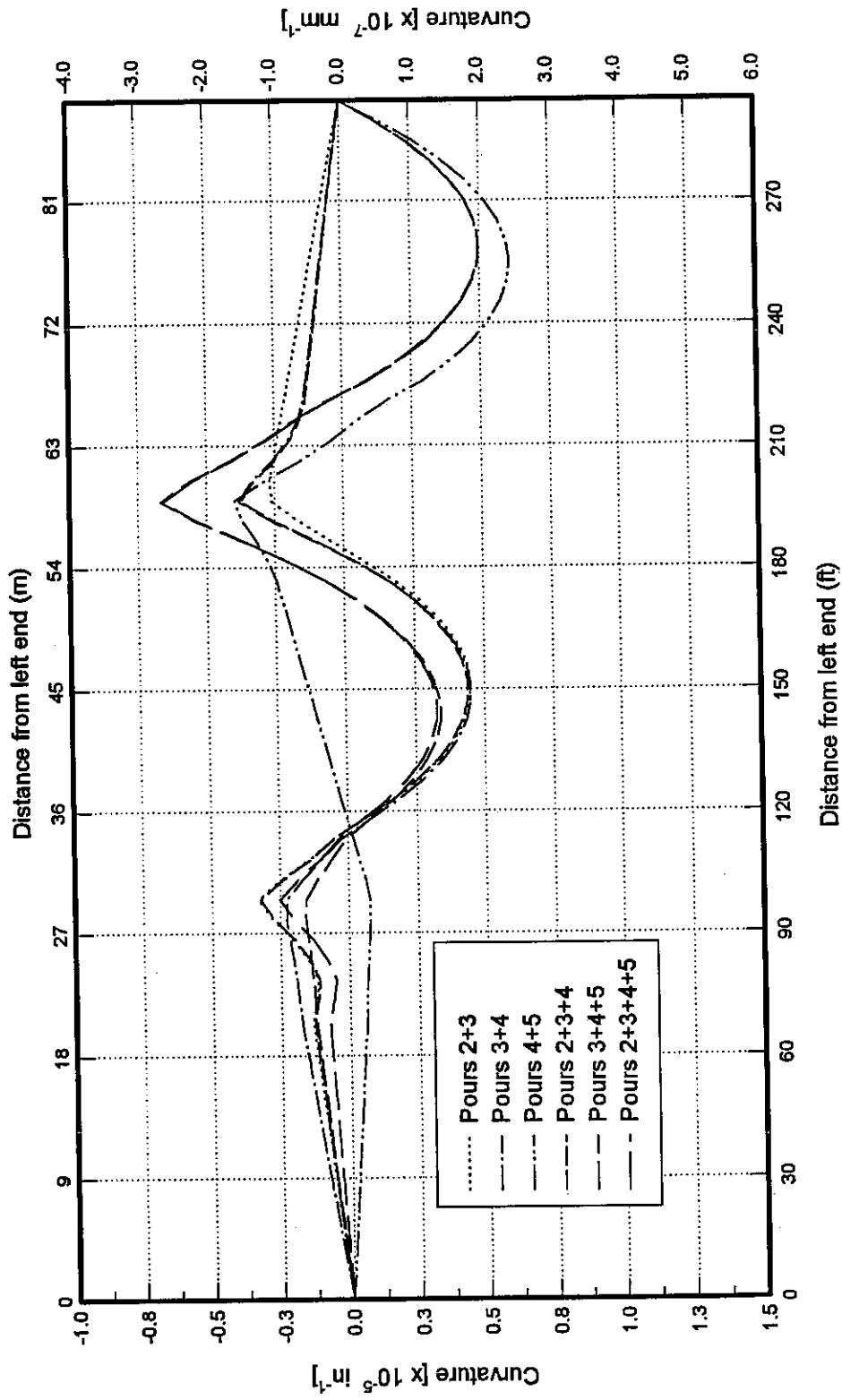


Figure C.41

```

CCCCCCCCCCCCCCCCCCCCCCCCCCCCCCCCCCCCCCCCCCCCCCCCCCCCCCCCCCCCCCCCCCCCCCCCCCCCCCCC
C                                                                 UIC at Chicago
C                                                                 BCL V1.02
C      Department of CME                                                                 April 1996.
CCCCCCCCCCCCCCCCCCCCCCCCCCCCCCCCCCCCCCCCCCCCCCCCCCCCCCCCCCCCCCCCCCCCCCCCCCCCCCCC
C      Program for calculating deformations of girder during
C      construction. Each step takes into account change in material and
C      stiffness characteristics of girders due to hardening of concrete.
C
C      This version takes into account effect of time on concrete
C      modulus of elasticity. It does not take into account influence of
C      specific weight of concrete on modulus of elasticity.
CCCCCCCCCCCCCCCCCCCCCCCCCCCCCCCCCCCCCCCCCCCCCCCCCCCCCCCCCCCCCCCCCCCCCCCCCCCCCCCC
      INCLUDE 'flib.fi'
      INCLUDE 'FGRAPH.FI'
C=====
      INCLUDE 'flib.fd'

      INTEGER lng, error
      CHARACTER*32 filename, fntmp, fntem, fnout, choice*1, menuname*9
      CHARACTER*32 fncrv, echoice*1
      LOGICAL si /.TRUE./

      CALL disclaimer(filename, si)

      DO WHILE (.TRUE.)
         fntmp = filename
         fntem = filename
         fntpr = filename
         fnout = filename
         fncrv = filename
         CALL ch_e(filename, 'dat', lng)
         CALL ch_e(fntmp, 'tmp', lng)
         CALL ch_e(fntem, 'tem', lng)
         CALL ch_e(fnout, 'out', lng)
         CALL ch_e(fncrv, 'crv', lng)

         CALL mainmenu(choice, filename, si)

      SELECT CASE (choice)
         CASE ('1', 'F', 'f')
            CALL takefn(filename, lng, si)

         CASE ('2', 'I', 'i')
            CALL datain(filename, si, error)
            IF (error .NE. 0) GOTO 999

         CASE ('3', 'S', 's')
            menuname = 'SUBMENU 3'
            CALL prg_header(filename, si, menuname)
            PRINT 241, ' OPENING FILES'

```

```

OPEN ( 7, FILE = filename, ACCESS = 'SEQUENTIAL',
+       ERR = 989, IOSTAT = error, STATUS = 'OLD')
IF (error .NE. 0) GOTO 999
OPEN ( 9, FILE = fntmp, ACCESS = 'SEQUENTIAL',
+       ERR = 988, IOSTAT = error, STATUS = 'UNKNOWN')
IF (error .NE. 0) GOTO 999
OPEN ( 6, FILE = fntem, ACCESS = 'SEQUENTIAL',
+       ERR = 988, IOSTAT = error, STATUS = 'UNKNOWN')
IF (error .NE. 0) GOTO 999

CALL prepare(error)
IF (error .NE. 0) GOTO 999

OPEN ( 8, FILE = fnout, ACCESS = 'SEQUENTIAL',
+       ERR = 988, IOSTAT = error, STATUS = 'UNKNOWN')
IF (error .NE. 0) GOTO 999
OPEN ( 5, FILE = fncrv, ACCESS = 'SEQUENTIAL',
+       ERR = 988, IOSTAT = error, STATUS = 'UNKNOWN')
IF (error .NE. 0) GOTO 999

CALL print_input(error)
IF (error .NE. 0) GOTO 999
CALL solvesys(error)
IF (error .NE. 0) GOTO 999
CALL curvature(error, fncrv, si)
IF (error .NE. 0) GOTO 999

PRINT 241, ' CLOSING FILES'
CLOSE (7, ERR = 999, IOSTAT = error)
CLOSE (9, ERR = 999, STATUS='DELETE', IOSTAT = error)
CLOSE (6, ERR = 999, STATUS='DELETE', IOSTAT = error)
CLOSE (8, ERR = 999, IOSTAT = error)
CALL wait()

CASE ('4', 'V', 'v')
CALL editmenu(echoice, filename, si)
SELECT CASE (echoice)
CASE ('1', 'V', 'v')
error = RUNQQ ('EDIT.BAT', fncrv)
CASE ('2', 'W', 'w')
error = RUNQQ ('EDIT.BAT', fnout)
CASE DEFAULT
END SELECT
IF (error .LT. 0 ) GOTO 987

CASE ('5', 'C', 'c')
CALL ch_infile(filename, fntem, lng, error, si)
CASE ('6', 'U', 'u')
CALL ch_si(filename, si)

CASE ('7', 'X', 'x')
EXIT

```



```

CALL pt(12,20,      '6')
CALL pt(13,20,      '7')

CALL pt(7, 41,      'F')
CALL pt(8, 31,      'I')
CALL pt(9, 24,      'S')
CALL pt(10,24,      'V')
CALL pt(11,24,      'C')
CALL pt(12,41,      'U')
CALL pt(13,25,      'X')
dummy = SETTEXTCOLOR(12)
CALL pt(16,15,'Type corresponding number or letter')
dummy = SETTEXTCOLOR(def_color)

DO WHILE (.NOT. pressed)
    pressed = PEEKCHARQQ()
END DO
choice = GETCHARQQ()
RETURN
221  FORMAT ( 2A )
END
C=====
SUBROUTINE editmenu(choice, filename,si)

INCLUDE 'flib.fd'
INCLUDE 'fgraph.fd'

INTEGER*2 dummy, def_color
CHARACTER choice*1, filename*(*), menuname*9
LOGICAL*4 pressed / .FALSE. /, si
menuname = 'VIEW MENU'
CALL prg_header(filename, si, menuname)

CALL pt(9, 22,      '- View curvatures only')
CALL pt(10,22,      '- view Whole output')
CALL pt(12,22,      '- exit to Main Menu')

def_color = SETTEXTCOLOR(15)
CALL pt(9, 20,      '1')
CALL pt(10,20,      '2')
CALL pt(12,20,      '3')

CALL pt(9, 24,      'V')
CALL pt(10,29,      'W')
CALL pt(12,25,      'X')
dummy = SETTEXTCOLOR(12)
CALL pt(16,15,'Type corresponding number or letter')
dummy = SETTEXTCOLOR(def_color)

DO WHILE (.NOT. pressed)
    pressed = PEEKCHARQQ()
END DO
choice = GETCHARQQ()

```

```

RETURN
221  FORMAT ( 2A )
END
C=====
SUBROUTINE prg_header(filename, si, menuname)

INCLUDE 'flib.fd'
INCLUDE 'fgraph.fd'

INTEGER*2 dummy
CHARACTER filename*(*), units*(5), menuname*9
LOGICAL*4 si

IF (si) THEN
    units = 'SI'
ELSE
    units = 'in-lb'
END IF

CALL cls()

CALL pt(1, 1,      ' BCL V1.02      File: ')
dummy = SETTEXTCOLOR(2)
CALL pt(1,26, filename)
dummy = SETTEXTCOLOR(dummy)
CALL pt(1,50,     'Units: ')
dummy = SETTEXTCOLOR(2)
CALL pt(1,57, units)
dummy = SETTEXTCOLOR(dummy)
CALL pt(1,67, menuname)
dummy = SETTEXTCOLOR(2)
CALL pt(2, 1, '_____')//
+'_____')
dummy = SETTEXTCOLOR(dummy)

RETURN
END
C=====
C  Pause
SUBROUTINE wait()

INCLUDE 'flib.fd'

CHARACTER key*1
PRINT 221, ' Press any key to continue!'
key = getcharqq()
RETURN
221  FORMAT ( 2A )
END
C=====
C  Pause for time t. (On 486DX2-50 k=3 333 333 ~ 1 sec)
SUBROUTINE pause_t( t )

```

```

INTEGER i, t, k
k = 3333333
DO i = 1, k*t
  CONTINUE
END DO

```

```

RETURN
END

```

```

C=====

```

```

C   Take name of the file and open it if exists.
SUBROUTINE takefn(fn, strlength, si)

```

```

  INCLUDE 'flib.fd'

```

```

  INTEGER strlength, i, j
  CHARACTER fnt*32,fn*32, menuname*9
  LOGICAL*4 si

```

```

  i = strlength
  fnt = fn
  menuname = 'SUBMENU 1'
  CALL prg_header(fn, si, menuname)

```

```

  CALL pt(10,20, 'Input new file name.')
  CALL pt(14,20, 'New file name ==> ')
  strlength=GETSTRQQ(fn)
  PRINT 221, ' '

```

```

  j = SCAN (fn, '.')
  IF (j .LT. strlength .AND. j .GT. 0) strlength = j

```

```

  IF ( strlength .EQ. 0 ) THEN
    fn = fnt
    strlength = i
  END IF
  RETURN

```

```

210  FORMAT ( A, \)
221  FORMAT ( 3A )

```

```

END

```

```

C=====

```

```

C   Change extension of filename.
C   Extension must have 3 characters.
SUBROUTINE ch_e(fn, ext, lng)

```

```

  INTEGER lng
  CHARACTER fn*(*),fnt*(32), ext*3

```

```

  fnt = '
  fnt = fn(1:lng) // '.' // ext
  fn = fnt

```

```
RETURN
END
```

```

=====
C Change system of units.
  SUBROUTINE ch_si(filename, si)

    INTEGER tmpi
    CHARACTER filename*32, menuname*9
    LOGICAL si
    menuname = 'SUBMENU 6'
    CALL prg_header(filename, si, menuname)

    CALL pt(11,20, 'Note: This affects new files only. ')
    IF (si) THEN
      CALL pt(10,20, 'Current units are in SI system. ')
      CALL pt(13,20, 'Change to INCH-POUND system of units? (Y/N) ')
      CALL YorN(tmpi)
      IF (tmpi .EQ. 1) si = .FALSE.
    ELSE
      CALL pt(10,20, 'Current units are in INCH-POUND system. ')
      CALL pt(13,20, 'Change to SI system? (Y/N) ')
      CALL YorN(tmpi)
      IF (tmpi .EQ. 1) si = .TRUE.
    END IF

    RETURN
210  FORMAT ( A, \)
211  FORMAT ( A )
    END
=====

```

```

=====
  SUBROUTINE pt(r,c,str)

    INCLUDE 'FGRAPH.FD'

    INTEGER r, c
    CHARACTER str*(*)
    RECORD / rccoord / curpos

    CALL SETTEXTPOSITION( INT2(r), INT2(c), curpos)
    CALL OUTTEXT(str)

    RETURN
  END
=====

```

```

=====
  SUBROUTINE cls()

    INCLUDE 'FGRAPH.FD'

    CALL CLEARSCREEN($GCLEARSCREEN)

    RETURN
=====

```

END

```

=====
C=====
SUBROUTINE disclaimer(filename, si)

  INCLUDE 'flib.fd'
  INCLUDE 'fgraph.fd'

  INTEGER*2 dummy, def_color
  CHARACTER choice*1, filename*(*), menuname*10
  LOGICAL*4 pressed / .FALSE. /, si

  menuname = 'DISCLAIMER'
  def_color = SETTEXTCOLOR(15)

  CALL prg_header(filename, si, menuname)

  CALL pt(7, 10,
+'The findings and conclusions expressed in this program')
  CALL pt(8, 14,
+'are those of the autors and not necessarily of')
  CALL pt(9, 11,
+'the State of Illinois Department of Transportation.')
  CALL pt(11,10,
+'It is responsibility of the user to verify all results')
  CALL pt(12,23,'produced by this program.')

  dummy = SETTEXTCOLOR(12)

  CALL pt(16,23,'Press any key to continue')
  dummy = SETTEXTCOLOR(def_color)

  DO WHILE (.NOT. pressed)
    pressed = PEEKCHARQQ()
  END DO
  choice = GETCHARQQ()
  SELECT CASE(choice)
    CASE ('V', 'v', 'I', 'i')
      CALL pt(15, 19,
+'University of Illinois at Chicago')
      CALL pt(16, 13,
+'Department of Civil and Materials Engineering')
      CALL pt(17, 30,
+'April 1996')
      CALL pt(18,19,
+'Program written by UIC')
      CALL pt(20,23,'Press any key to continue')

      DO WHILE (.NOT. pressed)
        pressed = PEEKCHARQQ()
      END DO
      choice.= GETCHARQQ()
    CASE DEFAULT
  END SELECT

```

```
      RETURN  
221  FORMAT ( 2A )  
      END  
CCCCCCCCCCCCCCCCCCCCCCCCCCCCCCCCCCCCC END CCCCCCCCCCCCCCCCCCCCCCCCCCCCCCCCCCCCCC
```

APPENDIX D

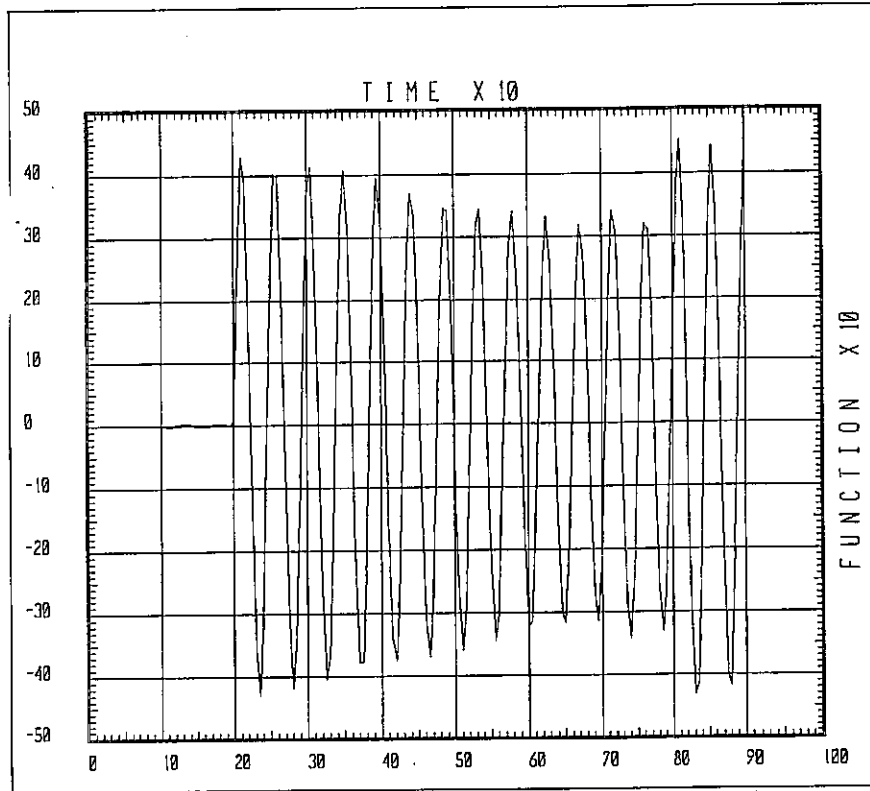


Figure D.1 Time history plot for typical shell element with respect to σ_{11} (Mode 4)

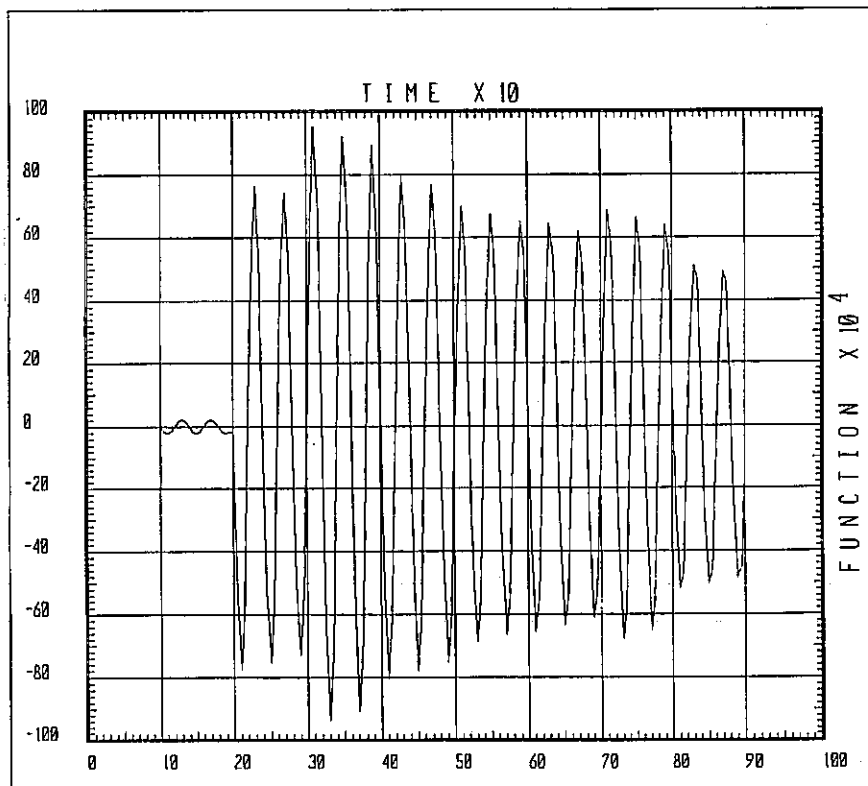


Figure D.2 Time history plot for typical shell element with respect to σ_{11} (Mode 5)

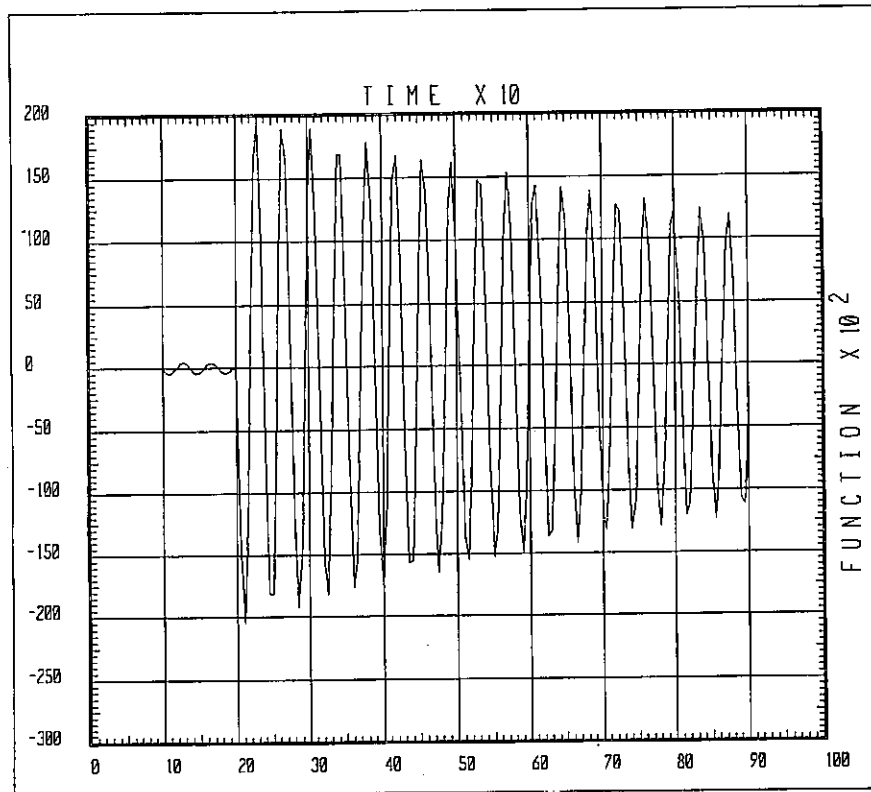


Figure D.3 Time history plot for typical shell element with respect to σ_{11} (Mode 6)

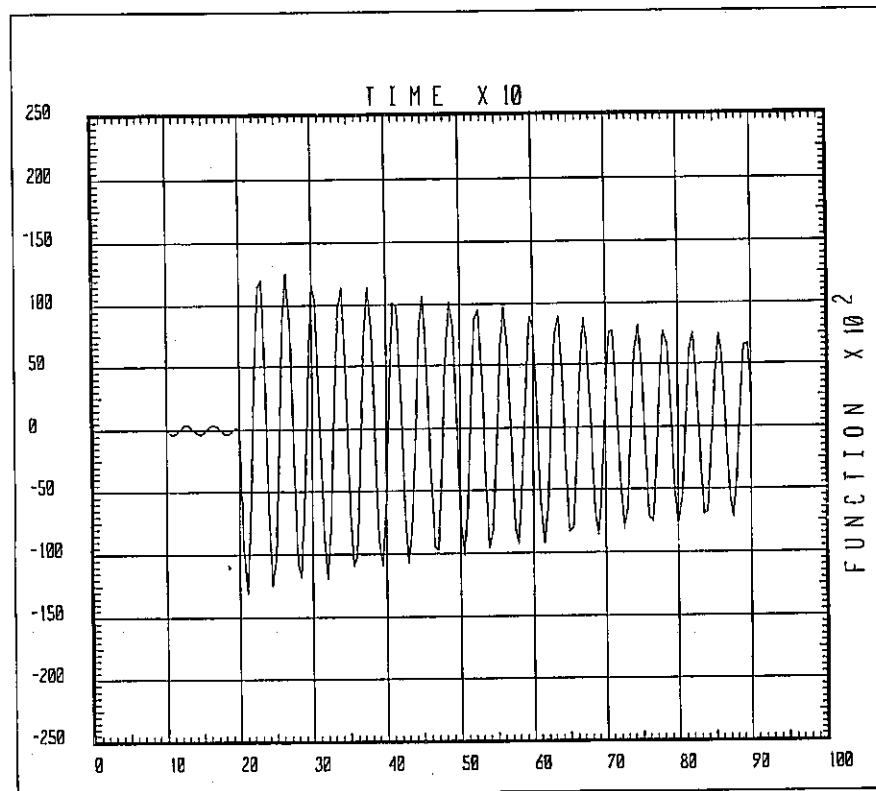


Figure D.4 Time history plot for typical shell element with respect to σ_{11} (Mode 7)

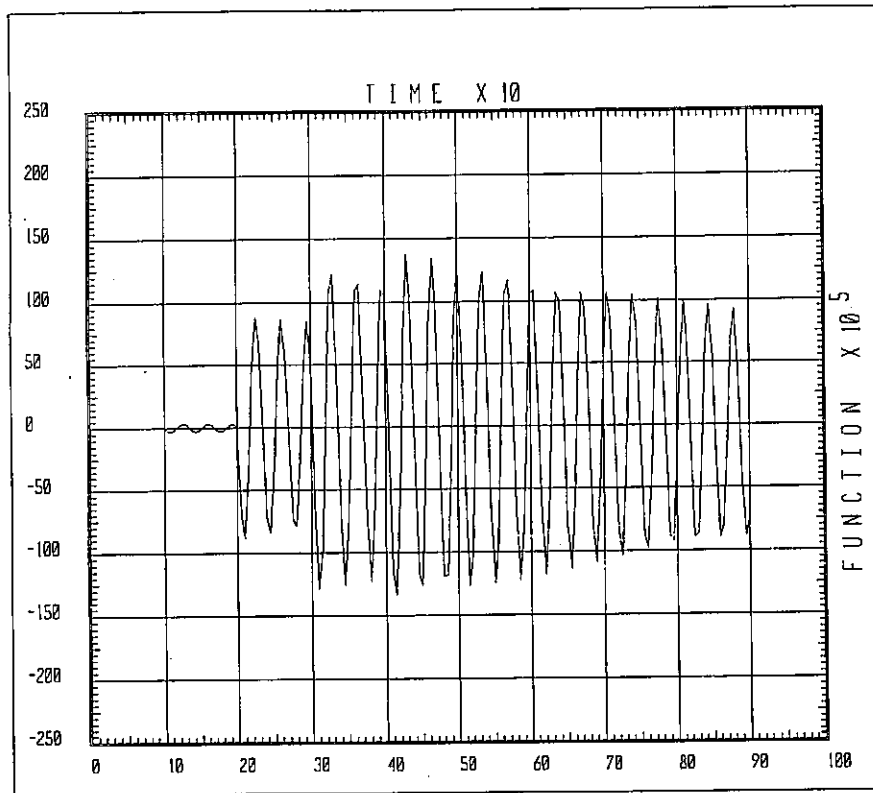


Figure D.5 Time history plot for typical shell element with respect to σ_{11} (Mode 8)

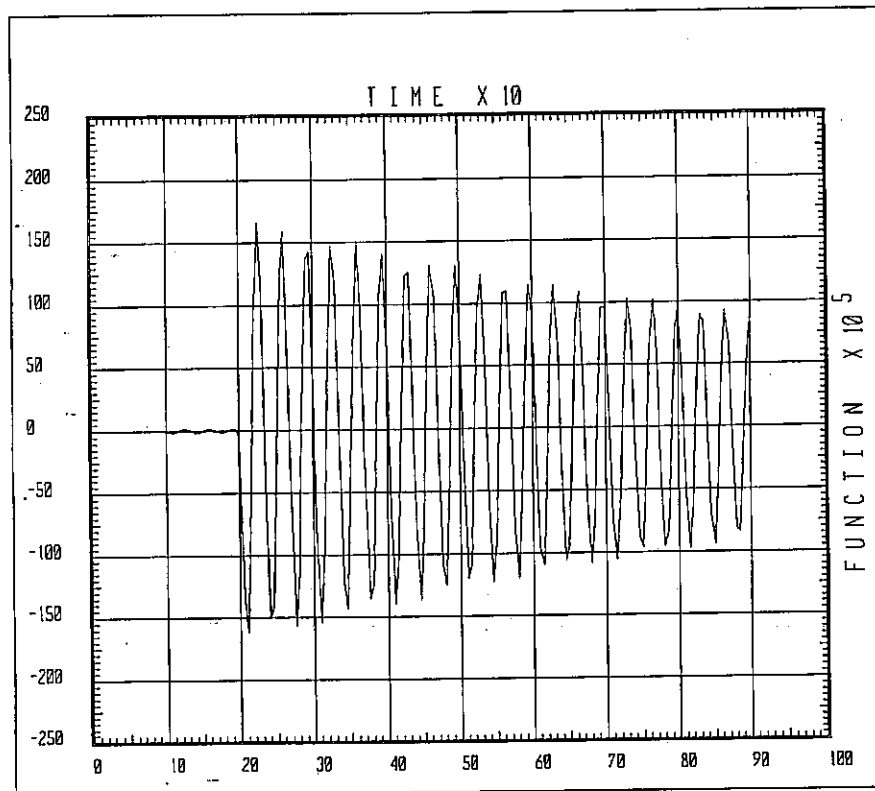


Figure D.6 Time history plot for typical shell element with respect to σ_{11} (Mode 9)

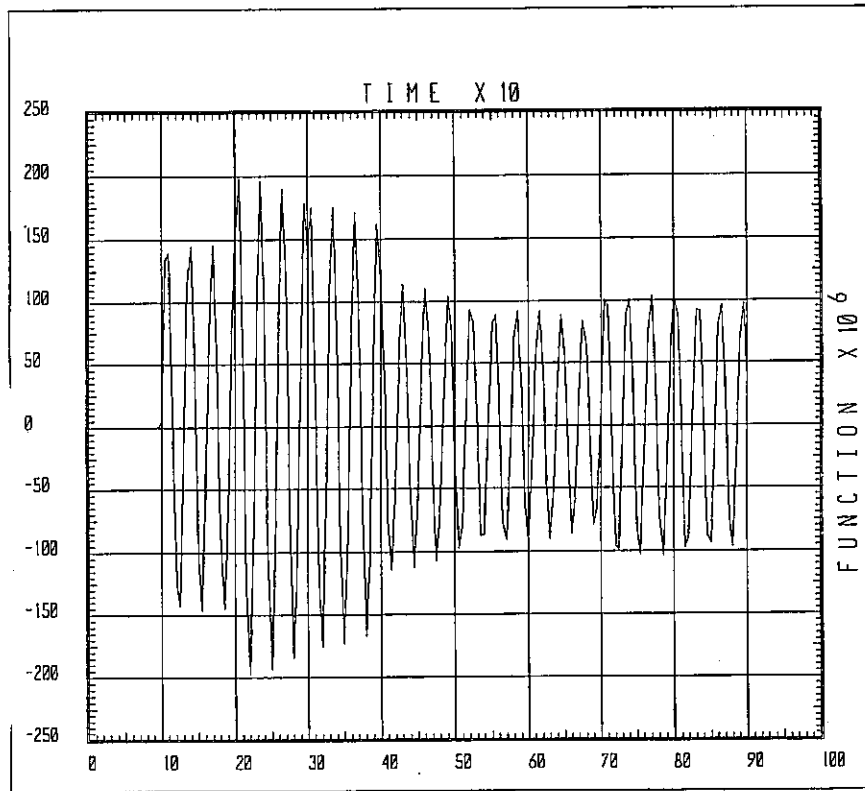


Figure D.7 Time history plot for typical shell element with respect to σ_{11} (Mode 10)

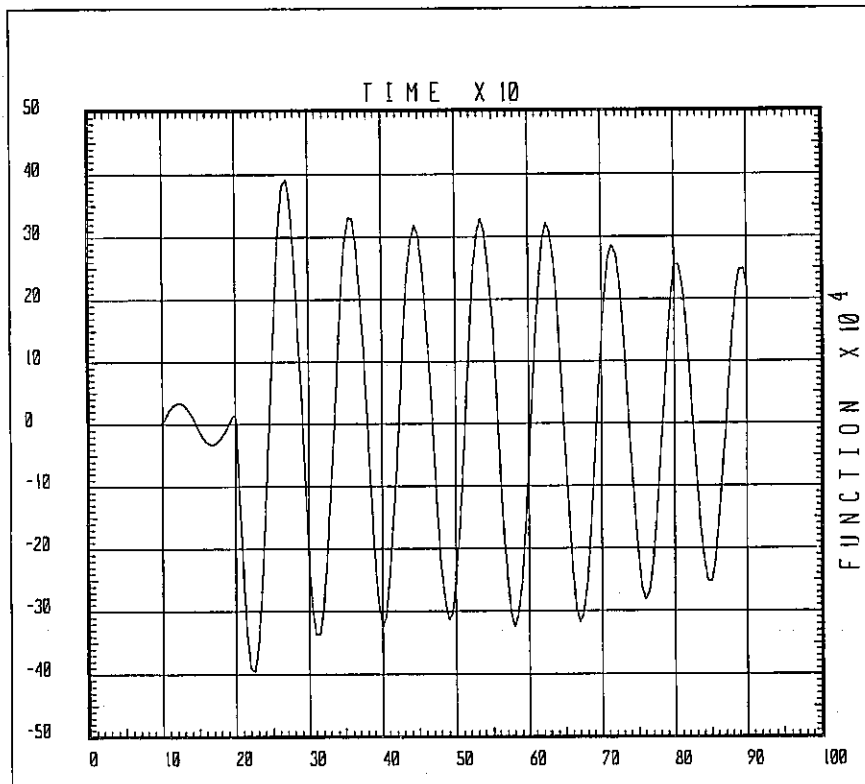


Figure D.8 Time history plot for typical joint with respect to displacement in z-axis (Mode 1)

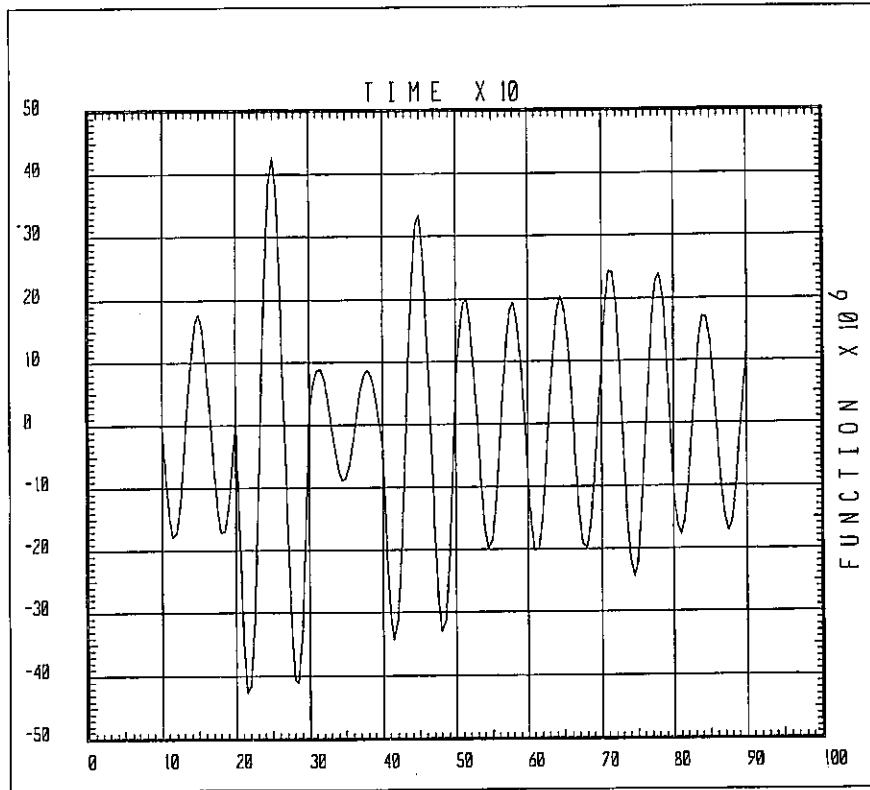


Figure D.9 Time history plot for typical joint with respect to displacement in z-axis (Mode 2)

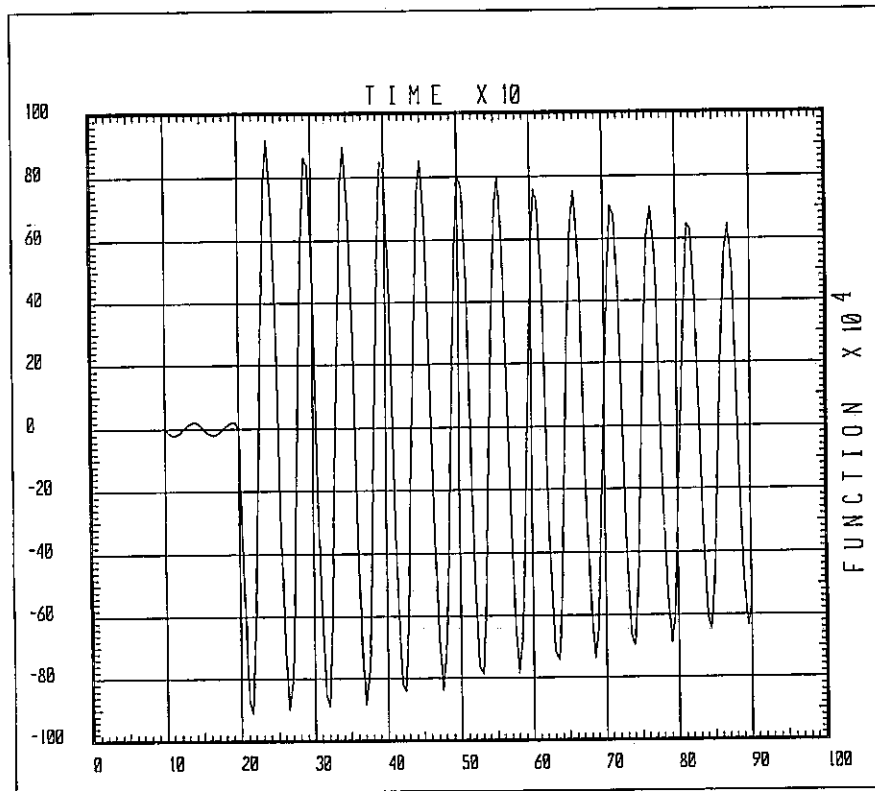


Figure D.10 Time history plot for typical joint with respect to displacement in z-axis (Mode 3)

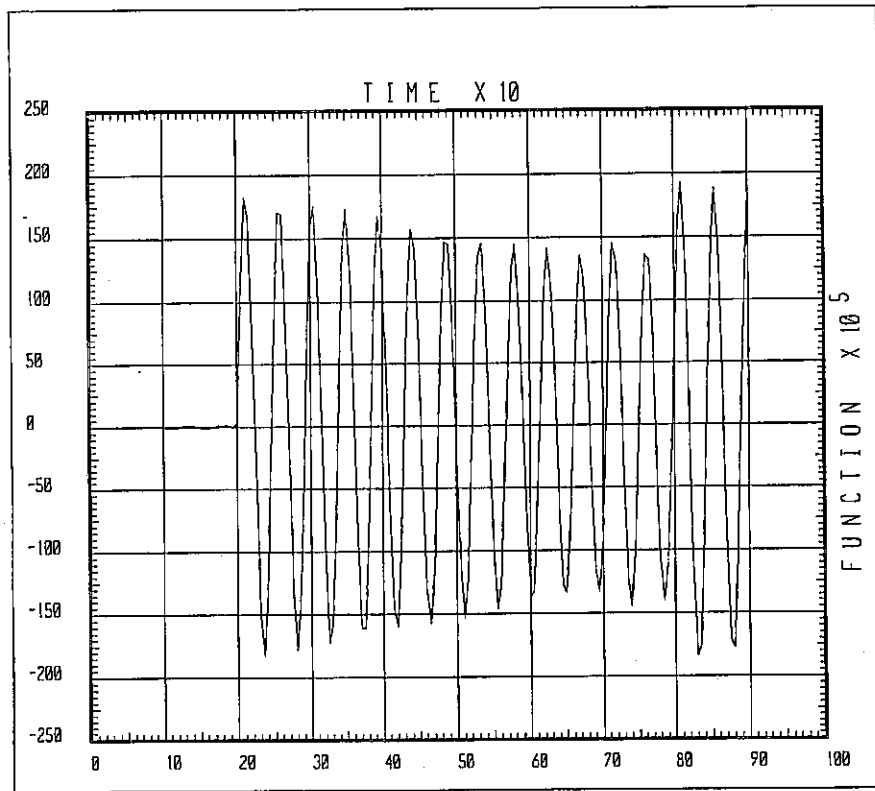


Figure D.11 Time history plot for typical joint with respect to displacement in z-axis (Mode 4)

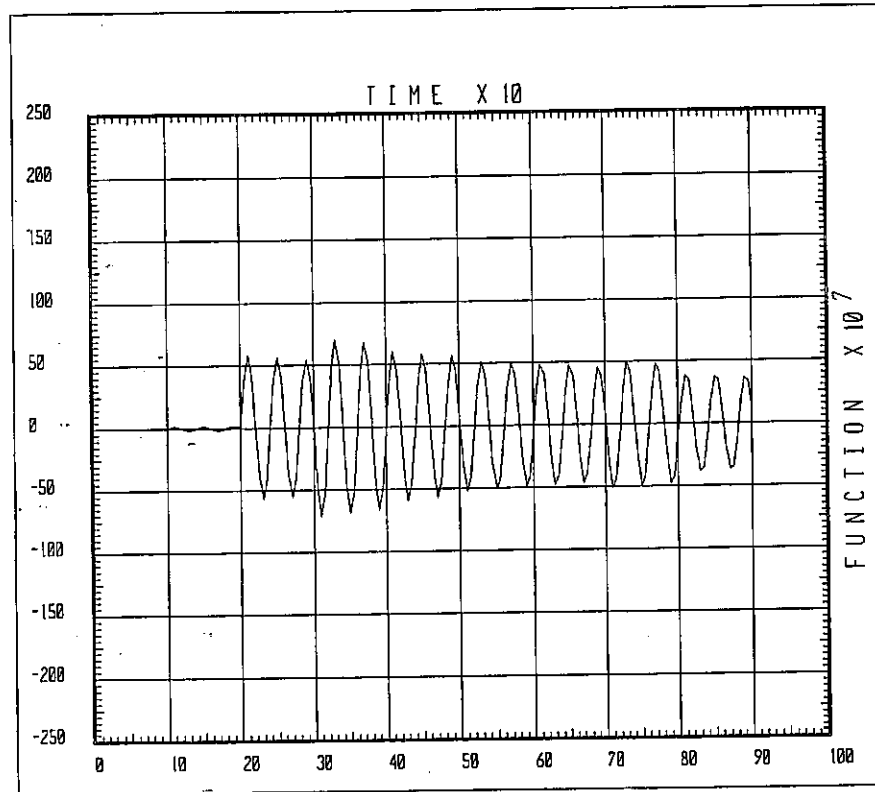


Figure D.12 Time history plot for typical joint with respect to displacement in z-axis (Mode 5)

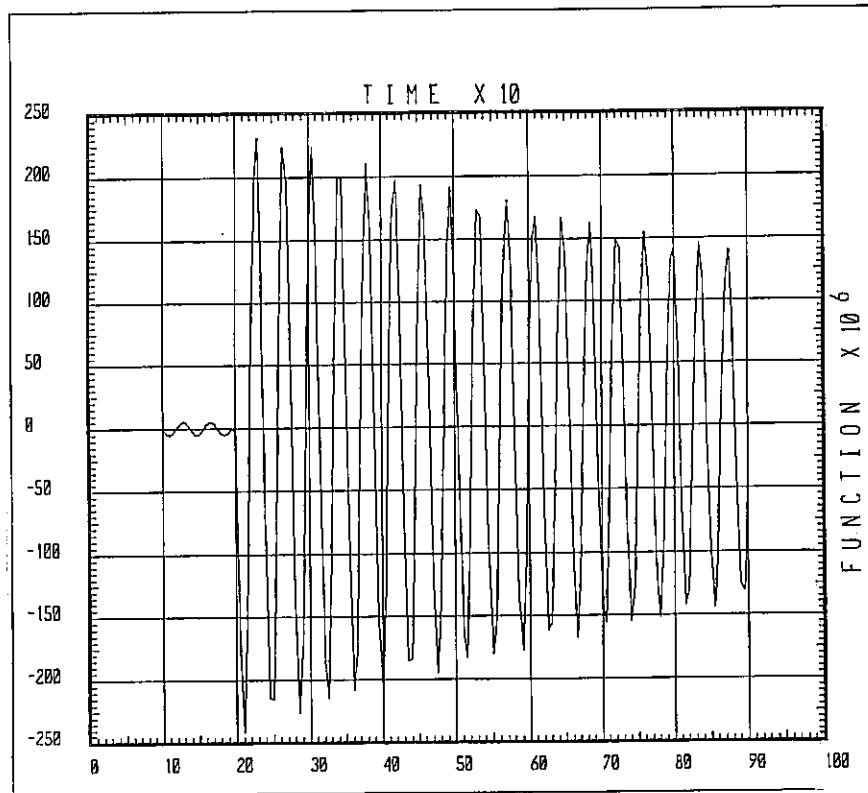


Figure D.13 Time history plot for typical joint with respect to displacement in z-axis (Mode 6)

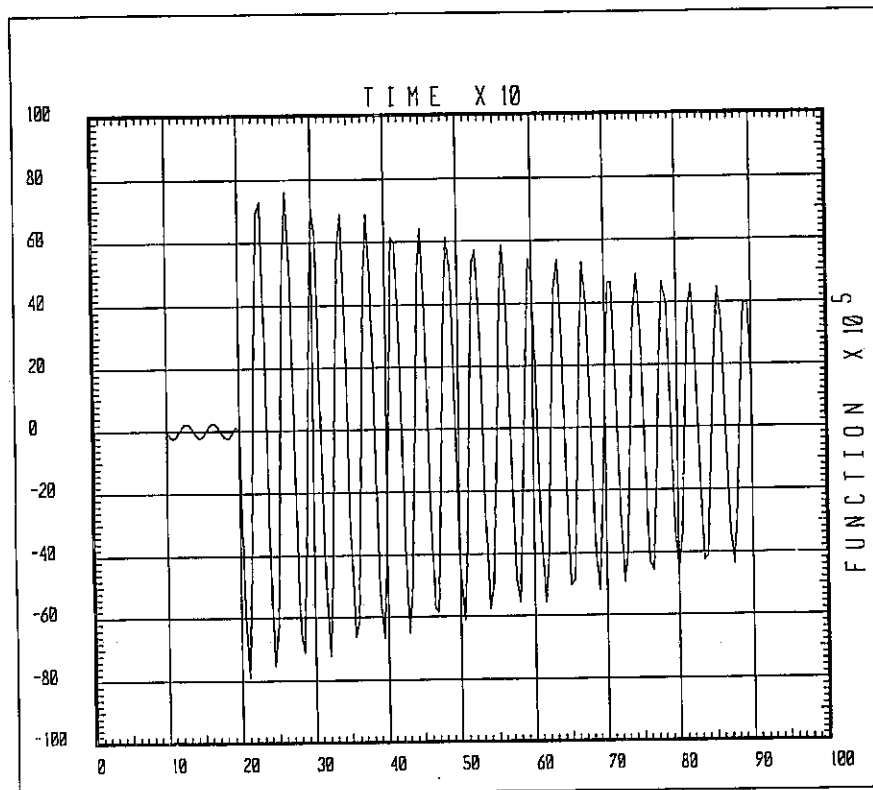
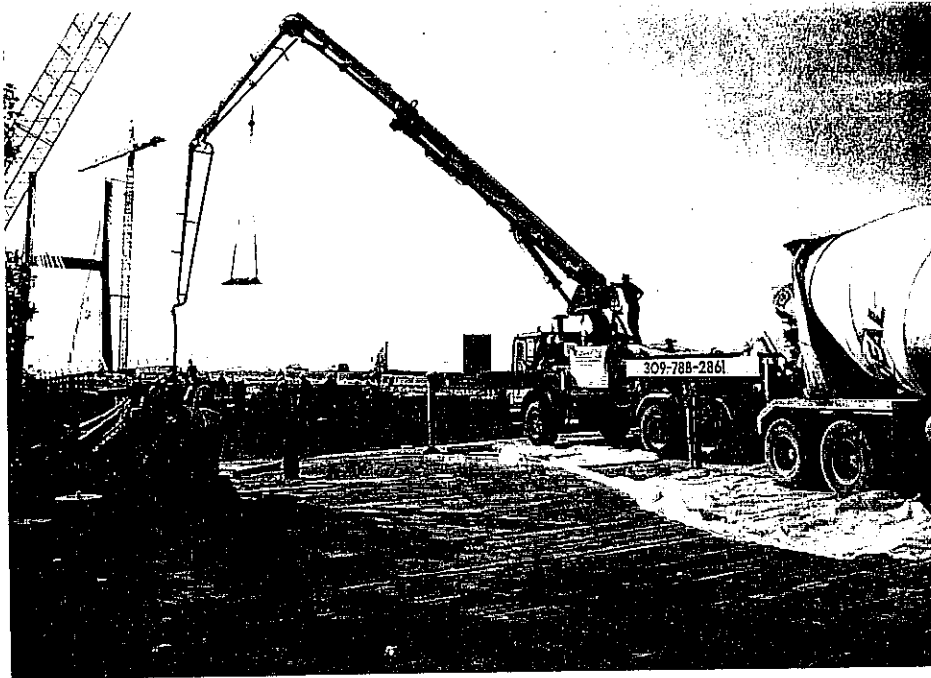


Figure D.14 Time history plot for typical joint with respect to displacement in z-axis (Mode 7)

FINAL REPORT

CONSTRUCTION LOADS AND VIBRATIONS

Project IA-H1, FY 1994



Prepared by

Mohsen A. Issa
Department of Civil and Materials Engineering
University of Illinois at Chicago
Chicago, Illinois

March 1998

· Illinois Transportation Research Center
Illinois Department of Transportation

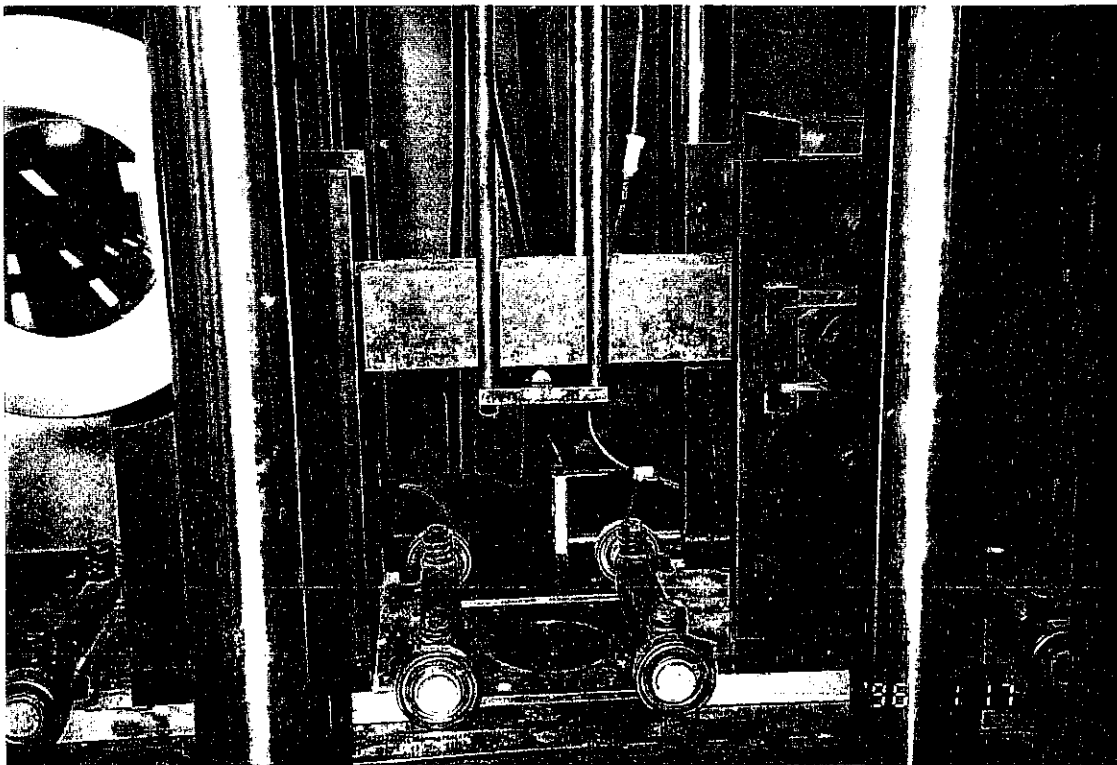
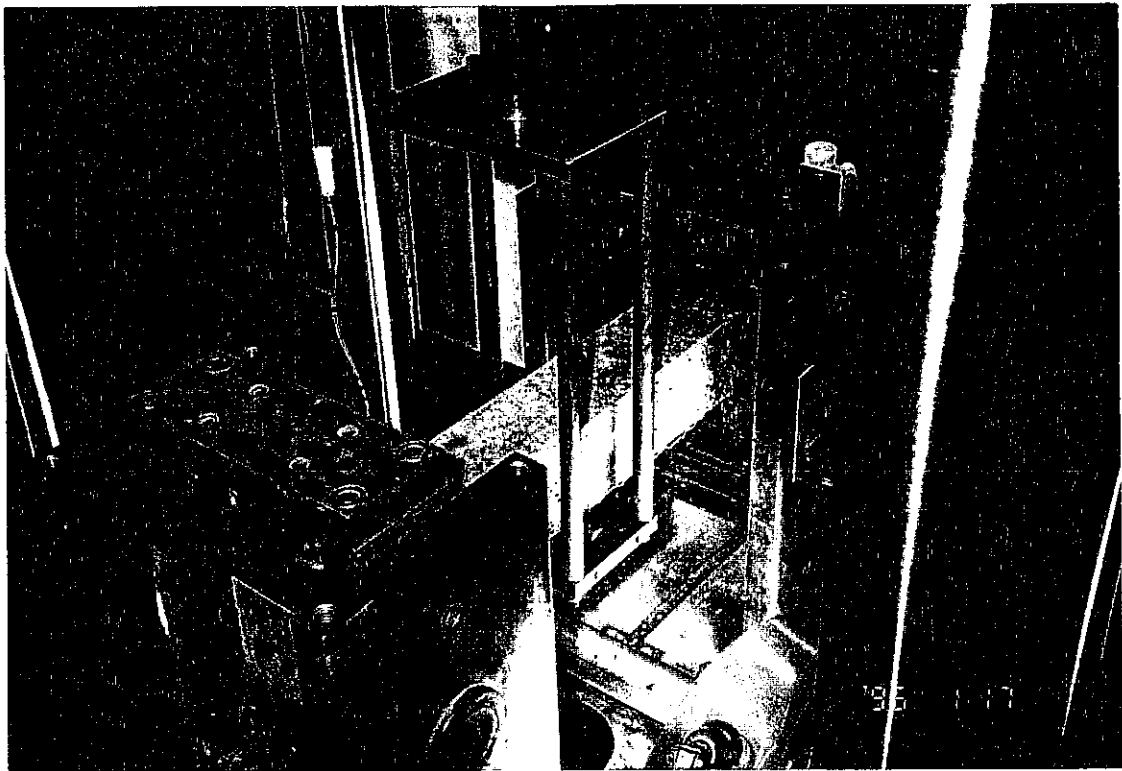


Figure 4.2 Experimental test setup